

**Age-, Sex-, and Diabetes-Determined Changes in the Structure and Mechanics of  
Human Sartorius Tendon Collagen**

by

Emile Joseph George Feniyanos

Submitted in partial fulfilment of the requirements  
for the degree of Master of Applied Science

at

Dalhousie University  
Halifax, Nova Scotia  
August 2019

© Copyright by Emile Joseph George Feniyanos, 2019

## Table of Contents

List of Tables .....	vii
List of Figures .....	viii
Abstract .....	xii
List of Abbreviations and Symbols Used .....	xiii
Acknowledgements .....	xv
Chapter 1: Introduction .....	1
1.1. Objectives .....	1
1.2. Soft Tissue Injuries .....	1
1.3. Tendon Overview .....	2
1.3.1. Tendon Anatomy & Composition .....	2
1.3.2. Tendon Structure .....	3
1.3.3. Collagen Structure .....	3
1.4. Crosslinking of Collagen .....	5
1.5. Enzymatic Crosslinking .....	5
1.6. Advanced Glycation End-Products .....	6
1.7. Thermal Stability .....	8
1.7.1. Differential Scanning Calorimetry .....	9
1.7.2. Hydrothermal Isometric Tension Analysis .....	10
1.8. Mechanical Behaviour of Tendons .....	13
1.8.1. In Vitro Mechanical Testing .....	15
1.9. Visualizing Modes of Damage .....	16
1.9.1. Discrete Plasticity .....	17
1.9.2. Bovine Tail Tendon Model .....	18
1.9.3. Bovine Forelimb Model .....	23
1.9.4. Human Distal Sartorius Tendon .....	27
1.10. Age-Determined Changes in Tendons .....	27
1.10.1. Structural and Compositional Changes in Aging Tendons .....	28
1.10.2. Alterations in Tendon Mechanics with Aging .....	29

1.11. Sex-Determined Changes in Tendons.....	29
1.11.1. Sex-Determined Changes in Tendon Structure and Mechanics .....	30
1.12. Diabetes Mellitus-Determined Changes in Tendons .....	31
1.12.1. Diabetes Mellitus-Determined Changes in Tendon Structure and Mechanics .....	32
Chapter 2: Thesis Rationale, Objectives and Hypotheses .....	33
2.1. Overview .....	33
2.2. Objectives and Hypotheses .....	34
2.2.1. Study #1: Assessing Collagen Structure and Thermal Stability .....	34
2.2.2. Study #2: Assessing Mechanical Behaviour of Tendon Collagen.....	35
2.2.3. Study #3: Assessing Overload Damage to Tendon Collagen .....	36
2.2.4. Study #4: General Histology & Immunohistochemistry .....	37
Chapter 3: Materials & Methodology.....	39
3.1. Sartorius Tendon Acquisition & Donor Demographic .....	39
3.2. Anatomy of the Distal Sartorius Tendon .....	39
3.3. Proposed Studies for Structural and Mechanical Analysis .....	40
3.4. Differential Scanning Calorimetry.....	45
3.4.1. DSC Test Protocol .....	47
3.4.2. Calculating DSC Parameters.....	47
3.5. Hydrothermal Isometric Tension Analysis .....	48
3.5.1. HIT Test Protocol .....	48
3.5.2. Calculation of HIT Parameters .....	49
3.6. Mechanical Overload Testing.....	54
3.6.1. Mechanical Overload Protocol .....	54
3.6.2. Calculation of Mechanical Parameters .....	55
3.6.3. SEM Preparation and Examination.....	57
3.7. Histology & Immunohistochemistry.....	57
3.7.1. Birefringence (Collagen Crimp) .....	59
3.7.2. Hematoxylin & Eosin .....	59
3.7.3. Immunostaining ( $\alpha$ -Pen12) .....	60

3.8. Statistical Analysis.....	60
3.9. Methodical Limitations.....	61
Chapter 4: Results.....	63
4.1. Structural Studies of Sartorius Tendon Collagen.....	63
4.1.1. Sartorius Tendon Collagen is Extremely Crosslinked and Thermally Stable.....	63
4.1.2. Sartorius Tendon Collagen Thermal Stability Decreases with Age in the Female and Male Non-Diabetic Populations .....	64
4.1.3. Isometric Contraction Occurs Prior to Denaturation .....	64
4.1.4. Isometric Contraction Occurs within the Isothermal Segment .....	70
4.1.5. Hydration may play a role in Sartorius Tendon Collagen Thermal Stability .	72
4.2. Mechanical Overload Studies of Sartorius Tendon Collagen.....	75
4.2.1. Sartorius Tendon Multi-Fascicle Subsample Failure Occurs via Stepwise Rupture of Fascicles.....	75
4.2.2. Sartorius Tendon Multi-Fascicle Subsample Strength Declined with Age in Female Donors .....	76
4.3. SEM Structural Studies and Failure Motifs of Sartorius Tendon Collagen.....	80
4.3.1. Unloaded Control Sample SEM Micrographs Reveal Relatively Tight-Packing and D-banding in Registry Amongst Neighboring Collagen Fibrils. ....	80
4.3.2. SEM Examination Reveals Damage Motifs Characteristic of High-Energy Elastic Piecewise Failure and Absence of Discrete Plasticity .....	80
4.4. Sex-Related Differences in Sartorius Tendon Collagen Structure and Mechanics .....	89
4.4.1. DSC and HIT Revealed Dense Crosslinking and No Differences in Structure Determined by Donor Sex.....	89
4.4.2. Sartorius Tendon Multi-Fascicle Subsamples from Female Donors have Reduced Strength, Extensibility and Ability to Absorb Strain Energy .....	89
4.5. Diabetes-Related Changes in Sartorius Tendon Collagen Structure and Mechanics .....	92
4.5.1. Appearance of Sartorius Tendon Collagen Unaltered by Diabetes .....	92

4.5.2. Sartorius Tendon Collagen Thermal Stability Largely Unchanged by Diabetes.....	92
4.5.3. Sartorius Tendon Multi-Fascicle Subsamples from Diabetic Donors Exhibit Brittle Behaviour.....	93
4.6. Sartorius Tendon Stiffness and Strength in Female Donors are Altered by Body Mass Index (BMI).....	96
4.7. Anatomical Location does not Alter Tendon Structure and Mechanics .....	96
4.8. Histology & Immunohistochemistry.....	98
4.8.1. Sartorius Tendon Collagen Crimp Appears to Diminish with Aging.....	98
4.8.2. Hematoxylin & Eosin Staining Reveals a High Density of Nuclei .....	100
4.8.3. Greater Pentosidine Epitope Concentration Observed in Sartorius Tendon Collagen with Diabetes and Aging .....	103
4.9. Summary of Results.....	106
Chapter 5: Discussion.....	107
5.1. Age-Related Changes in Sartorius Tendon Collagen Thermal Stability and Mechanics .....	107
5.1.1. Relationships Between Aging and Thermal Stability:.....	107
5.1.2. Relationships Between Aging and Tendon Mechanical Properties:.....	112
5.2. Sex-Related Changes in Sartorius Tendon Collagen Thermal Stability and Mechanics .....	115
5.2.1. Thermal Stability and Degree of Thermally Stable Crosslinking of Sartorius Tendon Collagen are Independent of Donor Sex .....	115
5.2.2. Relationships Between Donor Sex and Tendon Mechanics .....	115
5.3. Diabetes-Related Changes in Sartorius Tendon Collagen Thermal Stability and Mechanics .....	118
5.3.1. Relationships Between Diabetes and Tendon Collagen Thermal Stability ..	118
5.3.2. Relationships Between Diabetes and Mechanical Properties in Male Donors.....	119
5.3.3. Diabetic Tendon Coloration Remains Largely Unchanged .....	121
5.4. Tensile Failure Mechanics and SEM Structural Studies.....	122

5.4.1. Tensile Failure Mechanics of the Sartorius Tendon Reflects Dense Crosslinking .....	122
5.4.2. Discrete Plasticity is Absent in Overloaded Sartorius Tendon .....	123
5.5. Light Microscopy Studies of Structure and Composition.....	127
5.5.1. Birefringence: Collagen Crimp Flattening and Period Increases with Aging and Diabetes.....	127
5.5.2. H & E Staining: The Human Sartorius Tendon is Highly Cellular, Decreasing with Aging and Diabetes.....	127
5.5.3. $\alpha$ -PEN12: Qualitative Increases in $\alpha$ -PEN12 Epitope Concentration with the Combined Influence of Aging and Diabetes.....	128
5.6. Summary of Objectives and Hypotheses .....	130
5.6.1. Study #1 Assessing Collagen Structure and Thermal Stability .....	130
5.6.2. Study #2: Assessing Mechanical Behaviour of Sartorius Tendon Collagen	131
5.6.3. Study #3: Assessing Overload Damage to Tendon Collagen .....	132
5.6.4. Study #4: Histology & Immunohistochemistry .....	133
Chapter 6: Conclusion .....	134
6.1. Limitations .....	134
6.2. Future Research Suggestions .....	135
6.2.1. In-Depth Light and Scanning Electron Microscopy .....	135
6.2.2. In Vitro Diabetes Model .....	136
6.2.3. Crosslink Analysis and Identification.....	136
6.2.4. In-Depth Analysis of the Tendon Mechanics .....	137
6.2.5. Fatigue Subrupture Overload Testing and Usage of a Complementary Set of Human Tendons.....	137
6.3. Concluding Remarks.....	138
Reference List .....	139
Appendix A: Phosphate Buffer Saline DSC Study, Half-Time of Load Decay and Height-Related Data.....	165
Appendix B: Licenses for Copyrighted Material.....	171

## List of Tables

Table 4.1 Average thermomechanical and thermal properties of the sartorius tendon based on donor population across their respective age range (female non-diabetic: 16-60 years, male non-diabetic: 24-59 years, male diabetic: 46-60 years). .....	63
Table 4.2 Physical dimensions of the mechanical testing multi-fascicle subsamples. ....	76
Table 4.3 Comparison of HIT ( $n_{F,ND} = 6$ , $n_{M,ND} = 9$ ) and DSC ( $n_{F,ND} = 5$ , $n_{M,ND} = 9$ ) results between female non-diabetic and male non-diabetic donor populations spanning 16 to 59 years of age. ....	90
Table 4.4 Comparison of HIT and DSC ( $n_{M,ND} = 6$ , $n_{M,D} = 8$ ) results between male non-diabetic and male diabetic donor populations spanning 38 to 60 years of age. ....	94
Table 5.1 Summary of thermal studies (DSC and HIT) of tendon collagen performed in the Tissue Mechanics Lab demonstrating varying degrees of discrete plasticity damage. ....	109
Table 5.2 Evidence of the decreases in thermal stability of collagen in the presence of a salt ions evaluated via HIT and DSC. ....	113
Table 5.3 Summary of the effects of aging on in vitro mechanical properties of human lower limb tendons. ....	114
Table 5.4 Summary of in vitro mechanical studies identifying sex-determined differences in human lower limb tendon mechanical properties. ....	117
Table 5.5 Summary of thermal Studies (HIT/DSC) of tendon collagen subject to in vitro glycation or natural diabetes. ....	120
Table 5.6 Summary of the influence of diabetes on the in vitro mechanical properties of human lower limb tendons. ....	122
Table 5.7 Summary of in vitro mechanical properties of tendons tested in the Tissue Mechanics Lab demonstrating varying degrees of discrete plasticity damage. ....	124

## List of Figures

Figure 1.1 Diagram of the tendon hierarchical structure.....	4
Figure 1.2 Formation of the collagen fibril and molecule.....	4
Figure 1.3 Diagram of enzymatic and non-enzymatic crosslink formation.....	7
Figure 1.4 Energy states of collagen denaturation.....	9
Figure 1.5 DSC testing curve with the differential heat flow between the sample and the reference pan on the y-axis and temperature on the x-axis. ....	11
Figure 1.6 HIT Testing Curves with load (blue curve) or temperature (red curve) on the y axis and time on the x-axis.....	12
Figure 1.7 Representative tendon multi-fascicle subsample stress-strain curve displaying the toe, linear and yield regions.....	15
Figure 1.8 TEM micrograph of a longitudinal section of 5-week-old rat tail tendon collagen fibrils overloaded to 7% strain at 14,000x.....	18
Figure 1.9 TEM image of transverse section at 38,000x magnification displaying the formation of multiple kink deformations in neighboring 39-month old rat tail tendon fibrils overloaded to 4% strain indicated by the black arrows.....	19
Figure 1.10 SEM images of (A) undamaged and (B, C & D) damaged collagen fibrils .....	19
Figure 1.11 Thermal stability of BTT collagen evaluated using DSC. ....	21
Figure 1.12 SEM micrographs of collagen fibrils demonstrating differences in overload response to in vitro ribose incubation. ....	22
Figure 1.13 AFM deformation images of a native bovine tail tendon fibrils. ....	24
Figure 1.14 AFM deformation maps of BTT collagen fibrils exhibiting discrete plasticity before (A, B) and after (C, D) incubation with MMP-9 (D) and trypsin (C). ....	25
Figure 1.15 SEM micrographs displaying the difference in overload damaged tendon collagen from the bovine CDET (Top, Middle) and SDFT (Bottom).....	26
Figure 3.1 Stacked column graph showing individual donor counts grouped into age decades from the current study.....	41
Figure 3.2 (A) A stacked column graph was used to identify the number of individuals in each BMI category for each donor population from the current study. (B) A scatterplot displaying the donor BMI and age within each donor population from the current study. ....	42



Figure 3.3 (A) Anterior perspective view of the anatomy of the right lower limb. (B) Representative distal sartorius tendon collected from the NSHA Regional Tissue Bank prior to dissection.....	43
Figure 3.4 Partial assortment (12/24 individuals) of the collected sartorius tendons prior to gross dissection from donors varying in age, sex and diabetic status. ....	44
Figure 3.5 Hierarchical chart displaying the two comparative groups examined in this study to determine differences in human sartorius tendon collagen by age, BMI, sex and diabetic status. ....	45
Figure 3.6 Flowchart of the methodology followed in this study.....	46
Figure 3.7 Representative DSC endotherm from a sartorius tendon collagen sample.....	48
Figure 3.8 HIT Apparatus schematic wherein specimens are isometrically constrained in a 4L water bath by a fixed support and cantilever load cell. ....	49
Figure 3.9 Representative HIT test graph of sartorius tendon collagen. ....	50
Figure 3.10 Determination of the HIT parameters (A) denaturation temperature and (B) fractional differences in load pre- and post-denaturation.....	52
Figure 3.11 Representative isothermal segment evaluated 5,000-10,000 seconds from the beginning of the start of the segment. ....	53
Figure 3.12 Representative stress-strain curve for a mechanical overload rupture test.....	56
Figure 3.13 Composite SEM micrograph overview of a sample at 40x magnification.....	58
Figure 3.14 Histological tendon samples were dissected near the middle of the tendon in two 5x10mm pieces (green rectangles).....	58
Figure 4.1 Scatterplots of DSC (A) $T_{onset}$ and (B) $T_{peak}$ plotted against age using distilled water as the hydrating medium revealed that thermal stability of the male non-diabetic donor tendon collagen decreased significantly with increasing age.....	65
Figure 4.2 Scatterplots of additional DSC parameters evaluated versus age using distilled water as the sample hydrating medium.....	66
Figure 4.3 Representative DSC (Heat Flow) curves y-scale adjusted to reveal the differences in collagen thermal behaviour with age and diabetes.....	67
Figure 4.4 HIT denaturation temperature plotted against age revealed thermal stability declined with increasing age for both the female non-diabetic and male non-diabetic populations. ....	67
Figure 4.5 Scatterplots of the fractional differences in load (A) pre- $T_d$ and (B) post- $T_d$ versus age. ....	68
Figure 4.6 Stacked column graphs of the fractional difference in load pre- $T_d$ in HIT strip samples for each individual (denoted by their age) of a given donor population.....	69

Figure 4.7 Mosaic plot displaying the count and percentage of HIT strip samples from each donor population that underwent isometric contraction or relaxation pre- $T_d$ .....	70
Figure 4.8 Scatterplot of the fractional difference in load post- $T_d$ versus pre- $T_d$ . ....	71
Figure 4.9 Comparison of the contraction or decay behaviour during the isotherm. ....	72
Figure 4.10 Isothermal behaviour was classified into four categories: contraction, decay, constant loading or failure for each sample in a HIT test for a donor tendon. ....	73
Figure 4.11 Evaluating DSC parameters of the entire donor population revealed linear decreases with increasing water content when calculated for the entire donor population: (A) $T_{onset}$ , (B) $T_{peak}$ , (C) $FWHM$ and (D) $h_{wet\ mass}$ .....	74
Figure 4.12 Representative stress-strain curves of a tendon multi-fascicle subsample produced by an overload to rupture test using a strain rate of 0.25% strain/second.....	77
Figure 4.13 Scatterplot of tissue modulus versus UTS of tendon multi-fascicle subsamples. ....	77
Figure 4.14 Sequence of images capturing the failure of a sartorius tendon multi-fascicle subsample secured by the custom waveform crush grips strained at 0.25%/second. ....	78
Figure 4.15 Mechanical properties of the tendon collagen plotted versus age. ....	79
Figure 4.16 SEM micrographs of unloaded control images displaying neighboring fibrils with D-banding in registry. ....	81
Figure 4.17 Representative SEM composite micrographs at 40x magnification of (A) an unloaded control sample and (B) an overload damaged sample.....	83
Figure 4.18 SEM micrographs A and B reveal varying degrees of fibril hairpin turns. ....	84
Figure 4.19 SEM micrographs revealing regions of hairpin turns in neighboring fibrils.....	85
Figure 4.20 SEM micrographs displaying the different motifs of elastic recoil damage found in the sartorius tendon.....	86
Figure 4.21 SEM micrographs describing the varying degrees of fibril failure found in the sartorius tendon collagen.....	87
Figure 4.22 SEM micrographs revealing differing modes of plasticity damage in sartorius tendon samples from the young and tough male non-diabetic donors.....	88
Figure 4.23 Comparison of mechanical parameters based on donor sex across the ages 16-59 years ( $n_{F,ND} = 6$ , $n_{M,ND} = 9$ ) revealed three of the four mechanical parameters evaluated were significantly different.....	91
Figure 4.24 Example of the extremes of sartorius tendon collagen coloration observed. ....	93

Figure 4.25 $T_{onset}$ of tendon collagen was significantly increased in tendon collagen of male donors 38-60 years of age with diabetes ( $n_{M,ND} = 6, n_{M,D} = 8$ ). .....	94
Figure 4.26 Evaluation of diabetes-determined mechanical differences in sartorius tendon multi-fascicle subsamples from male donors aged 38-60 years of age ( $n_{M,ND} = 6, n_{M,D} = 8$ ) revealed significant results.....	95
Figure 4.27 Tendon multi-fascicle subsample (A) tissue modulus ( $p = 0.0026; r^2 = 0.74$ ) and (B) $UTS$ ( $p = 0.0089; r^2 = 0.85$ ) decreased with increasing BMI within the female donor population. ....	97
Figure 4.28 Longitudinal tendon sections of a young healthy (24 years of age, normal BMI) male non-diabetic (A & C) and an older unhealthy (50 years of age, obese BMI) male diabetic (B & D) shown at magnifications of 40x and 100x respectively. Birefringence examination of the longitudinal sections revealed a noticeably higher degree of collagen crimping in the younger donor tendon. ....	99
Figure 4.29 Transverse (Cross-sectional) sections of H & E stained tendon of a young healthy (24 years of age, normal BMI) male non-diabetic (A & C) and an older unhealthy (50 years of age, obese BMI) male diabetic (B & D) shown at magnifications of 40x and 100x respectively. ....	101
Figure 4.30 Longitudinal Sections of H & E stained tendon from a young healthy (24 years of age, normal BMI) male non-diabetic (A & C) and an older unhealthy (50 years of age, obese BMI) male diabetic (B & D) shown at magnifications of 40x and 100x respectively. ....	102
Figure 4.31 Control (A & C) and $\alpha$ -PEN12 immunostained longitudinal tendon sections of a young, healthy (24 years of age, normal BMI) male non-diabetic (A & C) shown at magnifications of 40x and 100x respectively. ....	104
Figure 4.32 Control (A & C) and $\alpha$ -PEN12 immunostained longitudinal tendon sections of an older, unhealthy (50 years of age, obese BMI) male diabetic (B & D) shown at magnifications of 40x and 100x respectively. ....	105
Figure 5.1 Graph of $\ln\left(\frac{Load}{Initial\ Load}\right)$ on the y-axis and the time from the start of the isotherm on the x-axis in order to illustrate the differences in thermally stable crosslinking and subsequent isothermal behaviour of the human sartorius tendon and the bovine SDFT. ....	110
Figure 5.2 Representative normalized stress-strain curves of the human sartorius tendon (blue) and the bovine CDET (red). ....	123
Figure 5.3 SEM micrographs of overloaded human sartorius tendons revealing hairpin turns, recoiled fibrils and overall disorganization. ....	126
Figure 5.4 TEM micrograph of local fibril failure (indicated by the black arrow heads) in a ruptured Achilles tendon from a 29-year old female ballet dancer at 38,000x.....	126
Figure 5.5 Light microscopy images at 40x and 100x magnification identifying the differences in positive and negative staining of the primary antibody with a clear border where the drop of $\alpha$ -PEN12 antibody was placed. ....	129

## Abstract

In an age where men and women are remaining physically active into the geriatric years, age-related changes in soft tissue injuries and healing are becoming more important to clinical care. Differences in structure and function of human tendons with aging, sex, and diabetes are poorly understood, despite reported differences in the frequencies of specific tendon injuries. The objectives of this thesis were to investigate whether variations occur in (i) molecular-level structure, (ii) multi-fascicle level mechanics and (iii) ultrastructural failure mechanisms in the human sartorius tendon that are determined by tissue bank donor age, sex and diabetic status.

Human sartorius tendons were collected from the NSHA Regional Tissue Bank (Halifax, N.S) from donors ranging in age from 16–56 (female, non-diabetic only) and 24–60 (male, non-diabetic or diabetic). Blinded donor information included height, weight and diabetic status. To assess molecular-level changes in structure, hydrothermal isometric tension (HIT) analysis and differential scanning calorimetry (DSC) were used. The mechanics of the sartorius tendon multi-fascicle subsamples were assessed using uniaxial tensile overload testing to rupture. After rupture, tendon collagen ultrastructure was examined using SEM and compared with undamaged samples. Histology and immunohistochemistry were performed on fixed tendon samples (from predominantly male diabetic and non-diabetic donors) to identify changes in (i) collagen crimp, (ii) cell nuclei content and (iii) pentosidine epitope concentration with aging and diabetes.

Results demonstrated that the sartorius tendon collagen is highly crosslinked, from early adulthood through early geriatric life. Under overload to rupture, this crosslinking results in high energy, sequential elastic rupture of individual tendon fascicles. Ultrastructural studies with SEM revealed fibril-level failure mechanisms consistent with elastic recoil (twisting, balling and knotting), hairpin turns, and local failure and complete breakage of isolated and neighboring fibrils – but with an absence of serial discrete plasticity kinking observed in other species.

Fascicle mechanical properties were largely maintained with age. Thermal stability and heterogeneity of collagen decreased modestly with age under HIT and DSC. In the non-diabetic donors, tendon samples from female donors were 25% weaker, 38% less tough and 16% less extensible than those from non-diabetic male donors. In males, diabetic tendon samples were 37% less tough and 20% less extensible than normal tendons, yet modulus and strength remained unchanged. A slight increase in collagen denaturation temperature was observed with diabetes, likely due in part to accumulation of advanced glycation product crosslinks. The combination of aging and diabetes qualitatively increased collagen crimp wavelength, decreased cell nuclei numbers and increased pentosidine epitope concentration.

The human sartorius tendon is a highly crosslinked structure that remains relatively unchanged with age, sex and diabetes, sacrificing the toughness mechanism discrete plasticity for molecular stability and elastic mechanical strength. This stability of structure with age is belied by the surprisingly high cellular density which is partially retained into early geriatric life. This study has contributed to advancing modern knowledge of tendon structure-function relations, with potential future applications in treatment of soft tissue injuries and engineering of tendon or ligament replacements.

## List of Abbreviations and Symbols Used

AGE	Advanced Glycation End-Product
ANOVA	Analysis of Variance
BMI	Body Mass Index
BTT	Bovine Tail Tendon
CSA	Cross-Sectional Area
CDET	Common Digital Extensor Tendon
CDHA	Capital District Health Authority
D	Diabetic
DAB	Diaminobenzidine
DSC	Differential Scanning Calorimetry
DW	Distilled Water
$E$	Tissue Modulus
F	Female
F.D.	Fractional Difference
$FWHM$	Full Width at Half-Maximum
$\Delta G$	Gibbs Free Energy
GAG	Glycosaminoglycan
$h$	Enthalpy
$h_{wet\ mass}$	DSC Wet Mass Specific Enthalpy of Denaturation
$h_{dry\ mass}$	DSC Dry Mass Specific Enthalpy of Denaturation
H & E	Hematoxylin and Eosin
HIT	Hydrothermal Isometric Tension
HRP	Horseradish Peroxidase
IHC	Immunohistochemistry
$k$	Relaxation Slope Constant
$Load$	HIT Isothermal Load
$Load_{Max}$	HIT Maximum Isothermal Load

M	Male
MTJ	Musculotendinous Junction
NSHA	Nova Scotia Health Authority
OTJ	Osteotendinous Junction
PBS	Phosphate Buffer Saline
<i>s</i>	Entropy
ND	Non-Diabetic
SD	Standard Deviation
SDFT	Superficial Digital Flexor Tendon
SEM	Scanning Electron Microscopy
<i>t</i>	Time
$t_{1/2}$	HIT Half-Time of Load Decay
TBS	TRIS Buffer Saline
$T_d$	HIT Denaturation Temperature
$T_{onset}$	DSC Onset Temperature
$T_{peak}$	DSC Peak Temperature
UTS	Ultimate Tensile Strength

## Acknowledgements

There are many people that require acknowledgements upon completion of this master's thesis. Firstly, I'd like to thank my co-supervisor Dr. J. Michael Lee for the opportunity to work on the project while providing insight, wisdom, and the random yet interesting one-liners and facts. Additionally, you helped to expand my musical knowledge of the jazz and classical genre. I'd like to thank Dr. Sarah Wells for being my other co-supervisor, you were always helpful in providing advice and assistance. I'd also like to thank Dr. Samuel Veres, who was always helpful and encouraged critical thinking, as I'd always leave a meeting with more questions than I had entered with. I'd like to thank my external examiner for the defense Dr. Derek Rutherford.

The thesis itself, relied on a series of mechanical, thermal, thermomechanical experiments and histological experiments. I would like to thank Sara Sparavalo (for the introduction to ultimate frisbee), for setting up the bulk of the experimental framework from her study and kindly walking me through many of the testing protocols. I'd like to thank Jasmin Astle, who acted as a mentor, and provided assistance (on crosswords) and advice when needed. Thanks to Tyler Herod, Brendan Grue and Meghan Martin, who provided help with lab work/presentations. I'd like to thank Darren Cole for his expertise with everything in the lab (and awful dad jokes). A thank you to Ping Li for assistance in scanning electron microscopy sample preparation with his sneaky humor. A sincere thank you to Patricia Scallion for her assistance with the scanning electron microscope. Thanks to Michel Johnson for his kind assistance with the differential scanning calorimeter. The histological work of this thesis wouldn't have been possible without Patricia Colp, who always had a smile on her face and provided assistance whenever needed.

As the author, I'd like to thank the funding sources for the project: The Natural Sciences and Engineering Research Council of Canada and the Canadian Institutes of Health Research. Further, I would like to thank the NSHA Regional Tissue Bank, specifically Charline Covin and Dr. Michael Gross.

Last, but certainly not least, I'd like to thank all my family and friends, especially my family, for their continued support throughout my thesis research.

# **Chapter 1: Introduction**

## **1.1. Objectives**

The overarching objective of this thesis was to investigate age-, sex-, and diabetes-determined differences in human distal sartorius tendon collagen structure and function by use of thermal, thermomechanical, mechanical and microscopy techniques. Thermal and thermomechanical testing was used to assess the structure (crosslinking and molecular packing) of the tendon collagen. Uniaxial tensile testing was used as a proxy to represent a single overload event on a tendon and characterize the subsequent damage to collagen ultrastructure.

## **1.2. Soft Tissue Injuries**

As men and women are encouraged and remain physically active into the geriatric years, changes in soft tissue injuries and healing with age are becoming more important to clinical care. Acute soft tissue injuries derive from sudden traumatic and forceful movements such as an acceleration-deceleration movement, twist or blow to the body that may produce a tear, strain (overextension of a tendon or muscle) or sprain (overextension of a ligament). Meanwhile chronic (overuse) soft tissue injuries are the result of repetitive forceful movements over time<sup>4</sup>. In the U.S. alone, acute sprains, strains and tears accounted for 421,610 days away from work<sup>45</sup>. Moreover, in Canada in 2013/2014, 15% (4.5 million) of Canadians reported overuse injuries due to repetitive strain in addition to the 8.15% (2.45 million) of Canadians that suffered from acute injuries (predominantly sprains)<sup>238</sup>.

Tendinopathy is the term used to encompass both acute (tendinitis) inflammation and chronic (tendinosis) non-inflammatory degenerative events<sup>273</sup>. Histologically, tendinopathy induces disorganization in the collagenous matrix, hypercellularity, and increases in proteoglycan and viscous nonfibrous matrix content<sup>92,131,273</sup>. Chronic microtrauma results in incomplete remodeling that adversely affects mechanical integrity leaving the tendon vulnerable to injury (rupture). Clinical observations have included swelling, pain and reduced range of motion<sup>130,212,229</sup>. Tendinopathy is commonly



observed in frequently strained, high load-bearing tendons (e.g. rotator cuff, Achilles and patellar tendons)<sup>273,278</sup>, and is considered to be facilitated by a multitude of intrinsic and extrinsic risk factors in addition to excessive mechanical loading. Intrinsic factors include genetics, sex, age, metabolic disorders (diabetes mellitus), obesity and biomechanical faults<sup>92,204</sup>. Extrinsic factors include loading pattern, environmental conditions, shoes and equipment<sup>65,212</sup>. Treatment strategies for tendinopathy vary from invasive surgery, exercise, short-term anti-inflammatory drug treatments and most recently cellular-molecular procedures (e.g. growth factors, stem cells)<sup>4,65</sup>.

### **1.3. Tendon Overview**

Tendons are soft multi-unit hierarchical fibrous tissues that are integral to the process of locomotion. The primary function of a tendon is to efficiently transmit high tensile forces generated by muscle contractions to bone to allow control of position and movement of the musculoskeletal system<sup>43,99</sup>. The primary component of tendons is collagen that is aligned in a hierarchical manner parallel to the primary loading axis, affording high tensile strength and stiffness.

#### *1.3.1. Tendon Anatomy & Composition*

Tendons typically appear as brilliant white densely fibrous soft tissues. Tendons are composed of a both cellular and extracellular components. The cellular component primarily consists of fibroblasts (tenoblasts and tenocytes) (95%), which synthesize and provide maintenance of fibers and viscous nonfibrous matrix<sup>82</sup>. The extracellular component includes collagen, elastin, and nonfibrous matrix. The viscous nonfibrous matrix is comprised of proteoglycans, structural glycoproteins and mucopolysaccharides, and water<sup>90,264</sup>. These components provide a basis for a viscous structural support system, allowing for spacing necessary for gliding of the various collagen hierarchy levels and for tissue metabolism<sup>90,211</sup>. Collagen, predominantly type I with minor components of type III and V, makes up 20-30% of the wet weight and 60-80% of the dry weight of a tendon<sup>185</sup>. Elastin and nonfibrous matrix respectively comprise approximately 1-2% of the tendon dry weight<sup>220</sup>. Water accounts for 60-80% of the total wet weight of tendon<sup>82</sup>.

### 1.3.2. Tendon Structure

The hierarchical structure of tendon may be divided into seven levels (Figure 1.1). The smallest structural unit of tendon is the tropocollagen molecule (~1.5 nm in diameter)<sup>202</sup>. Groups of five tropocollagen molecule assemble laterally in a quarter staggered parallel configuration to form a subfibril (~3.5 nm)<sup>18</sup>. Subfibrils form a twisted lattice network and pack together to form fibrils (~50-500 nm)<sup>125</sup>. Owing to the subfibril quarter stagger configuration, fibrils have a characteristic 64-67 nm axial D-banding (Figure 1.2B) pattern dependent on the hydration state<sup>28,68</sup>. Fibrils aggregate together into a fiber (~10-50  $\mu\text{m}$ )<sup>29,73</sup>. Unstrained fibers exhibit a sinusoidal waveform crimp structure<sup>68</sup>. A fiber bundle forms a fascicle (~50-300  $\mu\text{m}$ ) enclosed by endotenon<sup>125</sup>. Endotenon provides vascular, lymphatic and nerve supply to the fiber<sup>124</sup>. Fascicle bundles compose the whole tendon (~1-10mm) bound by a thin areolar connective tissue sheath, the peritendon<sup>263</sup>. The peritendon provides protection and lubrication for gliding of the tendon around structures<sup>82</sup>.

### 1.3.3. Collagen Structure

Collagen type I is a heterotrimeric fibrillar collagen. It consists of two identical  $\alpha\text{I(I)}$  and one  $\alpha\text{II(I)}$  left-handed helical chains of ~1000 amino acids in length<sup>39,217</sup>. The chains are characterized by the repeating amino acid sequence of Glycine-X-Y, where commonly X is proline and Y is post-modified hydroxyproline<sup>59,103</sup>. A glycine as every third amino acid allows for flexibility and close packing of the chain while proline and hydroxyproline provide stability forming intramolecular hydrogen bonds<sup>83</sup>. Three alpha chains form the molecular structure of a right-handed triple helix ~300 nm in length<sup>104</sup>.

In the formation of collagen molecules (Figure 1.2), procollagen is synthesized intracellularly with non-helical telopeptide ends (carboxy-terminal and amino-terminal)<sup>83</sup>. Prior to procollagen being transported extracellularly, post-translation modifications including hydroxylation of lysine and proline and glycosylation of specific hydroxylysines occurs<sup>186</sup>. Following which, the carboxy-terminal and amino-terminal propeptide ends are cleaved off by their respective procollagen C- and N-proteinases<sup>83</sup>.

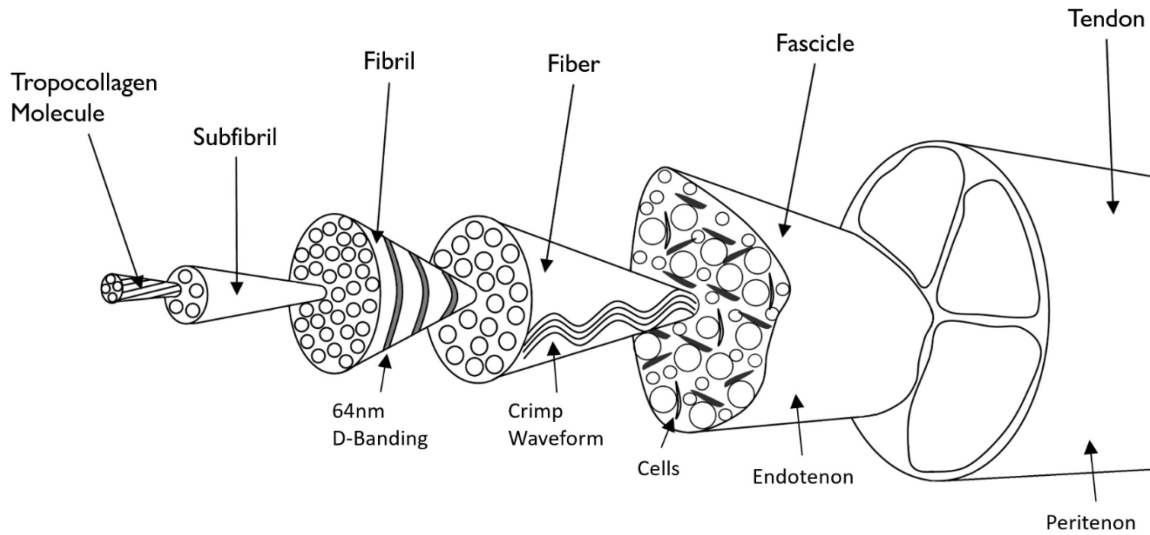


**Figure 1.1** Diagram of the tendon hierarchical structure. . In the present study, experimental testing is performed at the multi-fascicle structural level with scanning electron microscopy used to examine overload damage at the fibril structural level. Figure modified with permission (www.tandfonline.com)<sup>125</sup>.

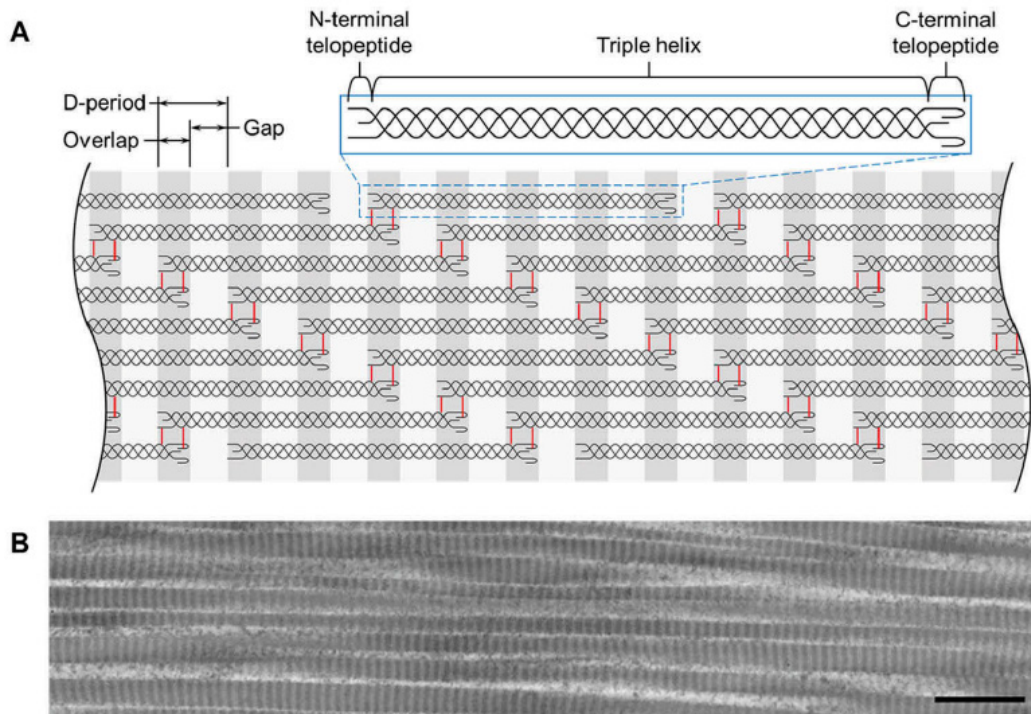


**Figure 1.2** Formation of the collagen fibril and molecule. After cleavage of the procollagen, collagen molecules form a triple helix with an N-terminal peptide and a C-terminal peptide. Collagen molecules are ordered in a quarter stagger arrangement with a D-period of 67nm. Intermolecular crosslinks are shown by the red lines. (B) Transmission electron microscopy image of collagen fibrils from a mouse supraspinatus tendon. (Scale bar = 500nm.) Reprinted with permission<sup>71</sup>.

Lastly, aggregation of molecules and covalent crosslinking occurs as shown in Figure 1.2A with the red lines indicating the location of the covalent crosslinks between molecules.

#### **1.4. Crosslinking of Collagen**

Crosslinking in collagen may occur via two mechanisms (Figure 1.3). The first is precision-controlled enzymatic crosslinking occurring through development and maturation to provide optimized tissue function (Figure 1.3A & B). The second is a non-enzymatic mechanism thought to occur post-maturation, with aging and deleteriously altering tissue function (Figure 1.3C).

#### **1.5. Enzymatic Crosslinking**

Enzymatic covalent crosslink formation in collagen is regulated by the enzyme lysyl oxidase<sup>15</sup>. Lysyl oxidase is a copper metalloenzyme necessary for converting the N- and C- terminal telopeptide lysine and hydroxylysine residues into the aldehydes allysine and hydroxyallysine respectively<sup>63,215</sup>. A telopeptide aldehyde may then react with another telopeptide aldehyde of the same molecule to form an aldol that provides an intramolecular crosslink<sup>20,258</sup>. Similarly, an aldehyde may react in a condensation reaction with the corresponding hydroxylysine or lysine from an adjacent molecule to form an immature, divalent intermolecular covalent crosslink, in a head-to-tail configuration (Figure 1.3A)<sup>74,258</sup>. The type of the crosslinking present in collagenous tissues depends on the extent of post-translational telopeptide lysyl hydroxylation, absolute age and turnover rate<sup>50,74</sup>. Covalent intermolecular crosslinks strengthen the lateral association between neighboring molecules by resisting slippage under tension<sup>266</sup>. Importance of enzymic crosslinking has been demonstrated by inhibition of lysyl oxidase activity under a lathyrictic diet<sup>258</sup>. Tail tendons from lathyrictic rats exhibited attenuated resistance to molecular slippage and decreased strength<sup>106</sup>.

Immature tendons contain both immature aldimine and ketoimine crosslinks. Reaction between allysine and helical lysine or hydroxylysine forms dehydro-hydroxylysinorleucine (deH-HLNL) or dehydro-lysinorleucine (deH-LNL) immature divalent crosslinks respectively<sup>15</sup>. The acid- and thermally-labile immature aldimines are prevalent in both skin and tendon where there is minimal lysine hydroxylation<sup>23,214</sup>. With

maturation, deH-HLNL may react with a histidine residue on an adjacent molecule to form a trivalent histidinohydroxylysinonorleucine (HHL) crosslink<sup>21</sup>. Amadori rearrangement of the Schiff base formed via the reaction of hydroxyallysine and helical lysine or hydroxylysine results in immature divalent hydroxylysino-5-ketonorleucine (HLKNL) or lysino-5-ketonorleucine (LKNL) crosslinks<sup>74</sup>. Predominantly found in bone and cartilage<sup>31</sup>, the immature ketoimine crosslinks are acid- and thermally-stable<sup>258</sup>.

Over time, HLKNL may react with a hydroxyallysine to form a hydroxylysylpyridinoline (Hyl-Pyr) or a lysine to form a hydroxylysyl pyrrole (H-Pyrrole) mature trivalent crosslink<sup>134</sup> (Figure 1.3B). Common trivalent crosslinks in mature tendons are HHL, pyridinolines and pyrroles<sup>185</sup>. With maturation, it has been observed that the level of immature crosslinking remains similar, but the proportion of immature to mature crosslinks decreases<sup>50,275</sup>, perhaps contributing to increases in mechanical strength<sup>15</sup>. The crosslink profile is dependent upon the nature of the tendon and corresponding loading endured *in vivo*<sup>128</sup>. The dominant crosslinks found in the structurally proximate, yet functionally different rabbit forelimb flexor and extensor tendons are ketoimine and aldimine respectively<sup>128</sup>. High load-bearing tendons (Achilles tendon) contain a greater concentration of stable mature crosslinking than do non-weight bearing tendons (e.g. rat tail tendon (RTT))<sup>74,243</sup>.

## 1.6. Advanced Glycation End-Products

Collagen is a long-lived protein that is susceptible to the stochastic formation and accumulation of non-enzymatic advanced glycation end products (AGEs) that occur with aging and diabetes. AGEs may be produced endogenously by metabolic reactions or stimulated exogenously by ingestion of foods and tobacco smoke<sup>108,184</sup>. Endogenous glycation occurring via the Maillard reaction is dependent on the concentration and reactivity of an open chain carbohydrate (typically glucose) and the concentration of specific  $\epsilon$ -amino side chains (e.g. lysine) in proteins (collagen), lipids and nucleic acids<sup>232</sup>. Generally, intracellular sugars (ex. glucose-6-phosphate) have a faster reactivity rate than does glucose, due to its stable ring structure<sup>44,244</sup>. Formation of an AGE may affect only a sole molecule (termed a covalent adduct); however, an adduct may spontaneously react with a neighboring amino side chain to form a covalent

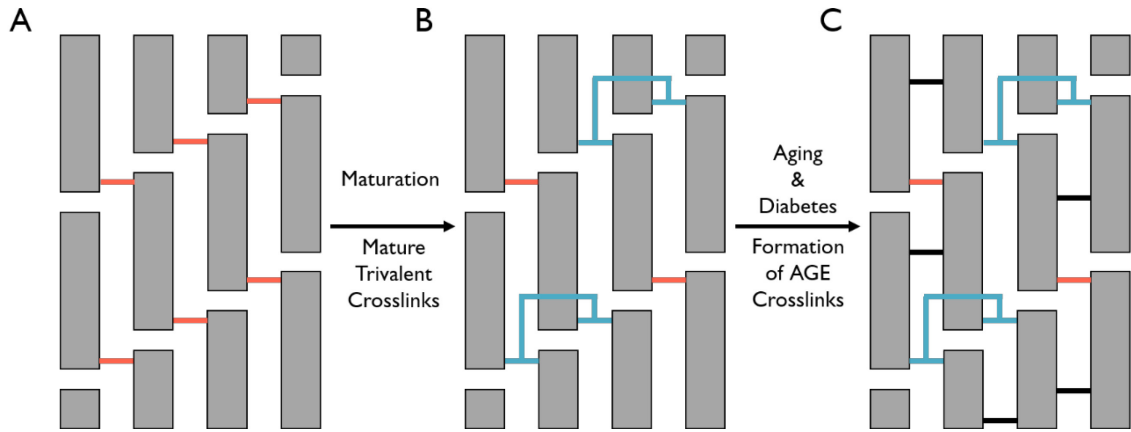


**Figure 1.3 Diagram of enzymatic and non-enzymatic crosslink formation.** An immature starts with immature aldimine and ketoimine divalent crosslinks (red lines) in a head-to-tail configuration. As a tissue matures, the lateral association between neighboring grows tighter with the formation of the mature trivalent crosslinks (blue hooks). With aging and diabetes, adventitious formation of divalent glycation (AGE) crosslinks (black lines) occurs within the triple helical region.

intermolecular crosslink. In contrast to enzymatic crosslinks, AGE crosslinks are thought to form between triple helical regions of adjacent collagen molecules<sup>21,179</sup>. Common intermolecular covalent AGE crosslinks include pentosidine and glucosepane. Pentosidine, a fluorescent biomarker for AGE accumulation<sup>226</sup>, occurs in one per several hundred collagen molecules<sup>16,27</sup>. Accumulation of fluorescent AGEs contributes to the change in appearance of collagenous tissues with aging and diabetes, from a brilliant white to a golden-brown<sup>226</sup>.

Biologically, AGEs disrupt the function of collagen via alteration of molecular conformation and packing, resulting in altered surface charges<sup>19,23</sup>. Thus, changes in cell-cell and cell-matrix interactions may lead to prolonged inflammation and impaired wound healing. Multi-ligand receptors for AGEs (RAGE) are expressed on a variety of cells (e.g. macrophages)<sup>203</sup>. AGE-RAGE interaction induces oxidative stress and activates downstream signaling pathways that lead to the production of pro-inflammatory cytokines, vasoconstriction, prothrombotic gene expression and free radicals (reactive oxygen species)<sup>113</sup>. AGE-RAGE interaction on fibroblasts is thought to modulate collagen production<sup>191</sup>.

Mechanically, non-enzymatic intermolecular crosslinks are thought to increase tendon stiffness, strength and brittleness<sup>13,87</sup>. Due to this increase in brittleness, accumulation of AGEs may be correlated with more mechanically fragile tissue<sup>81</sup>.

Recently, an in vivo study reported Achilles tendon strength (rather than stiffness) being correlated to pentosidine concentration<sup>58</sup>. An in vitro study revealed increasing presence of AGEs induced a pronounced transition in deformation behaviour causing decreased fibre sliding relative to fibre stretching<sup>154</sup>. Furthermore, glycation increases resistance to enzymatic degradation, decreases solubility<sup>128,223,245</sup> and impairs intermolecular receptor recognition<sup>233</sup>. AGEs are thought to be eliminated from the body via enzymatic degradation (proteolytic and lysosomal) and renal excretion<sup>113,233</sup>.

### 1.7. Thermal Stability

Thermal denaturation of collagen occurs with the disruption of the hydrogen bonds and unfolding of the peptide chains, leading to rearrangement of the native triple helix into a near-random coil configuration (Figure 1.4). The thermal stability of the collagen molecule can be thermodynamically quantified using Gibbs free energy, looking at the irreversible rate-governed transition from the native state to the denatured state:

$$\Delta G = \Delta H - T\Delta S \quad (1)$$

Where the enthalpy term ( $\Delta H$ ), measured via DSC, is representative of the net heat contribution from the endothermic (e.g. rupture of the hydrogen bonds) and exothermic reactions (e.g. disruption of hydrophobic reactions) occurring within the collagen triple helix<sup>42</sup>. The entropy term ( $\Delta S$ ), measured via HIT, describes the disorder within a system and physically, the changes in molecular kinetic and intermolecular potential energy (e.g. spatial configuration)<sup>42,151</sup>.

When thermal denaturation occurs, it is thought to commence locally with the scission of hydrogen bonds at the thermally labile domains of the collagen molecule<sup>166</sup>. These domains are characterized by a void of hydroxyproline and are found in the gap region of the quarter-staggered collagen arrangement. In collagen type I, three thermally labile domains are found in a 65-residue length chain near the C-terminus and two regions in the N-terminus 26 residues in length<sup>166</sup>. At the end of each domain is the location of enzymatic crosslink formation. Steric hindrance of the molecules and thermally labile domains occurs by increasing the density of the collagen molecules within the fiber lattice. This results in a decrease in the configuration entropy ( $\Delta S$ ) and increase in the activation energy required to initiate local thermal denaturation in the

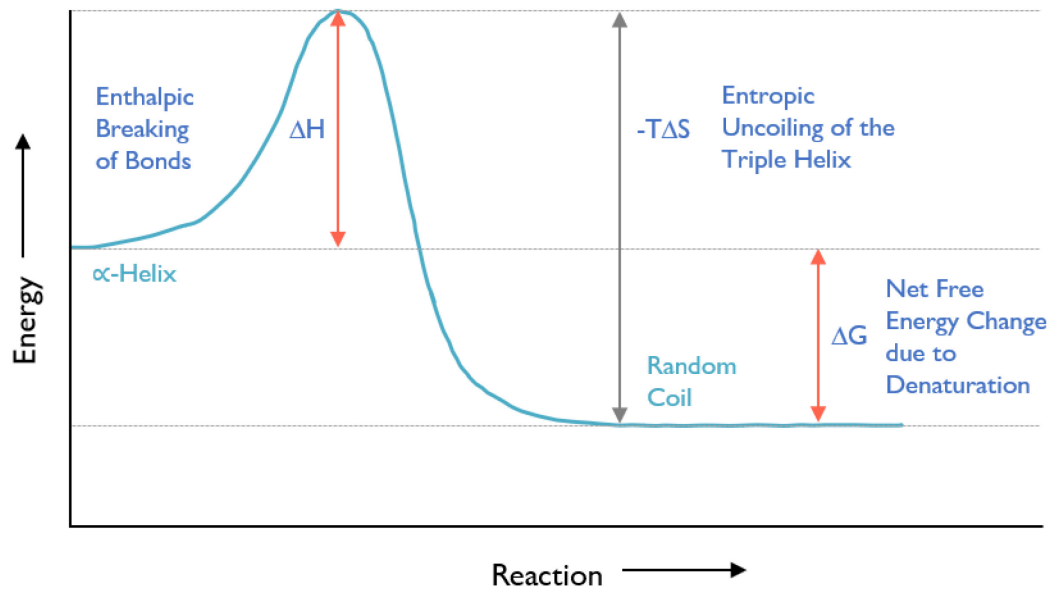


**Figure 1.4 Energy states of collagen denaturation.** Upon denaturation, when sufficient thermal energy has been transferred to overcome the enthalpic activation energy required to rupture the hydrogen bonds, the collagen backbone unravels to a lower energy amorphous random coil configuration state. Modified with permission from J. Michael Lee.

thermally labile domains<sup>169,170</sup>. This description is the essence of the polymer-in-a-box theory<sup>170</sup>. As a comparison, in a dilute solution, the denaturation temperature of the loosely-packed collagen is significantly lower than that of native collagen (fiber-lattice-confined) by  $\sim 27^{\circ}\text{C}$  (slightly above body temperature)<sup>167</sup>. It's been shown that factors including ionic concentration<sup>7</sup>, hydration and crosslinking may affect the denaturation temperature on the order of a few degrees celcius<sup>22,167,168,170</sup>. Differential scanning calorimetry (DSC) and hydrothermal isometric tension (HIT) testing of thermal stability provide a proxy for implicitly evaluating the degree of collagen crosslinking and molecular packing.

### 1.7.1. Differential Scanning Calorimetry

DSC is a powerful technique that allows researchers to follow the kinematics of a thermal transition of a biological molecular system (e.g. collagen). The technique allows for direct measurement of the enthalpy, in particular, the thermal transition in minuscule samples which cannot be mechanically gripped<sup>33,77</sup>. In a DSC set-up, two pans are heated at a constant rate such that the temperatures of the two pans are identical. One of the



sealed pans containing the sample of interest is run against a (generally empty) reference pan. Discrete measurements of the differential heat flow ( $\Delta\dot{Q}$ ) between a sample ( $\dot{Q}_S$ ) and a reference ( $\dot{Q}_R$ ) pan are recorded as a function of temperature and time. Scanning may occur at lower rates to avoid the effects of superheating, produced by the increasing temperature lag between sample and platform<sup>122</sup>.

$$\Delta\dot{Q} = \dot{Q}_S - \dot{Q}_R \quad (2)$$

With linearly increasing temperature, collagen is thought to undergo a melting process, synonymous with the denaturation or unfolding of the triple-helix<sup>170</sup>.

Denaturation results in a characteristic endothermic peak, the area under which is the enthalpy of denaturation (Figure 1.5). The shape of the resultant endotherm provides valuable information on the structure. A narrowed, deeper endotherm represents a more cooperative and homogenous population of activation energies in the bonds that are ruptured. In contrast a broader and shallower peak represents a more heterogeneous population of activation energies of bonds that must be overcome<sup>42</sup>. Be that as it may, DSC typically does not permit the determination of the quantity or type of bonds that exist<sup>77</sup>. As DSC is insensitive to entropic events, it is suggested that it be used in tandem with an alternative technique (HIT) to further evaluate collagen crosslinking and molecular packing.

### 1.7.2. *Hydrothermal Isometric Tension Analysis*

HIT analysis allows for rapid investigation of the alterations in collagen structure during (i) denaturation and (ii) post-denaturation where collagen has been described by Flory *et al.* as being rubber-like<sup>78</sup>. In a HIT set-up, a strip-sample of collagenous tissue is mounted to the apparatus via two grips. The lower grip acts as a fixed mount whereas the upper grip is attached to a force transducer. The samples are isometrically constrained parallel to the primary orientation of the fibers. Thereafter, testing reflects the thermally induced structural changes in the load-bearing collagen. The apparatus is immersed in an aqueous environment (distilled deionized water). The temperature of the water bath, and therefore of the samples are increased from room temperature to 90-97°C at a fixed rate ( $\sim 1^\circ\text{C}/\text{min}$ )<sup>12,149</sup>. The isothermal segment occurs once the desired temperature is reached

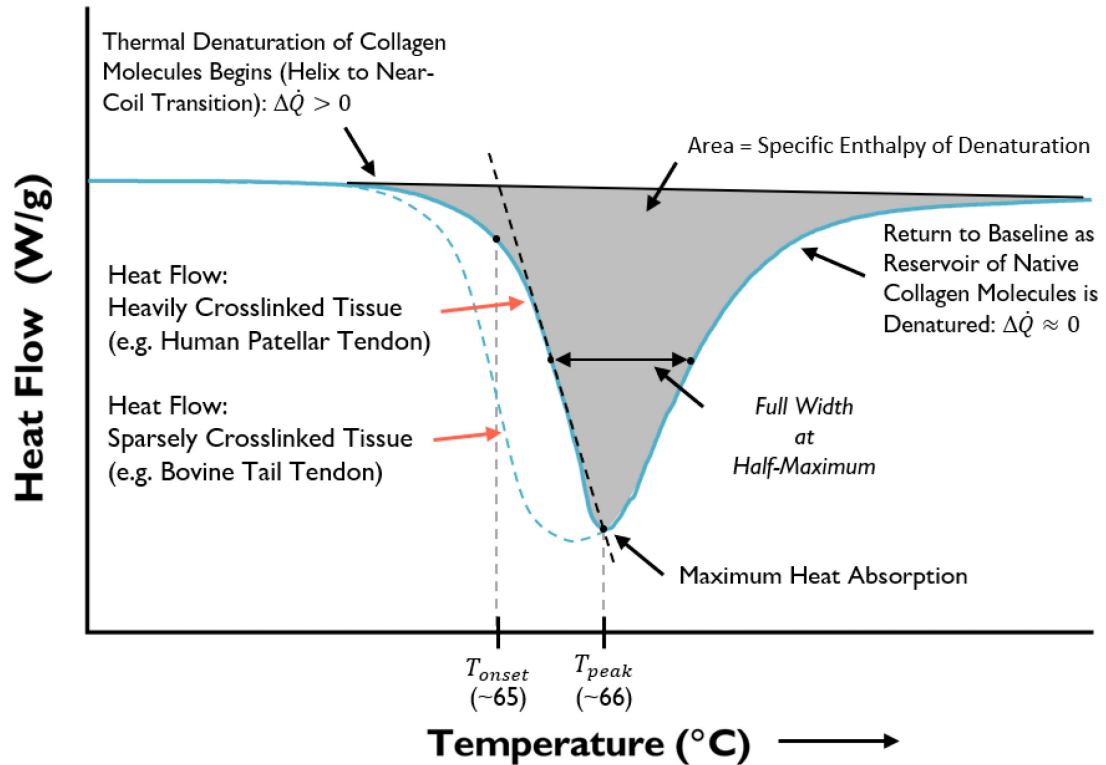
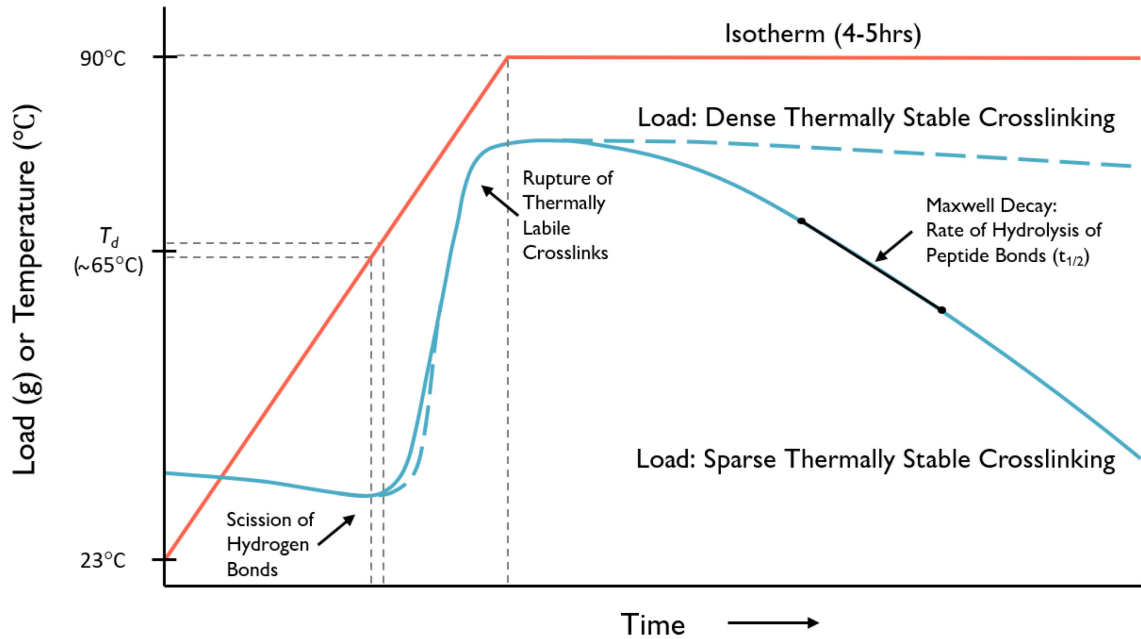


Figure 1.5 DSC testing curve with the differential heat flow between the sample and the reference pan on the y-axis and temperature on the x-axis. The temperature is increased from  $\sim 20^{\circ}\text{C}$  to  $90^{\circ}\text{C}$  at a linear rate of  $5^{\circ}\text{C}/\text{minute}$ . As the temperature increases, thermal denaturation of the collagen molecules occurs causing an increase in heat flow into the sample. The intersection of the linear baseline (solid black line) and tangent line of the heat flow curve (dashed black line) is termed the onset temperature ( $T_{onset}$ ). The temperature at which maximum heat flow into the sample is termed the peak temperature ( $T_{peak}$ ). As the reservoir of native collagen molecules is denatured, the heat flow is reduced, and the curve returns to baseline. The width of the resultant endotherm peak corresponding to the distribution of thermal stabilities is termed the full width at half-maximum (FWHM). The area of the endotherm peak under the linear baseline is the total energy absorbed by the sample during the helix to near-coil transition of the total collagen in the sample, termed the specific enthalpy of denaturation ( $h$ ). The shape and peak of the endotherm may be changed to reflect the degree of the crosslinking as demonstrated by representative curves of a heavily crosslinked tissue (solid blue curve) and a sparsely crosslinked tissue (dashed blue line).

and is held for an extended period of time. The heat-induced tension generated during the process is recorded as a function of temperature and time (Figure 1.6).

Thermally-induced structural alterations assessed include: (i) the denaturation temperature ( $T_d$ ) that is a measure of triple-helix thermal stability and (ii) the rate of load decay ( $t_{1/2}$ ) observed at high isothermal temperatures, a measure of peptide bond hydrolysis and total thermally stable crosslinking (Figure 1.6)<sup>149</sup>.  $T_d$  is reached once sufficient thermal energy has been transferred to the sample to overcome the activation



**Figure 1.6** HIT representative test curves with load (blue curve) or temperature (red curve) on the y axis and time on the x-axis. The temperature is gradually increased from room temperature to 90°C at which point it is held for 4-5 hours, termed the isotherm. At the denaturation temperature ( $T_d$ ), at approximately 65°C, the structure of the collagen triple helix begins the transition to random coil configuration with rupturing of the hydrogen bonds and alpha chains. The grey dashed lines indicate the differences in denaturation temperatures of the respective representative curves. Due to the isometric constraint, the desired shrinkage is registered as an increase in load. Following denaturation, thermally labile crosslinks begin to rupture contributing to pre-isothermal contraction. During the isotherm, stress relaxation causing load decay due to hydrolysis of peptide bonds occurs. Demonstrated by the blue solid and dashed curves, the quantity of load decay that occurs reflects the density of thermally stable crosslinking in a tissue preventing molecular slippage. Modified with permission from J. Michael Lee.

energy barrier to rupture hydrogen bonds and subsequently reconfigure collagen molecules from helix to amorphous coil conformation<sup>33</sup>. Due to the isometric constraints, desired shrinkage is registered as a sharp increase in tensile force as shown in Figure 1.6.

Measurement of  $T_d$  by HIT is representative of the combined thermal stability of the mechanically relevant collagen population<sup>11</sup>.  $T_d$  is thought to be affected primarily by intramolecular crosslinks and secondarily by intermolecular crosslinks<sup>149,266</sup>.

Intramolecular crosslinks contribute to increasing the enthalpic and decreasing the entropic activation energy required by preventing unwinding of the triple-helices<sup>266</sup>.

Intermolecular crosslinks contribute to decreasing the entropic activation energy required by reducing the number of potential molecular conformations and increasing molecular packing<sup>170,266</sup>.

Le Lous *et al.*<sup>144</sup> first described the isometric load decay at near-boiling temperatures by a Maxwellian model. Maxwell-type relaxation is described in detail elsewhere<sup>11,266</sup>, and the equations of which are covered in Section 3.5.2. The presence of mature thermally stable non-reducible intermolecular crosslinks reduces slippage between adjacent collagen molecules, maintaining force transmission under tension in a denatured collagen matrix<sup>266</sup>. Thus,  $t_{1/2}$  may be used as a proxy tool to measure the presence of the thermally labile crosslinks in a given tissue.

Sodium borohydride (NaBH<sub>4</sub>) may be used to stabilize immature reducible thermally labile crosslinks, allowing evaluation of the total crosslinking in a collagenous tissue. Stabilization treatment provide a means of assessing the proportion of thermally labile crosslinks in a given tissue by comparing the values of  $t_{1/2}$  between untreated and NaBH<sub>4</sub>-stabilized samples<sup>181,266</sup>.

## 1.8. Mechanical Behaviour of Tendons

Tendons are tasked with a primary mechanical role of transmitting tensile loads generated by muscular contractions to the skeleton, thereby allowing for smooth motion and stability of joints. Tendon collagen aligned primarily along the axis of tensile load transmission, affords remarkable anisotropic mechanical properties, and acts as a “biological spring”<sup>30,228,280</sup>. Like other collagenous soft tissues (e.g. skin and ligament), tendons exhibit viscoelastic behaviour. Viscoelasticity allows for the tendon to exhibit both compliant and stiff behaviours due to the time-dependent strain sensitivity<sup>2,127</sup>. At higher strain rates, tendons exhibit increased stiffness and load transmission, whereas at lower strain rates they allow for increased extensibility and energy absorption<sup>263</sup>. Time-dependent sensitivity may be attributed to the complex interactions between ECM components, revealed by the viscoelastic behaviour exhibited: stress-relaxation, creep and hysteresis<sup>48,199</sup>. Work done stretching the tendon is stored elastically and the energy input is efficiently recovered (~75-95%) when the tensile loading is removed and the tendon recoils<sup>83,160</sup>. Applied to locomotion, these characteristics results in the conversion of potential and kinetic energy into strain energy under ground reaction impact forces<sup>8,52</sup>. When the foot leaves the ground, tendon elastic recoil allows for the strain energy to be converted into potential and kinetic energy at the end of a gait cycle<sup>9</sup>. The importance of

the high efficiency energy transfer afforded by the elasticity of tendons has been demonstrated in terms of the savings of metabolic energy that would otherwise be required for gait<sup>10,52</sup>.

To simulate tensile behaviour of tendons in vivo, in vitro tensile testing via application of external loads is performed to produce a stress-strain curve (Figure 1.7). The initial phase of the stress-strain curve is the toe region that represents low-stress extensibility<sup>40,140</sup>. In this region the stress-strain curve appears concave towards the load axis. The primary characteristic of this region is the flattening of the collagen fibre crimp<sup>176,209</sup> accompanied by the straightening of fibrillar kinks<sup>171,267</sup>. With increasing strain, collagen fibrils are aligned parallel to the loading axis, leading into the beginning of the linear elastic region where strain and stress are proportional. Linear regression of the curve in this region yields a near constant peak elastic or tissue modulus. The linear region is characterized by longitudinal sliding of neighboring collagen molecules and stretching of the cross-linked telopeptides<sup>79,178</sup>. Connected collagen molecules form the load-bearing core of the collagen fibril<sup>71</sup>. Failure of fibrils with further elongation marks the start of the yield (plastic) region known as the yield point. The yield region displays a non-linear curve shape with plastic behaviour and macroscopic failure<sup>126,283</sup>. Ultimately, the end of the yield region is indicated by loss of structural integrity reflected by a substantial decrease in load: tendon rupture.

Although all tendons share the generic non-linear tensile behaviour described above, differing mechanical requirements alter the structure, composition and corresponding function of tendons. The length of the toe section is dependent on the crimp wavelength of the tissue which typically decreases with age<sup>250</sup>. The length of the yield region may reflect the number of constitutive fascicles and/or degree of crosslinking. A tendon composed of many fascicles or a low density of crosslinking may display an elongated near-zero slope plateau indicating that the rate of structural plastic deformation matches the applied strain<sup>126</sup>. Alternatively, a tendon with few fascicles or a high degree of crosslinking may fail suddenly in a brittle manner as a singular load-bearing unit.

While all tendons store energy upon extension, functionally, it has been suggested that there are been two wide-ranging divisions of tendons: positional and energy-

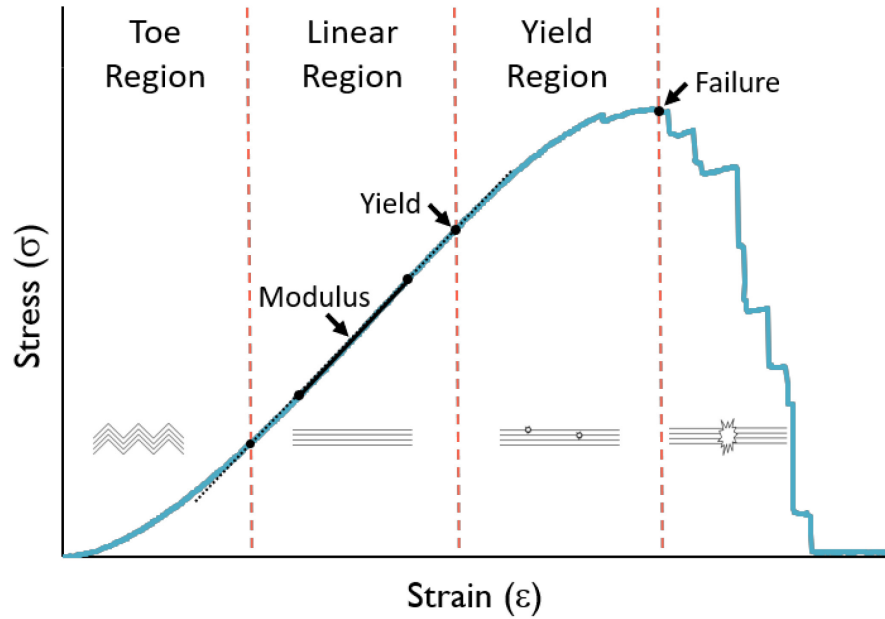


**Figure 1.7 Representative tendon multi-fascicle subsample stress-strain curve displaying the toe, linear and yield regions.**

storing<sup>225</sup>. Positional tendons (ex. common digital extensor tendon) require high stiffness and low extensibility to transmit rapid precision motion. In contrast, energy-storing tendons (e.g. superficial digital flexor, patellar and Achilles tendon) necessitate high strength and extensibility to grant maximal energy transfer under repetitive and high loading conditions<sup>61,228,247</sup>.

### 1.8.1. *In Vitro Mechanical Testing*

In vitro tensile testing of tendons has been performed for over 82 years<sup>61</sup>. Typically, in vitro methods have been performed by means of a tensile tester with the isolated sample being stretched under controlled deformation or load. Resulting deformation and force data are converted to stress and strain upon measurement of the sample length and cross-sectional area (CSA). At the tissue and fascicle scale, methods to accurately determine the CSA of a sample include non-contact techniques (laser micrometry<sup>246,265</sup> and photography<sup>255</sup>).

When testing, improper gripping may lead to slippage or stress-concentrations contributing to overestimates of deformation and underestimates of strength. At the tendon and fascicle level, alternative gripping solutions have been implemented (ex.

direct<sup>282</sup>, serrated jaw<sup>230</sup>, and cryo-gripping<sup>67</sup>) with varying degrees of success. While testing at the tissue scale may ideally probe mechanical properties at a physiological relevant scale, slippage may be exacerbated when testing due to the tendon's inherent geometry (ex. Achilles tendon).

Dissection of the tendon into easily isolated hierarchical substructures (fascicles) provides samples of near-ideal geometry (high aspect ratio) mitigating slippage and stress-concentration<sup>24</sup>. Tensile testing of isolated fascicles also provides the ability to perform multiple experiments (HIT, DSC) and repeated tensile tests to calculate averages and identify local variations of mechanical parameters within a given tendon. Furthermore, it bypasses the laborious dissection procedures (decellularization) and technologically demanding test set-ups required for study of isolated fibrils and collagen molecules.

In general, it is thought that as one progresses down the structural hierarchy that the elastic modulus increases, evidenced by the comparison of modulus values at the tissue (0.3-0.7 GPa) and molecule (0.4-12 GPa) levels<sup>66,286</sup>. Increased modulus may perhaps be attributed to attenuation of complex ECM interactions. Evaluation of the hierarchical structure allows for determination of not only the mechanical response within each hierarchical level, but also investigation of the underlying the complex mechanisms within multi-level load transfer.

## **1.9. Visualizing Modes of Damage**

Light microscopy is used to evaluate fibre-level changes in tendon structure. Histological techniques are advantageous in examination of microscopic structural and cellular changes that occur with aging<sup>159</sup>, diabetes<sup>72,158</sup>, overuse<sup>93</sup>, and rupture of tendon samples<sup>120,157,159,269</sup>. Compared to the ordered structure of unloaded samples, diseased or damaged samples may contain a disordered collagen structure<sup>120,159</sup>, disordered arrangement of fibers<sup>269</sup>, increased matrix deposition or increased cellularity<sup>93,131</sup>. Utilization of polarized light microscopy has revealed key features inherent to tendon extensibility, flexibility and function in vivo (e.g. collagen crimp)<sup>73,209</sup>. The lowest level of hierarchy observed with light microscopy is the collagen fiber<sup>259</sup>. Investigation of the fibrillar and subfibrillar structures require resolution on the magnitude of the nanoscale.

Nanoscale fibrillar structure may be examined using x-ray diffraction and/or electron microscopy techniques. X-ray diffraction is a powerful tool for investigating the axial and lateral packing of collagen allowing observation of particles less than  $20\text{\AA}$ <sup>29,267</sup>. X-ray diffraction has been used to study how aging<sup>29,126,182</sup>, diabetes and glycation<sup>118,244</sup> affects the crystallographic fibril structure in tendons. X-ray diffraction studies revealed diabetes-induced axial structure and lateral packing of collagen molecules alterations in human toe extensor tendons<sup>118</sup>. An advantage of X-ray and synchrotron radiation is simultaneous observation of intra-fibrillar deformation mechanisms during uniaxial overload testing<sup>79,171,222</sup>.

Electron microscopy has been similarly used to directly examine fibrillar structures. Transmission electron microscopy (TEM) used for ultrastructural examination requires thin sections of intact specimens stained with heavy metals, requiring meticulous preparation<sup>111,217</sup>. Investigations using TEM to identify collagen fibrillar deformation mechanisms post-yield in rat tail tendons (RTT) revealed a common motif: shredding and dissociation of fibrils into their subfibrillar components<sup>133,183,250</sup>. The dissociation of fibrils (Figure 1.8) was exhibited in both the transverse and longitudinal axes<sup>133,249</sup>. Repeated subrupture and rupture overloading produced dissociation of fibrils into fine substructure<sup>249,250</sup>. TEM examination revealed a second motif of severely bent or kink-like deformation of fibrils (Figure 1.9) observed in RTT<sup>123,183,249</sup> and human Achilles tendon<sup>164</sup>. It's possible that the fibril damage motifs of dissociation and kinking may be dependent on the crosslink density of the tissues which restrict intrafibrillar sliding.

### 1.9.1. *Discrete Plasticity*

In the Tissue Mechanics Lab through the years, discrete plasticity has been studied and described as a kinking/toughening mechanism in mechanically overloaded collagen fibrils that provides absorption of strain energy<sup>254,255,256,257</sup>. This characteristic structural motif is thought to be a toughening mechanism by which formation of discrete zones of plastic deformation containing denatured collagen molecules is accompanied by the loss of the native D-banding along fibril surface at and between the discrete plasticity kink sites<sup>257</sup>. The presence of the nanoscale damage previously observed in RTT<sup>183,249</sup> was confirmed in the bovine tail tendon model (BTT)<sup>257</sup>. The following sections describe



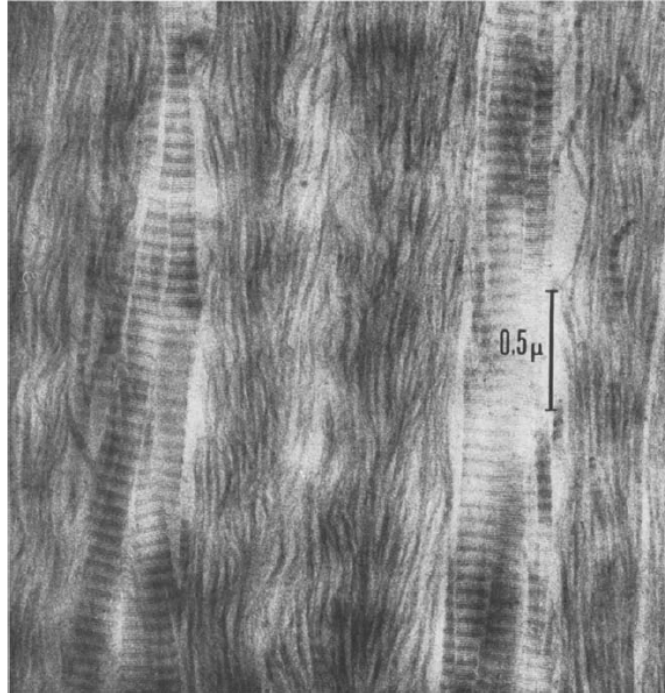


**Figure 1.8 TEM micrograph of a longitudinal section of 5-week-old rat tail tendon collagen fibrils overloaded to 7% strain at 14,000x. (Scale bar = 0.5 μm) Reprinted with permission<sup>183</sup>.**

models that have been used in the characterization of collagen damage in vitro via mechanical overload testing.

### 1.9.2. Bovine Tail Tendon Model

Much of the work to date on discrete plasticity has been performed on a BTT model. In preliminary studies, BTT were mechanical overloaded to rupture, with subsequent digestion of the denatured collagen via the serine proteases acetyltrypsin and  $\alpha$ -chymotrypsin<sup>277</sup>. Study results showed an increase in proteolysis of collagen thought to be due to micro-unfolding of overloaded collagen molecules, prompting further investigation by means of scanning electron microscopy (SEM)<sup>277</sup>.

In the first study by Veres *et al.*, mechanical overload to rupture of bovine tail tendons was performed and induced damage observed via SEM<sup>257</sup>. This technique was used to explore how overload alters conformation of the constituent collagen molecules and structure of the fibrils. Three sample groups were utilized and compared, a control group of samples, a mechanically overloaded group and a digested, mechanically overloaded

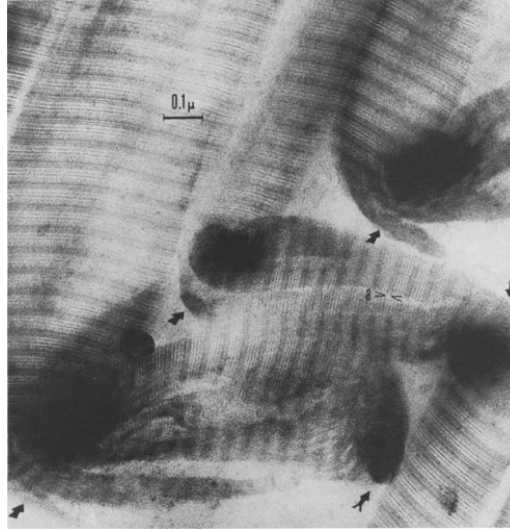


Figure 1.9 TEM image of transverse section at 38,000x magnification displaying the formation of multiple kink deformations in neighboring 39-month old rat tail tendon fibrils overloaded to 4% strain indicated by the black arrows. Furthermore, dissociation of subfibrillar components and intact D-banding prior to kink sites is observed. (Scale bar = 0.1  $\mu\text{m}$ ) Reprinted with permission<sup>183</sup>.

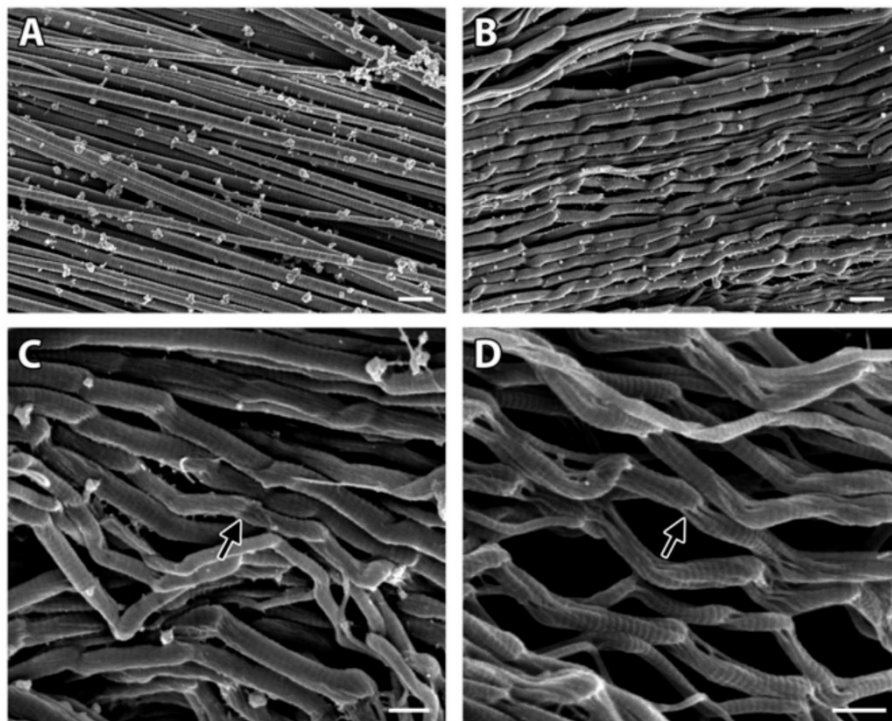


Figure 1.10 SEM images of (A) undamaged and (B, C & D) damaged collagen fibrils . Damaged fibrils exhibited regions of the damage motif “Discrete Plasticity”, the repetitive kinking morphology with loss of D-banding at the kink sites. SEM micrograph (D) of the trypsin incubated BTT shows voids (indicated by the black arrow) where denatured collagen has been removed. (Panel A and B: Scale bar = 500 nm, Panel C and D: Scale bar = 300 nm) Reprinted with permission<sup>257</sup>.

group (Figure 1.10). Serine proteases similar to those used by Willett *et al.*<sup>277</sup> were used in the digestion of denatured collagen<sup>257,277</sup>.

The undigested mechanical overload group showed serial zones of pronounced plasticity longitudinally along fibrils, a feature absent in the control group. Selective molecular denaturation was displayed as repeating kink sites with heterogenous inter-kink spacing with an approximate minimum of 300 nm<sup>257</sup>. The frequency of the kink sites increased with subrupture cyclical loading<sup>255</sup>, thought to be a consequence of heterogeneity in structure and loading of fibrils and subfibrils. Between kink sites, it was observed that at times D-banding striations were not visible on the fibril surface, that being covered by a fuzzy surface layer of denatured collagen<sup>257</sup>.

In the digested mechanical overload group, both the kink locations and the interkink surface layer were subject to enzymolysis, removing apparently denatured collagen. In the former, the previously dense appearing kink locations were filled with voids, leaving sparse undamaged collagen subfibrils. The D-banding on these subfibrils was conserved<sup>257</sup>. In the latter, the surface layer of denatured collagen in each specimen was digested, rendering the underlying D-banding striations visible. In a separate study, the authors set to determine whether phagocytes can recognize and target strain-damaged collagen fibrils that displayed characteristics of discrete plasticity. Macrophage-like U937 cells were cultured on exposed internal surfaces of both control and overloaded tendons<sup>253</sup>. The cells preferentially degraded damaged collagen fibrils displaying characteristics of discrete plasticity, and were found to have elongated and ruffled membranes in the presence of damage. Results indicate that U937 macrophage-like cells were able to discriminate between damaged and undamaged fibrils, altering their functional morphology in the presence of collagen fibril damage.

Furthermore, *in vitro* ribose incubation of BTT was performed for 28 days to simulate the accumulation of long-term AGE crosslinking. The purpose of the investigation was to observe if the high degree of AGE crosslinking would suppress intermolecular sliding thought to consequently induce discrete plasticity damage. Ribose crosslinking induced more brittle behaviour under tensile testing and a higher degree of thermal stability evaluated by DSC (Figure 1.11). SEM confirmed that changes in mechanical behaviour and thermal behaviour were reflected by inhibition of the discrete

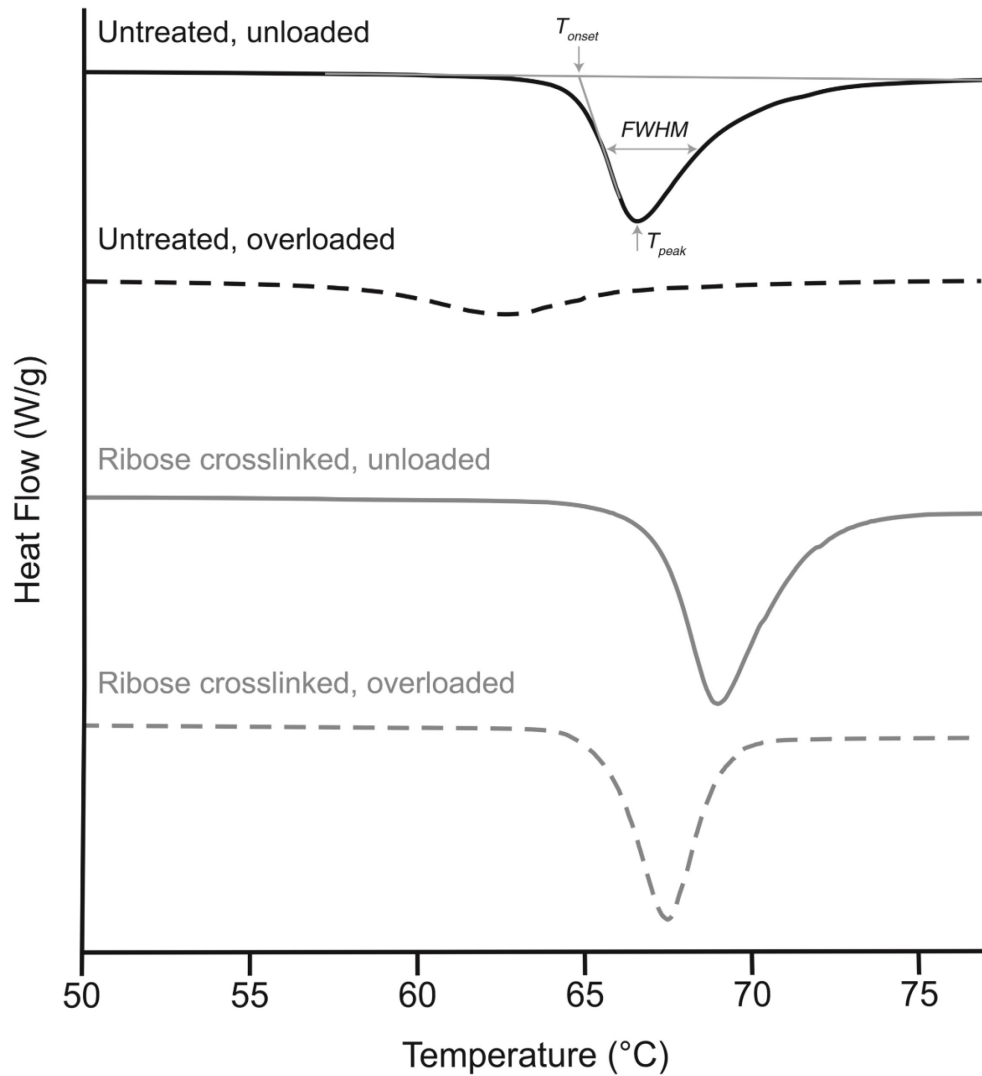


**Figure 1.11 Thermal stability of BTT collagen evaluated using DSC. Ribose incubation (grey curves) increased the thermal stability of the unloaded BTT collagen (shifted endotherm peak to the right) and reduced the impact of mechanical subrupture overload testing (grey dashed curve) in destabilizing the collagen molecule (decreased thermal stability). Reprinted with permission<sup>150</sup>.**

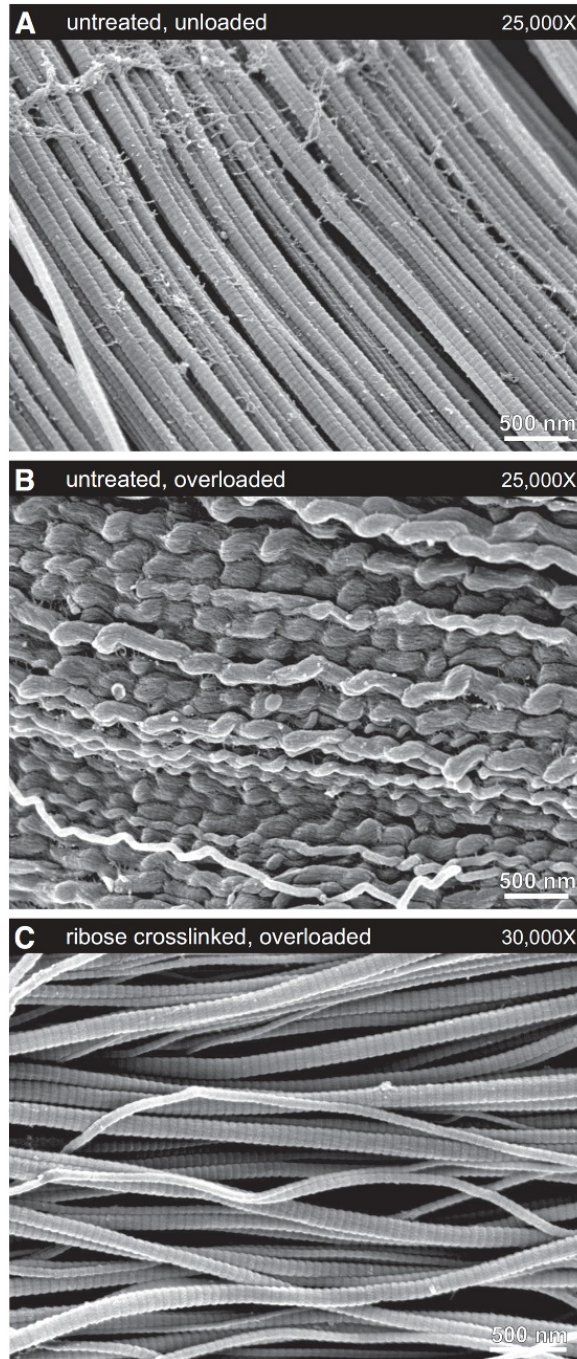


**Figure 1.12 SEM micrographs of collagen fibrils demonstrating differences in overload response to in vitro ribose incubation. (A) Untreated and unloaded collagen fibrils reveal absence of damage. (B) Untreated, overloaded collagen fibrils display discrete plasticity. (C) Ribose crosslinking in overloaded fibrils suppresses the formation of discrete plasticity. (Scale bars = 500 nm) Reprinted with permission<sup>150</sup>.**

plasticity failure mechanism in the ribose-crosslinked BTT (Figure 1.12C)<sup>150</sup>. The results are indicative of a pathological suppression of discrete plasticity, thought to be an important physiological mechanism in tissue remodeling, that may occur in humans with dense crosslinking due to aging or diabetes.

The interior structure of decellularized collagen type I fibrils extracted from unloaded and subrupture-overloaded BTT were also probed using AFM (Figure 1.13)<sup>24</sup>. Dehydrated unloaded control fibrils displayed intact D-banding and undisturbed morphology<sup>26</sup>. Overloaded fibrils revealed the discrete plasticity damage motif with a kinked and twisted morphology<sup>24</sup>. D-banding was absent at the turn and kink sites, but recovered between kink sites as previously seen with SEM<sup>257</sup>. When fibrils were hydrated, significant swelling occurred, providing difficulties in observing the D-banding in both control and overload samples. Hydrated control images similarly revealed an undisturbed morphology and intact D-banding (Figure 1.13A). Hydrated overload samples revealed a swollen highly penetrable shell layer overlaying the collagen fibril in which kink sites were visible (Figure 1.13B & C)<sup>24</sup>. Most recently, AFM has been used to investigate the role of matrix metallo-proteinases (MMP-2 and MMP-9) located in vivo and their role in wound healing on collagen fibrils from overloaded BTTs exhibiting the toughening mechanism discrete plasticity<sup>25</sup>. It was found that the enzyme MMP-9 was able to selectively cleave the shell of non-D-banded material from the overloaded collagen fibrils (Figure 1.14D). Thus, further supporting the role of the toughening mechanism discrete plasticity as a marker of collagen fibril damage in the process of tendon remodeling in vivo.

### 1.9.3. Bovine Forelimb Model

In a study performed by Herod *et al.*<sup>109</sup>, the discrete plasticity work was expanded to a bovine forelimb model. Drawing on previous literature<sup>208,228</sup>, this model compared two structurally proximate but functionally distinct tendons, the energy storing superficial digital flexor (SDFT) and the positional common digital extensor tendon (CDET). With significant differences in crosslinking identified via DSC and HIT testing, differences in the presence of discrete plasticity were observed upon SEM examination (Figure 1.15). In the more thermally stable crosslinked SDFT, as identified by  $t_{1/2}$ , when mechanically

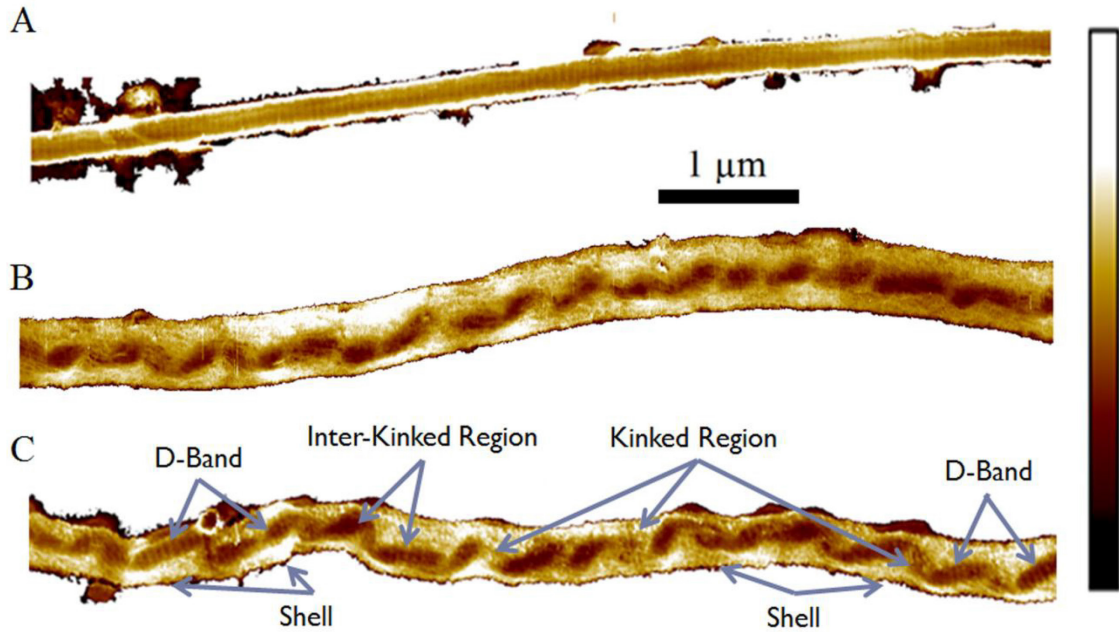


**Figure 1.13** AFM deformation images of a native bovine tail tendon fibrils. Image A displays hydrated control fibril exhibiting undisturbed intact D-banding and Images B & C display hydrated damaged fibrils. (B) Hydrated damaged fibril displayed kinking regions and a loss of observable D-banding due to the swelling. (C) A swollen damaged fibril revealed (1) kinked regions, (2) a penetrable shell layering, and (3) D-banding present in the inter-kinked regions, all of which are identified by the grey arrows. Intensity bar indicates the deformation depth. (Scale bar = 1 μm) Reprinted with permission<sup>24</sup>.

overloaded to rupture, discrete plasticity was rarely observed using SEM. In contrast, the less thermally stable crosslinked CDET, when mechanically overloaded to rupture, resulted in discrete plasticity damage present in the form of dense serial kinking containing disrupted or broken fibrils throughout as observed using SEM<sup>109</sup>. Differences in fibril mechanics and damage motifs between functionally distinct bovine forelimbs were confirmed via AFM<sup>200</sup>, likely the result of differences in kinking containing disrupted or broken fibrils throughout as observed using intermolecular crosslinking<sup>109</sup>. AFM, second harmonic generation (SHG) imaging and confocal microscopy revealed upon rupture, an absence of fibrillar plasticity damage was observed in the SDFT, whereas kink formation and denaturation along the length of the CDET collagen fibrils occurred, matching the behaviour observed via SEM<sup>109,200</sup>.

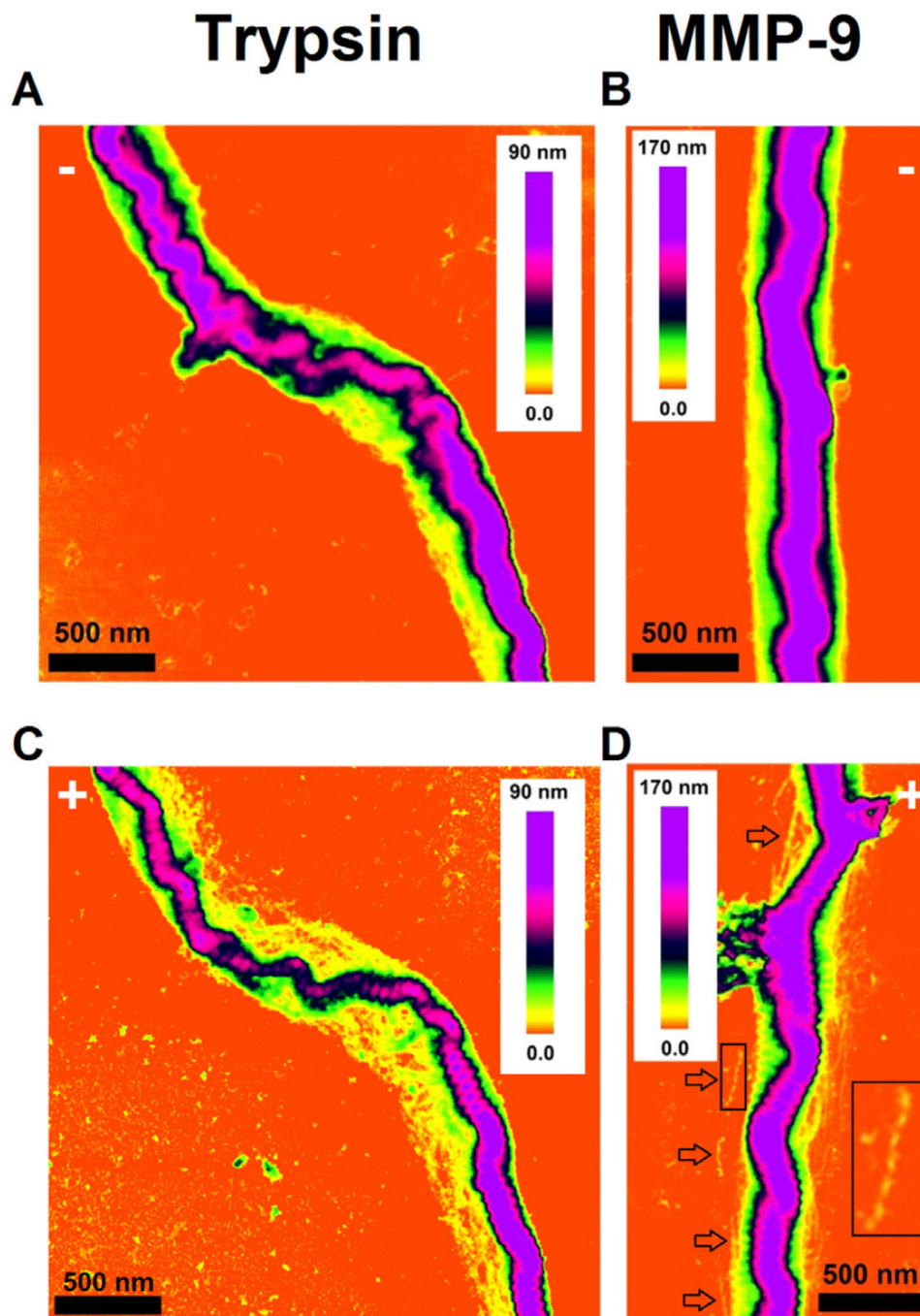
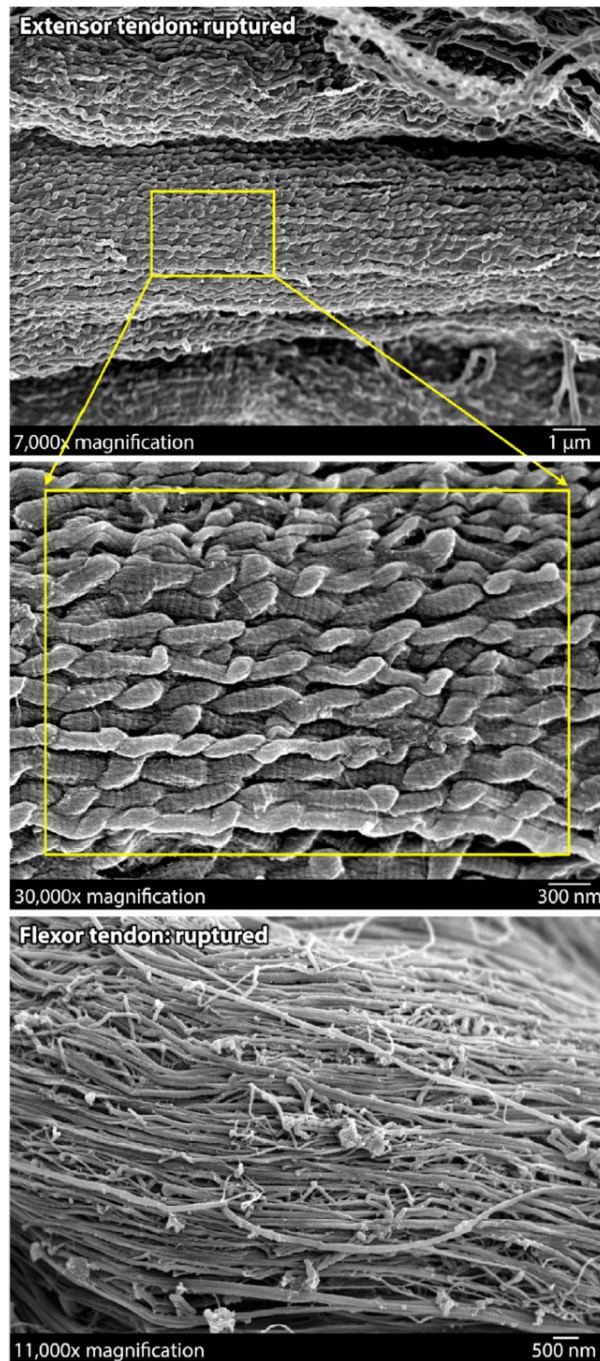


Figure 1.14 AFM deformation maps of BTT collagen fibrils exhibiting discrete plasticity before (A, B) and after (C, D) incubation with MMP-9 (D) and trypsin (C). (D) MMP-9 selectively removes the denatured collagen shell leaving the remaining collagen with D-banding intact in compared to (C) non-specific removal of denatured collagen with trypsin incubation. (Scale bar = 500 nm) Reprinted with permission<sup>25</sup>.





**Figure 1.15 SEM micrographs displaying the difference in overload damaged tendon collagen from the bovine CDET (Top, Middle) and SDFT (Bottom). In the CDET, dense regions of discrete plasticity were observed, whereas in the SDFT discrete plasticity was sparsely observed. This difference in damage mechanisms are likely the result of changes in crosslinking profile between the two structurally proximate but functionally different tendons. Reprinted with permission<sup>109</sup>.**

#### 1.9.4. *Human Distal Sartorius Tendon*

Most recently, discovery of the discrete plasticity toughening mechanism in the bovine model begged the question of whether discrete plasticity would be observed in a more physiologically relevant human model. Human distal sartorius tendons were collected from a local tissue bank (NSHA Regional Tissue Bank, Halifax, N.S.) from non-diabetic donors ranging in age from 20-60 years<sup>237</sup>. Unloaded sartorius tendon samples examined via SEM showed intact D-banding in registry across tightly packed fibril bundles and relatively homogenous fibril diameters. Examination of tendon samples subject to mechanical overload to rupture, revealed an absence of discrete plasticity in both younger and older tendon donors. Although sparse sites of fibrillar plasticity damage were observed, the quantity and density of the damage observed in the human tendons was far less than that found in the bovine tendons. Macroscopic observation of structure revealed a highly disrupted and disorganized structure. Fibrillar level damage revealed motifs of high energy elastic recoil damage. Damage motifs included balled and bundled fibrils, multiple hairpin turns, and kinks with slight loss of D-banding striation only at the turn sites. There was no supporting evidence for age dependent damage motifs. Within the human sartorius tendon, the notion of dense thermally stable crosslinking was evidenced by the high denaturation temperatures (DSC/HIT) and an absence of HIT isothermal load decay. Furthermore, in the human sartorius tendon, similar to the bovine SDFT<sup>109</sup> and in vitro glycated BTT<sup>150</sup>, that the toughening mechanism discrete plasticity may be suppressed in heavily crosslinked tissues.

#### **1.10. Age-Determined Changes in Tendons**

Aging is a non-pathological process that results in the progressive loss of physical function and ability. The rate of aging is highly individual, with influencing factors including lifestyle, disease (ex. diabetes), genetics, injuries and hormonal changes<sup>165</sup>. The present study focuses on the age-related alterations in tendons that occur from maturation, through adulthood, and into geriatric age. In a society that is physically active into geriatric life, it is important to consider soft tissue aging and the corresponding increase in injuries. Anatomical location and the absolute age of the tissue components

are two factors that contribute to the age-related changes observed in tendon structure and function. For example, AGE accumulation may have a more prominent influence over the lifespan of a human (~80 years<sup>239</sup>) versus a smaller animal (ex. mice: ~1-5 years)<sup>175</sup>. In aging human patellar tendon the concentration of pentosidine was found to increase seven-fold<sup>56</sup>. Although changes in structure, composition and mechanics have been identified, the underlying mechanisms behind aging in tendons are, to date, not well understood.

#### 1.10.1. *Structural and Compositional Changes in Aging Tendons*

Alterations in tendon structure and composition occurs with aging in both humans and animals, potentially influencing the function of the tissue. Evidence in thoroughbred horses suggests that structural changes in tendon occur predominantly during maturation, and only minimally with further aging<sup>195</sup>. Important structural changes in human tendons with aging, that potentially lead to changes in function, include both the cross-sectional area (CSA) and collagen fiber crimp. Previous studies in humans have found that the patellar and Achilles tendon CSA increases<sup>161,240</sup>, remains unchanged<sup>51,56,227</sup>, and decreases<sup>189</sup> with aging. However, these changes or lack thereof may be in part modulated by the physical activity level of the individual<sup>57,272</sup>, seemingly as an adaptive response to changes in average stresses without altering the material properties. CSA aside, collagen fiber crimp wavelength in the Achilles tendon has been found to increase with age<sup>241</sup>.

Changes in tendon composition with aging has been identified in terms of cellular, ECM and nonfibrous matrix components. In aging tendons, the quantity and volume density of cells (fibroblast and tenocytes) decreases accompanied by changes in morphology and function<sup>242</sup>. The ability of the cell to synthesize proteins decreases with age, attributing to the reduced collagen turnover rate<sup>107,130</sup>. The reduction in collagen turnover rate is further supported by evidence of the absolute collagen content remaining relatively unchanged<sup>57</sup> and decreasing<sup>56</sup> in the human patellar tendon. Some changes in animal and human tendons have been reported in relation to the volume fraction<sup>194,250,281</sup> and distribution of diameters of tendon collagen fibrils<sup>193,241</sup>. However, the effect of aging

on the collagen molecular packing remains unclear, as contrasting studies have found both increased<sup>88,182</sup> and unchanged<sup>118</sup> spacing.

With aging, formation of AGE crosslinking occurs adventitiously and appears to contribute to surprising increases in molecular spacing<sup>135,248</sup>, resistance to enzymatic degradation<sup>118,182</sup> and tissue dehydration. Extracellular water content has been observed to dramatically decrease with maturation, and to a lesser extent with further aging<sup>5,228,252</sup>, modulated in part by a decrease in mucopolysaccharides<sup>5,114,217</sup>. Evidence of changes in MRI signal intensity in the imaging human patellar tendons in vivo suggests that ultrastructural age-related changes in tendons does occur<sup>51</sup>. Overall, the influence of age on tendon composition and structure is unclear; nonetheless it appears to produce a heavily crosslinked, decreasingly cellular, and dehydrated tendon.

#### 1.10.2. *Alterations in Tendon Mechanics with Aging*

With conflicting reports of compositional and structural changes in the literature, it is also not clear how the mechanics of tendons are altered with aging. Consensus across in vivo and in vitro studies in human tendons<sup>57,112,210</sup>, primarily focusing on the patellar tendon<sup>51,56,105,121</sup>, is that tendon mechanics remain more or less unchanged through adulthood. Minor decreases in modulus and tensile strength are observed, while extensibility and toughness remain unchanged. Biomechanical properties derived from in vivo testing, which is commonly performed using ultrasound to measure deformation, and dynamometry to measure forces<sup>66</sup>, depends on the maximum voluntary muscular contraction (MVC) of the individual. The portion of the stress-strain curve that can be probed by this technique is thus determined by the force exerted on the tendon. Furthermore, individual variability in human tendon mechanics with aging is multifactorial, as previously mentioned (disease, diet, injury history, exercise).

### 1.11. **Sex-Determined Changes in Tendons**

Sex-determined differences in the rate of injuries, mechanics and structure of tendons have been reported, with differences in soft tissue injury rates between sexes seemingly related to age, sex hormone concentrations, neuromuscular balance, biomechanics and anatomical location<sup>3,92,213</sup>. In the case of ligament injuries, it has been

seen in females that there is a greater frequency in anterior cruciate ligament (ACL) ruptures and ankle sprains, especially in young females<sup>115,129,198</sup>. Males have a higher occurrence of Achilles tendon ruptures<sup>102,192,262</sup>. In post-menopausal aging, the sex-discrepancy is reduced<sup>156</sup>, perhaps due to comparable levels of estrogen<sup>234</sup>. Contradictory studies have found that soft tissue injury rate is either increased in males<sup>17,70</sup> or independent of sex<sup>75,115,219</sup>. Overall, sex-determined differences in overall soft tissue injury rate remain inconclusive<sup>92,115,119,197</sup>. In sports, factors independent of sex, including activity type, exposure time, and environment, may regulate the frequency of soft tissue injuries<sup>17,115,119,213</sup>.

#### 1.11.1. *Sex-Determined Changes in Tendon Structure and Mechanics*

With inconsistent findings in sex-determined tendon injury rates, structural studies based on lower limb tendons of both animals and humans are beginning to accumulate. In the animal Achilles and human patellar tendons, changes in ECM composition (collagen type I, type III) and nonfibrous matrix (major proteoglycan content) components have been found to be independent of sex<sup>152,192,221</sup>. However, the total collagen dry weight and total collagen content per wet weight have been found to be lower in human female patellar tendons<sup>152</sup>, perhaps the result of a lowered collagen synthesis rate<sup>162</sup>. In support of the changes in ECM synthesis rates observed in the human patellar tendon, the CSA of lower limb tendons have been consistently smaller<sup>80,138,190,240</sup>, with an attenuation or absence of tendon hypertrophy (increased CSA) in response to frequent training/physical activity in females<sup>152,162,227</sup>. To the authors knowledge, no studies have investigated the sex-determined changes in molecular packing and crosslinking in either animal or human tendons which may help to explain potential changes in tendon mechanics.

In humans, both in vivo and in vitro studies have reported conflicting sex-determined differences in tendon mechanics. In the Achilles tendon, in vivo studies have shown the tendon modulus to be higher in males<sup>46,138,240</sup>, consistent with in vitro tensile testing findings of increased modulus and strength of isolated fascicles<sup>162</sup>. Likewise in patellar tendon studies, modulus has been found to be dependent<sup>110</sup> and independent<sup>187,190,268</sup> of an individual's sex. It may be possible that rather than sex, lower

limb tendon mechanics may be determined by muscle contraction force<sup>51,177,180</sup> and tendon mass density<sup>105</sup>. In general, female lower limb tendons have been found to have greater energy efficiency<sup>80,102,138</sup> and extensibility in vivo<sup>51,138,190</sup>, which may increase the susceptibility to injury. With inconsistent findings in tendon structure and mechanics, further in-depth studies of sex-determined differences in baseline tendon properties could lead to sex-specific training strategies and treatment of tendon injuries.

### **1.12. Diabetes Mellitus-Determined Changes in Tendons**

Diabetes mellitus (DM) is one of the most prevalent diseases around the world, with approximately 415 million people worldwide suffering from diabetes mellitus as of 2015, and the number expected to rise to 615 million by 2040<sup>53</sup>. Clinically, there are two distinct types of diabetes. Type I (juvenile) diabetes occurs due autoimmune elimination of insulin-producing beta islet cells of the pancreas, resulting in little to no insulin production. Type II diabetes, present in 91% of diabetic adults<sup>53</sup>, occurs when bodily resistance to insulin is increased, thus, insufficient quantities of insulin are endogenously produced<sup>235</sup>. Insulin is a hormone that upregulates the transport of glucose in the blood to muscle and fat cells. The burdensome nature of diabetes may lead to poor regulation of glucose levels in the blood stream causing extended periods of hyperglycemia. Increased extracellular glucose may lead to musculoskeletal degeneration amongst other complications<sup>53,96,235</sup>. Accumulation of AGEs due to aging is thought to be accelerated with diabetes (hyperglycemia)<sup>101,135</sup>.

Previous clinical studies have suggested diabetes has deleterious effects on native connective tissue (e.g. limited joint mobility)<sup>49,216</sup>. Tendon pathological changes are evidenced by an increased risk of tendon ruptures requiring hospitalization<sup>284</sup> and increased rate of tendinopathy (3.67:1)<sup>204</sup>. Obesity, an independent risk factor for tendon disorders is a common comorbidity of type II diabetes<sup>3,86</sup>. Therefore, obesity likely contributes to changes in tendon pathology and incidence of tendinopathy by increased loading and biochemical changes, further highlighting the importance of exercise in the management of diabetes.

### 1.12.1. *Diabetes Mellitus-Determined Changes in Tendon Structure and Mechanics*

Clinical studies have been performed to reveal diabetes mellitus-related changes in structure of a variety of human tendons (e.g. Achilles, rotator cuff). These have included both ex-vivo (histology/EM) and in vivo (ultrasound/MRI) studies. Most strikingly, diabetic tendons were characterized by a loss of their typical brilliant pearl white appearance<sup>155,231</sup> and frequent occurrences of structural abnormalities<sup>64</sup>. Structural abnormalities reported include twisted, curved and disorganized collagen ultrastructure (fibers and fibrils)<sup>64,95,98</sup>. Moreover, significant increases in tendon thickness and/or volume<sup>1,6,38,60,62</sup> have been observed. Similar structural changes were observed in a pair of reviews on induced diabetic rat models, predominantly examining the Achilles tendon<sup>188,231</sup>. Clinically, Achilles tendon shortening and strain attenuation have been reported in diabetic individuals<sup>60,62,64</sup>, possibly due to increased stiffness as observed in vivo<sup>58,196</sup>. Changes in mechanics in vivo would contribute to a higher metabolic cost for locomotion. In vitro, Guney *et al.*<sup>98</sup> reported inferior Achilles tendon mechanics (modulus, strength and toughness) in diabetic individuals. Additional factors that may affect diabetic tendon mechanics include accelerated tenocyte senescence<sup>3</sup>, decreased PG content<sup>47</sup>, and reduced healing capacity<sup>236</sup>. These factors may be explained by the elevated AGE accumulation within tissues during diabetes<sup>218,261</sup>. The underlying mechanisms in vivo behind diabetes-related changes in tendon structure and mechanics in humans remains inconclusive.

## Chapter 2: Thesis Rationale, Objectives and Hypotheses

### 2.1. Overview

As men and women are remaining physically active later in life, the prevalence of soft tissue injuries and need for healing are becoming of importance to clinical care. Aging has been found in the literature to produce a less crimped, more heavily (formation of AGEs) crosslinked, decreasingly cellular and dehydrated tendon. However, these changes in tendon structure are not reflected by consistent changes in mechanics throughout adulthood in humans, in part due to the degeneration of muscle mass, strength and physical activity levels with age. Considering the variable of sex of the individual/donor, differences in soft tissue injury rates between groups are based on a multitude of factors (e.g. anatomical location) are not explained by the inconsistencies in tendon structure and mechanics across the literature. Meanwhile in diabetic individuals, a disease with a hallmark of hyperglycemia, the rate of tendinopathy has been found to increase by nearly four-fold<sup>204</sup>, possibly due to the impact of impaired tendon remodeling on tendon structure and mechanics.

In the Tissue Mechanics Lab over the years, the toughening mechanism of discrete plasticity was first uncovered in overload damaged BTT<sup>257</sup>. Using SEM, the primary damage motifs identified included serial kinking along collagen fibrils and a loss of D-banding between and at kink locations, supporting previous studies of RTT<sup>183,250</sup>. This model was then extended into a bovine forelimb model in which structurally proximate but functionally different SDFTs and CDETs were compared<sup>109</sup>. SEM investigations revealed discrete plasticity formed frequently in the CDET and sparsely in the SDFT when subject to overload damage, thought to be the result of changes in thermally stable crosslinking. This hypothesis is supported by in vitro glycation of BTT wherein introduction of AGE crosslinking completely suppressed the formation of discrete plasticity<sup>150</sup>. Most recently, discrete plasticity has been shown to be a marker of collagen fibril damage for tendon remodeling, exhibited by the selective damaged material removal by MMP-9<sup>25</sup>. From these bovine studies, this begged the question whether the formation of discrete plasticity occurs in human tendons, leading to present study, a current extension of the works performed by Sparavalo<sup>237</sup> wherein structural and



biomechanical characterization of age-related changes in human distal sartorius tendons harvested from male non-diabetic donors across four decades of adulthood (20-60 years of age) were performed. In the present study, a series of thermal, thermomechanical, mechanical, histological and immunohistochemical experiments were performed to accomplish the objectives of uncovering age-, sex-, and diabetes-determined changes in distal sartorius tendon collagen structure and mechanics and to potentially suggest underlying mechanisms.

## **2.2. Objectives and Hypotheses**

### *2.2.1. Study #1: Assessing Collagen Structure and Thermal Stability*

**Rationale:** Collagen, the primary mechanical component in tendons, allows bearing of frequent and high mechanical loads necessary for locomotion without failure. Increases in thermal stability may be indicative of a higher degree of thermally stable crosslinking and increased molecular packing. Although enzymatic crosslinking may plateau with maturation, the slow turnover of collagen allows for further formation of intermolecular AGE crosslinks with aging and diabetes. Studies of the differences in tendon collagen crosslinking or thermal stability by sex have not been performed to date. Methods like DSC and HIT may be used as proxies to evaluate the crosslinking profile and molecular organization of tendon collagen, improving fundamental knowledge of molecular level changes that occur with aging, sex, and diabetes.

**Objective:** To determine if any differences in thermal properties of collagen occur in the human sartorius tendon: by sex, diabetes, or age over four decades of adult life (16-60 years)

**Hypothesis #1:** Thermomechanical behaviour will depend significantly on donor age. With aging, increases in thermally stable crosslinks will further confine the fiber lattice and increase molecular packing resulting in increased overall thermal stability. Aging will result in a decreased distribution of thermal stabilities and an increase in thermally stable crosslinks.

**Hypotheses #2:** Thermomechanical behaviour of tendon collagen over all age ranges will be independent of donor sex. Given the high load-bearing nature of the sartorius tendon and similar tendon compositions between sexes, it is expected that the overall collagen thermal stability, distribution of thermal stabilities (*FWHM*) and thermally stable crosslinking will be independent of sex over all age ranges.

**Hypothesis #3:** Within each sex, diabetic status will significantly determine thermomechanical behaviour of tendon collagen over all age ranges. Accelerated accumulation of intermolecular glycation crosslinks in tissues from diabetic donors, with regards to the polymer-in-a-box theory<sup>170</sup>, will further increase molecular packing and restrict conformational freedom. Overall collagen thermal stability and total thermally stable crosslinking will be increased, accompanied by a decreased distribution of thermal stabilities in sartorius tendon collagen from the diabetic donors.

#### *2.2.2. Study #2: Assessing Mechanical Behaviour of Tendon Collagen*

**Rationale:** Given the critical function of tendons, tensile testing provides a fundamental and repeatable test to understand bulk mechanical properties. Uniaxial overload to rupture tests of tendon fascicles will be performed at a strain rate of 0.25%/sec, as per previous studies of human sartorius tendon<sup>237</sup> and BTT<sup>257</sup>. Overload to rupture testing provides a replicable test to simulate in vivo overload damage to collagen ultrastructure. As thermal techniques are used to probe the type and amount of crosslinking, changes in crosslinking should be reflected in the mechanical properties of tendons at high extensions<sup>106</sup>. With aging, sex, and diabetes, differences in injury rates have been reported<sup>85,204</sup>, however, it is unclear how each intrinsic factor independently influences the mechanics in a high-load human tendon. Characterizing differences in tendon mechanical properties between donor populations may assist in improving clinical care.

**Objective:** To determine if any differences in mechanics of collagen occur in the human sartorius tendon: by sex, diabetes, or age over four decades of adult life (16-60 years)

**Hypothesis #1:** Mechanical behaviour of tendon multi-fascicle subsamples will depend significantly on donor age. With anticipated changes in collagen content and crosslinking

profile of aging tendons<sup>66,242</sup>, aging is expected to result in a stiffer, more brittle tissue within each donor population.

**Hypotheses #2:** Mechanical behaviour of tendon multi-fascicle subsamples over all age ranges will be independent of the donor sex. Although minor changes in composition have been observed in human Achilles and patellar tendon studies between sexes<sup>152</sup>, bulk mechanical properties will be independent of sex.

**Hypothesis #3:** Within each sex, diabetic status will significantly determine the Mechanical behaviour of the sartorius tendon multi-fascicle subsamples over all age ranges. Further increases in AGE intermolecular crosslink formation will negatively impact tendon multi-fascicle subsample mechanical behaviour, resulting in a stiffer and more brittle tissue.

### 2.2.3. Study #3: Assessing Overload Damage to Tendon Collagen

**Rationale:** Mechanisms of failure in tendon ultrastructure subject to biomechanical overload in vivo are poorly understood. The earliest studies of overload damage in RTT<sup>183,250</sup> and human Achilles tendon<sup>164</sup> revealed fibril dissociation and kink-deformations. These findings were later augmented in the study of BTT and bovine forelimb models where a kinking morphology termed discrete plasticity was revealed<sup>109,257</sup>. Most recently, in human sartorius tendons from non-diabetic donors, overload damage was found not to cause discrete plasticity; rather, it induced fibril disruption, hairpin turns and rare disruption of subfibrillar structures<sup>237</sup>. It remains to be discovered whether similar damage motifs are observed by sex, age and diabetic status. Overall, it is important to understand the underlying failure mechanisms of the primary load-bearing elements in tendon injury, collagen, in order to deliver more effective clinical treatment.

**Objective:** To determine the mechanisms by which the human sartorius tendon fails in biomechanical overload.

**Hypothesis #1:** Failure mechanisms, as described by an absence of discrete plasticity in a previous study<sup>237</sup>, of tendon collagen will not depend significantly on donor age.

**Hypothesis #2:** Failure mechanisms of tendon collagen over all age ranges will be independent of the donor sex.

**Hypothesis #3:** Within each sex, diabetic status will significantly determine the failure mechanisms of tendon collagen over all age ranges. Evidence of more brittle fractures of tendon collagen fibrils from diabetic donors is anticipated.

#### 2.2.4. Study #4: General Histology & Immunohistochemistry

**Rationale:** Histology and immunohistochemistry in tandem may reveal important changes in tendon collagen structure not identified by thermal and mechanical techniques. Birefringence may be used to examine collagen fibre crimp which is known to vary with age and contributes to low stiffness and extensibility. Use of H&E staining will provide information on the cellularity of the tendon, as previously studies have indicated changes in cellular content and morphology with aging and diabetes<sup>242,252</sup>. The degree of pentosidine concentration, the best characterized glycation crosslink<sup>16</sup>, across high-load bearing tissues with diabetes and age is unclear<sup>242</sup>. As such, this work provides the first immunohistochemistry experiment to qualitatively examine changes in pentosidine concentration in a high load bearing tendon model.

**Objectives:** To qualitatively determine differences in cellularity, crimp, and presence of the pentosidine epitope ( $\alpha$ -PEN12), the biomarker for AGEs, in a preliminary study intended to both (1) partially illuminate the observations in other parts of the thesis, and (2) pave the way for possible in-depth studies by comparing tendon collagen from (i) a 24-year-old non-diabetic and (ii) a 50-year-old diabetic donor.

**Hypothesis #1** In tendon collagen from (i) the older male diabetic donor, expectations are that an increase in collagen crimp wavelength will occur when compared to the tendon from (ii) the young male non-diabetic donor. With the suggested lowered turnover of tendon collagen in the old donor, the increased physical age of the fiber will result in a qualitative increase in the crimp wavelength.

**Hypothesis #2** In tendons from (i) the old diabetic donor, expectations are that a decreased nuclei content via H & E staining will occur when compared to the tendon

from (ii) the young non-diabetic donor. With aging and diabetes, marked qualitative decreases in cellular content is anticipated.

***Hypothesis #3:*** In the tendon from (i) the older diabetic donor, expectations are that an increased presence of the pentosidine epitope ( $\alpha$ -PEN12) will occur when compared to the tendon from the (ii) young non-diabetic donor.

## Chapter 3: Materials & Methodology

### 3.1. Sartorius Tendon Acquisition & Donor Demographic

Distal human sartorius tendons were collected from the Nova Scotia Health Authority (NSHA) Regional Tissue Bank (Halifax, N.S.) within 24 hours of tissue harvest. Tendons were transferred to the Tissue Mechanics Lab (Dalhousie University, Halifax, N.S.) on ice. Upon arrival, tendons were immediately wrapped in gauze soaked in 0.1M phosphate buffered saline (pH 7.4) containing a 1% Penicillin/Streptomycin and 1% Amphotericin B solution, and placed in a polypropylene tube. Tendons were stored at -86°C until testing. The tissue harvesting protocol was accepted by the Research Ethics Board of the Capital District Health Authority (CDHA-RS/2015-168 and renewals).

Information collected and recorded for each donor included the age, sex, diabetic health status, weight, height and the number of tendons donated. Tendon donors collectively spanned four decades of adulthood from 16-60 years of age in this study as shown in Figure 3.1. The female non-diabetic population consisted of six sets of paired (contralateral and ipsilateral) tendons, spanning 16-58 years of age. The male non-diabetic population consisted of nine sets of paired tendons spanning 24-59 years of age in order to replicate previous work by Sparavalo<sup>237</sup>. The male diabetic population consisted of both diabetes types ( $n_{Type I} = 1$ ,  $n_{Type II} = 7$ ), with six paired sets and two unpaired (i.e. single) tendons spanning 46-60 years of age. A donor's body mass index (BMI) (Figure 3.2) was calculated using their height and weight in the following equation<sup>100</sup>:

$$BMI = \frac{mass_{kg}}{height_m^2} = \frac{kg}{m^2} \quad (3)$$

Although BMI is a limited proxy for obesity, it was the best option with the information available in this study to be used in determining the influence of health on sartorius tendon structure and mechanics.

### 3.2. Anatomy of the Distal Sartorius Tendon

The flat, parallel-fibered sartorius (“tailor’s”) tendon is one of three tendons comprising the pes anserinus, forming at the anteromedial aspect of the proximal tibia<sup>142</sup>.

The pes anserinus (“goose’s foot”) consists of, from anterior to posterior, the gracilis, semitendinosus and sartorius muscle tendinous insertions<sup>89,148</sup>. The biarticular (hip and knee) strap-like sartorius muscle is the longest muscle (~50cm) in the body<sup>69</sup>. Its function is to provide lateral rotation and flexion of the thigh in addition to flexion and medial rotation of the leg<sup>163</sup>. The sartorius muscle is thought to play an important role in stabilizing the pelvis<sup>172</sup> (Figure 3.3).

Aside from the donor-dependent variations in morphology, the distal sartorius tendons (Figure 3.4) that were harvested by the residents at the NSHA Regional Tissue Bank were also variable in the degree of intactness (occasional missing portions) and in the appearance (e.g. color, fat and muscle content). Previously reported dimensions of distal sartorius tendons have varied in width (1-2.5 cm) and in length (4.4-17 cm)<sup>69,285</sup>. The harvested tendons used in this study fell within these ranges of measurements. Structurally, the tendon has been described consisting of two tracts (superior and inferior) at the osteotendinous junction (OTJ). The differences in the two tracts were thought to be fibre packing, fibre length and insertion locations<sup>69</sup>. Tract and junction (osteotendinous and musculotendinous) sampling locations were mapped and investigated to compare the thermal and mechanical properties of the collagen at the different anatomical locations within the tendon.

Distal sartorius tendon injuries are rarely documented in the literature as they are difficult to diagnose clinically<sup>89,139,207</sup>. The most common injuries are “snapping sartorius syndrome”, tendinitis and bursitis<sup>37,89,117</sup>. The limited literature on the distal sartorius tendon is growing, due to the increasing usage of pes anserinus grafts (semitendinosus and gracilis distal tendons) in anterior cruciate ligament reconstruction<sup>84,279,285</sup>. Typically discarded by the resident upon tissue (pes anserinus) harvesting, the sartorius tendon provided a means of studying human tendon collagen structure, mechanics and overload damage.

### **3.3. Proposed Studies for Structural and Mechanical Analysis**

Two comparison groups were investigated in this study: the (i) sex- and (ii) diabetes-determined differences in human sartorius tendon collagen behaviour (Figure 3.5). Age- and BMI-related changes in sartorius tendon collagen behaviour within each

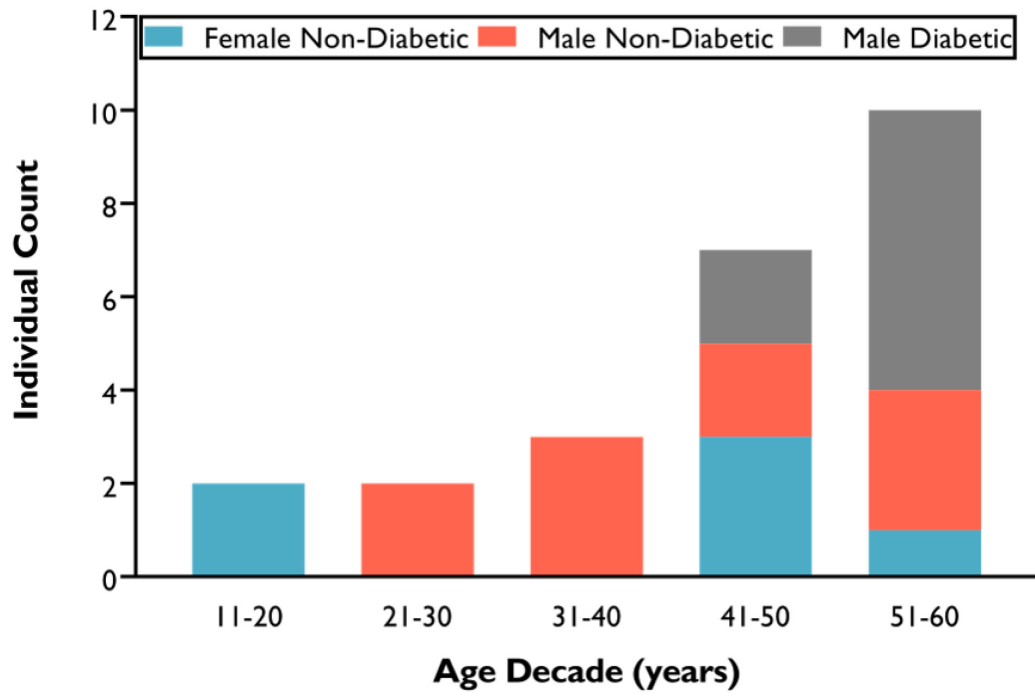


**Figure 3.1** Stacked column graph showing individual donor counts grouped into age decades from the current study. Ten male non-diabetic donors spanned 24-59 years of age, donated as paired tendons. Eight male diabetic donors spanned 46-60 years of age, two of which donated as a single unpaired tendon. Six female non-diabetic donors spanned 16-58 years of age, giving a clear younger and older cohort, all of which were donated as paired tendons.



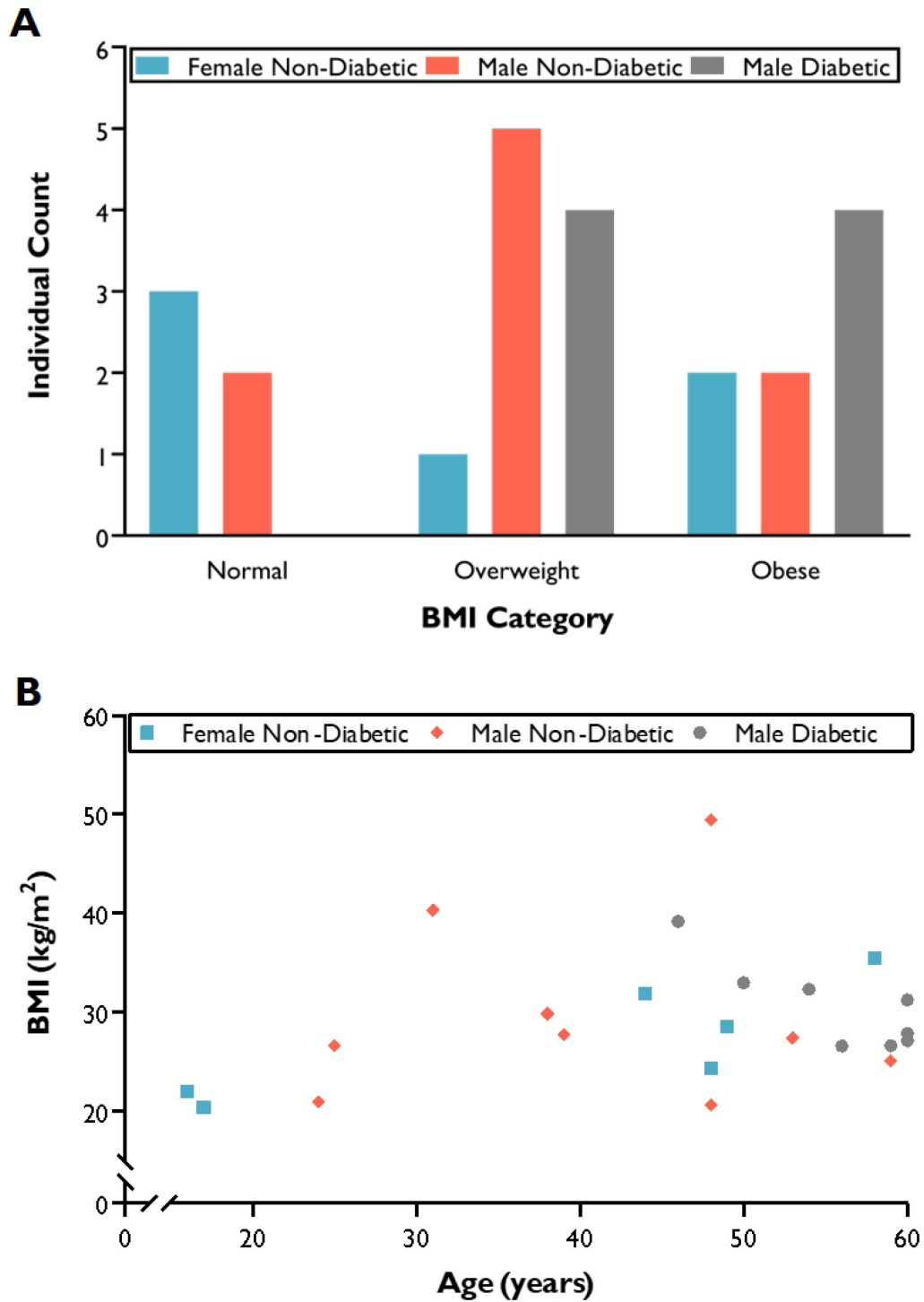
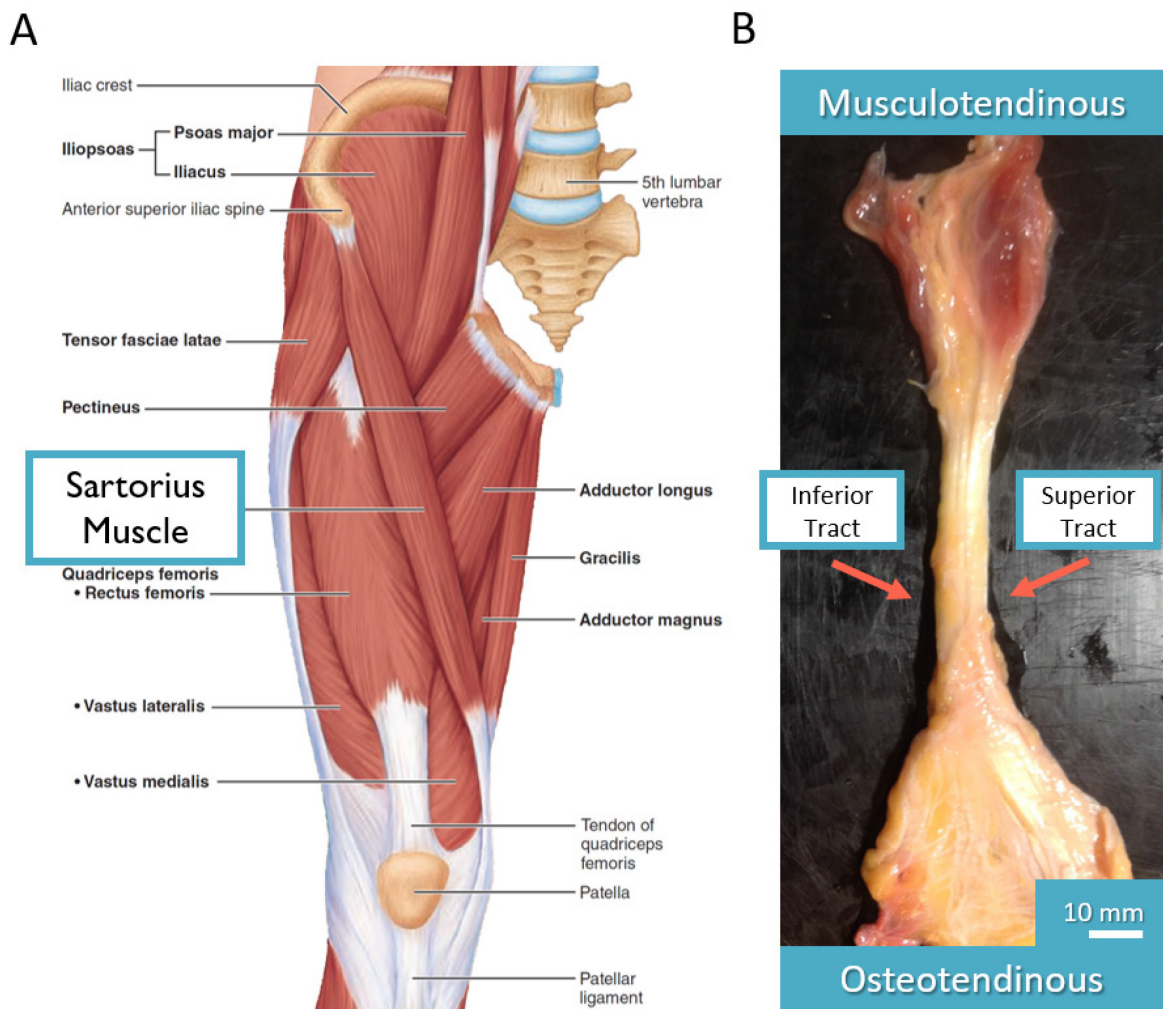


Figure 3.2 (A) A stacked column graph was used to identify the number of individuals in each BMI category for each donor population from the current study. (B) A scatterplot displaying the donor BMI and age within each donor population from the current study.



**Figure 3.3 (A) Anterior perspective view of the anatomy of the right lower limb. (B) Representative distal sartorius tendon collected from the NSHA Regional Tissue Bank prior to dissection. Although there was large variability in the morphology of the sartorius tendons, there were defined musculotendinous (MTJ) and osteotendinous (OTJ) junctions. Sampling locations were recorded to identify possible changes in structure and mechanics throughout the study. Figure modified from MARIEB, ELAINE N.; HOEHN, KATJA, HUMAN ANATOMY & PHYSIOLOGY, 9th, ©2013. Reprinted by permission of Pearson Education, Inc., New York<sup>163</sup>.**



Figure 3.4 Partial assortment (12/24 individuals) of the collected sartorius tendons prior to gross dissection from donors varying in age, sex and diabetic status.

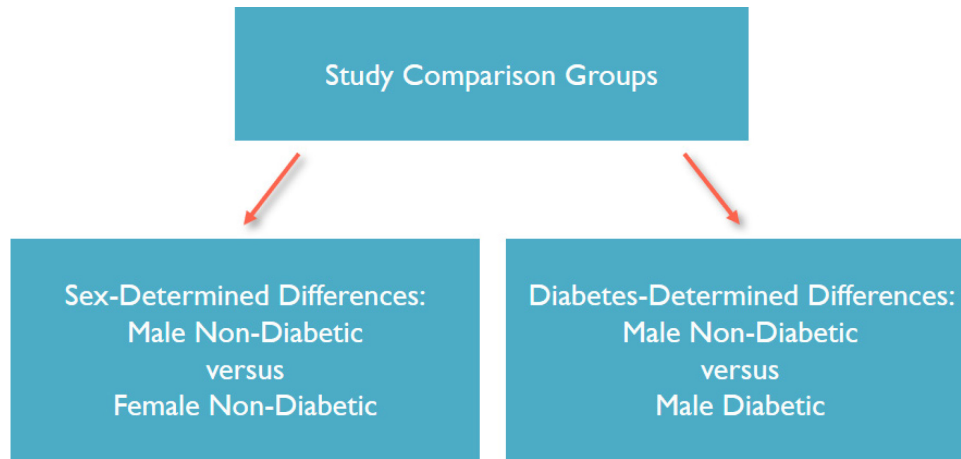


**Figure 3.5 Hierarchical chart displaying the two comparative groups examined in this study to determine differences in human sartorius tendon collagen by age, BMI, sex and diabetic status.**

donor population were also studied. Standardized handling procedures were used for each tendon sample to ensure consistent treatment prior to all testing<sup>237</sup>. Sartorius tendon collagen behaviour was investigated using the established techniques of hydrothermal isometric tension (HIT) analysis, differential scanning calorimetry (DSC) and mechanical uniaxial tensile overload to rupture. Rupture testing provided both mechanical properties and, using scanning electron microscopy (SEM), allowed for the observation of failure mechanisms at the nanoscale (fibril level) of the tendon collagen. Histology and immunohistochemistry (IHC) were used to investigate structural differences in tendon collagen based on donor diabetic health status and age. Shown in Figure 3.6 is a flowchart demonstrating the different methodologies used in this study for a set of paired tendons from a single donor. The tendon from one leg of the pair (labeled B upon collection) was used for light microscopy (histology and IHC) and thermomechanical evaluation. The tendon from the opposite leg (labeled A upon collection) tendon was used for uniaxial overload to rupture to reveal tendon mechanical properties and subsequent ultrastructural evaluation of overload damage motifs via SEM.

### 3.4. Differential Scanning Calorimetry

Differential Scanning Calorimetry was performed on  $n = 22$  tendons from female non-diabetic ( $n_{F,ND} = 5$ ), male non-diabetic ( $n_{M,ND} = 9$ ) and male diabetic ( $n_{M,D} = 8$ ) donors.

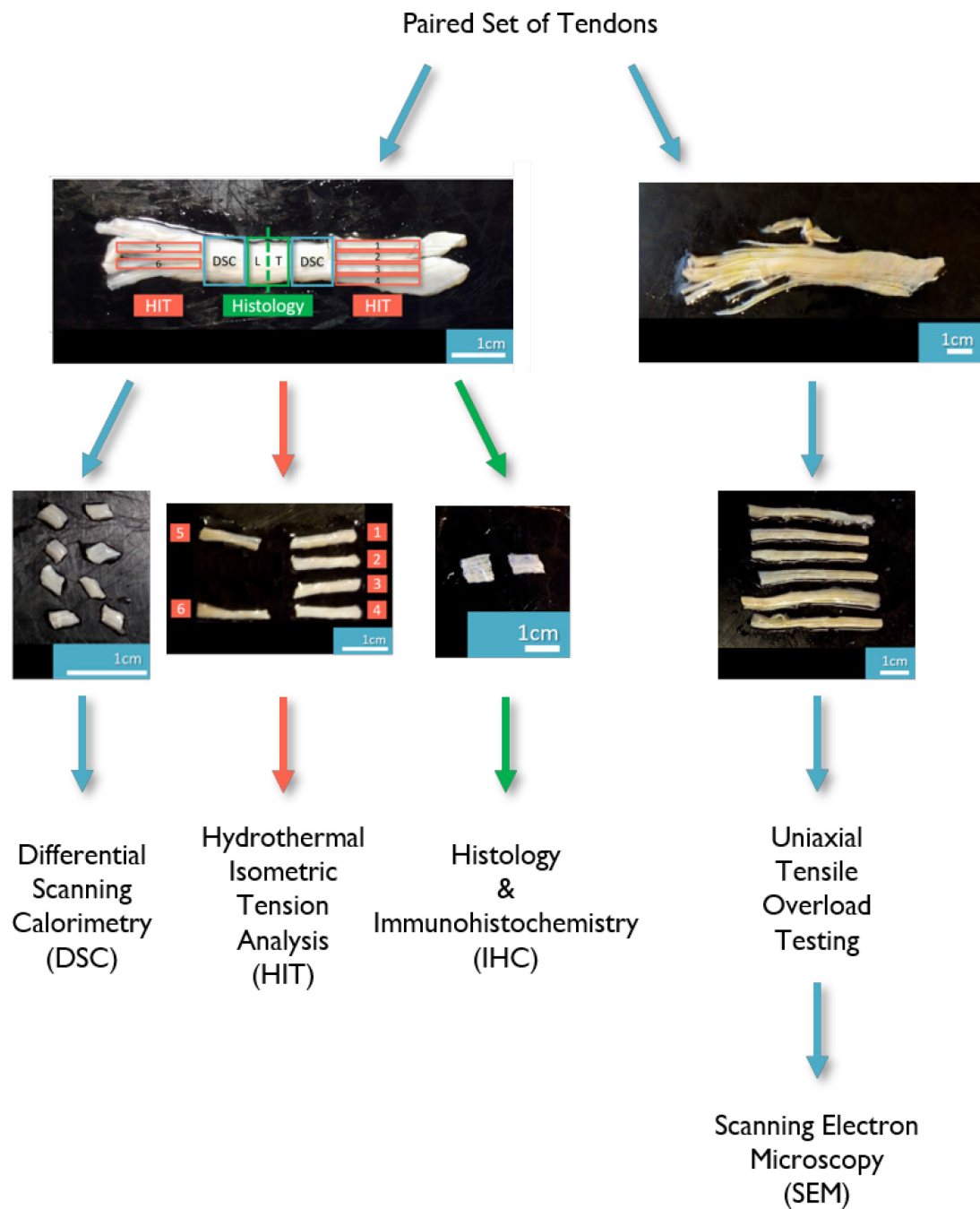


**Figure 3.6** Flowchart of the methodology followed in this study. Using paired tendons from a donor, the ipsilateral tendon underwent thermomechanical and histological characterization. The contralateral tendon underwent uniaxial overload to rupture testing to extract both mechanical properties and ultrastructural control and damage motifs (via SEM).

### 3.4.1. DSC Test Protocol

For DSC testing, tendon pieces were taken from two ~10 x 10 mm square sections near the middle of the tendon (Figure 3.6). This resulted in multiple ~2.5 x 2.5 mm samples each weighing  $15 \pm 5$  mg. Samples were placed in either 40 mL of freshly prepared phosphate buffer saline or distilled water. Samples were double rinsed with their respective solutions and stored at 4°C overnight. DSC samples were blotted dry to remove excess water from the surface and weighed before being individually placed and hermetically sealed in 20 $\mu$ L aluminum pans. DSC was performed using a Q200 differential scanning calorimeter (TA Instruments, New Castle, DE) that was calibrated prior to testing with an indium standard. Samples were run against an empty hermetically sealed reference pan. Pan temperatures were equilibrated at 30°C and the temperature was increased at a linear rate of 5°C per minute to 90°C. During testing, data was recorded at 10 Hz with the resultant endotherm analyzed using Universal Analysis 2000 software (Version 4.5A, TA Instruments). After testing, sealed pans were pierced using a hypodermic needle and stored in a vacuum desiccator with the sample dry mass being weighed once every 24 hours until the mass stabilized.

### 3.4.2. Calculating DSC Parameters

Resultant endotherm peaks were evaluated with reference to a linear baseline from 65°C to 80°C (Figure 3.7). Parameters that were extracted include the onset temperature ( $T_{onset}$ ), peak temperature ( $T_{peak}$ ), full width at half-maximum ( $FWHM$ ), and the specific enthalpy of denaturation ( $h$ ).  $T_{onset}$  was defined as the temperature at which thermal denaturation commences, calculated as the intersection of the tangent line of the endotherm slope and the endotherm baseline.  $T_{peak}$  was defined as the temperature of maximum heat flow into the sample, where denaturation of collagen molecules is occurring at its fastest rate. The full width at half-maximum was calculated as the percent range of the temperatures at 50% of the heat flow values between  $T_{peak}$  and the baseline heat flow, a measure of the distribution of thermal stabilities. The specific enthalpy of denaturation was calculated as the area under the DSC endotherm using both the sample wet mass ( $h_{wet\ mass}$ ) and dry mass ( $h_{dry\ mass}$ ).

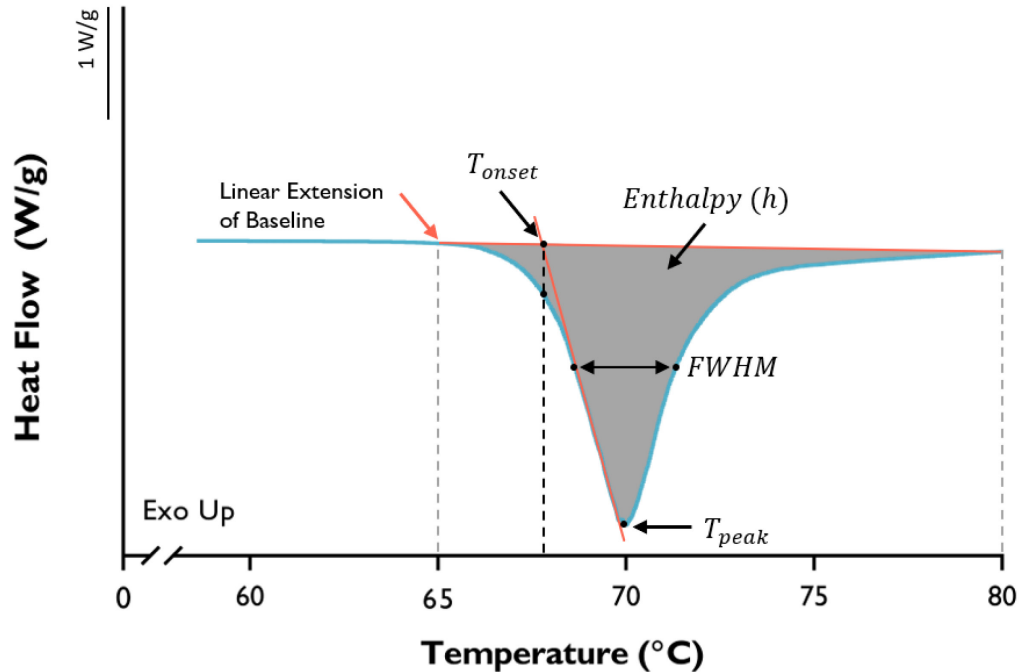


Figure 3.7 Representative DSC endotherm from a sartorius tendon collagen sample. With reference to a linear baseline from 65°C to 80°C, parameters extracted from an endotherm included onset temperature ( $T_{onset}$ ), peak temperature ( $T_{peak}$ ), full width at half-maximum ( $FWHM$ ) and specific enthalpy of denaturation ( $h_{wet\ mass}$ ,  $h_{dry\ mass}$ ).

### 3.5. Hydrothermal Isometric Tension Analysis

Hydrothermal Isometric Tension (HIT) analysis was performed on  $n = 23$  tendons comprised of female non-diabetic ( $n_{F,ND} = 6$ ), male non-diabetic ( $n_{M,ND} = 9$ ) and male diabetic ( $n_{M,D} = 8$ ) donors.

#### 3.5.1. HIT Test Protocol

Strip samples measuring nominal dimensions of 15 x 2.5 mm (Figure 3.6), three or four from the OTJ and two from the MTJ, were secured into a six-sample custom apparatus (Figure 3.8) that has been previously described<sup>149,181,266</sup>. Sensors consisted of six 1000-gram cantilever load cells (Transducer Techniques, Temecula, CA) and a thermocouple placed in the middle of the apparatus. Briefly, samples were secured by a spring-loaded clamp at each end, leaving an intergrip distance of ~8 mm. Once the samples were secured, the mounting apparatus was immersed into a 4 L beaker of distilled water.

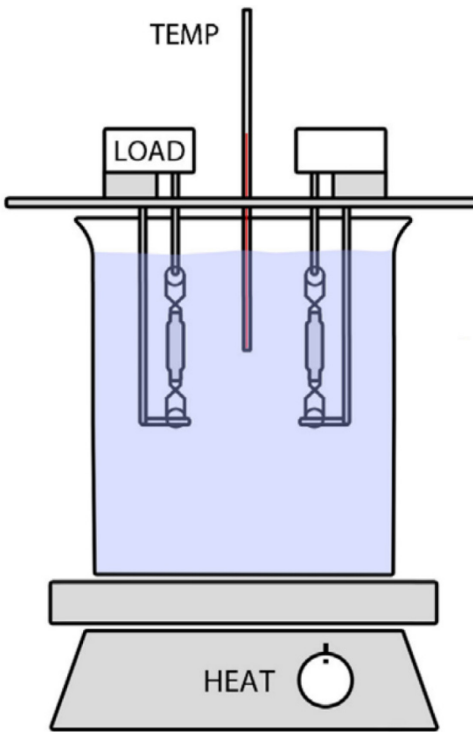


**Figure 3.8 HIT Apparatus schematic wherein specimens are isometrically constrained in a 4L water bath by a fixed support and cantilever load cell. The water bath was then placed on a computer-controlled hot plate during testing, with the temperature readings by a thermocouple in the center of the apparatus. Figure modified with permission<sup>254</sup>.**

The HIT apparatus was controlled by a custom software in LabVIEW (Version 6.1, TA Instruments). Samples were preloaded to 60 grams and remained undisturbed for 10 minutes prior to heating, allowing for stress relaxation to occur. Using computer on/off control of a hotplate, the temperature of the water bath was increased from room temperature at a near-constant rate of  $\sim 1.3^{\circ}\text{C}/\text{minute}$  to  $75^{\circ}\text{C}$  and a rate of  $\sim 0.7^{\circ}\text{C}$  from  $75^{\circ}\text{C}$  to  $90^{\circ}\text{C}$ . Once the temperature of the bath reached  $90^{\circ}\text{C}$ , the temperature was maintained at  $90.0 \pm 0.2^{\circ}\text{C}$  for 5 hours (Figure 3.9). Time (sec), load (g) and temperature ( $^{\circ}\text{C}$ ) data were recorded at 0.2 Hz.

### 3.5.2. Calculation of HIT Parameters

Analysis of the data was conducted using custom-written software in MATLAB (Version R2017b, Mathworks). Data were averaged over time using a five-point moving average



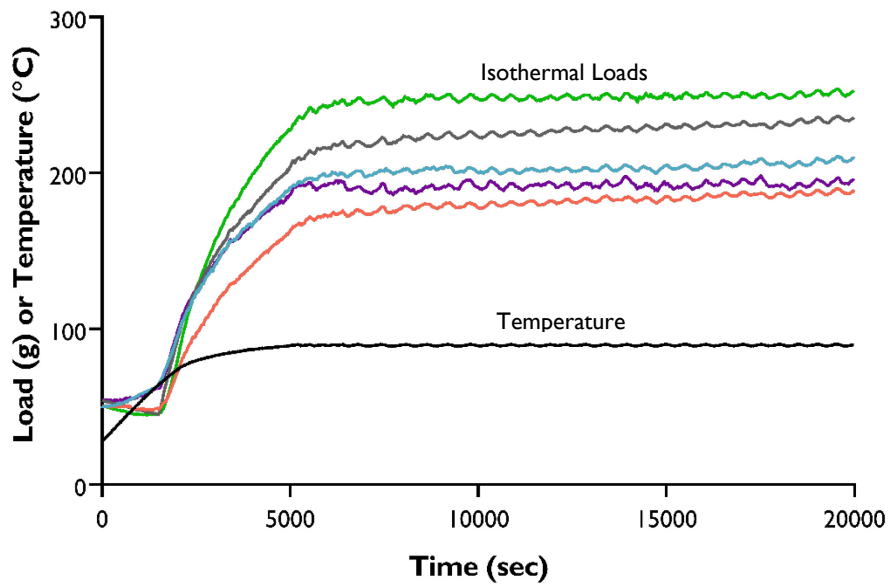


**Figure 3.9 Representative HIT test graph of sartorius tendon collagen. HIT samples were dissected into 6 strip samples measuring 15 x 2 mm (Figure 3.6), were isometrically constrained in the HIT apparatus (Figure 3.8) and placed in a 4L water bath. A ramp from room temperature to 90°C was followed by an isothermal segment at 90°C to produce the representative graph where load (multicolor curves), temperature (black curve) and time were recorded.**

filter (centered at the third point) prior to analysis<sup>266</sup>. Parameters of interest calculated include: denaturation temperature ( $T_d$ ), the fractional differences (F.D.) in load pre- and post- $T_d$ , the sample's half-time of load decay ( $t_{1/2}$ ) under the isotherm and the type of collagen isothermal segment behaviour observed separated into four defined categories.

$T_d$  was defined as the temperature at which a distinctive monotonic increase in load is generated by the inhibited contraction of the sample under isometric constraints. Evaluation of  $T_d$  was performed by drawing a manual line of best fit over the few degrees prior to the generated tension observed in the load-temperature curves (Figure 3.10A) that were created using custom-written software in MATLAB (Version R2017b, Mathworks).

The fractional differences in load pre- $T_d$  (29°C to  $T_d$ ) and post- $T_d$  ( $T_d$  to 90°C) (Figure 3.10B) were used to determine the fractional amount of contraction or relaxation over those two regions of the load-temperature curves:

$$\text{Pre-Denaturation F. D. in Load} = \frac{\text{load}_{T_d} - \text{load}_{29^\circ\text{C}}}{\text{load}_{29^\circ\text{C}}} \quad (4)$$

$$\text{Post-Denaturation F. D. in Load} = \frac{\text{load}_{90^\circ\text{C}} - \text{load}_{T_d}}{\text{load}_{T_d}} \quad (5)$$

Two alternative methods were chosen to describe the isothermal behaviour of the sartorius tendon collagen. The first means of isothermal analysis was a characterization based on whether the tendon strip samples exhibited signs of decay, isothermal contraction, constant load or breakage in the isotherm. Again, the load for each sample was examined between 5,000-10,000 seconds after the start of the isothermal segment to avoid any thermoelastic effects<sup>266</sup>. Linear least squares regression was used to assess the sample behaviour across the 5,000 second period (Figure 3.11), with a significant positive and negative slope indicating contraction and decay respectively ( $p < 0.05$ ). Failure was defined as a sudden major decrease in load ( $> 5\text{g}$ ). A slope of the line of best fit that is not statistically different from zero ( $p > 0.05$ ) denoted constant load in the samples.

The second isotherm analysis used was the calculation of the half-time of load decay using the Maxwell model of the hydrolysis of the peptide bonds of the collagen network<sup>144,181</sup>. Looking at a window of 5,000 to 10,000 seconds after the start of the isotherm, the isothermal load behaviour was represented as a ratio of the logarithm of the load at a specified time  $t$  to the logarithm of the maximum load that was found over the 5,000 second interval.

$$\frac{\text{Load}(t)}{\text{Load}_{max}} = e^{-kt} \quad (6)$$

Where  $-k$  is the relaxation slope constant calculated using a linear regression of the ratio of  $\text{Load}(t):\text{Load}_{max}$  versus time ( $t$ ). For a rubber, the relaxation constant is directly proportional to the rate of bond rupture and inversely proportional to the number of intact polymeric chains at a given time<sup>143,145</sup>. Rearranging Equation 4, the half-time of load decay ( $t_{1/2}$ ) was able to be calculated in the following equation:

$$t_{1/2} = -\frac{\ln\left(\frac{1}{2}\right)}{k} \quad (7)$$

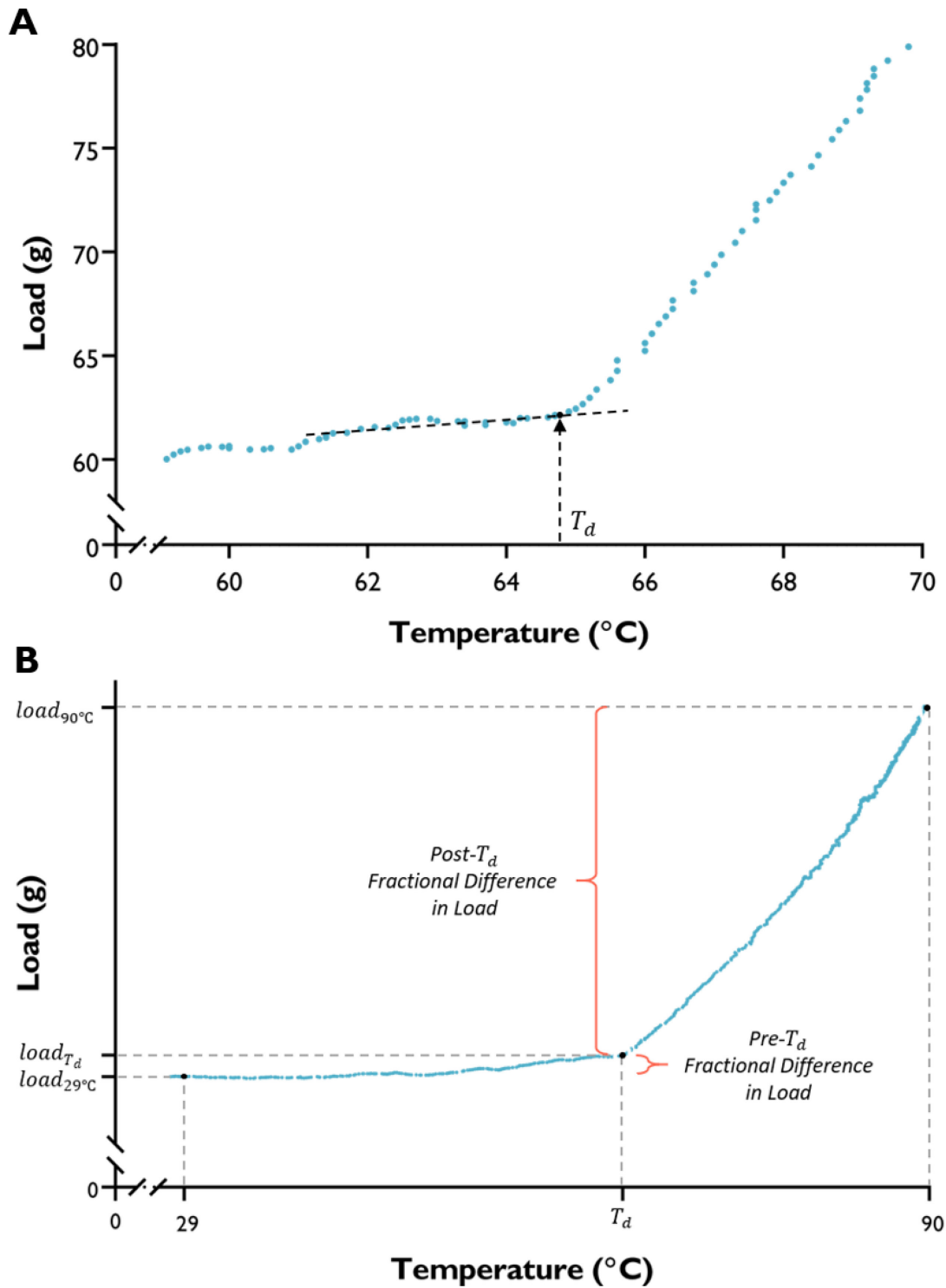


**Figure 3.10** Determination of the HIT parameters (A) denaturation temperature and (B) fractional differences in load pre- and post-denaturation. (A) Determination of the HIT denaturation temperature ( $T_d$ ) for a given sample. A manual line of best fit was constructed to assist in evaluating the temperature at which the monotonic increase in load first occurs ( $T_d$ ). (B) Determination of the fractional differences in load (i) pre- $T_d$  (29°C to  $T_d$ ) and (ii) post- $T_d$  ( $T_d$  to 90°C) are shown by the red brackets by dividing the difference in load between two temperature points and an initial temperature point as identified on the graph.

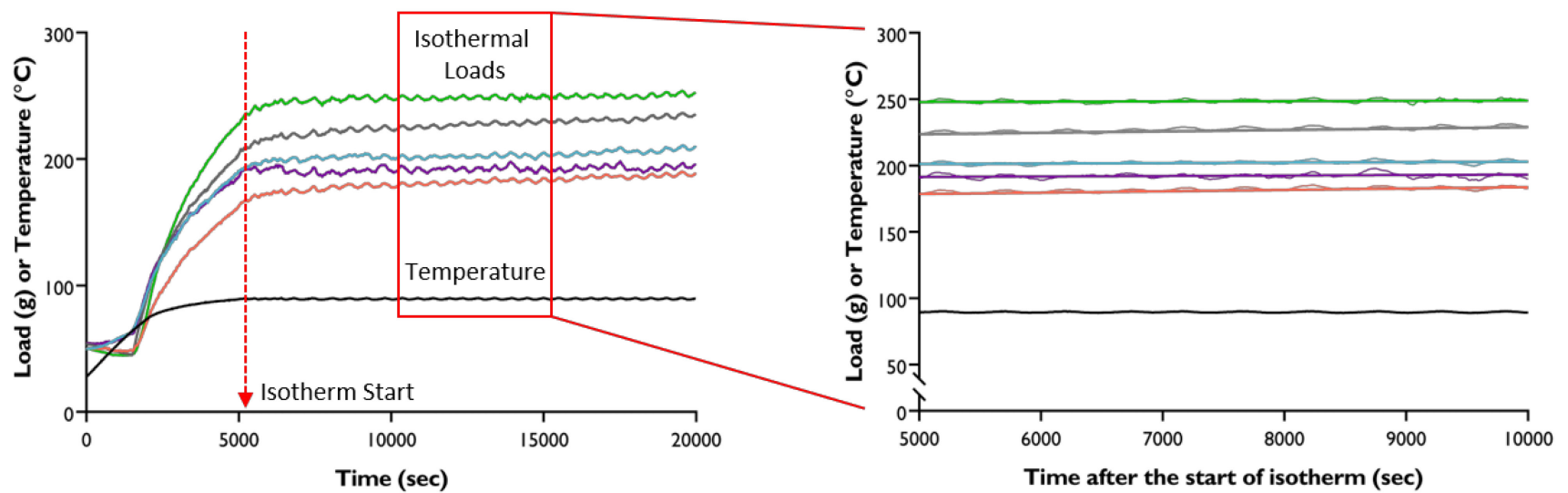


Figure 3.11 Representative isothermal segment evaluated 5,000-10,000 seconds from the beginning of the start of the segment. Linear least squares regression was used to evaluate the isothermal behavior of a given strip sample using the resulting slope and significance values.

It was only possible to calculate this parameter in tendon samples that displayed load decay – and most did not.

### **3.6. Mechanical Overload Testing**

Mechanical overload to rupture testing was performed on  $n = 23$  tendons comprised of female non-diabetic ( $n_{F,ND} = 6$ ), male non-diabetic ( $n_{M,ND} = 9$ ) and male diabetic ( $n_{M,D} = 8$ ) donors.

#### *3.6.1. Mechanical Overload Protocol*

Tendon samples were dissected using a scalpel under the 40x magnification Nikon SMZ 800 dissection microscope (Nikon, Tokyo, Japan). A minimum of six multi-fascicle subsamples were cut from each tendon using a scalpel to approximate dimensions of 35 mm in length and 2 mm in width. During dissection, multi-fascicle bundles were separated using a scalpel such that multiple fascicles – thought to range individually from 50 – 300  $\mu\text{m}$  in diameter<sup>125</sup> – were apparently enveloped within an endotenon covering with clearly defined edges. This separation of multi-fascicle units was assisted by the presence of this endotenon: it prevented cutting of fascicles and fibers within the multi-fascicle subsamples by splaying open as the scalpel blade progressed through the tendon sample along the edge of the assumed bundle of fascicles. One of the subsamples was used as a control sample and a minimum of five subsamples were placed in PBS in a 6-well plate after dissection prior to the overload testing described below to ensure the samples maintained proper hydration.

Uniaxial overload testing was conducted using a servo-hydraulic material testing system (MTS 458-series, MTS, Eden Prairie MN) controlled in LabVIEW (Version 2010, National Instruments, Austin, TX) using custom-written software. Samples were mounted into custom waveform-crush grips padded with cotton fabric squares to reduce potential slippage and secured with noticeable slack. At this point the 100lbs load cell (Transducer Techniques, Temecula, CA) was zeroed. Samples were extended to a detected load of  $0.5 \pm 0.25$  N with a nominal intergrip distance of 15.0 mm that was measured and input as the actuator maximum displacement. Mechanical overload to rupture then commenced at a variable extension speed to attain a nominal strain rate of 0.25% strain/second. During

overload to rupture, drops of PBS were dispensed along the sample regularly to maintain hydration. Tests were visually recorded using an OEM-Optical HD133DV HD (OEM-Optical, Danville, CA) video camera with Zoom7000 macro video lens (Nativar Inc., Rochester, NY) and a video capture board (Intensity, Blackmagic Design, Burbank, CA) to observe the induced fascicle damage. Actuator position, time and load were recorded at 10 Hz (Figure 3.12). Post-testing, the crushed gripped ends of each sample were removed using a razor blade. The remaining samples, both unloaded control and overloaded, approximately 15 mm in length, were prepared for examination of damage using scanning electron microscopy.

### 3.6.2. Calculation of Mechanical Parameters

#### *Determination of Cross-Sectional Area*

Prior to testing, each sample to be overloaded was vertically suspended from one end using a custom apparatus and photographed with a scalebar at 90° rotation increments ( $D_{0^\circ}$ ,  $D_{90^\circ}$ ,  $D_{180^\circ}$  and  $D_{270^\circ}$ ) using a 12.0-megapixel Nikon digital camera (Nikon, Tokyo, Japan). Using Image J (Version 1.51, National Institutes of Health) software, the photos were used to capture the sample's minor ( $D_{Minor}$ ) and major axis diameters ( $D_{Major}$ ) at the thinnest location a minimum of 10 mm from each end of the sample. The minor and major axes were used to calculate the elliptical cross-sectional area with the following equation:

$$CSA = \frac{\pi}{4} (D_{Minor})(D_{Major}) = \frac{\pi}{4} \left( \frac{D_{90^\circ} + D_{270^\circ}}{2} \right) \left( \frac{D_{0^\circ} + D_{180^\circ}}{2} \right) \quad (8)$$

#### *Determination of Mechanical Properties*

Custom MATLAB software (version 2017b, Mathworks) was used to extract the stress, strain, tissue modulus, ultimate tensile strength ( $UTS$ ), strain at  $UTS$  and toughness of a ruptured sample (Figure 3.12). Stress,  $\sigma$  (MPa), was calculated using the recorded force (N) and the cross-sectional area ( $\text{mm}^2$ ) with the following equation:

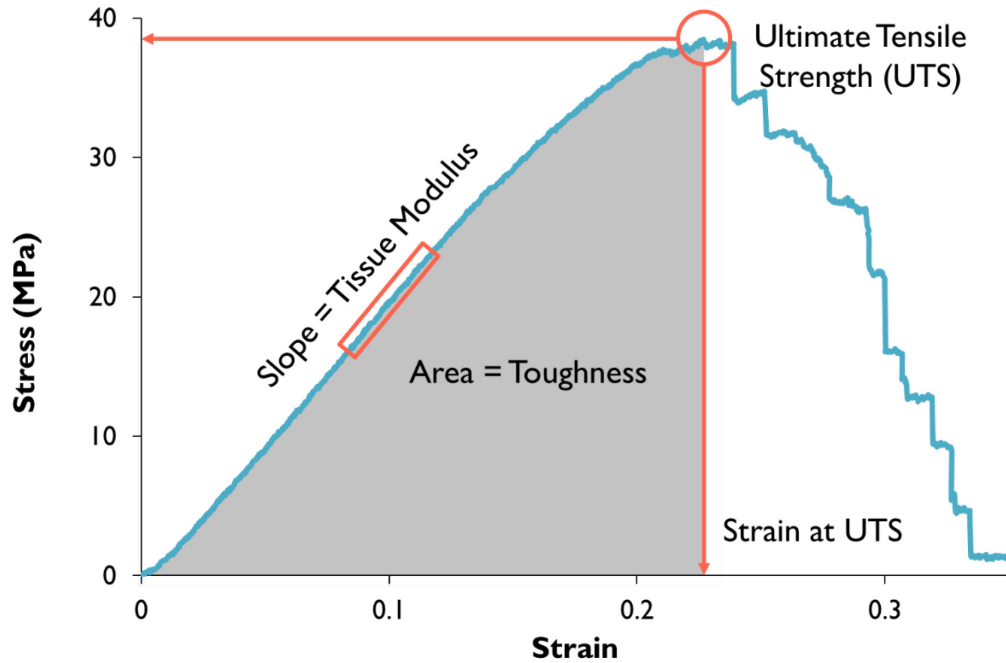


Figure 3.12 Representative stress-strain curve for a mechanical overload rupture test. Mechanical parameters evaluated include tissue modulus ( $E$ ), ultimate tensile strength ( $UTS$ ), strain at  $UTS$  and toughness.

$$\sigma = \frac{\text{Force}}{\text{Cross-Sectional Area}} \quad (9)$$

Strain ( $\epsilon$ ), the fractional change in length of the sample, was calculated using the actuator displacement,  $\Delta l$  (mm), and initial sample intergrip length,  $l_o$  (mm), shown below:

$$\epsilon = \frac{\Delta l}{l_o} = \frac{l - l_o}{l_o} \quad (10)$$

Tissue Modulus,  $E$  (MPa), was calculated as the steepest slope in the linear region of the stress-strain curve over an interval of 150 data points. Ultimate tensile strength ( $UTS$ ) was taken as the maximum stress that the sample was able to withstand prior to or at failure. The strain at  $UTS$  value was taken as the corresponding strain value at the  $UTS$ . Toughness was calculated by integration of the curve from the start of the test to the strain at  $UTS$  value using the trapezoidal rule.

### 3.6.3. SEM Preparation and Examination

Following mechanical overload testing, samples were prepared for ultrastructural assessment via SEM. Both control and overloaded samples were individually placed in a 12 well plate containing 2.5% SEM-grade glutaraldehyde (Sigma, St. Louis, MO) in PBS and stored for 24 hours at 4°C. Fixed samples were triple-rinsed for ten minutes in distilled water and gently shaken. Rinsed samples were bisected longitudinally using a scalpel to expose the internal surface, then dehydrated using graded aqueous ethanol for 10-minute intervals at the following concentrations: 30%, 50%, 70%, 90%, 95% and 100%. Dehydrated samples were critical point-dried using a Leica EM CPD300 (Leica Microsystems, Ontario, Canada) with liquid CO<sub>2</sub>, and mounted on aluminum stubs using carbon tape with each sample's internal surfaces facing upwards. The samples were then sputter-coated with gold palladium using a Low Vacuum Coater Leica EM ACE200 (Leica Microsystems, Ontario, Canada). The diffuse coating setting was used for 60 seconds with a current of 30mA, resulting in a ~6 nm thick layer. Samples were examined at a minimum of five locations along the length of each bisected piece (Figure 3.13) using magnifications up to 200,000x in a Hitachi S-4700 scanning electron microscope (Hitachi, Chula Vista, CA) operating at an accelerating voltage of 3kv and current of 15µA.

### 3.7. Histology & Immunohistochemistry

Within one hour of extraction from the -86°C freezer, tendon samples measuring approximately 5mm x 10mm in size (Figure 3.14) were dissected and laid flat in 10% acetate-buffered neutral formalin for 96 hours at 4°C. Following fixation, samples were double rinsed in 70% ethanol and placed in tissue cassette containers. Cassettes were stored in 70% ethanol until tissue processing and paraffin-embedding by the Histology and Research Services Laboratory (Department of Pathology, Dalhousie University). Two different orientations of the tendon were examined, (1) the longitudinal (L) plane that was parallel to the fibers and (2) the transverse cross-sectional area (T) plane perpendicular to the fibers. Paraffin-embedded samples were stored at -10°C prior to serial sectioning at 5µm thickness using a Leica 4000 Microtome (Leica Biosystems,



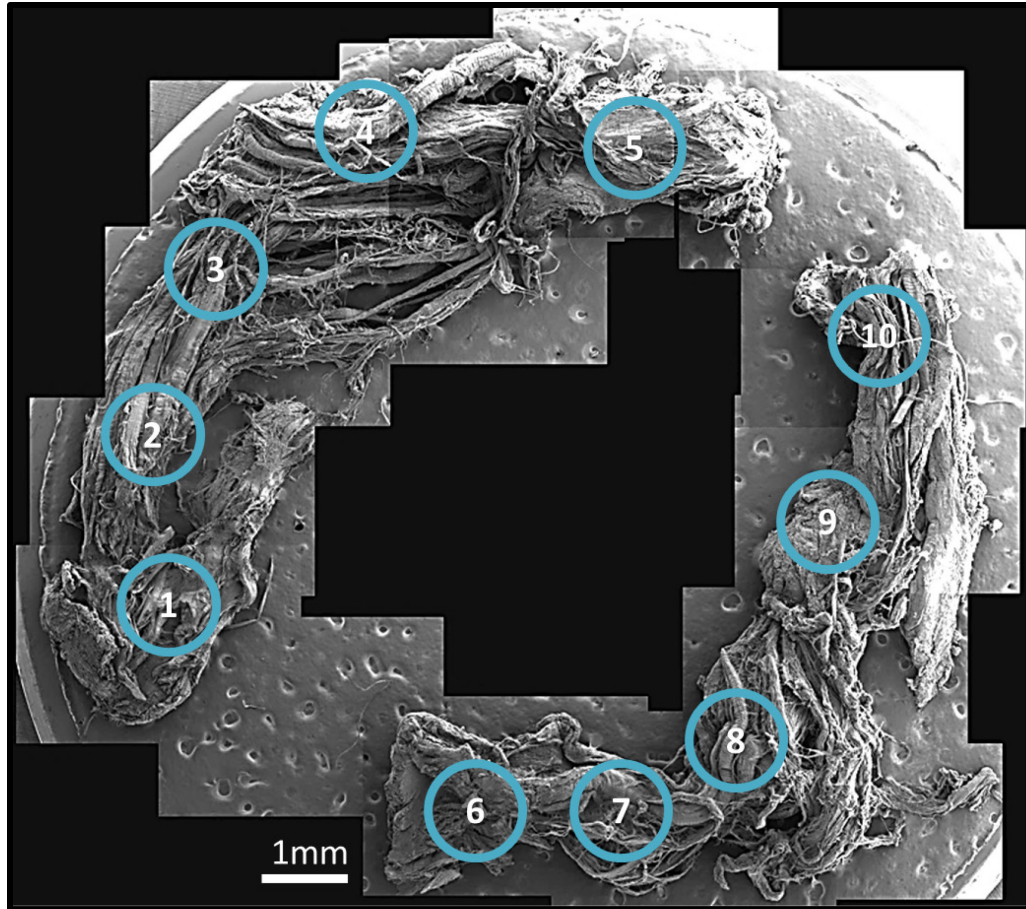


Figure 3.13 Composite SEM micrograph overview of a sample at 40x magnification. Regions investigated (blue circles) along the cross section of the sample at locations included areas near the ends, middle and alternative areas where the fibrils appear damaged.

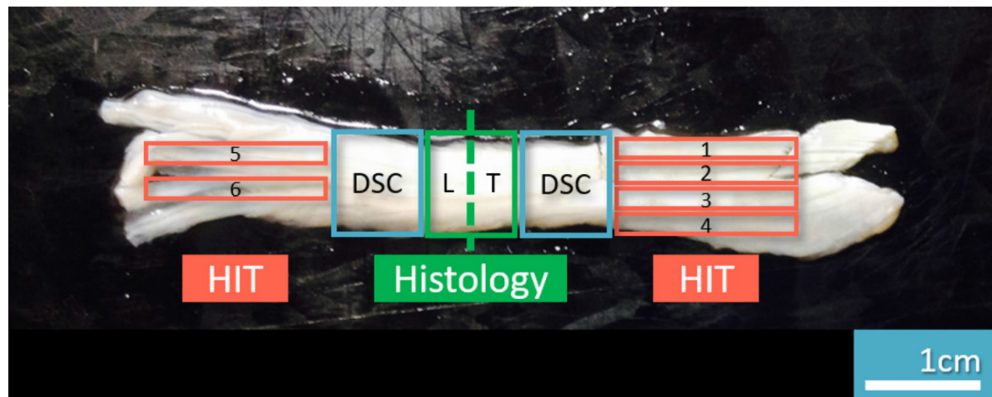


Figure 3.14 This is a magnification of an image in Figure 3.6 showing that the histological tendon samples were dissected near the middle of the tendon in two 5x10mm pieces (green rectangles). The two pieces were used for a longitudinal (L) and transverse (T) sections respectively.

Ontario, Canada). Tissue sections were placed on positively charged microscope slides (Fisherbrand) and stored at 37°C for 48-72 hours after sectioning.

For the histology and immunohistochemistry experiments, the analysis was performed primarily in the male (non-diabetic and diabetic) donor population due to the experimental progress – paired tendons from 4/6 female non-diabetic donors having been used for thermal and mechanical testing – prior to the light microscopy studies being confirmed.

### 3.7.1. *Birefringence (Collagen Crimp)*

Birefringence of unstained samples was explored to reveal collagen fiber arrangement and crimp using a Nikon Eclipse E600 light microscope (Nikon, Tokyo, Japan) equipped with a polarizing filter set and a quarter-wave plate analyser. Images were captured using a 10 MP AmScope digital camera and IS Listen software (Version 2.0, AmScope).

### 3.7.2. *Hematoxylin & Eosin*

Cell nuclei and collagen were visualized by staining slides using hematoxylin and eosin (H & E). Slides were deparaffinized with three five-minute washes in xylene and rehydrated using graded ethanol solutions (100%, 100%, 100%, 95%, 95%, 95%, 70%). Hydrated samples were rinsed in a bath of running water for 1 minute to remove residual ethanol. Slides were placed in Harris's Hematoxylin (Sigma-Aldrich) for five minutes and washed in a running water bath until the water became clear. Rinsed slides were then placed in Scott's H<sub>2</sub>O for two, two-minute washes separated by a quick dip in 0.1% picric acid. After rinsing in the water bath, slides were dipped in Eosin Y (Sigma) 15 times and dehydrated using 20 dips at each concentration of graded ethanol (70%, 95%, 95%, 95%, 100%, 100%, 100%) and placed in xylene. Stained sections were covered and sealed using 24x50 mm glass coverslips (VWR) and Cytoseal XYL mounting media (Thermo Scientific) respectively. Sealed slides were set in a fume hood to adhere for 24-48 hours prior to examination.

### 3.7.3. Immunostaining ( $\alpha$ -Pen12)

AGE pentosidine epitope content was qualitatively examined by staining slides using an anti-pentosidine antibody ( $\alpha$ -Pen12, mouse monoclonal IgG1, Transgenic Inc., Kobe, Japan). Slides were deparaffinized and hydrated using the same protocol as for H & E staining (see above). Slides were rinsed using TRIS-buffered saline (TBS) (Sigma-Aldrich) three times prior to applying a protein block (Background Punisher, BioCare Medical) for 10 minutes at room temperature in a humid chamber. Samples were rinsed once more using TBS prior to application of the primary antibody ( $\alpha$ -Pen12) using a working dilution of 5.0 $\mu$ g/mL in TBS overnight in a humid chamber at room temperature. Slides were rinsed with TBS three times, blotted and then incubated with a secondary anti-mouse antibody (MACH 4 Mouse Probe, Biocare Medical) in a humid chamber for 15 minutes at room temperature. Slides were rinsed once with TBS and incubated in a humid chamber for 15 minutes at room temperature with a horseradish peroxidase (HRP) polymer (MACH 4 HRP-Polymer, Biocare Medical). Slides were rinsed with TBS three times, washed with 3% hydrogen peroxide for 10 minutes at room temperature to block endogenous peroxidase staining<sup>93</sup>, and subsequently rinsed in TBS three times. Slides were then stained using 3,3'-Diaminobenzidine (DAB) (BioCare Medical) for 10 minutes. Post-staining, the slides were washed in a water bath and then counterstained for nuclei by placing them in Mayer's Hematoxylin (Dako) for 5 minutes. Slides were placed in the water bath, dipped in Scott's H<sub>2</sub>O until nuclei were stained blue and then washed in water. The slides were covered using glass 24x50mm coverslips (VWR), then were mounted and sealed using mounting media (VectaMount), and left to dry for 24 hours prior to evaluation. Control slides were processed as described above absent the primary antibody.

### 3.8. Statistical Analysis

Results were analyzed using JMP software (Version 14.0, SAS Institute). Dataset normality was assessed using Shapiro-Wilk tests. Parametric student-t tests were used to compare unpaired groups of normally distributed data. Non-parametric Mann-Whitney tests were used to compare unpaired groups of data in the event of non-normal datasets.

An ordinary one-way ANOVA was used to compare normally distributed data across BMI divisions. Non-parametric Kruskal-Wallis tests were used to compare non-normal datasets across BMI divisions. An ordinary two-way ANOVA was used to evaluate changes in thermal stability using either distilled water or PBS as the hydrating solution within the young and older donor cohorts.

Linear least squares regression was used to evaluate tendon collagen properties relationships with independent variables (e.g. donor age and BMI). Chi-Squared tests were used to evaluate the proportion of samples displaying load decay (i) prior to  $T_d$  and (ii) during the isotherm. A minimum level of statistical significance in this thesis was taken to be  $p < 0.05$ , although  $p$  values as large as 0.10 are reported as indicators of possible trends in the data which might be evaluated through further experiments. Unless otherwise stated, values presented in tables and text are in the format mean  $\pm$  standard deviation (S.D.).

Outliers were defined as points ranging outside of the Tukey Outlier Range shown in the following equation:

$$Outlier = \begin{cases} Value < (First\ Quartile - 1.5(IQR)) \\ Value > (Third\ Quartile + 1.5(IQR)) \end{cases} \quad (11)$$

Where IQR (Interquartile range) is defined as the range between the first and third quartile of the of the dataset. For mechanical testing, other samples were excluded including samples which had slipped, as shown by a rounded peak or a noticeable change in slope of the linear portion of the stress-strain curve without any signs of fiber rupture, resulting in a lowered  $UTS$  and increased strain at the  $UTS$ . Tukey outlier box plots were used in comparisons of tendon properties. The lines within the boxes corresponded to the median. The boxes extended to the first and third quartile of the data. Whiskers were determined by the maximum and minimum data points if the outlier criteria as shown in Equation 10 was not fulfilled. Outliers were displayed on graphs when present.

### 3.9. Methodical Limitations

The influence of diabetes on sartorius tendon collagen structure and mechanics was limited by the absence of female diabetic donors in the current study. Thus, findings of the influence of diabetes may only be inferred from the male diabetic data. Moreover, the

age range (46-60 years) prevented comparison of structure and mechanical properties of a young (20-40 years) and old (41-60 years) cohort, simultaneously negating potential significant relationships with age.

## Chapter 4: Results

### 4.1. Structural Studies of Sartorius Tendon Collagen

#### 4.1.1. Sartorius Tendon Collagen is Extremely Crosslinked and Thermally Stable

Thermal studies revealed through the range of average values of DSC  $T_{onset}$  (68.35 – 69.22°C),  $T_{peak}$  (69.78 – 70.48°C) and HIT  $T_d$  (65.57 – 66.36°C) that the sartorius tendon collagen is a highly crosslinked and densely packed structure (Table 4.1). The high degree of thermal stability was observed consistently across donor populations with respect to age, sex and diabetic status. Dense thermally stable crosslinking found in the sartorius tendon collagen was reflected in evaluation of the collagen isotherm behaviour wherein resistance to load decay was frequently observed. Overall, 63% of the total strip-samples tested via HIT resisted load decay under a 90°C isotherm. The average half-time of load decay values ( $t_{1/2}$ ) that were calculated when possible varied from 482 – 1,490 hours. Moreover, the range of FWHM values (1.73 – 1.99°C) and average water content (73.39 – 77.3%) of the sartorius tendon samples prepared for DSC testing were not significantly different between donor sample populations. Altogether, these parameters are indicative of dense heat-stable crosslinking which contribute to maintaining the structural integrity of the sartorius tendon collagen.

**Table 4.1 Average thermomechanical and thermal properties of the sartorius tendon based on donor population across their respective age range (female non-diabetic: 16-60 years, male non-diabetic: 24-59 years, male diabetic: 46-60 years). Values presented as mean ± SD.**

Method	Parameter	Female Non-Diabetic	Male Non-Diabetic	Male Diabetic
DSC	$T_{onset}$ (°C)	68.4 ± 1.1	69.2 ± 0.8	69.2 ± 0.7
	$T_{peak}$ (°C)	69.8 ± 1.3	70.3 ± 0.8	70.5 ± 0.8
	FWHM (°C)	1.91 ± 0.24	1.99 ± 0.28	1.73 ± 0.15
	Water Content (%)	77.3 ± 6.6	76.5 ± 4.1	73.5 ± 5.0
HIT	$T_d$ (°C)	65.84 ± 1.13	66.4 ± 1.0	65.6 ± 1.0
	$t_{1/2}$ (hrs)*	482 ± 568	1,490 ± 2,370	757 ± 677

\*Value calculated when applicable.

#### 4.1.2. Sartorius Tendon Collagen Thermal Stability Decreases with Age in the Female and Male Non-Diabetic Populations

Evaluation of thermal stability via DSC using distilled water as the sample hydrating medium, revealed decreases in  $T_{onset}$  ( $p = 0.0065$ ) and  $T_{peak}$  ( $p = 0.0025$ ) within the aging male non-diabetic donor population (Figure 4.1). Moreover,  $FWHM$  ( $p = 0.0477$ ) and  $h_{wet\ mass}$  ( $p = 0.0453$ ) significantly declined with age, indicative of a more homogenous collagen population in the older male non-diabetic population (Figure 4.2A & C). In tendon collagen from the female donor population, thermal stability ( $T_{onset}$ ,  $T_{peak}$ ) (Figure 4.1) and range of thermal stabilities ( $FWHM$ ) were not significantly related to age ( $p > 0.2794$ ), however, a decrease in  $h_{wet\ mass}$  ( $p = 0.0893$ ) was suggested with aging (Figure 4.2A & C). Meanwhile in tendon collagen from the respective donor populations,  $h_{dry\ mass}$  was not significantly related to age (Figure 4.2B). The changes in thermal stability with aging and diabetes evaluated by DSC may be observed in the representative endotherms in Figure 4.3, where the peak shifts left to the lower temperatures and change in shape (narrowing) is observed. Evaluating the thermal stability of the tendon collagen using HIT, it was found that in both the female non-diabetic and male non-diabetic donor population that  $T_d$  decreases with aging (Figure 4.4). Changes in the fraction of pre- $T_d$  and post- $T_d$  contraction were not related to age in respective donor populations. Despite the observed changes in thermal stability, the isotherm behaviour and average  $t_{1/2}$  did not vary significantly with age within each donor population. Due to the limited age range (46 to 60 years) of the male diabetic donors observed in the present study, relations of thermal stability determined by age were not significant.

#### 4.1.3. Isometric Contraction Occurs Prior to Denaturation

Thermally induced isometric contraction occurred prior to denaturation in 82% of the total samples in the entire donor population (Figure 4.6). The frequency and magnitude of the pre- $T_d$  contraction was consistent across each donor population. This behaviour was atypical to that observed in studies of bovine tendons<sup>275</sup> where stress relaxation occurs prior to denaturation. The amount of pre- $T_d$  and post- $T_d$  contraction

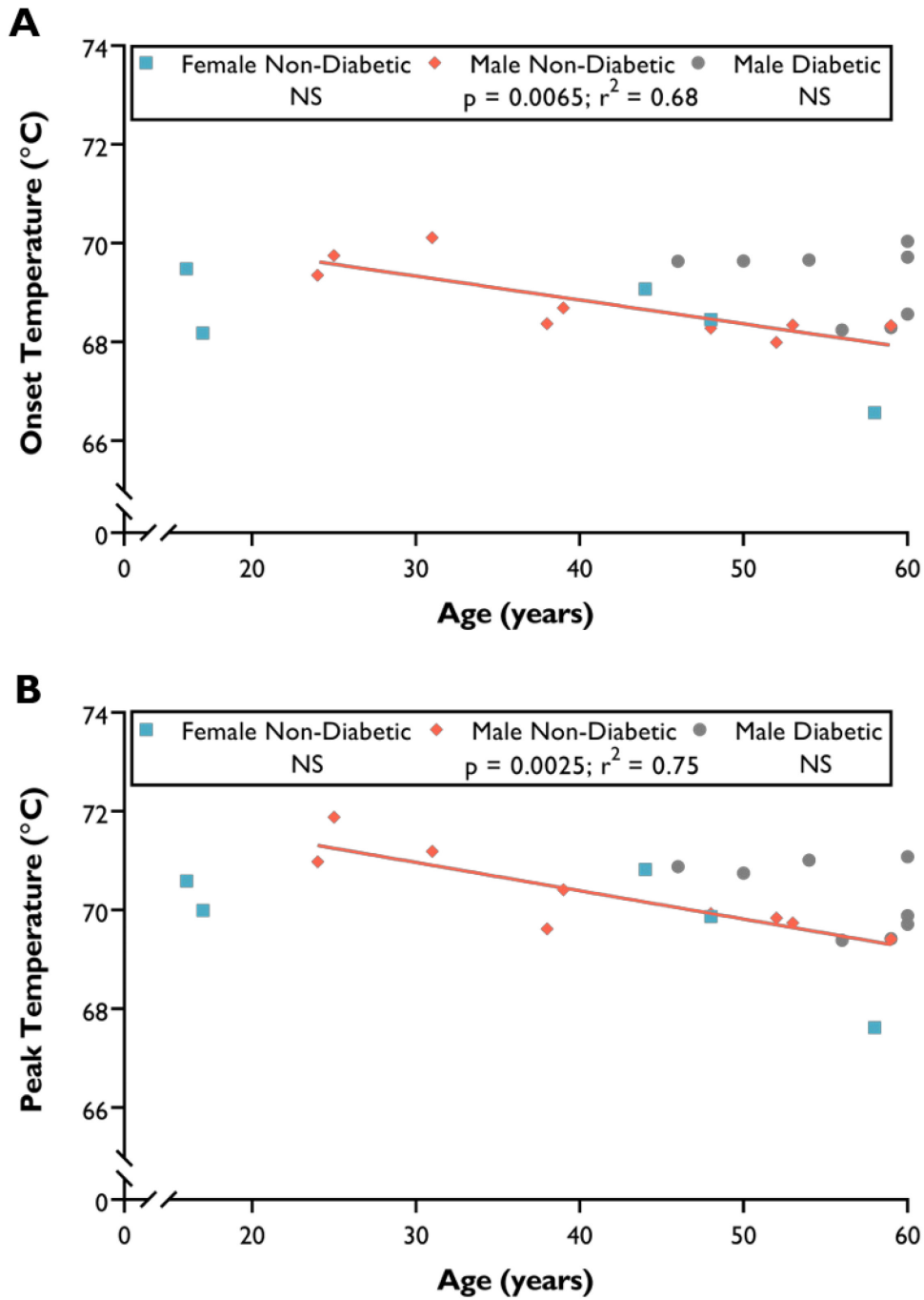


Figure 4.1 Scatterplots of DSC (A)  $T_{onset}$  and (B)  $T_{peak}$  plotted against age using distilled water as the hydrating medium revealed that thermal stability of the male non-diabetic donor tendon collagen decreased significantly with increasing age.



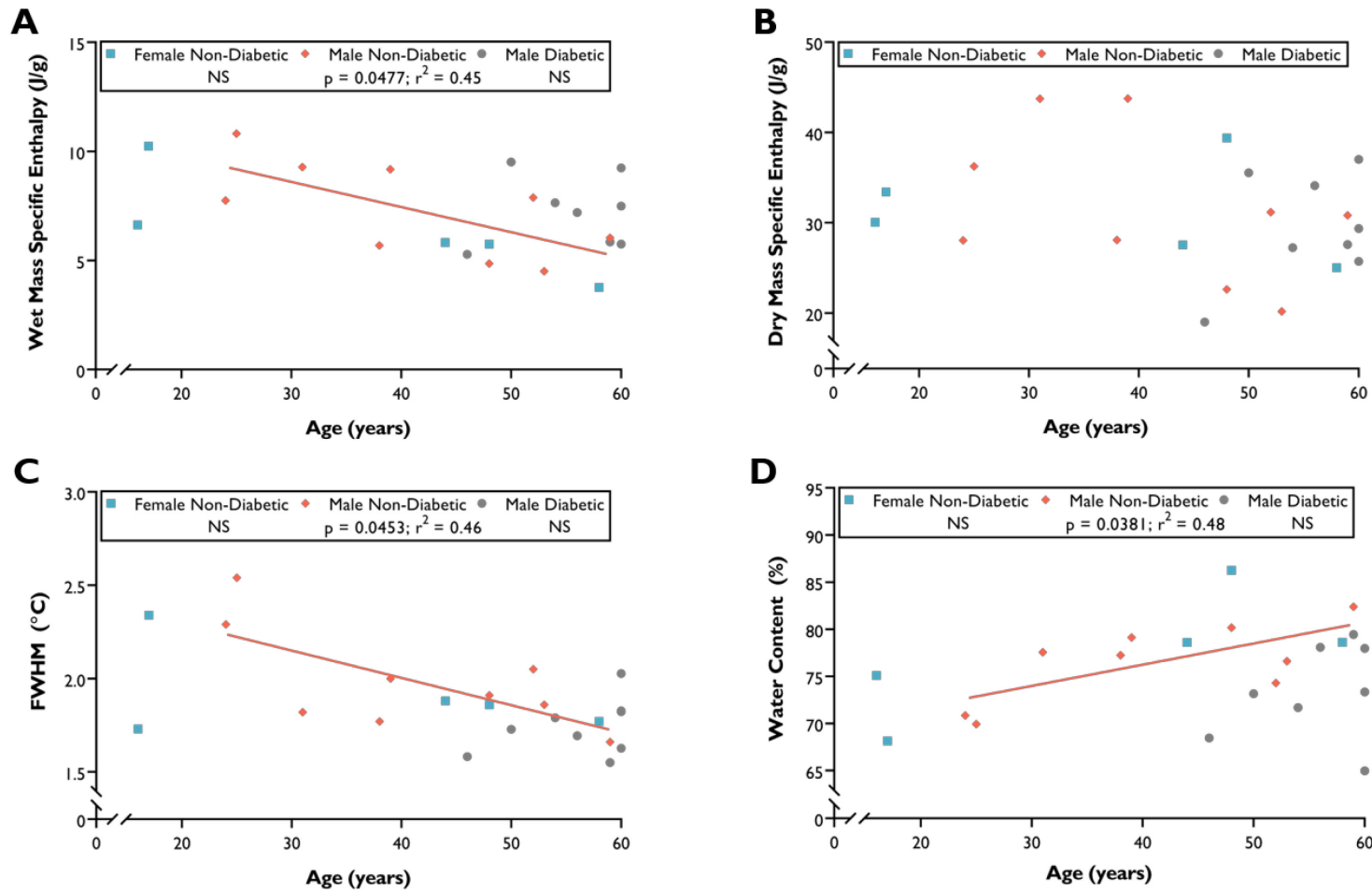


Figure 4.2 Scatterplots of additional DSC parameters evaluated versus age using distilled water as the sample hydrating medium. Scatterplots of (A)  $h_{wet\ mass}$  ( $p = 0.0477$ ) and (C)  $FWHM$  ( $p = 0.0453$ ) showed declining relations with increasing age within the male non-diabetic donor population. (B)  $h_{dry\ mass}$  appears to remain unchanged with age in tendon collagen from each donor population. (D) Average tendon sample water content was shown to increase with age within the male non-diabetic donor population.

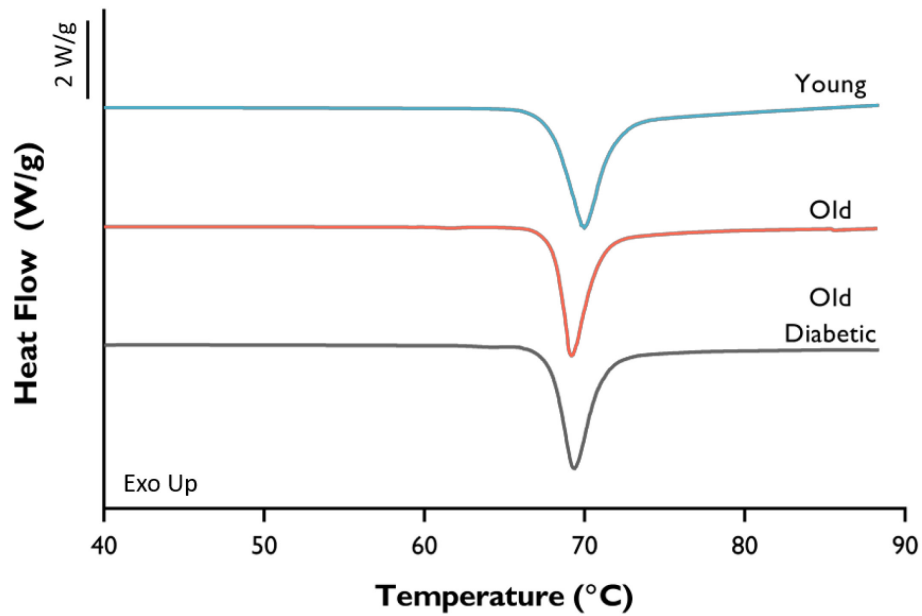


Figure 4.3 Representative DSC (Heat Flow) curves y-scale adjusted to reveal the differences in collagen thermal behaviour with age and diabetes. The noticeable shifting of the endotherm peak to the left with aging and diabetes to the left is indicative of a lowered  $T_{onset}$  and  $T_{peak}$ . Similarly, a narrowing of the endotherm peak may be observed indicating a smaller range of thermal stabilities ( $FWHM$ ). The young curve (blue) was taken from a 24-year old male non-diabetic donor. The old curve (red curve) was taken from a 59-year old male non-diabetic donor. The old diabetic curve (grey curve) was taken from a 54-year old male diabetic donor. (Scale bar is 2W/g.)

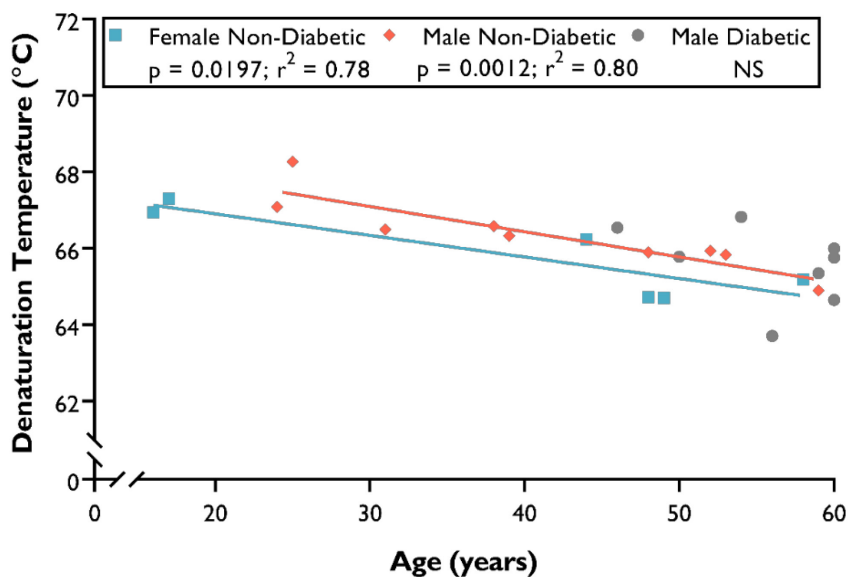


Figure 4.4 HIT denaturation temperature plotted against age revealed thermal stability declined with increasing age for both the female non-diabetic and male non-diabetic populations. The slopes of the regression lines were not significantly different. The y-intercept values varied significantly ( $p = 0.0261$ ) with a slight increase in the male non-diabetic compared to the female non-diabetic population ( $69.07^{\circ}\text{C}$  to  $68.03^{\circ}\text{C}$ ).

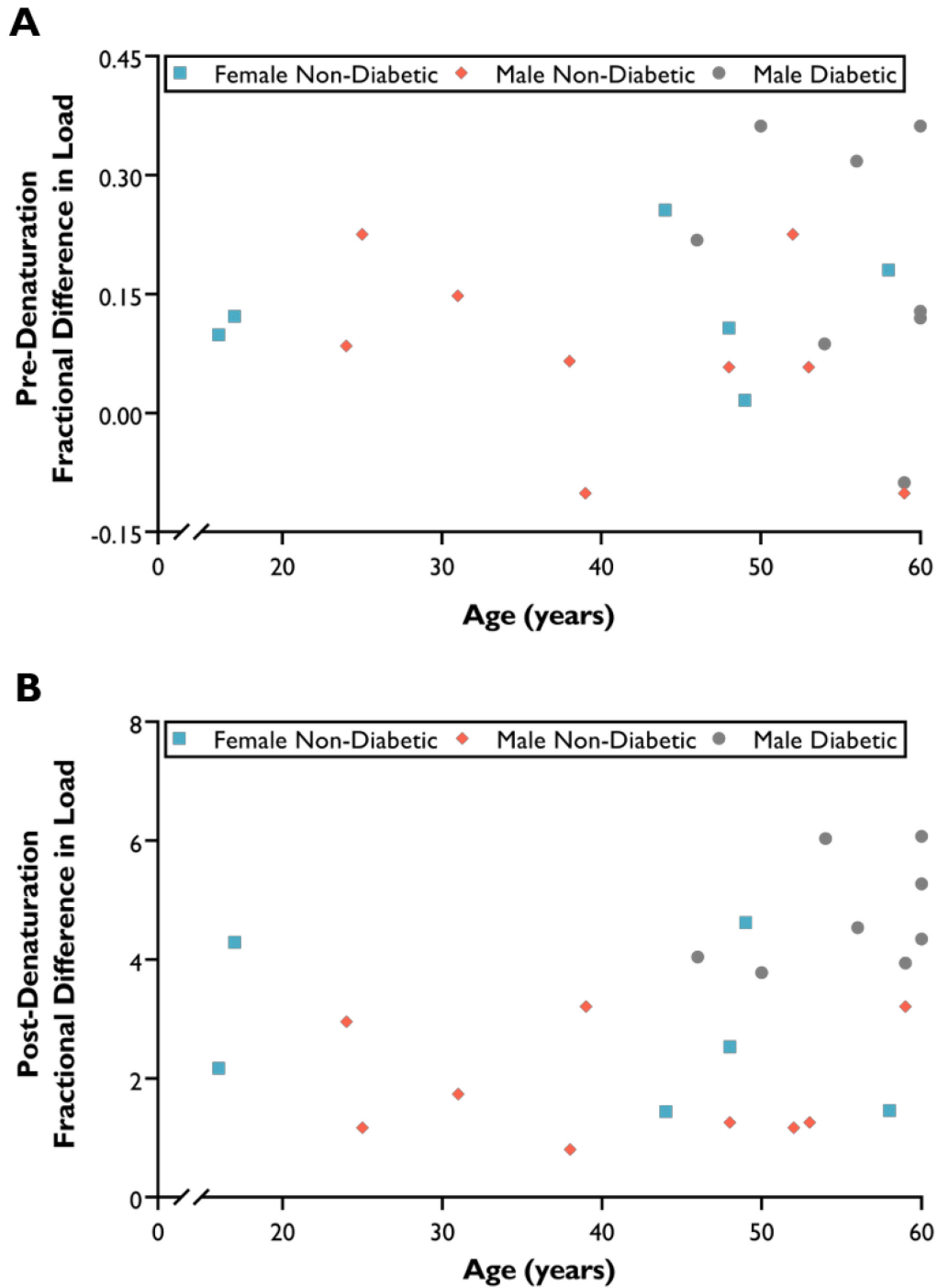


Figure 4.5 Scatterplots of the fractional differences in load (A) pre- $T_d$  and (B) post- $T_d$  versus age. The amount of contraction pre- and post- $T_d$  was not governed by age and was not significantly different between donor populations.

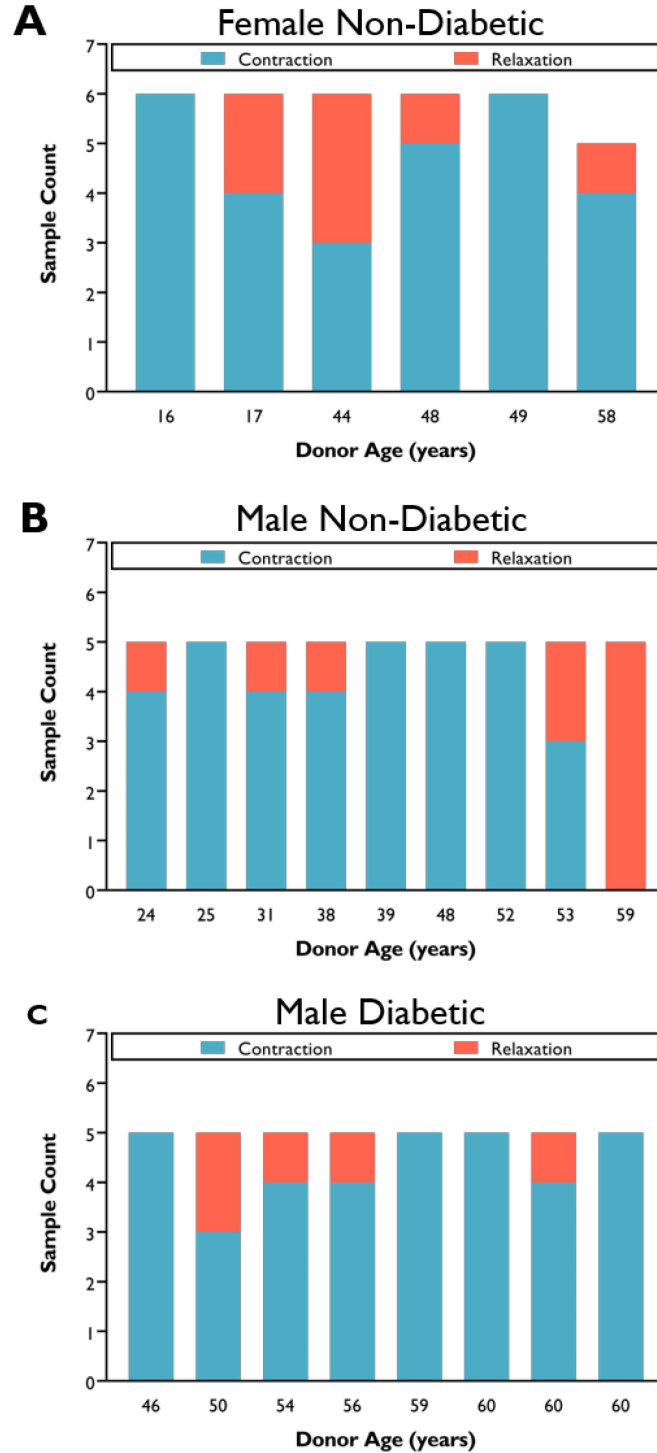
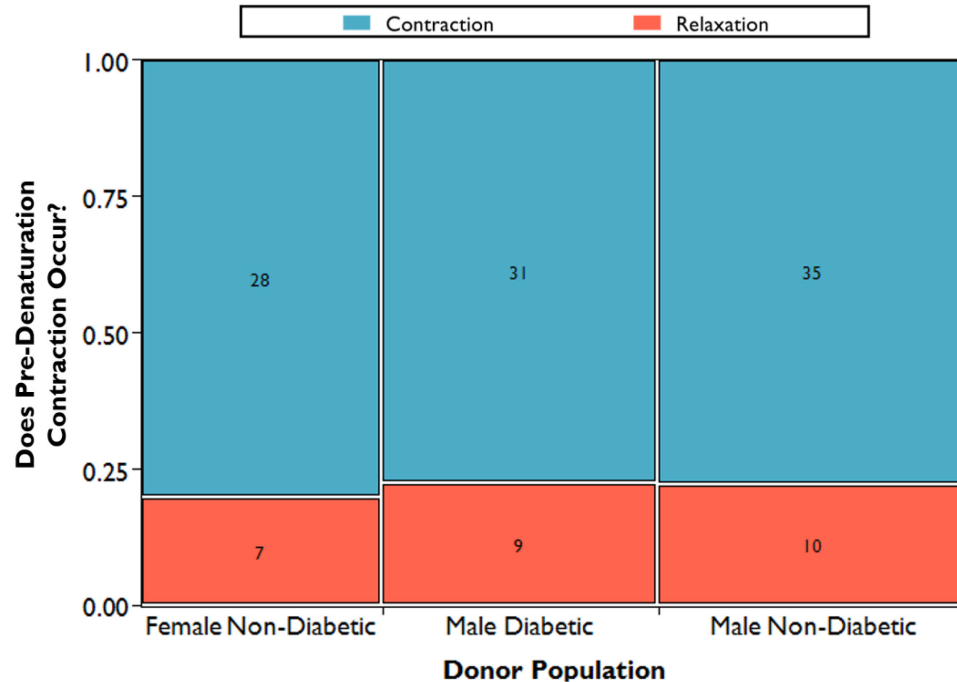


Figure 4.6 Stacked column graphs of the fractional difference in load pre- $T_d$  in HIT strip samples for each individual (denoted by their age) of a given donor population. The blue represents the samples that contracted, and the red represents the samples that relaxed during the period of temperatures prior to denaturation. Graphs A, B, and C represent the female non-diabetic, the male non-diabetic and the male diabetic donor populations respectively. Overall, a high percentage of the samples do contract prior to  $T_d$ .



**Figure 4.7** Mosaic plot displaying the count and percentage of HIT strip samples from each donor population that underwent isometric contraction or relaxation pre- $T_d$ . A chi-squared test revealed there was no significant likelihood that the donor population impacted the fraction of samples that contracted pre- $T_d$  ( $\chi^2 = 0.9442$ ).

was not significantly dependent on age (for each donor population:  $p > 0.30$  and  $r^2 < 0.16$ ). A chi-squared analysis (Figure 4.7) revealed that the proportion of contraction to relaxation prior to  $T_d$  was independent of donor population ( $\chi^2 = 0.9442$ ). In the male non-diabetic donor population, the fraction of post- $T_d$  contraction significantly decreased with increasing pre- $T_d$  contraction ( $p = 0.0363$ ;  $r^2 = 0.49$ ) as shown in Figure 4.8. A similar trend was observed when evaluating the entire donor population ( $p = 0.0146$ ;  $r^2 = 0.25$ ), suggesting that there is a finite amount of thermally induced contraction that occurs within a tendon collagen strip sample across all donor populations.

#### 4.1.4. Isometric Contraction Occurs within the Isothermal Segment

Investigating the interval of 5,000 to 10,000 seconds after the start of the isothermal segment (Figure 4.9) revealed that a high percentage of samples displayed isometric contraction (Figure 4.10). Classification of the isothermal behaviour in four categories: contraction (55%), constant load (8%), relaxation (34%), or failure (3%) revealed that a high quantity of samples (63%) underwent contraction or remained in

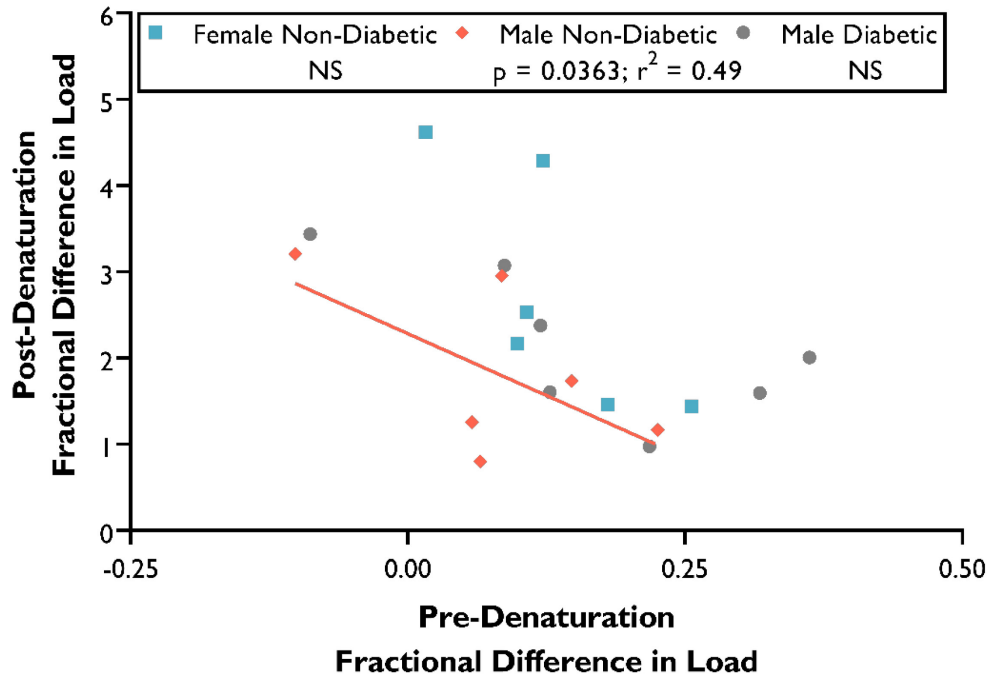
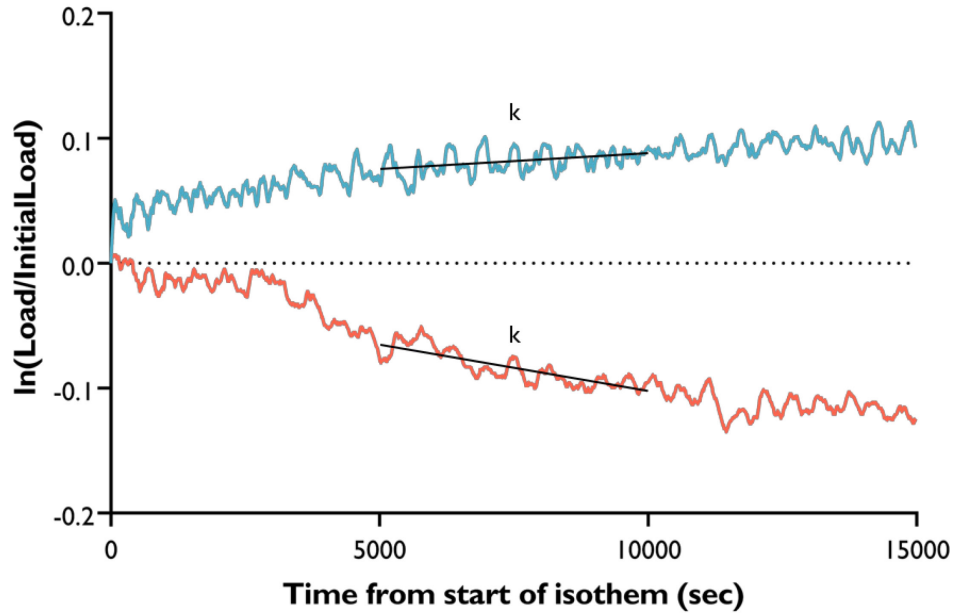


Figure 4.8 Scatterplot of the fractional difference in load post- $T_d$  versus pre- $T_d$ . In the Male ND donor population, a significant declining relationship ( $p = 0.0363$ ;  $r^2 = 0.49$ ) was observed. As a combined population ( $p = 0.0146$ ;  $r^2 = 0.25$ ), a significant declining relationship that weakly suggested that a specific degree of contraction occurs across all sample populations.

constant isometric loading. This isothermal behaviour has not been observed in the bovine tendon models previously explored<sup>109,255,275</sup>. In combination with the elevated denaturation temperatures, this isothermal behaviour suggests that the sartorius tendon collagen is a densely crosslinked structure independent of sex, age and diabetes. Average values of  $t_{1/2}$  for the proportion (37%) of samples demonstrating load decay from a given donor and donor population may be found in the Appendix A, however, the values are limited in their usefulness as they are not representative of the entire sample population. Occasionally, contraction or load decay would occur from 5,000 – 10,000 seconds after the start of the isotherm only to plateau over the last few thousand seconds of testing and vice versa. Additional analyses would be to compare the behaviour at the two time points in the isotherm.



**Figure 4.9 Comparison of the contraction or decay behaviour during the isotherm. The slope value  $k$  is calculated between 5,000 and 10,000 seconds from the start of the isotherm. Load decay occurred in 42/120 (35%) and rupture in 5/120 (4.5%) of the total HIT strip samples tested across the entire donor population. In the absence of load decay, the Maxwell-type analysis is invalid and would not yield a meaningful constant  $k$ .**

#### 4.1.5. Hydration may play a role in Sartorius Tendon Collagen Thermal Stability

The average water content of the sartorius tendon DSC samples across the entire donor population was  $75.62 \pm 5.08\%$ . DSC sample water content was found to be independent of sex and diabetes (Table 4.1). Water content increased with age in the sartorius tendon collagen from male non-diabetic donors ( $p = 0.0381$ ;  $r^2 = 0.48$ ), yet was unchanged with age in the female donor population ( $p = 0.1651$ ). Moreover, water content was not significantly related with age when accounting for the entire donor population ( $p = 0.2176$ ). Evaluation of DSC parameters versus water content in the entire donor population (Figure 4.11) revealed declining relationships in  $T_{onset}$  ( $p = 0.0148$ ;  $r^2 = 0.26$ ),  $T_{peak}$  ( $p = 0.0311$ ;  $r^2 = 0.26$ ),  $FWHM$  ( $p = 0.0406$ ;  $r^2 = 0.26$ ) and  $h_{wet\ mass}$  ( $p = 0.0311$ ;  $r^2 = 0.26$ ). The low  $r^2$  values indicate that water content, although significant, is not a strong predictor of collagen thermal stability due to the high degree of variability in the data. Combining the female and male non-diabetic donor populations as shown in Figure 4.12, HIT  $T_d$  significantly decreased ( $p < 0.0001$ ) with increasing DSC sample water content, indicative of changes in the molecular packing.

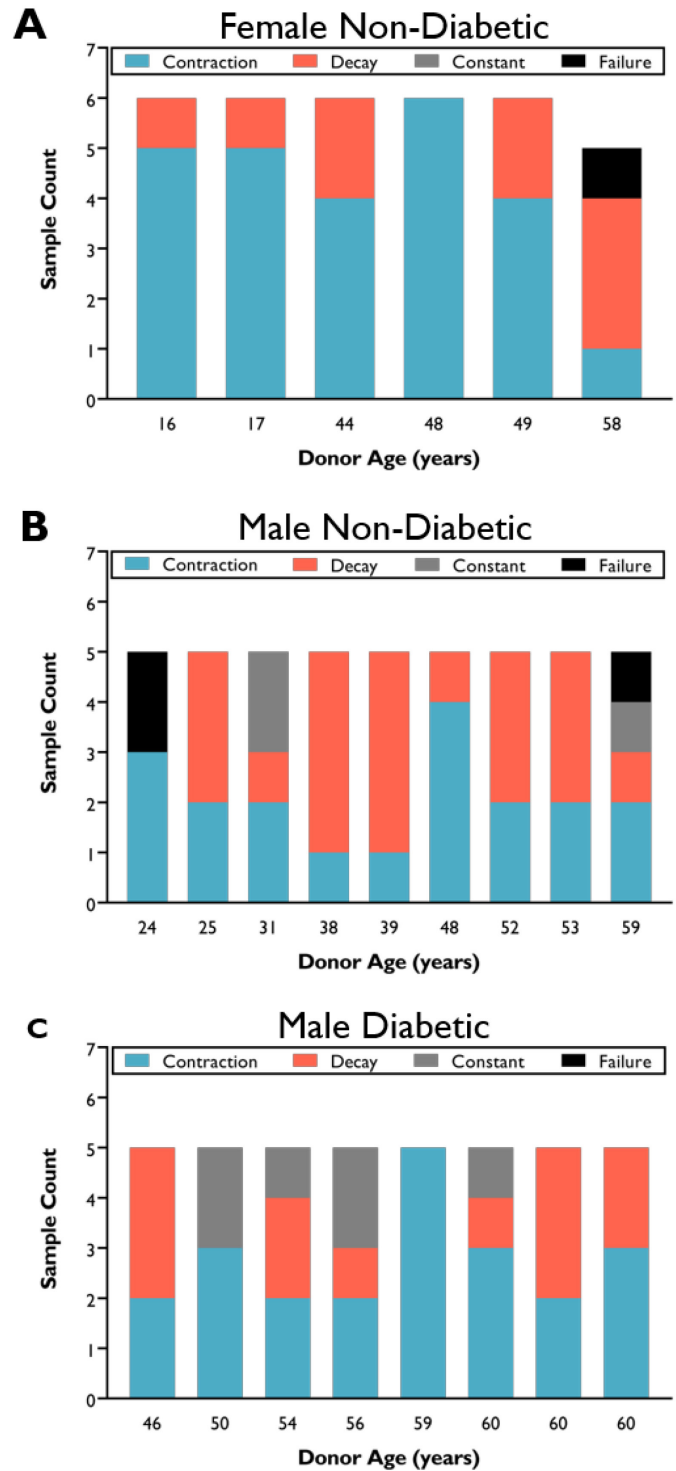


Figure 4.10 Isothermal behaviour was classified into four categories: contraction, decay, constant loading or failure for each sample in a HIT test for a donor tendon. Columns were divided by the donor ages. Graphs A, B, and C represent the female non-diabetic, the male non-diabetic and the male diabetic donor populations respectively. No relationships were found comparing the behaviour of the number of samples that contracted, decayed, remained at a constant loading or failed between and within donor populations



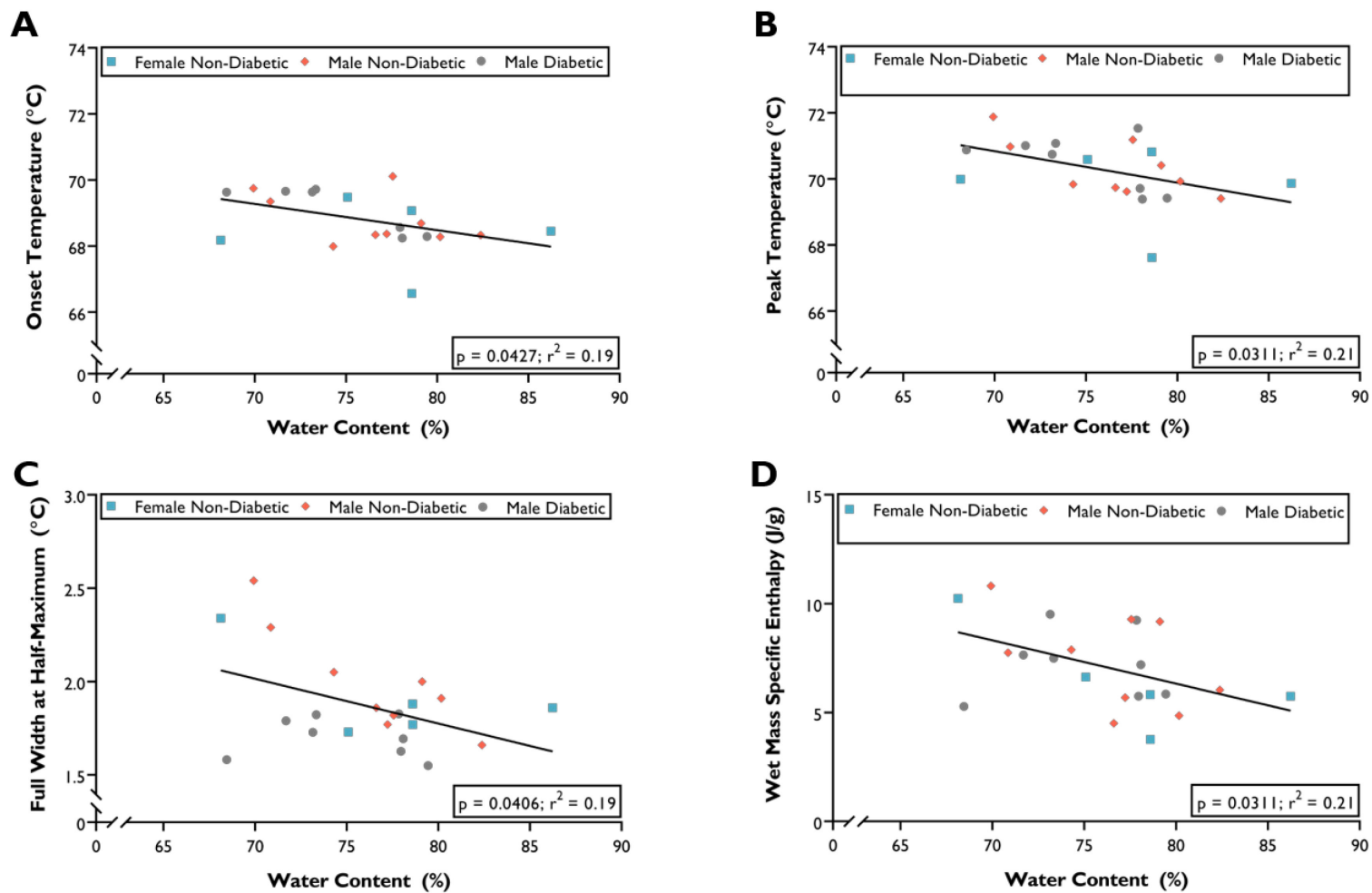


Figure 4.11 Evaluating DSC parameters of the entire donor population revealed linear decreases with increasing water content when calculated for the entire donor population: (A)  $T_{onset}$ , (B)  $T_{peak}$ , (C)  $FWHM$  and (D)  $h_{wet\ mass}$ . Although each relationship was significant, poor  $r^2$  values obtained indicate that water content is not a strong predictor of collagen thermal behaviour.

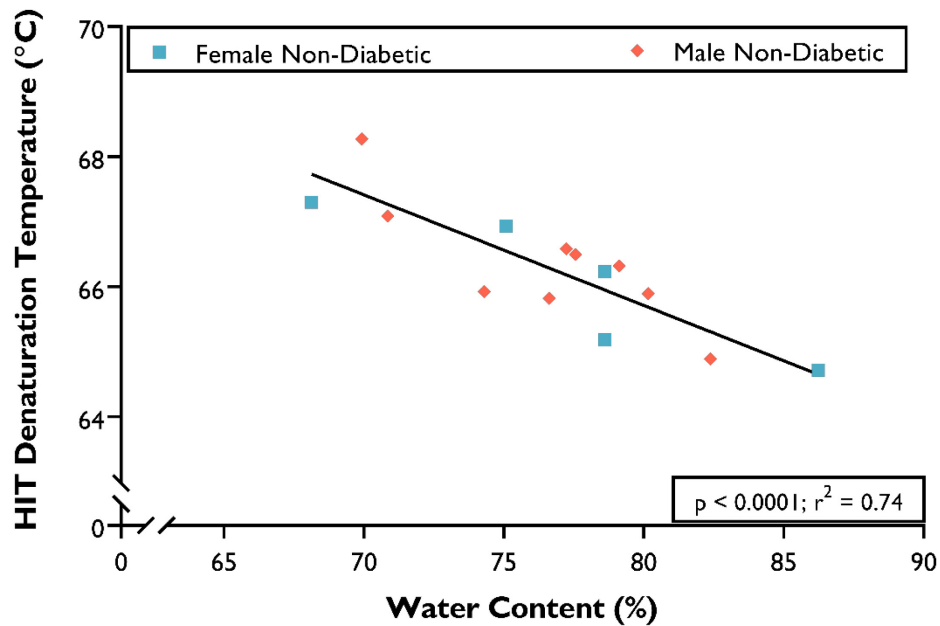


Figure 4.12 Scatterplot of HIT denaturation temperature versus DSC sample water content. A negative linear relationship with HIT denaturation temperature and water content was found in a pooled female non-diabetic and male non-diabetic donor population ( $p < 0.001$ ;  $r^2 = 0.74$ ). Furthermore, this decreasing relationship was likewise found for the female non-diabetic ( $p = 0.0360$ ;  $r^2 = 0.81$ ) and male non-diabetic ( $p = 0.0054$ ;  $r^2 = 0.69$ ) donor populations.

## 4.2. Mechanical Overload Studies of Sartorius Tendon Collagen

### 4.2.1. Sartorius Tendon Multi-Fascicle Subsample Failure Occurs via Stepwise Rupture of Fascicles

With a multi-fascicle subsample secured properly in the custom waveform grips, constitutive fascicles (fibre bundles) ruptured in a stepwise manner as illustrated by the representative curves in Figure 4.13. The high elastic energy snapping of the individual fibre bundles was clearly audible, even over the sound of the servo-hydraulic system. Based on the loading distribution, the number of discrete bundles providing mechanical integrity of a subsample ranged from as little as three to as many as fifteen discrete bundles, indicated by the number of piecewise failures in the stress-strain curves. Across the entire donor population, the average gauge length was  $14.5 \pm 2.5$  mm and the average cross-sectional area was  $1.82 \pm 0.82$  mm<sup>2</sup> of the multi-fascicle subsamples. The sample gauge length and CSA for each of the donor populations are reported in Table 4.2. The

manner wherein individual fascicle first failed varied from test to test. During a test, the first fascicle failure would occur either at the extremities of or near the middle of the CSA. Both modes of fascicle rupture provided a narrowing of the CSA of the sample as observed in Figure 4.15. Furthermore, the sample failures typically occurred in the mid-substance of the samples and not near the grip edges where stress concentrations may occur. Proper mounting of the samples would prevent edge stress concentrations that would lead to premature failure. Consistency of the testing methodology was reflected in a scatterplot of modulus versus strength wherein relationships of or approaching significance were observed within each donor population (Figure 4.14). Throughout the study, no differences were observed in the manner that failure (upon examination of the stress-strain curves) of the multi-fascicle subsamples occurred based on sex, diabetes, and age.

**Table 4.2 Physical dimensions of the mechanical testing multi-fascicle subsamples. Values expressed as mean  $\pm$  SD.**

<b>Donor Population</b>	<b>Sample Gauge Length (mm)</b>	<b>Cross-Sectional Area (mm<sup>2</sup>)</b>
<b>Female Non-Diabetic</b>	14.8 $\pm$ 2.3	2.25 $\pm$ 0.79
<b>Male Non-Diabetic</b>	13.5 $\pm$ 2.8	1.54 $\pm$ 0.75
<b>Male Diabetic</b>	15.3 $\pm$ 1.9	1.88 $\pm$ 0.81
<b>Total Population</b>	14.5 $\pm$ 2.5	1.82 $\pm$ 0.82

#### 4.2.2. *Sartorius Tendon Multi-Fascicle Subsample Strength Declined with Age in Female Donors*

As previously discussed (Section 4.1.2), investigations of the tendon collagen crosslinking revealed declining thermal stability with age through DSC ( $T_{onset}$ ) and HIT ( $T_d$ ). However, using a nominal strain rate of 0.25% strain/second, the only mechanical property (Figure 4.16) found to reflect these structural changes was the declining tendon strength ( $p = 0.0232$ ) in the female donor population with aging. Moreover, a declining relationship with toughness and aging was almost significant ( $p = 0.0708$ ) in the female donor population. Curiously, in the tendon collagen from male non-diabetic and diabetic

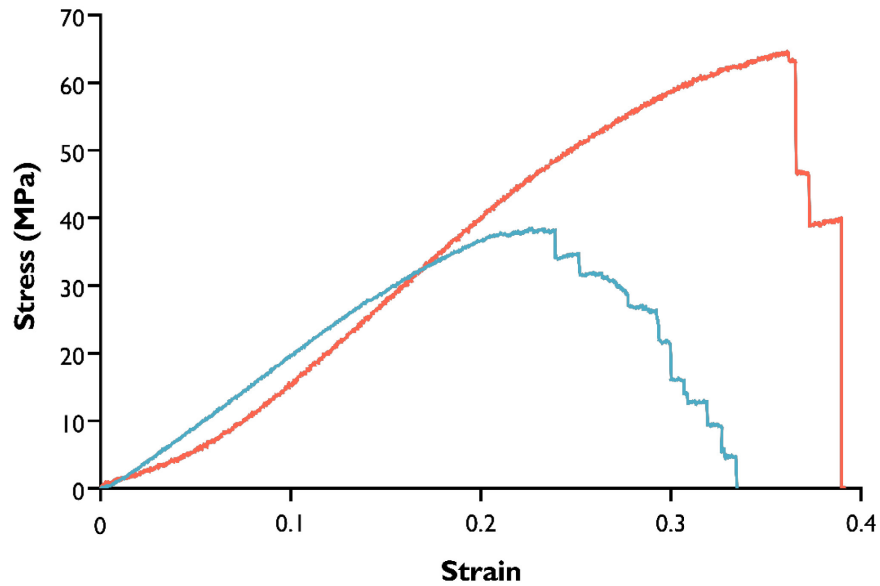


Figure 4.13 Representative stress-strain curves of tendon multi-fascicle subsamples produced by overload to rupture testing using a strain rate of 0.25% strain/second. The feature of note is the stepwise failure of fascicular subcomponents prior to loss of total mechanical integrity. The blue curve (female non-diabetic, 16-years of age) represents a sample made up of multiple load-bearing fascicles. The red curve (male non-diabetic, 48-years of age) represents a sample made up of few load-bearing fascicles.

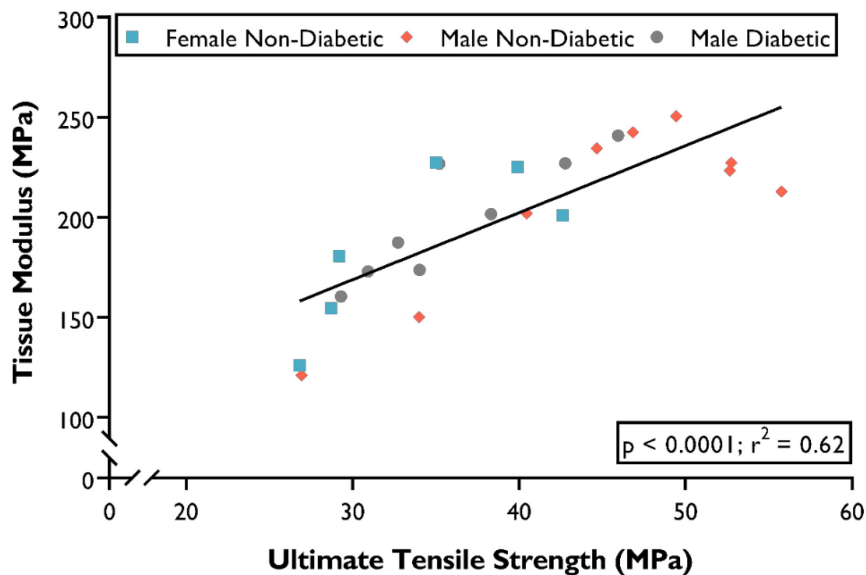
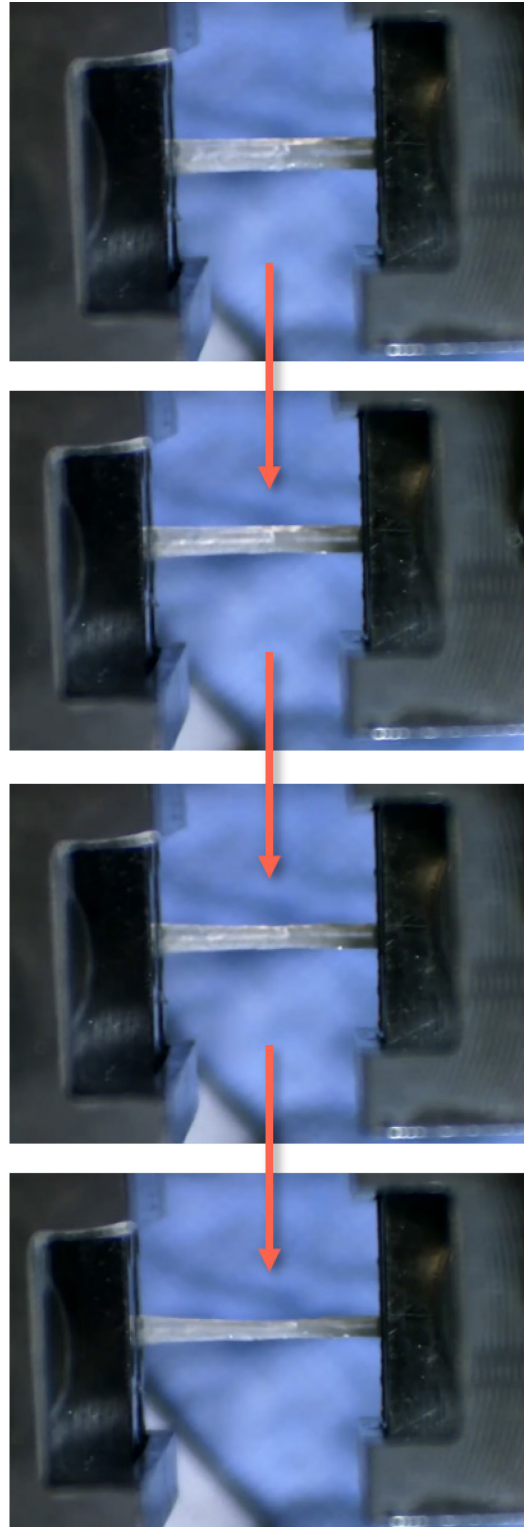


Figure 4.14 Scatterplot of tissue modulus versus UTS of tendon multi-fascicle subsamples. Samples from male non-diabetics ( $p = 0.0046$ ,  $r^2 = 0.71$ ) and diabetics ( $p = 0.004$ ,  $r^2 = 0.77$ ) each displayed significant increasing relationships, whereas female non-diabetic data suggests a similar increasing relationship of UTS and tissue modulus. When pooling the entire donor population, a significant increasing relationship of tissue modulus and strength was identified ( $p < 0.0001$ ;  $r^2 = 0.62$ ).



**Figure 4.15** Sequence of images capturing the failure of a sartorius tendon multi-fascicle subsample secured by the custom waveform crush grips strained at 0.25%/second. Fibre bundles fail in a stepwise manner observed by the reduction in cross-section in the images and in the stress-strain curve (Figure 4.13).

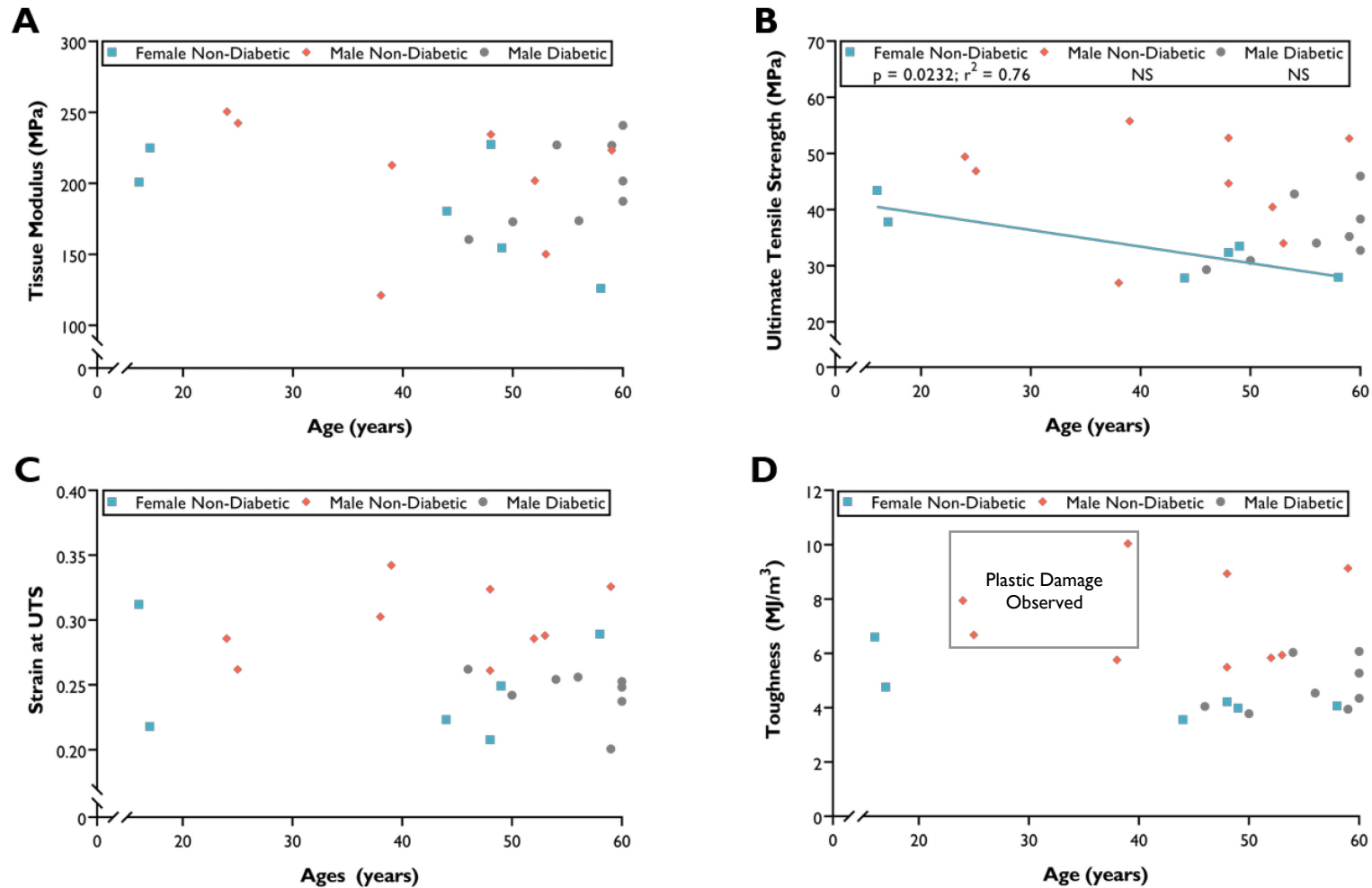


Figure 4.16 Mechanical properties of the tendon collagen plotted versus age. Mechanical parameters (A) tissue modulus, (C) strain at *UTS* and (D) toughness were independent of age for all donor populations. The shaded box highlights the tendons in which plastic deformation of collagen fibrils was observed via SEM. (B) *UTS* declined with age in the female non-diabetic population.

donor populations, none of the mechanical testing parameters approached significance with a high degree of variability between donors of similar age. This large variation was likely in part to donor dependent factors (e.g. genetics, lifestyle) not accounted for in the present study.

#### **4.3. SEM Structural Studies and Failure Motifs of Sartorius Tendon Collagen**

Scanning Electron Microscopy was used to evaluate evidence of structural disruption and damage in tendon samples from each donor population after overload to rupture ( $n_{F,ND} = 6$ ,  $n_{M,ND} = 8$ ,  $n_{M,D} = 8$ ). For each donor, an unloaded control and a minimum of 4 ruptured tendon samples were evaluated.

##### *4.3.1. Unloaded Control Sample SEM Micrographs Reveal Relatively Tight-Packing and D-banding in Registry Amongst Neighboring Collagen Fibrils.*

SEM micrographs of the unloaded/untested control samples from each donor did not show the presence of flattened regions indicative of fibrils which had uniformly straightened out by applied overload. Even at the lower magnifications ( $\sim 2000\times$ ), although collagen crimp waveform was observed at lower magnifications, evidence of densely packed fibril bundles was observed. At higher magnifications ( $\sim 15,000$ - $70,000\times$ ), SEM micrographs revealed tightly packed collagen fibrils and intact D-banding (Figure 4.17). Neighboring fibrils exhibited D-banding in registry and a retention of clear D-banding. The presence of non-collagen extracellular matrix components was suggested by a filamentous webbing occasionally covering the fibril surfaces.

##### *4.3.2. SEM Examination Reveals Damage Motifs Characteristic of High-Energy Elastic Piecewise Failure and Absence of Discrete Plasticity*

Overall, regions of tendon damage in the ruptured samples of sartorius tendon were sparse and infrequent. Adding to the difficulties in exploration of these samples were limitations based on the orientation of the bisected samples on the carbon taped stubs. To expedite tendon sample scanning, examination of select locations included across the cross-section of the longitudinal ends, middle and flattened regions was performed. In contrast to bovine tendon studies performed by Veres *et al.*<sup>257</sup> and

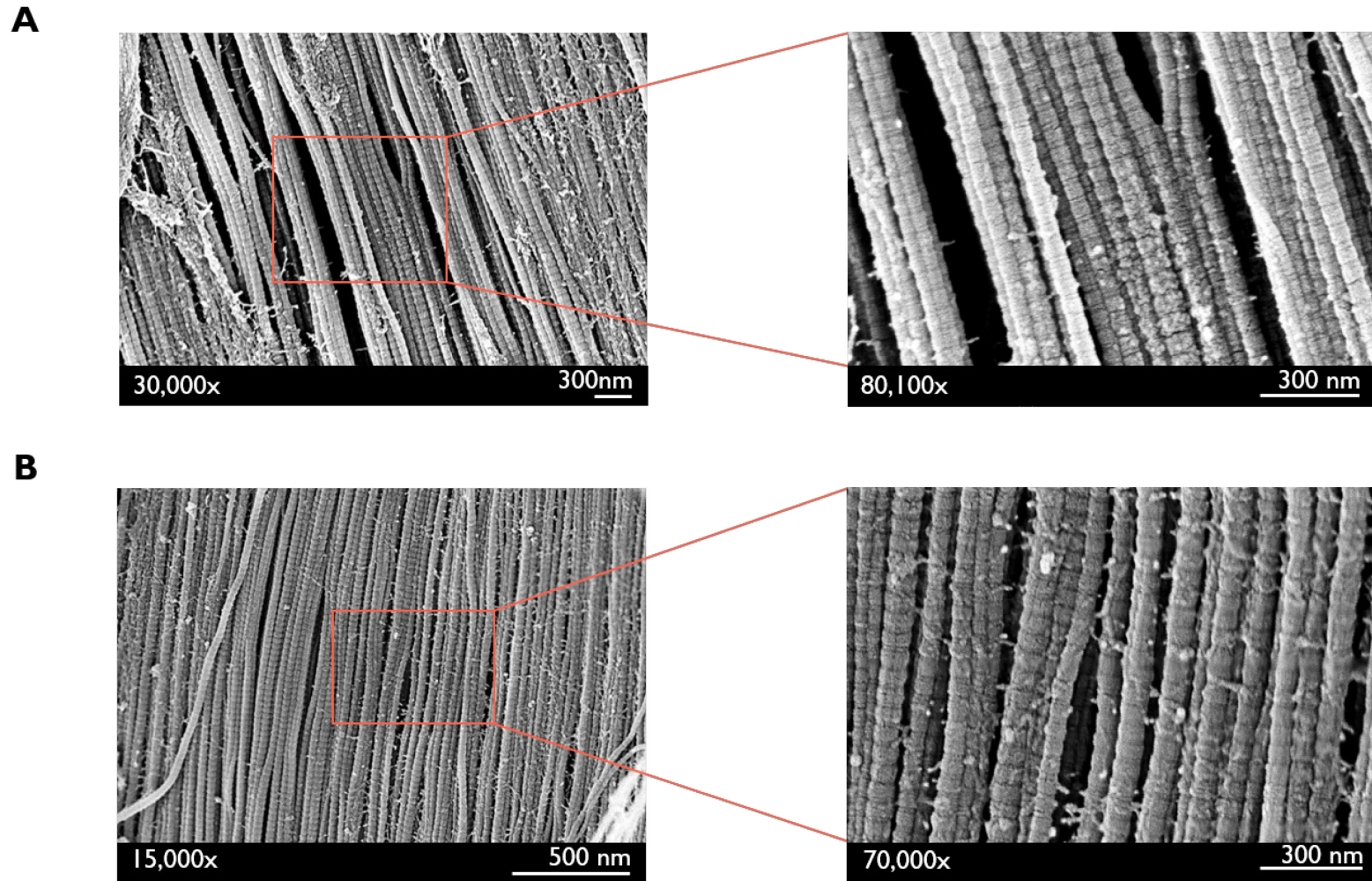
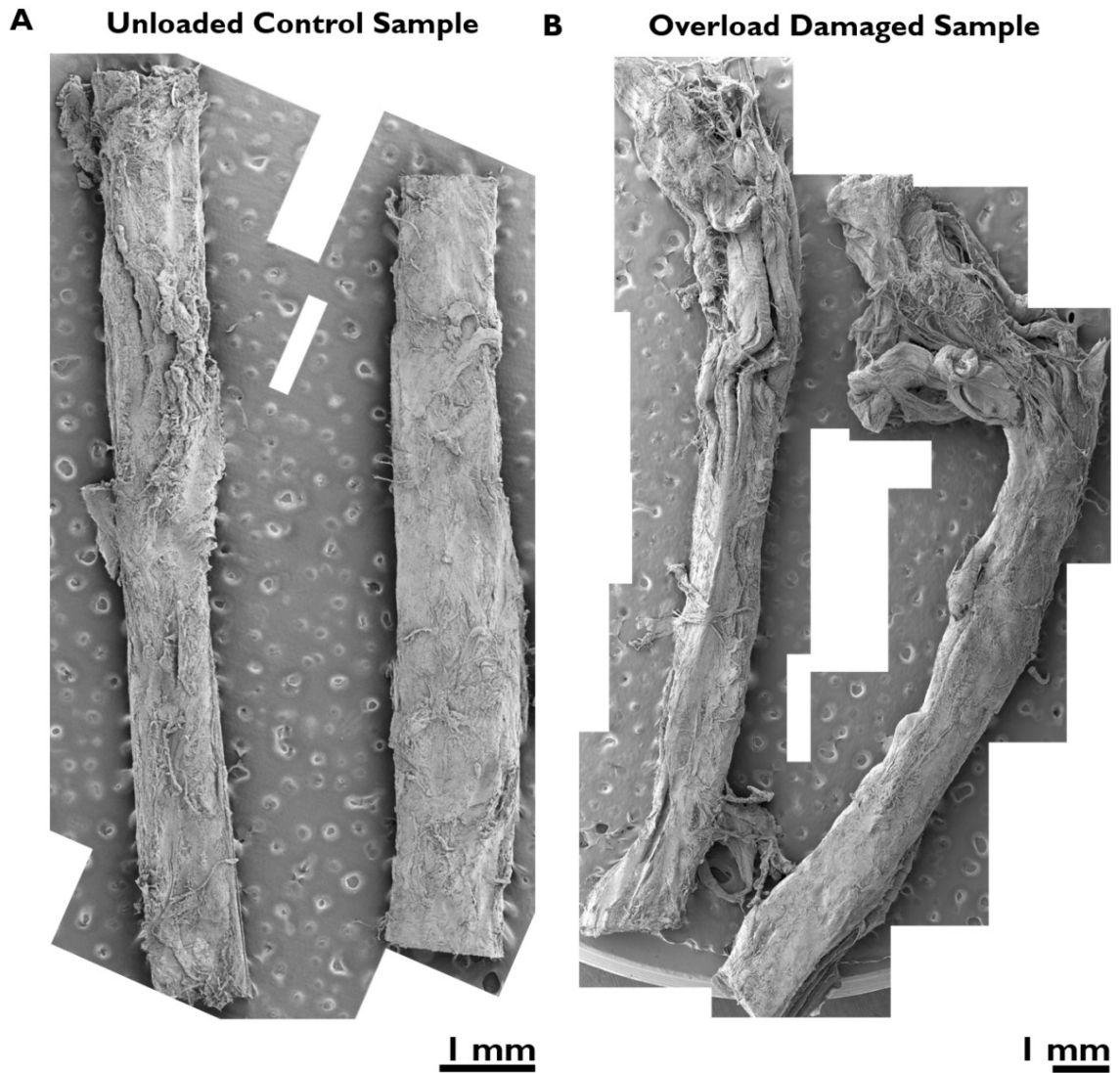


Figure 4.17 SEM micrographs of unloaded control images displaying neighboring fibrils with D-banding in registry. High and low magnification micrographs reveal dense fibril packing. The presence of ECM components is suggested by the debris covering the fibril surfaces.



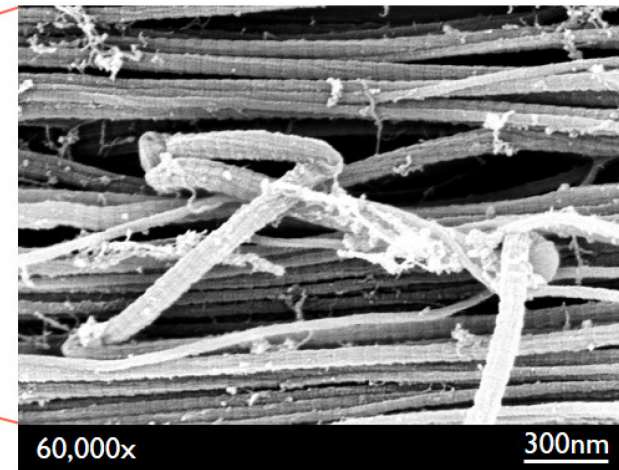
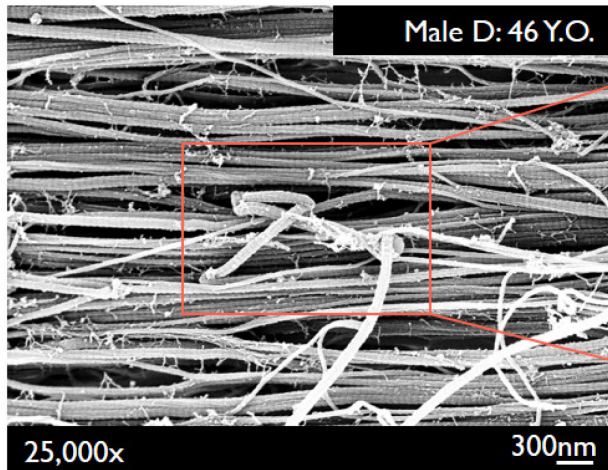
Herod *et al.*<sup>109</sup>, where discrete plasticity motifs are observed, discrete plasticity was absent in the human sartorius tendon samples. In the bovine tendon models, extensive regions of collagen fibrils were found to be kinked at regular intervals with loss of D-banding between or at the kink sites.

In the sartorius tendon, although a few distinct damage motifs were identified as follows, composite overview micrographs (40x magnification) displayed some evidence of structural disorganization between undamaged and damaged samples (Figure 4.18). Firstly, many isolated fibril hairpin turns were observed. Often in these scenarios, it was single fibrils affected (Figure 4.19); however, at times multiple fibrils were affected (Figure 4.20). Within these hairpin turns, the D-banding was preserved and the subfibril structure was often revealed. As shown in Figure 4.20C, the substructure of the fibrils could often be observed in otherwise undamaged fibrils throughout tendon samples from varying donors. Collagen fibrils undergoing hairpin turns likewise occurred at a lowered frequency within unloaded control samples. High energy elastic fibre snapping and recoil was observed during testing and recorded as discrete down-steps in the stress-strain curve were reflected in the second motif, structural disorder accompanied by twisting (Figure 4.21B), tangling and balling of ruptured fibrils (Figure 4.21A, C & D). Local failure and complete breakage was observed in both isolated (Figure 4.22A & B) and neighboring fibrils (Figure 4.22C). Disruption of the fibrillar substructure and loss of D-banding occurred only at the damage sites. Third, examples of plastic damage were found in tendon samples from the tougher younger male (non-diabetic) donor population (refer to box in Figure 4.16D). These minuscule regions of damage extending at maximum ~200  $\mu\text{m}$ , appeared noticeably flattened and straightened at low magnifications (40x). At higher magnifications (>15,000x), those fibrils displayed kinking, subfibrillar disruption, and softening of appearance (loss of D-banding) are defined as plastic deformation (Figure 4.23). In micrograph B of Figure 4.23, loss of D-banding and disrupted structure in the form of dark spots in the twisted collagen fibrils, however interkink D-banding is preserved. This behaviour occurred in a number of fibrils in the damaged regions, however it lacked the consistent serial kinking along a fibril shown with the previously described discrete plasticity damage in the bovine tendon models<sup>109,257</sup>. However, the areas of plastic damage, but not discrete plasticity, is consistent with what was found for



**Figure 4.18** Representative SEM composite micrographs at 40x magnification of (A) an unloaded control sample and (B) an overload damaged sample. Differences are observed in the level of structural disorganization between the two representative sample micrographs. Micrographs of tendon multi-fascicle subsamples are from a 16-year old female non-diabetic donor.

**A**



**B**

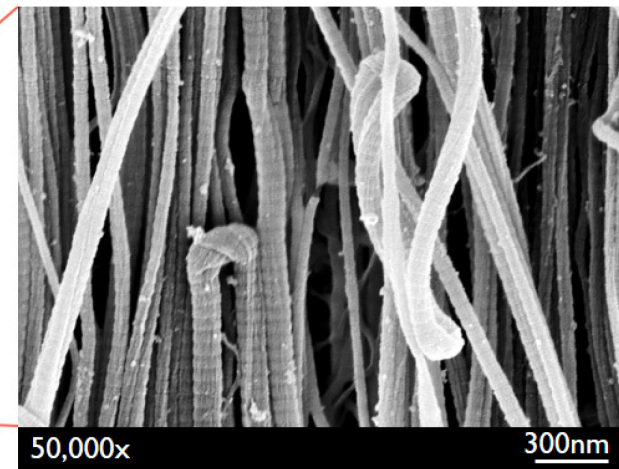
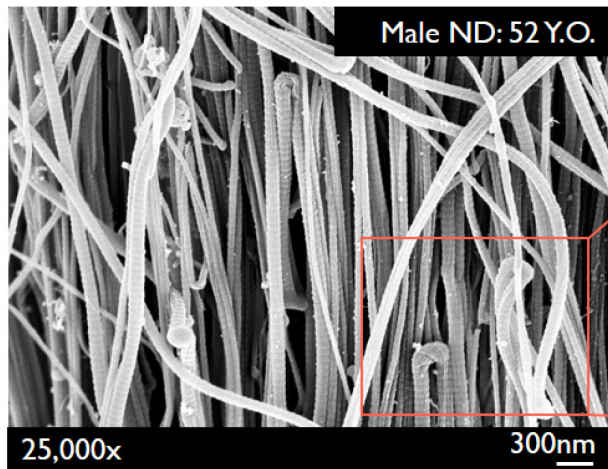
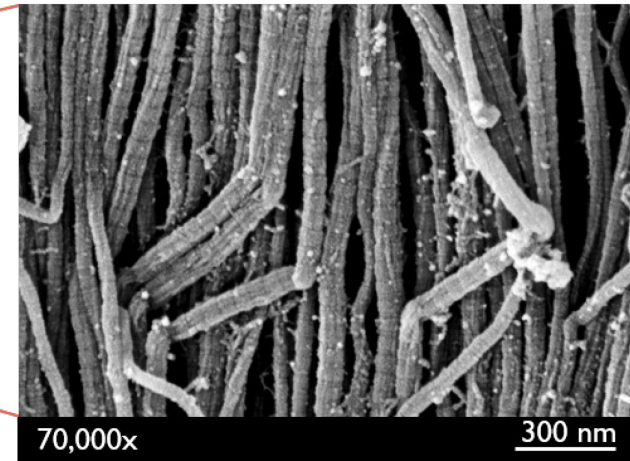
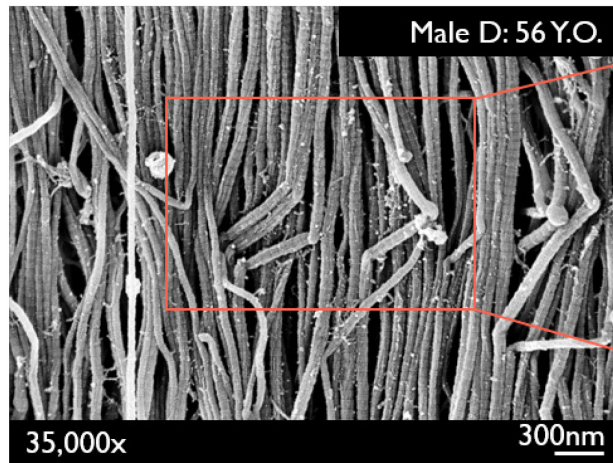
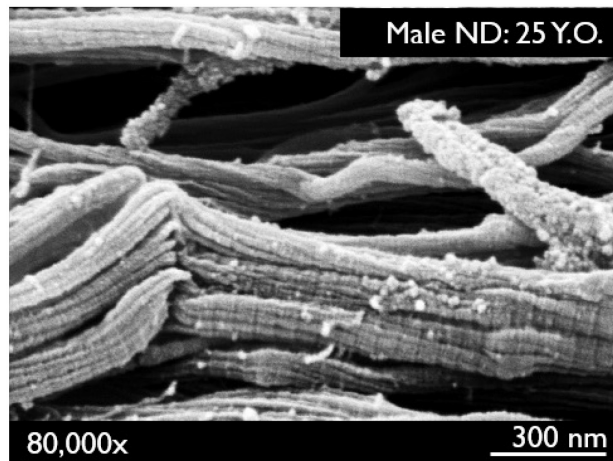
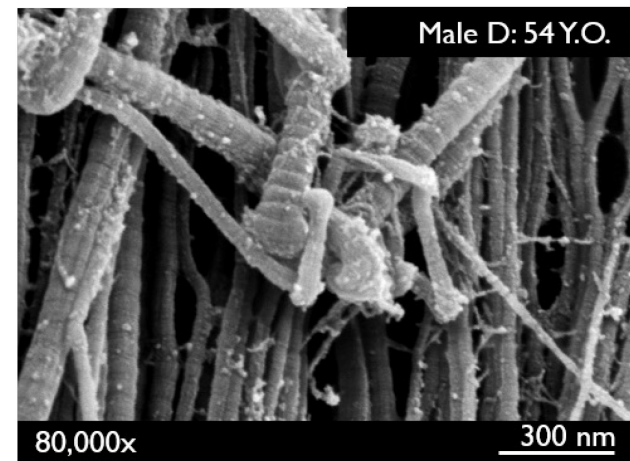


Figure 4.19 SEM micrographs A and B reveal varying degrees of fibril hairpin turns. Hairpin turns were often observed in isolated fibrils as shown in micrograph A. Micrograph B displays a region where multiple fibrils display the hairpin behaviour. Subfibril structure may clearly be observed at the turn sites. D-banding is present throughout the turn sites.

**A****B****C**

**Figure 4.20** SEM micrographs revealing regions of hairpin turns in neighboring fibrils. Micrograph A & B reveal bundles of neighboring fibrils exhibiting hairpin turns. In micrograph B the subfibril structure may be observed as the twisting of the internal structure. Image C reveals tangled fibrils that were found undergoing multiple hairpin turns. These motifs were regularly seen across all donor populations irrespective of age.

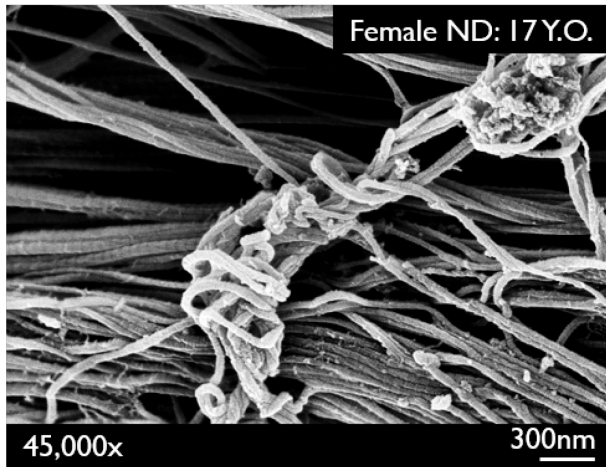
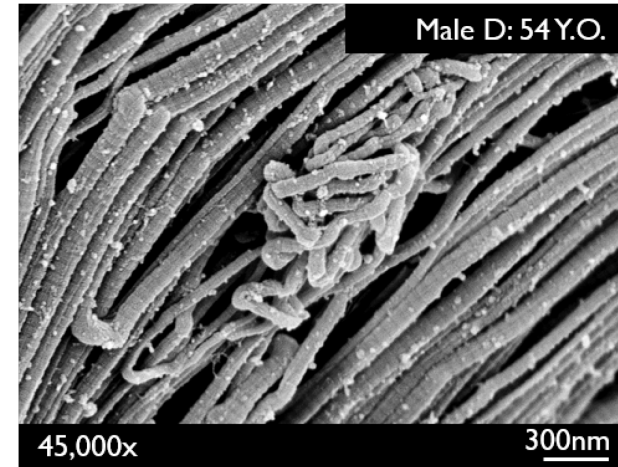
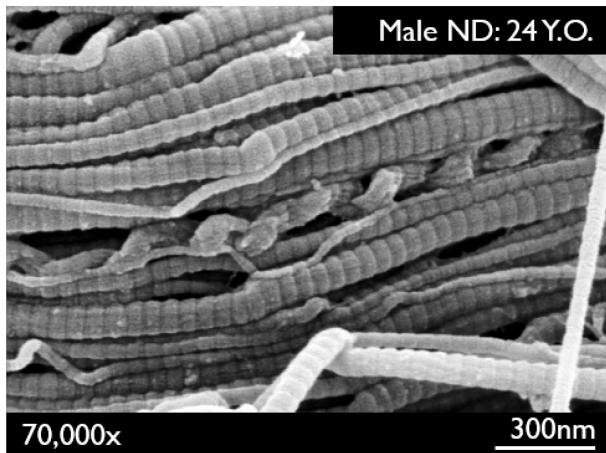
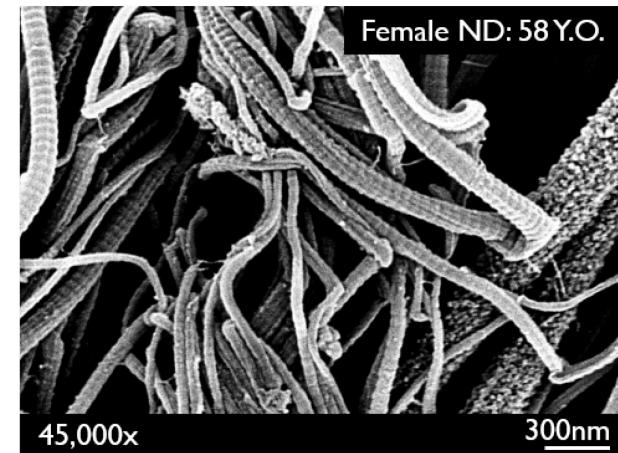
**A****B****C****D**

Figure 4.21 SEM micrographs displaying the different motifs of elastic recoil damage found in the sartorius tendon. At 45,000x, micrographs A, B & C show a mixture of recoiled fibrils showing tangling, twisting and balling. At 70,000x, micrograph C reveals an isolated fibril with a continuous twisting morphology. Micrograph D displays elastically recoiled fibrils and overall disruption.

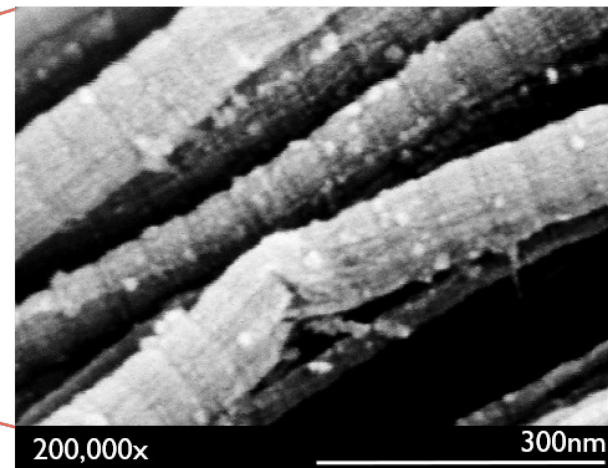
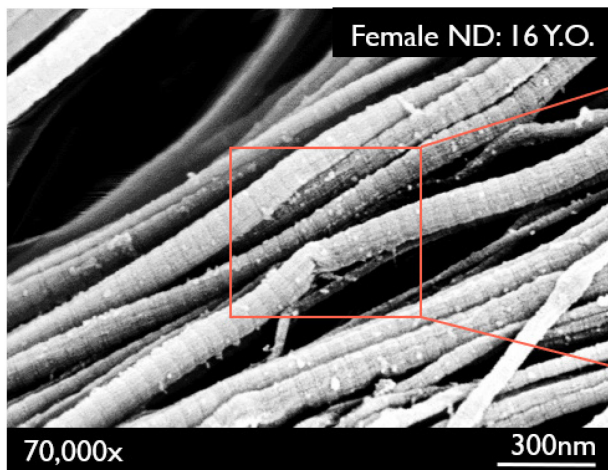
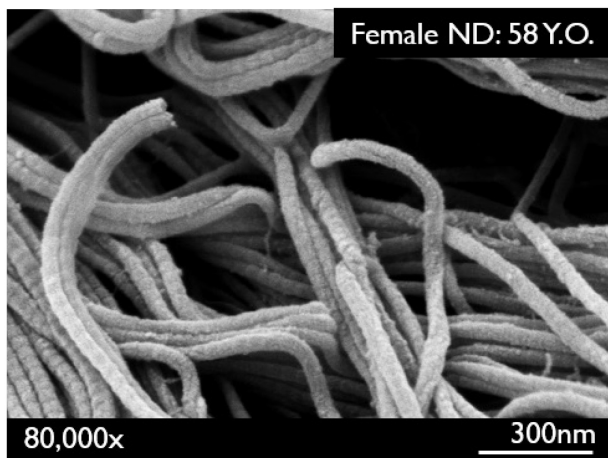
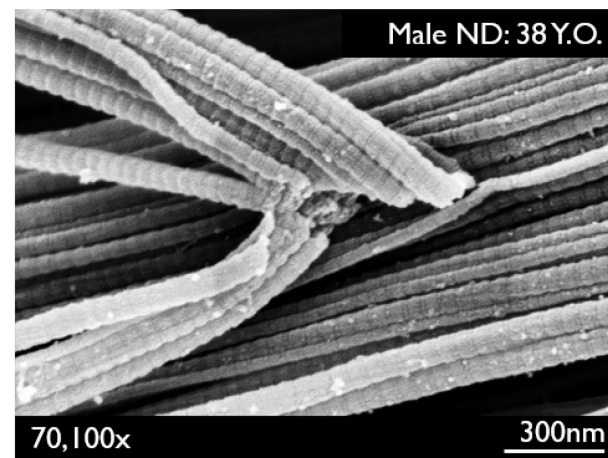
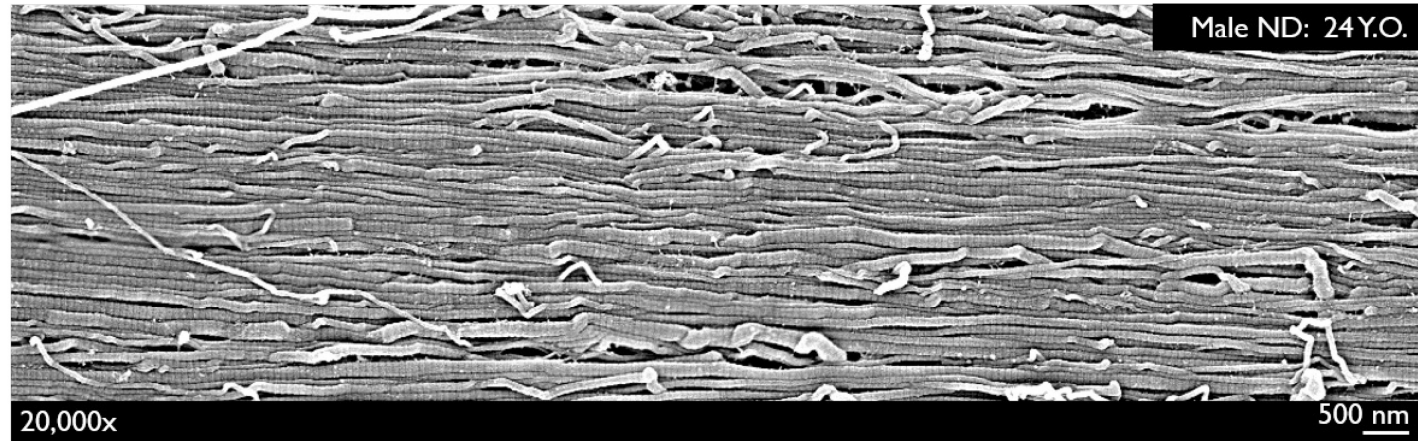
**A****B****C**

Figure 4.22 SEM micrographs describing the varying degrees of fibril failure found in the sartorius tendon collagen. SEM micrograph set A reveals local fibril disruption at magnifications of 70,000x and 200,000x. Micrographs B and C display fibril failure at 80,000x and fibril bundle failure at 70,100x magnification respectively.

A



B

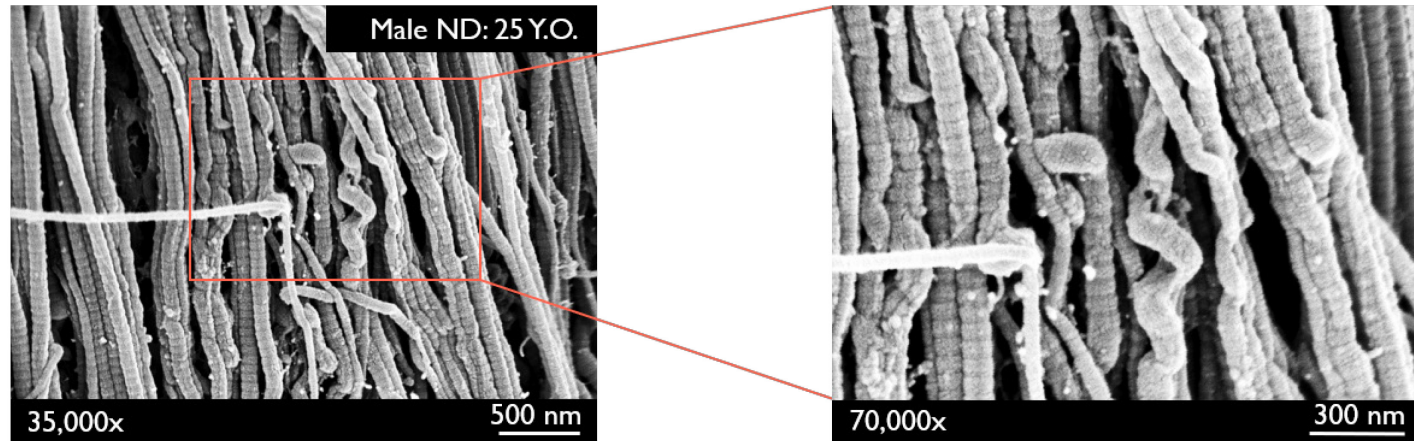


Figure 4.23 SEM micrographs revealing differing modes of plastic damage in sartorius tendon samples from the young and tough male non-diabetic donors. Donors where plasticity damage was found are indicated by the box located in Figure 4.16D. In micrographs A & B, rare and small regions exhibiting plasticity damage revealed kinking and twisting plasticity of collagen fibrils. Typically, the kinking plasticity damage was not observed serially along fibrils or in registry across neighboring fibrils. An overview is presented in the panoramic composite micrograph A.

the SDFTs by Herod and coworkers<sup>109</sup>. It could be suggested that in these damaged regions the diameters of the plastically damaged fibrils were larger than the undamaged fibrils; however, a more thorough study would be required to reach a conclusion on this point. Overall, in addition to the absence of discrete plasticity, evidence of differences in damage motifs based on age, sex and diabetes were not found.

#### **4.4. Sex-Related Differences in Sartorius Tendon Collagen Structure and Mechanics**

##### *4.4.1. DSC and HIT Revealed Dense Crosslinking and No Differences in Structure Determined by Donor Sex*

DSC and HIT testing were used to reveal structural changes between sartorius tendon collagen from female and male non-diabetic donors over four decades of age. These techniques revealed similar changes in thermal stability with aging (16-59 years) independent of sex. Furthermore, no changes in thermal stability were observed when separated into young (16-40 years) and old (41-59 years) cohorts. DSC testing revealed that thermal stability ( $T_{onset}$ ,  $T_{peak}$ ), range of thermal stabilities ( $FWHM$ ) and enthalpy of denaturation ( $h_{wet\ mass}$ ,  $h_{dry\ mass}$ ) were independent of sex as shown in Table 4.3. Within each donor sex, HIT  $T_d$  declined with age (female:  $p = 0.0197$ , male:  $p = 0.0012$ ), with their respective regression lines having similar slopes ( $p = 0.6248$ ). The intercept of the regression line was significantly increased ( $p = 0.0261$ ) in the male non-diabetic donor tendon population (69.07°C versus 68.03°C), perhaps an indicator of increased crosslinking and molecular packing. When comparing the average  $T_d$  between donor sexes, no significant difference was observed ( $p = 0.1996$ ). Comparison of the fractional differences in load pre- and post- $T_d$  resulted in no significant differences between donor sexes. Overall, dense thermally stable crosslinking was indicated by the absence of change in tendon collagen isotherm behaviour (contraction) in samples based on donor sex.

##### *4.4.2. Sartorius Tendon Multi-Fascicle Subsamples from Female Donors have Reduced Strength, Extensibility and Ability to Absorb Strain Energy*

Uniaxial overload to rupture testing revealed changes in the mechanics of the



sartorius tendon multi-fascicle subsamples determined by sex across four decades of age (16-59 years). Tendon samples from the female non-diabetic donors exhibited significantly lower strength, toughness, and extensibility ( $p = 0.0274$ ,  $p = 0.0211$  and  $p = 0.0041$  respectively) in comparison to samples from the male non-diabetic donor population (Figure 4.24). Tendon sample tissue modulus meanwhile remained independent of sex ( $p = 0.3556$ ). Without any alterations in molecular packing and crosslinking identified by HIT and DSC, it is curious that the mechanical behaviour nonetheless varied by sex. Differences observed in mechanics via overload testing did not result in changes in the modes of structural failure revealed by SEM examination.

**Table 4.3 Comparison of HIT ( $n_{F,ND} = 6$ ,  $n_{M,ND} = 9$ ) and DSC ( $n_{F,ND} = 5$ ,  $n_{M,ND} = 9$ ) results between female non-diabetic and male non-diabetic donor populations spanning 16 to 59 years of age. Values expressed as mean  $\pm$  SD.**

Method	Parameter	Male Non-Diabetic	Female Non-Diabetic	p-value
DSC	$T_{onset}$ ( $^{\circ}\text{C}$ )	$68.8 \pm 0.7$	$68.3 \pm 1.1$	0.3435
	$T_{peak}$ ( $^{\circ}\text{C}$ )	$70.3 \pm 0.8$	$69.8 \pm 1.3$	0.3044
	$FWHM$ ( $^{\circ}\text{C}$ )	$1.99 \pm 0.28$	$1.91 \pm 0.24$	0.5680
	$h_{wet\ mass}$ (J/g)	$7.3 \pm 2.1$	$6.4 \pm 2.4$	0.4475
	$h_{dry\ mass}$ (J/g)	$32 \pm 8$	$31 \pm 6$	0.8862
HIT	$T_d$ ( $^{\circ}\text{C}$ )	$66.3 \pm 1.0$	$65.6 \pm 1.0$	0.1996
	Slope of $T_d$ vs. Age ( $^{\circ}\text{C}/\text{year}$ )	-0.066	-0.056	0.6248
	Y-Intercept of $T_d$ vs. Age ( $^{\circ}\text{C}$ )	$69.1 \pm 1.3$	$68.0 \pm 1.8$	<b>0.0261</b>
	F.D. in Load Pre- $T_d$	$0.073 \pm 0.119$	$0.130 \pm 0.081$	0.4029
	F.D. in Load Post- $T_d$	$1.86 \pm 0.98$	$2.75 \pm 1.39$	0.1216

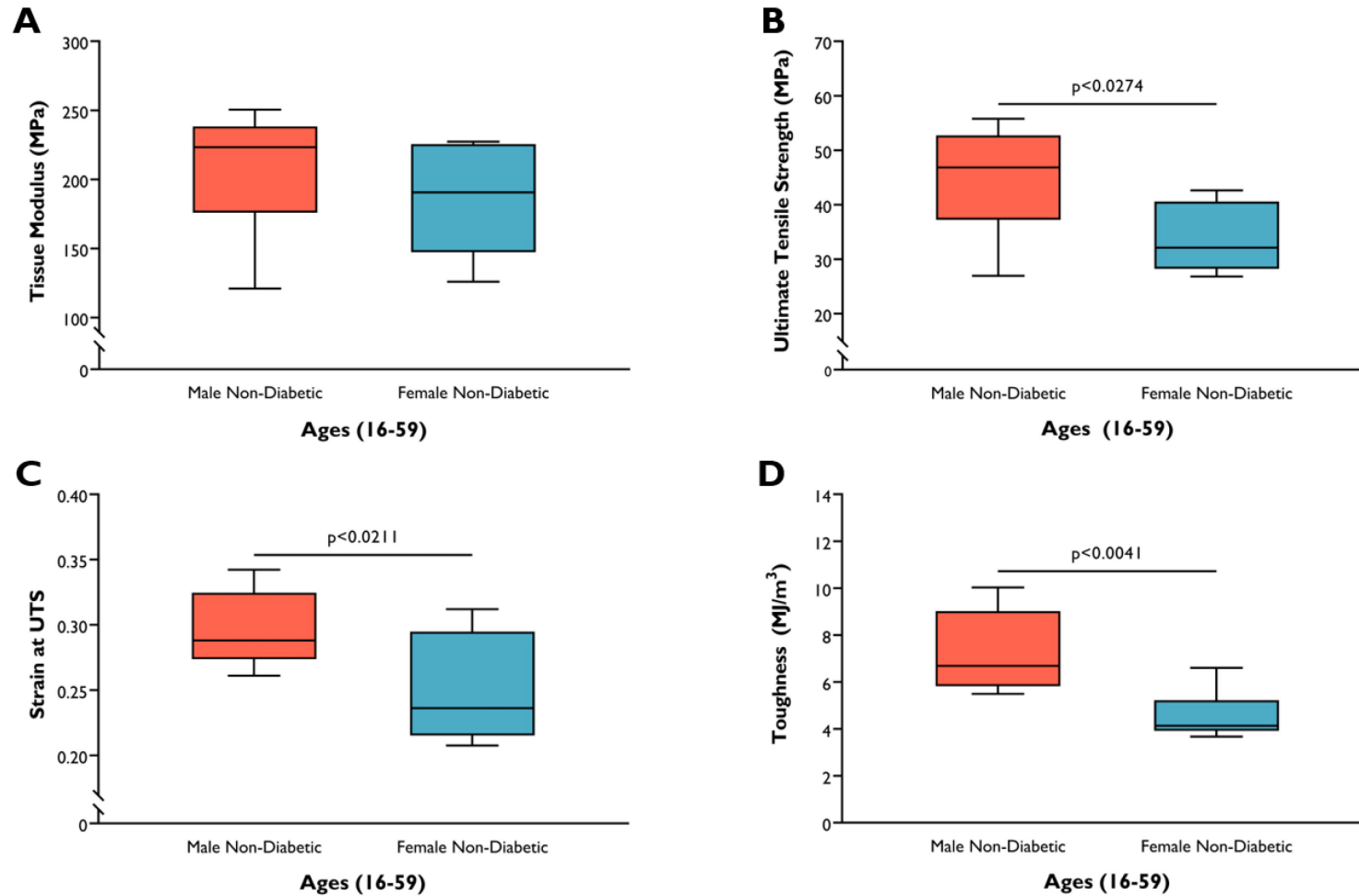


Figure 4.24 Comparison of mechanical parameters based on donor sex across the ages 16-59 years ( $n_{F,ND} = 6$ ,  $n_{M,ND} = 9$ ) revealed three of the four mechanical parameters evaluated were significantly different. (A) Tissue modulus was found to remain unchanged by donor sex. Moreover, (B) UTS ( $p = 0.0274$ ), (C) Strain at UTS ( $p = 0.0211$ ) and (D) Toughness ( $p = 0.0041$ ) were significantly reduced in tendons from female non-diabetic donors.

## 4.5. Diabetes-Related Changes in Sartorius Tendon Collagen Structure and Mechanics

### 4.5.1. Appearance of Sartorius Tendon Collagen Unaltered by Diabetes

Upon gross dissection of the sartorius tendon, in comparison to the tendons from non-diabetic donors, diabetes did not produce a consistent yellow discoloration. A few times in the older diabetic and non-diabetic older population, the tendons appeared golden-yellow, replacing the brilliant pearl white of the tendons seen otherwise. The overall absence of change in appearance (Figure 4.25) of golden-yellowing was inconsistent with the literature of collagenous tissues having undergone natural<sup>95,174,236</sup> or simulated diabetes<sup>41,81,135,150,231,260</sup>. Variability in the appearance of the sartorius tendon coloring may vary on a multitude of factors associated with donor health. Qualitative differences in tendon thickness were also not observed between the diabetic and non-diabetic tendons commonly recorded in tendons<sup>47,91,95,188</sup>.

### 4.5.2. Sartorius Tendon Collagen Thermal Stability Largely Unchanged by Diabetes

Interestingly, the influence of diabetes on tendon collagen thermal stability was revealed by a higher average DSC  $T_{onset}$  from diabetic compared to non-diabetic male donors over an age range of 38-60 years (Figure 4.26, Table 4.4). The difference in the average  $T_{onset}$  and lack of change in the average  $T_{peak}$  leads to the suggestion of a significant narrowing occurs in the range of thermal stabilities ( $FWHM$ ,  $p = 0.0944$ ) and some changes in molecular packing in the diabetic population. Changes in enthalpic energy required to denature the tendon collagen was not significantly determined by diabetes when considering the wet mass ( $h_{wet\ mass}$ ) and dry mass ( $h_{dry\ mass}$ ) of the DSC samples. When evaluating tendon collagen thermal stability using PBS as the hydrating solution, significant increases in  $T_{onset}$  and  $T_{peak}$  were similarly observed ( $p = 0.0033$  and  $p = 0.0079$  respectively) when compared to distilled water as the hydrating solution (refer to appendix).

HIT testing revealed no significant changes in the evaluated parameters  $T_d$  and the fractional differences in load pre- and post- $T_d$ . Moreover, the isotherm behaviour did



**Figure 4.25** Example of the extremes of sartorius tendon collagen coloration observed. While atypical, the tendon subsample from an older and/or diabetic donor (left) was of a golden yellow appearance - likely the result of hyperglycemia - in comparison to the brilliant pearl white tendon collagen of a young non-diabetic donor (female non-diabetic, 16 years of age).

not vary by diabetic status, indicative of the dense thermally stable crosslinking in the sartorius tendon collagen, irrespective of a possible increase in AGE intermolecular crosslinking induced by hyperglycemia.

#### *4.5.3. Sartorius Tendon Multi-Fascicle Subsamples from Diabetic Donors Exhibit Brittle Behaviour*

Tensile overload to rupture testing revealed that significant decreases in sartorius tendon subsample extensibility ( $p = 0.0003$ ) and ability to absorb strain energy ( $p = 0.0020$ ) occurred in donors with diabetes (Figure 4.27). Furthermore, it could be suggested that strength ( $p = 0.1006$ ) decreases, yet tissue modulus ( $p = 0.8767$ ) remains unchanged in sartorius tendon subsample from male donors with diabetes. These modifications in mechanical behaviour were not reflected in changes in the modes of structural failure assessed via SEM.

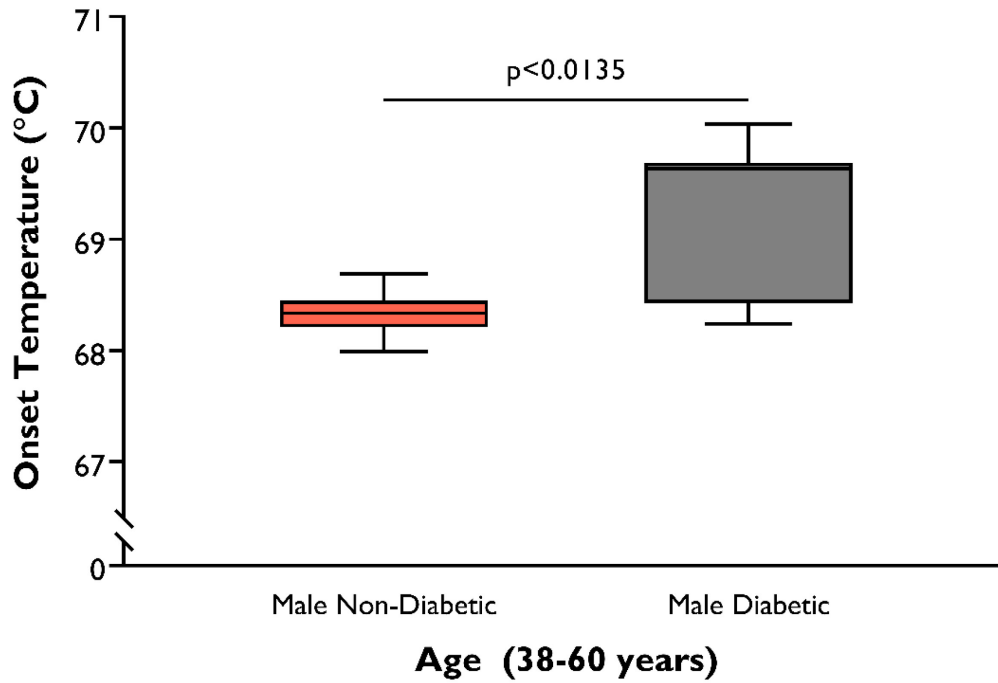


Figure 4.26  $T_{onset}$  of tendon collagen was significantly increased in tendon collagen of male donors 38-60 years of age with diabetes ( $n_{M,ND} = 6$ ,  $n_{M,D} = 8$ ). The DSC sample hydrating medium was distilled water.

Table 4.4 Comparison of HIT and DSC ( $n_{M,ND} = 6$ ,  $n_{M,D} = 8$ ) results between male non-diabetic and male diabetic donor populations spanning 38 to 60 years of age. Values expressed as mean  $\pm$  SD.

Method	Parameter	Male Non-Diabetic	Male Diabetic	p-value
DSC	$T_{onset}$ (°C)	68.5 $\pm$ 0.6	69.2 $\pm$ 0.7	<b>0.0135</b>
	$T_{peak}$ (°C)	70.1 $\pm$ 0.8	70.5 $\pm$ 0.8	0.4999
	$FWHM$ (°C)	1.88 $\pm$ 0.29	1.73 $\pm$ 0.15	0.0944
	$h_{wet\ mass}$ (J/g)	7.0 $\pm$ 2.3	7.3 $\pm$ 1.7	0.7454
	$h_{dry\ mass}$ (J/g)	30 $\pm$ 8	29 $\pm$ 5	0.6370
HIT	$T_d$ (°C)	66.25 $\pm$ 1.04	65.6 $\pm$ 1.0	0.1996
	F.D. in Load Pre- $T_d$	0.061 $\pm$ 0.133	0.188 $\pm$ 0.157	0.0976
	F.D. in Load Post- $T_d$	1.72 $\pm$ 1.03	2.14 $\pm$ 0.81	0.4600

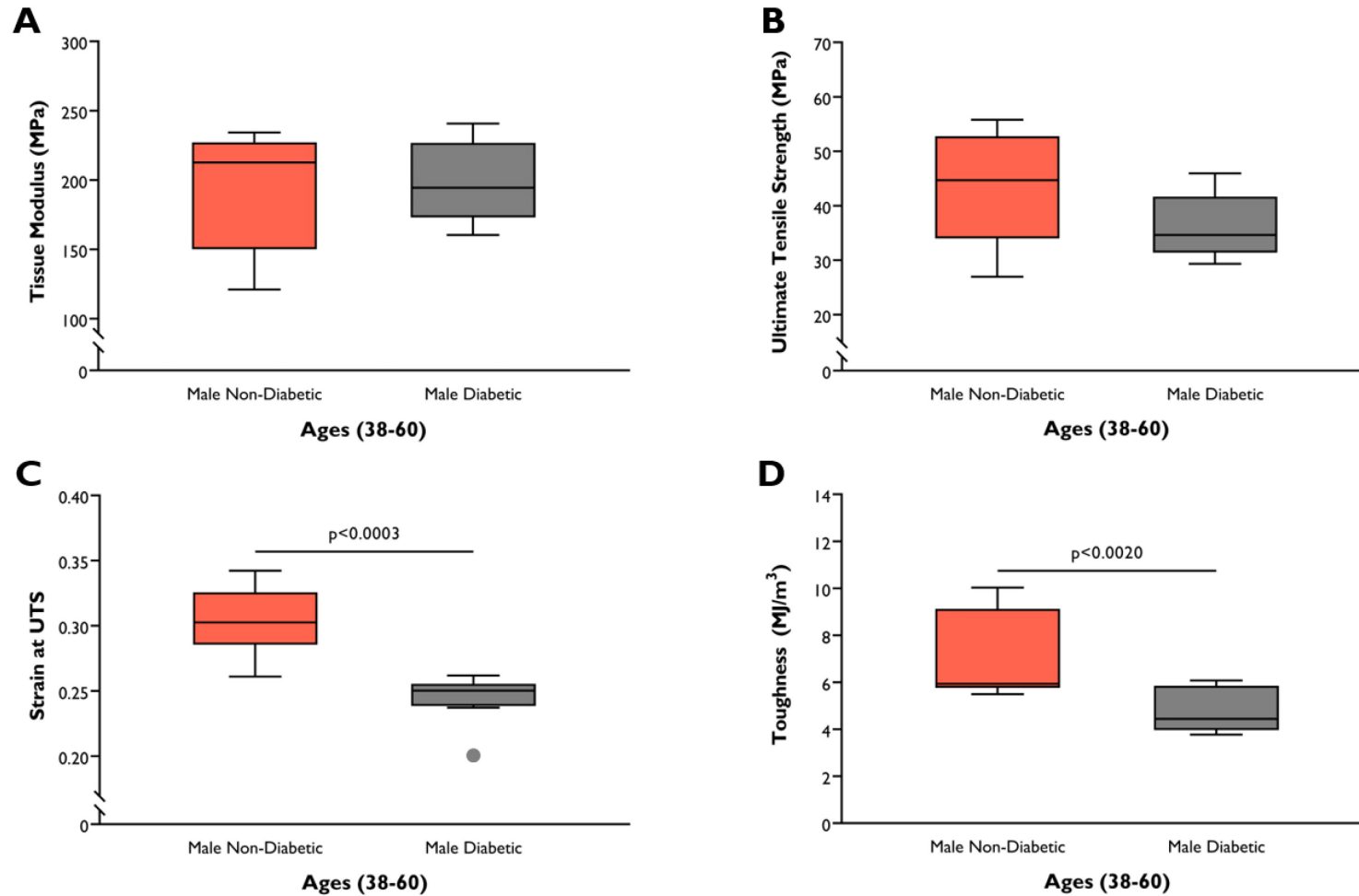


Figure 4.27 Evaluation of diabetes-determined mechanical differences in sartorius tendon multi-fascicle subsamples from male donors aged 38-60 years of age ( $n_{M,ND} = 6$ ,  $n_{M,D} = 8$ ) revealed significant results. The (C) strain at *UTS* and (D) toughness were shown to be significantly lowered in the diabetic donor population. The data also suggests that the tendon subsample strength ( $p = 0.1006$ ) decreases in the presence of diabetes.

#### **4.6. Sartorius Tendon Stiffness and Strength in Female Donors are Altered by Body Mass Index (BMI)**

BMI appears to play a minor role in determining the structure and mechanical behaviour of the sartorius tendon collagen in the female non-diabetic donor population, but curiously absent a role in the male non-diabetic and diabetic population. Female sartorius tendon multi-fascicle subsample strength and tissue modulus ( $p = 0.0089$  and  $p = 0.0026$  respectively) declined significantly with increasing BMI. Furthermore, the  $h_{wet\ mass}$  ( $p = 0.1000$ ) suggested a possible slight inverse relationship with BMI in the female donor population. Although significant, it is likely that these relationships were influenced by BMI in combination with age. Overall, changes in thermal stability were not influenced by the BMI of the donor in each population. Significant differences were not obtained when comparing testing parameters based on donor BMI division (normal, overweight and obese) when analysed using an ordinary one-way ANOVA or Kruskal-Wallis test dependent on dataset distributions. Surprisingly, donor weight did not influence structural and mechanical properties of the sartorius tendon collagen whereas the height of the donor played a significant positive linear relationship in determining the extensibility of the sartorius tendon subsamples ( $p = 0.0497$ ;  $r^2 = 0.24$ ) when evaluating the entire donor population (Figure A.4)

#### **4.7. Anatomical Location does not Alter Tendon Structure and Mechanics**

Anatomical location did not play a role in altering the structural and mechanical characteristics of the sartorius tendon collagen as evaluated via ordinary one-way ANOVA. Comparison of tendon collagen thermal stability and crosslinking by HIT and DSC reveal no effect of sampling location. Mechanical testing likewise revealed no changes in mechanical properties based on sampling location. Qualitative assessment of the tensile behaviour under overload to failure and loss of mechanical integrity of the multi-fascicle subsample was found to remain unchanged by sampling location.

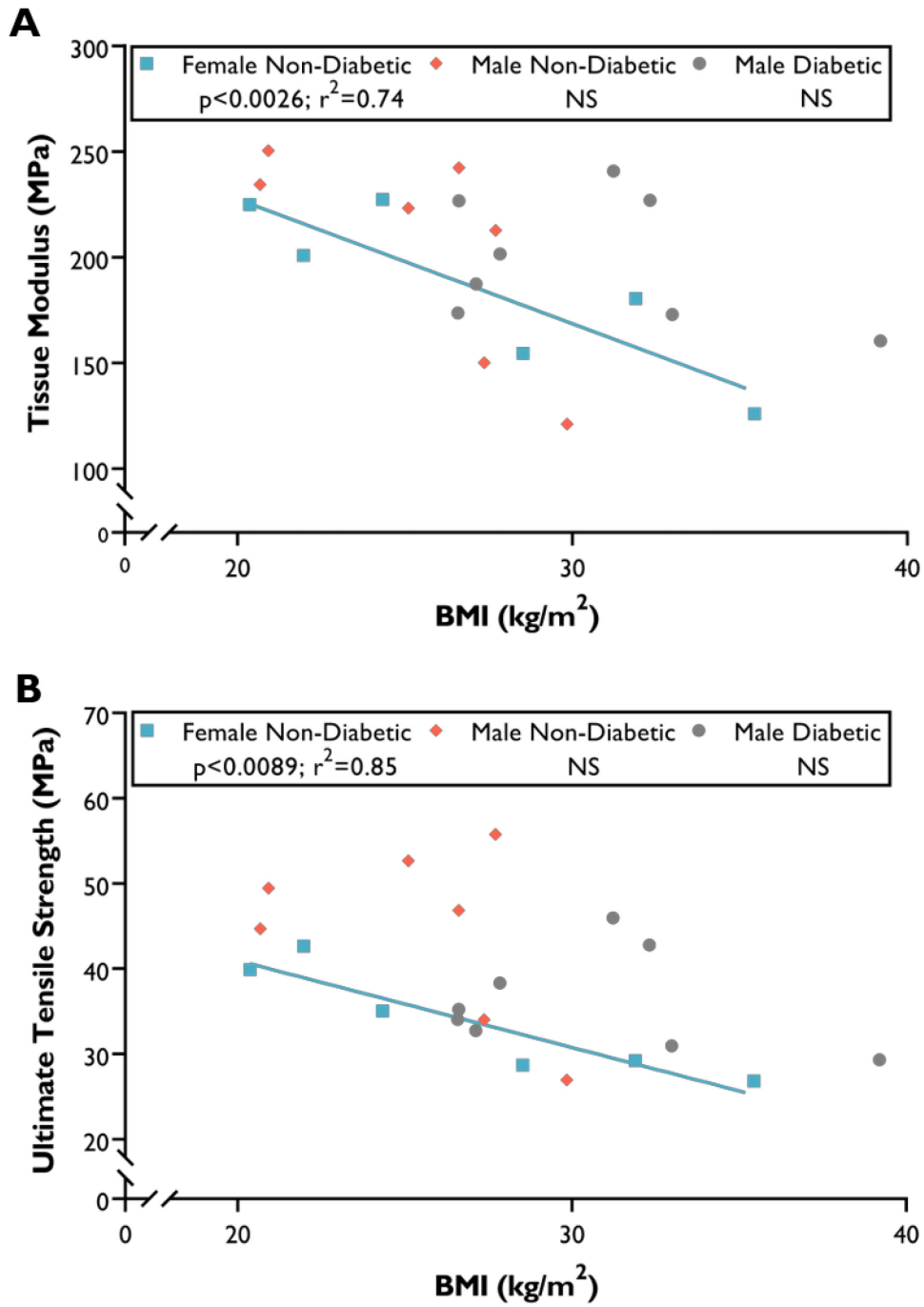


Figure 4.28 Tendon multi-fascicle subsample (A) tissue modulus ( $p = 0.0026$ ;  $r^2 = 0.74$ ) and (B) UTS ( $p = 0.0089$ ;  $r^2 = 0.85$ ) decreased with increasing BMI within the female donor population.



## **4.8. Histology & Immunohistochemistry**

### *4.8.1. Sartorius Tendon Collagen Crimp Appears to Diminish with Aging*

Birefringence was used to assess the degree of crimp and orientation of the tendon collagen fibers at 40x and 100x magnification. Birefringence examination of the longitudinal sections (Figure 4.29) revealed that in the younger donor tendons, the collagen was highly crimped. Longitudinal tendon sections from aged and/or diabetic donors exhibited a near absence of crimping. Alongside the reduction in crimp frequency was an observable flattening of the crimp waveform in the older tendon sections. The change in crimp waveform amplitude, noticeable in the birefringence images, was further evidenced by the changes in staining intensity of the tendon sections from younger donors (Figure 4.33). Tendon sections also appeared more susceptible to fragmentation with increasing donor age. Interestingly, qualitative changes in fiber thickness and spacing were not observed to be altered with age or diabetes.

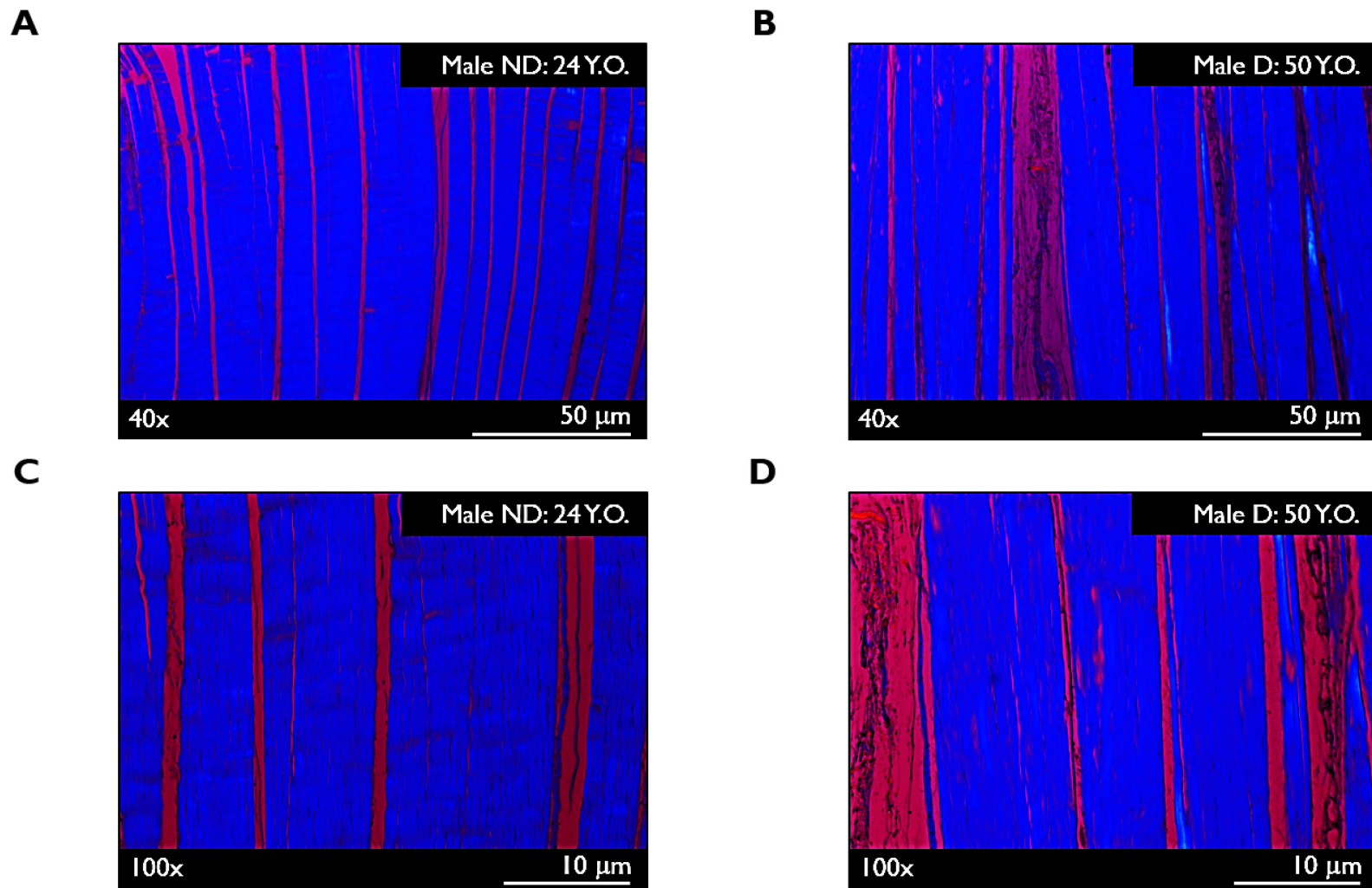
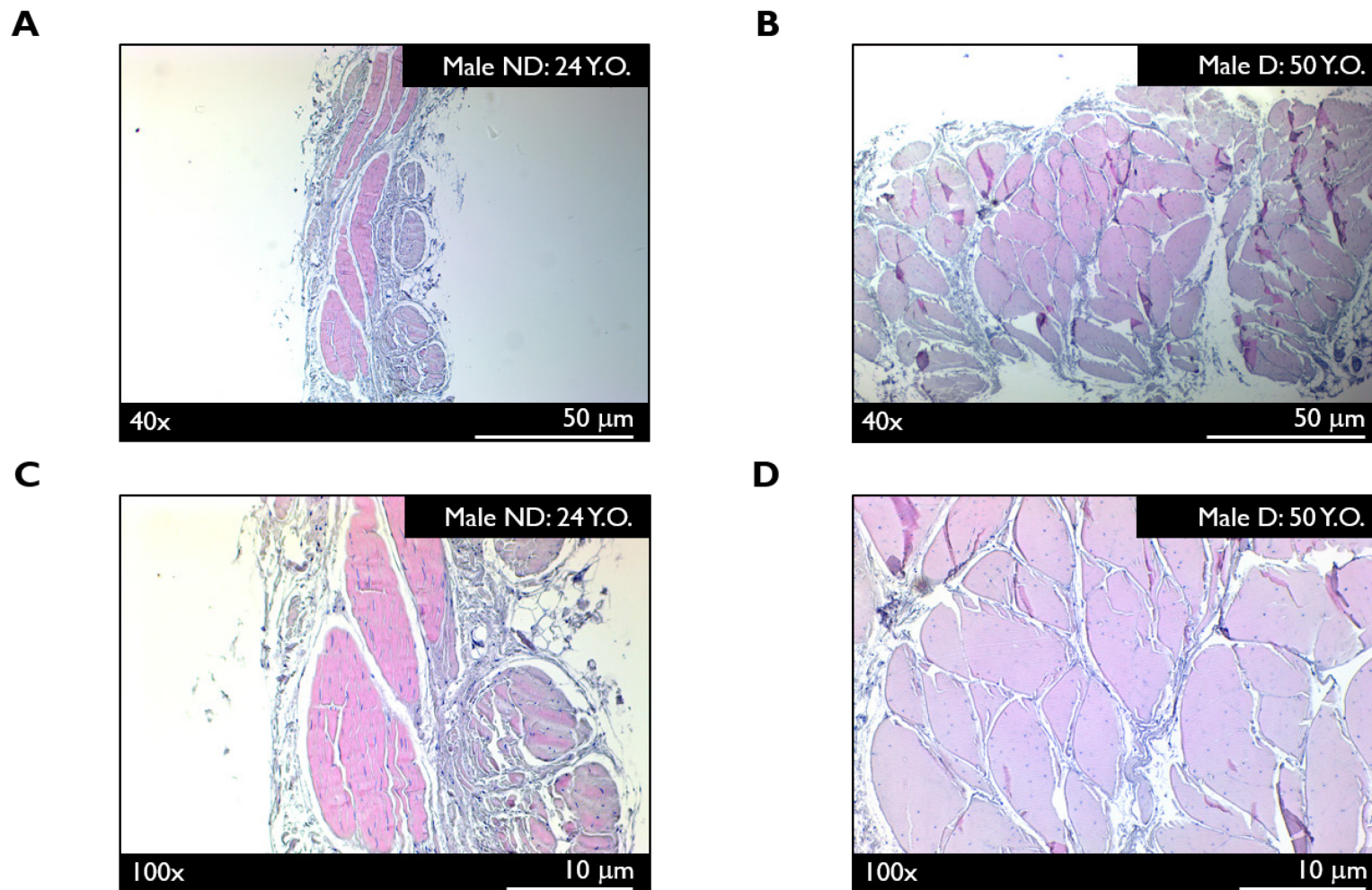


Figure 4.29 Longitudinal tendon sections of a young healthy (24 years of age, normal BMI) male non-diabetic (A & C) and an older unhealthy (50 years of age, obese BMI) male diabetic (B & D) shown at magnifications of 40x and 100x respectively. Birefringence examination of the longitudinal sections revealed a noticeably higher degree of collagen crimping in the younger donor tendon.

#### 4.8.2. *Hematoxylin & Eosin Staining Reveals a High Density of Nuclei*

H & E staining was used to characterize changes in tendon structure. Examination of stained transverse sections at 40x and 100x magnification respectively (Figure 4.30) revealed that nuclei appeared relatively dense and uniformly distributed throughout the transverse section of the collagen fibers. Occasional non-specific staining of the neighboring muscle fibers occurred as shown in Figure 4.30C. Hematoxylin staining uncovered a high concentration of nuclei between collagen fibers. Investigation of the stained longitudinal sections (Figure 4.31) revealed elongated nuclei present in the grooves of the collagen fibers in an undulated distribution. There were instances where the nuclei were found in serial chains in both young and old tendon sections. Although DSC and HIT revealed dense crosslinking in both young and old donors, hematoxylin staining uncovered a surprisingly high degree of nuclei density. However, in the older donors, qualitative decreases in nuclei content were observed with aging and diabetes, consistent with the literature of aging tendons<sup>242</sup>. Qualitatively, the intensity of the eosin staining of collagen was found to be independent of age. Evaluation of serial sections from the mid, and extremes of a tendon would give a better representation of the distribution of nuclei content throughout the tendon thickness laterally and the length longitudinally.



**Figure 4.30** Transverse (Cross-sectional) sections of H & E stained tendon of a young healthy (24 years of age, normal BMI) male non-diabetic (A & C) and an older unhealthy (50 years of age, obese BMI) male diabetic (B & D) shown at magnifications of 40x and 100x respectively. Both donor tendons appear cellular, however the nuclei in the younger donor tendon appear to be more elongated, contrasting the fine rounded nuclei in the older donor tendon.

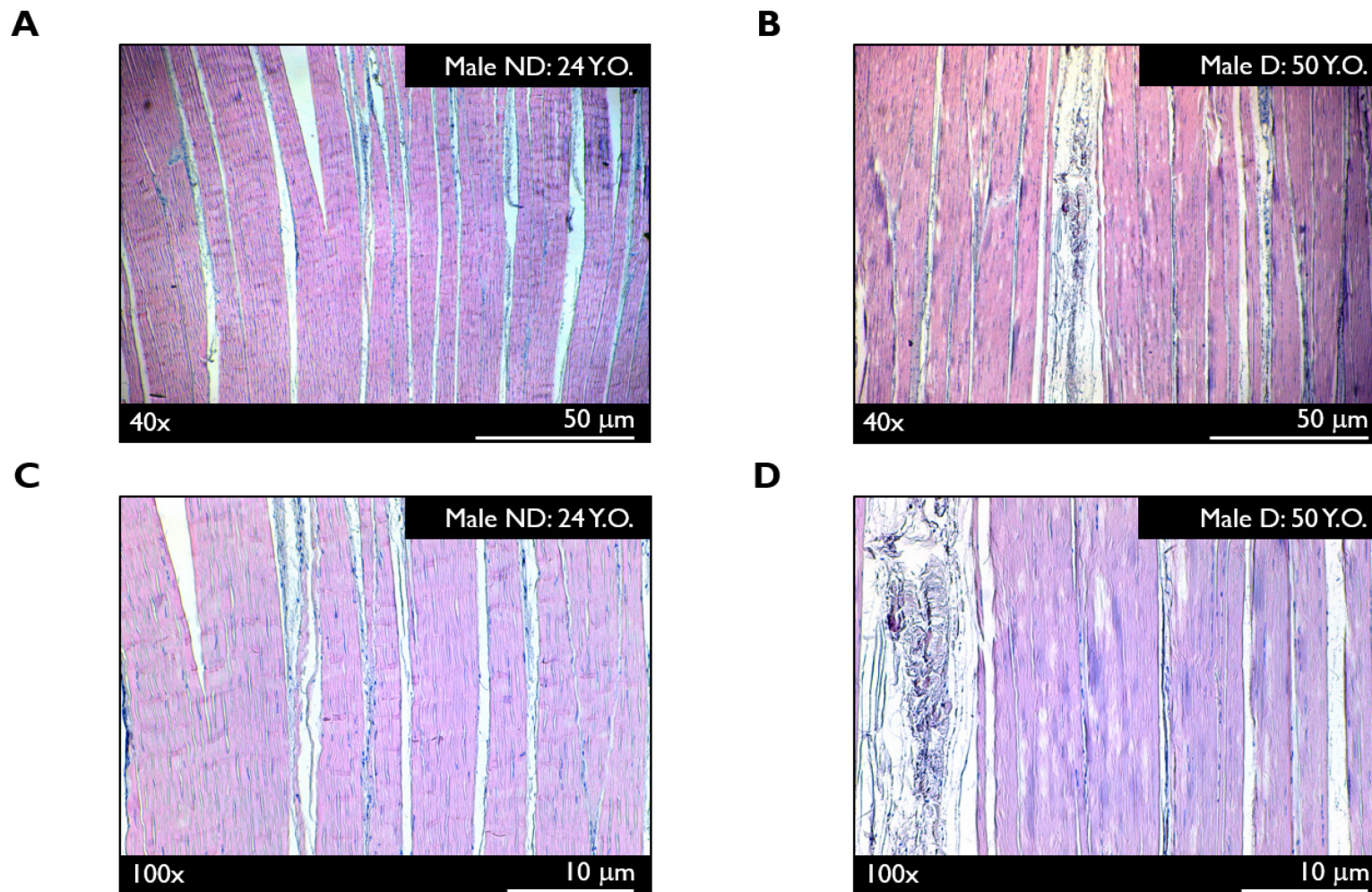


**Figure 4.31** Longitudinal Sections of H & E stained tendon from a young healthy (24 years of age, normal BMI) male non-diabetic (A & C) and an older unhealthy (50 years of age, obese BMI) male diabetic (B & D) shown at magnifications of 40x and 100x respectively. Tendons from both donors appear relatively cellular with the presence of elongated nuclei. Qualitatively at higher magnifications, the younger donor tendon appears to have a higher density of nuclei. Similar observations were made in other donor tendons.

#### *4.8.3. Greater Pentosidine Epitope Concentration Observed in Sartorius Tendon Collagen with Diabetes and Aging*

In this preliminary immunohistochemistry study, presence of the  $\alpha$ -PEN12 epitope for the sugar crosslink pentosidine was examined using DAB labelling, resulting in brown staining where present (magnifications of 40x and 100x). Control tendon sections (Figure 4.32A & C, Figure 4.33A & C), absent the  $\alpha$ -PEN12 antibody, were counterstained with hematoxylin and displayed collagen fibers of a brilliant blue coloring with nuclei observable. Examination of the stained longitudinal sections from the younger donor (Figure 4.32B & D) revealed a slight positive staining that was not found to be uniform in the collagen fibers, perhaps due to collagen crimp. In the older diabetic tendon sections (Figure 4.33B & D), the collagen fibers were uniformly stained positive for the pentosidine epitope. In both the young non-diabetic and the old diabetic donor longitudinal tendon sections, significant non-specific background staining of the ECM components was observed between collagen fibers (Figure 4.32, 4.33)

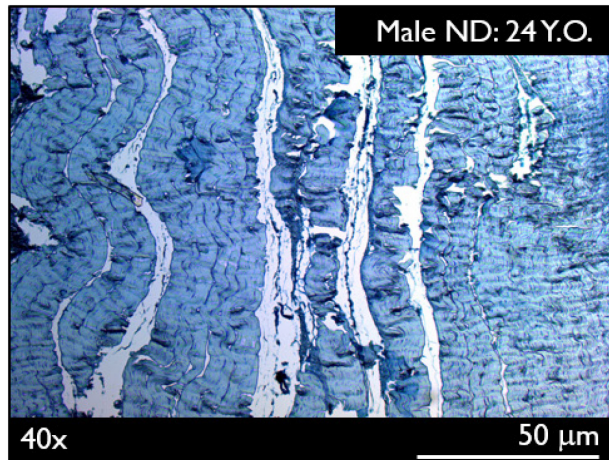
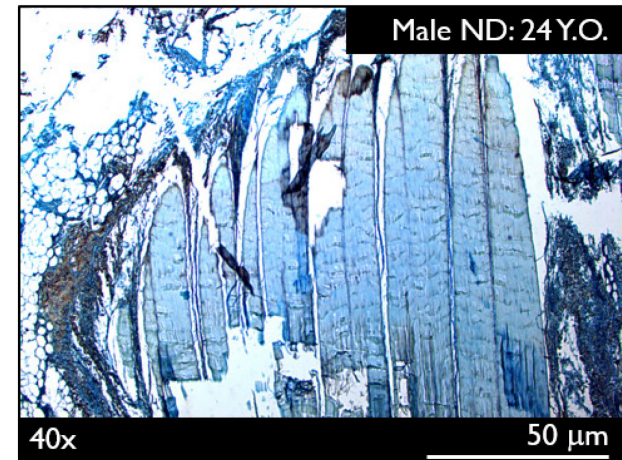
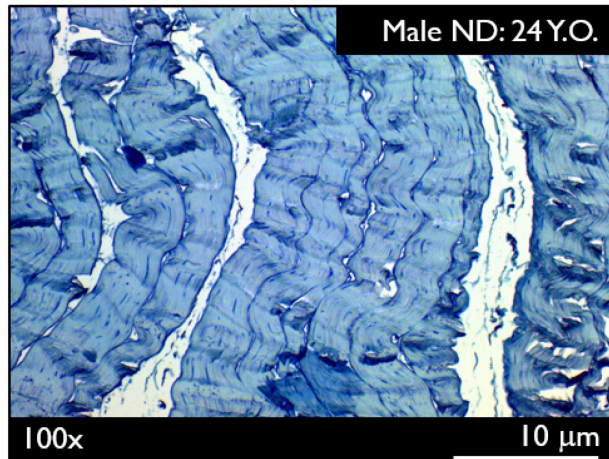
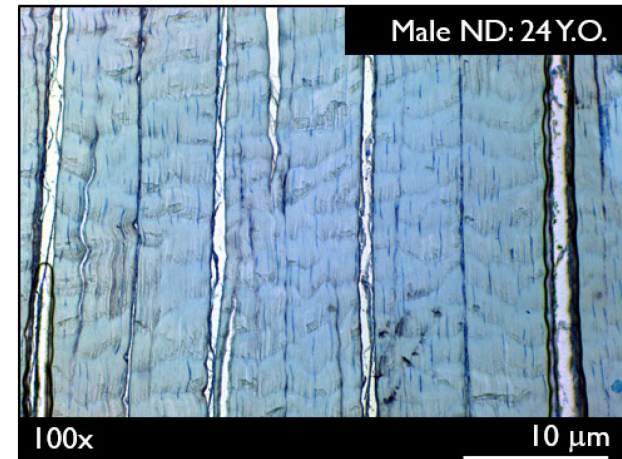
**A****B****C****D**

Figure 4.32 Control (A & C) and  $\alpha$ -PEN12 immunostained (B & D) longitudinal tendon sections of a young, healthy (24 years of age, normal BMI) male non-diabetic shown at magnifications of 40x and 100x respectively. Sections stained brown with DAB ( $\alpha$ -PEN12) were counterstained with Meyer's Hematoxylin. At 100x, image D shows a slight amount of positive staining on the collagen fibers contrasting the blue found in the control image (C).

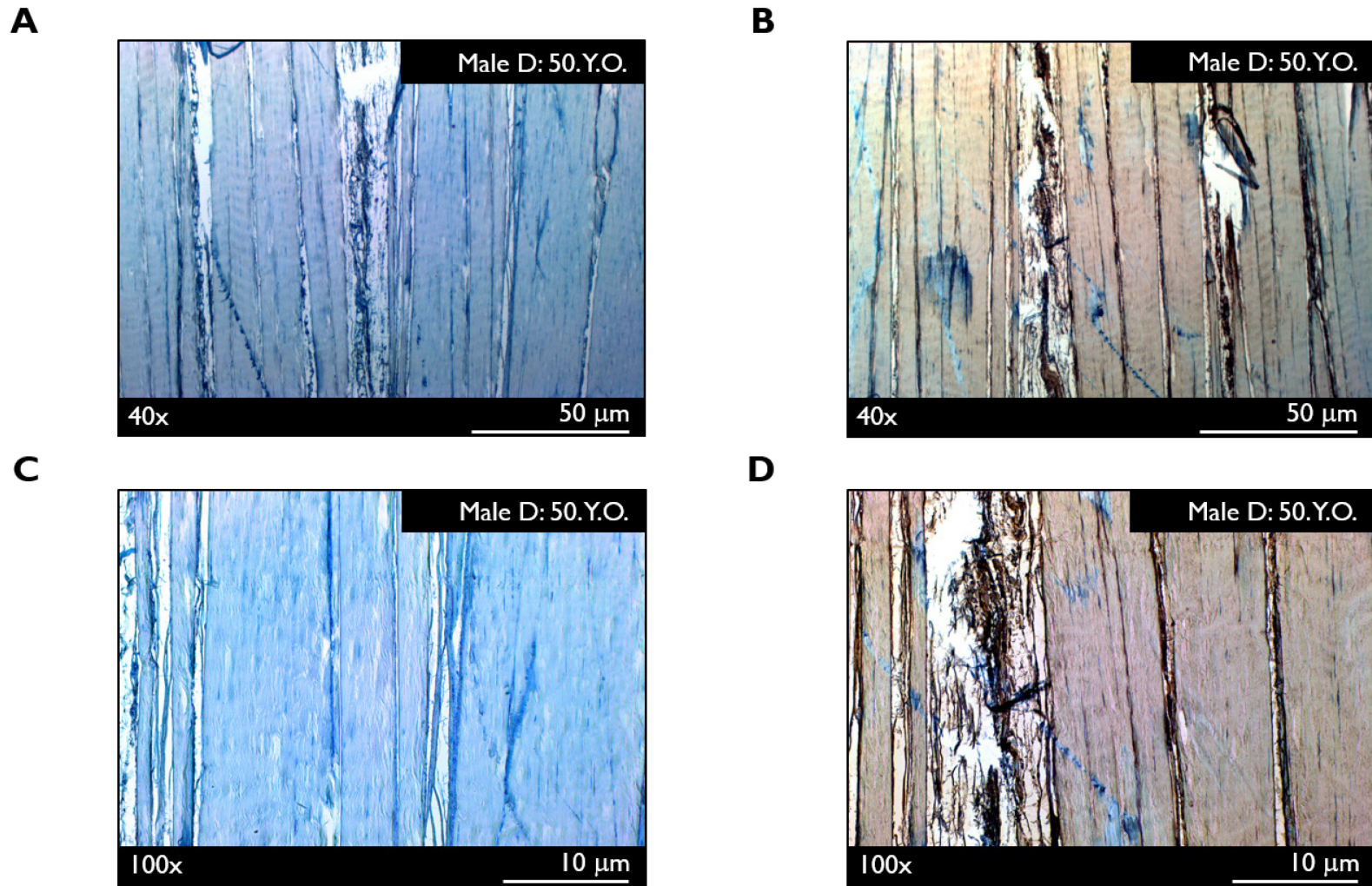


Figure 4.33 Control (A & C) and  $\alpha$ -PEN12 immunostained (B & D) longitudinal tendon sections of an older, unhealthy (50 years of age, obese BMI) male diabetic shown at magnifications of 40x and 100x respectively. Sections stained brown with DAB ( $\alpha$ -PEN12) were counterstained with Meyer's Hematoxylin. IHC revealed in the older donor tendons there was a noticeable amount of positive staining when compared to the control sections.



#### 4.9. Summary of Results

Investigation of the structure of the sartorius tendon collagen using HIT and DSC as proxies for crosslinking and molecular packing revealed that the tendon collagen is a densely crosslinked structure. With age, tendon collagen structure was modulated with slight changes in denaturation temperatures independent of sex. Changes in collagen structure with aging were reflected by a significant declining strength solely observed in the multi-fascicle tendon subsamples from female donors. BMI was likewise significantly related to a decline in strength and tissue modulus solely in tendon samples from the female donors. Although tendon collagen structure was found to be independent of sex, lowered average strength, extensibility and toughness was found in tendon samples from female donors over four decades of age. In terms of the influences of diabetes, a significantly higher tendon collagen  $T_{onset}$  was observed in the older (38-60 years) male donor population with diabetes. Meanwhile, the sole changes in mechanics observed were reduced extensibility and toughness in tendon samples from the diabetic donor population.

Observation of overload damage to tendon collagen via SEM revealed structural damage motifs of isolated hairpin turns, elastic recoil, local isolated fibril damage, complete fibril breakage, and plastic damage. Discrete plasticity motifs – loss of D-banding and serial kinking along fibrils - were absent across all tendons examined under SEM. The type of damage motifs observed were not influenced by sex, by diabetes or by age.

In preliminary light microscopy experiments, birefringence examination revealed a decrease in the tendon collagen crimp waveform frequency and amplitude with aging. H & E studies revealed a surprisingly dense nuclei content despite the heavy crosslinking indicated by DSC and HIT experiments. However, the amount and density of nuclei content, although not measured, appeared to decrease with age. Initial IHC experiments uncovered an increase in pentosidine epitope ( $\alpha$ -PEN12) concentration with age and diabetes. Further histological studies are required independently investigate the relationship between aging and pentosidine epitope concentration.

## Chapter 5: Discussion

From the outset of this thesis, an extension of previous work by Sparavalo<sup>237</sup>, the overarching objectives were to determine (i) age- (16-60 years), (ii) sex-, and (iii) diabetes-related variations in sartorius tendon collagen molecular structure, multi-fascicle mechanics and fibrillar overload damage mechanisms. With aging, it was found that although decreases in thermal stability occurred in tendon collagen from both the female and male non-diabetic donor population, the mechanics were largely unchanged. Considering donor sex, it was found that while thermal stability was independent of sex, sartorius tendon multi-fascicle subsamples from the female donors were weaker, less tough, and less extensible. Finally, diabetes induced minor changes in structure and more brittle mechanical behaviour. The combined effects of diabetes and 30 years of aging were revealed in the light microscopy findings of a less crimped, less cellular tissue with a higher concentration of pentosidine epitopes. SEM examination identified overload damage motifs consistent with the high-energy elastic snapping observed during testing – but with the absence of the toughening mechanism discrete plasticity. This was found to be independent of donor age, sex and diabetic status. Overall, it appears that the sartorius tendon collagen is a densely crosslinked structure that is modestly modulated over four decades of adulthood, in individuals of either sex and/or diabetic status.

### 5.1. Age-Related Changes in Sartorius Tendon Collagen Thermal Stability and Mechanics

This section serves as an extension of a previous study by Sparavalo<sup>237</sup> who investigated age-related changes in the sartorius tendon's collagen (thermal stability and mechanics) from male, non-diabetic donors only.

#### 5.1.1. *Relationships Between Aging and Thermal Stability:*

##### *Sartorius Tendon Collagen Thermal Stability Declines with Age*

Evaluation using DSC (enthalpic) and HIT (entropic) methods uncovered

decreases in thermal stability of sartorius tendon collagen with age. In the male non-diabetic donor population, decreasing thermal stability was found with age via both DSC ( $T_{onset}$ :  $p = 0.0065$ ) and HIT ( $T_d$ :  $p = 0.0012$ ). Meanwhile, significant decreases in thermal stability of the female tendon collagen was only found using HIT ( $T_d$ :  $p = 0.0197$ ). It is possible that in the female donor population, the DSC analysis was limited by the sample size ( $n = 5$ ). The decreases in thermal stability observed in the male non-diabetic donor population may be associated with an increase in pentosidine concentration with aging, similar to that observed in the gracilis and semitendinosus tendons<sup>88</sup>. While the formation of AGEs would restrict conformational freedom, increasing the thermal stability, the effect of the increased lateral molecular spacing decreasing the thermal stability may be greater. Further, it is possible the decrease in thermal stability may be associated with the decreased distribution of thermal stabilities with aging (decreased  $FWHM$ :  $p = 0.0477$ ). The narrowing endotherm with aging may be indicative of a more uniform organization of the collagen molecules and a cooperative reduction in the thermal energy required to disrupt hydrogen bonds responsible for maintaining molecular structure<sup>42,251</sup>.

Despite the decrease in thermal stability with aging, in comparison to previous studies of bovine tissues, the sartorius tendon collagen denaturation temperatures evaluated by HIT ( $T_d$ ) and DSC ( $T_{onset}$ ,  $T_{peak}$ ) were higher (despite of the change in hydrating medium from PBS to distilled water for DSC) as observed in Table 5.1. Unexpectedly, the sartorius tendon collagen was more thermally stable when compared to other human lower limb tendons (e.g. patellar, Achilles)<sup>271</sup>, although this may be the result of a difference in heating rates between studies (0.3°C/min vs. 5°C/min).

*Despite Sartorius Tendon Thermal Stability Decrease, Crosslinking Remains Largely Unchanged with Aging*

In the human sartorius tendon across male and female non-diabetic donors, decreases in thermal stability were found to occur despite dense thermally stable crosslinking across four decades of age ( $t_{1/2}$ ). The dense crosslinking was reflected across the entire donor population as 61% of the total strip-samples *resisted* load decay

**Table 5.1 Summary of thermal studies (DSC and HIT) of tendon collagen performed in the Tissue Mechanics Lab demonstrating varying degrees of discrete plasticity damage. Values expressed as mean  $\pm$  SD.**

<b>Tissue</b>	$T_{onset}$ (°C)	<i>FWHM</i> (°C)	$T_d$ (°C)	$t_{1/2}$ (hrs)	<b>Degree of Discrete Plasticity?</b>
Steer Tail Tendon (24-30 M.O.) <sup>274</sup>	64.5 $\pm$ 0.5	4.2 $\pm$ 1.4	65.5 $\pm$ 1.2	Failure Prior to Isotherm	Extensive
Glycated Steer Tail Tendon (24-30 M.O.) <sup>8,150</sup>	66.9 $\pm$ 0.3	2.6 $\pm$ 0.4	-	-	Absent
Bovine CDET (24-36 M.O.) <sup>109</sup>	63.1 $\pm$ 1.0	2.7 $\pm$ 0.5	62.7 $\pm$ 0.4	Failure Prior to Isotherm	Extensive
Bovine SDFT (24-36 M.O.) <sup>109</sup>	65.4 $\pm$ 0.7	1.7 $\pm$ 0.1	65.4 $\pm$ 0.7	6 $\pm$ 2	Sparse
Human Sartorius Tendon <sup>237</sup> (Male ND: 20-60 Y.O.)	67.2 $\pm$ 0.8	1.7 $\pm$ 0.2	66.5 $\pm$ 0.4	55 $\pm$ 55**	Absent
<b>Human Sartorius Tendon*</b> <b>(16-60 Y.O.)</b>	<i>69.2 <math>\pm</math> 0.7</i>	<i>2.0 <math>\pm</math> 0.3</i>	<i>66.0 <math>\pm</math> 1.0</i>	<i>774 <math>\pm</math> 1340**</i>	<i>Absent</i>

\* Inclusive of male non-diabetic, male diabetic and female non-diabetic donor populations. \*\*Load decay only occurred in a portion of the samples. *Italicized data are from current study.*

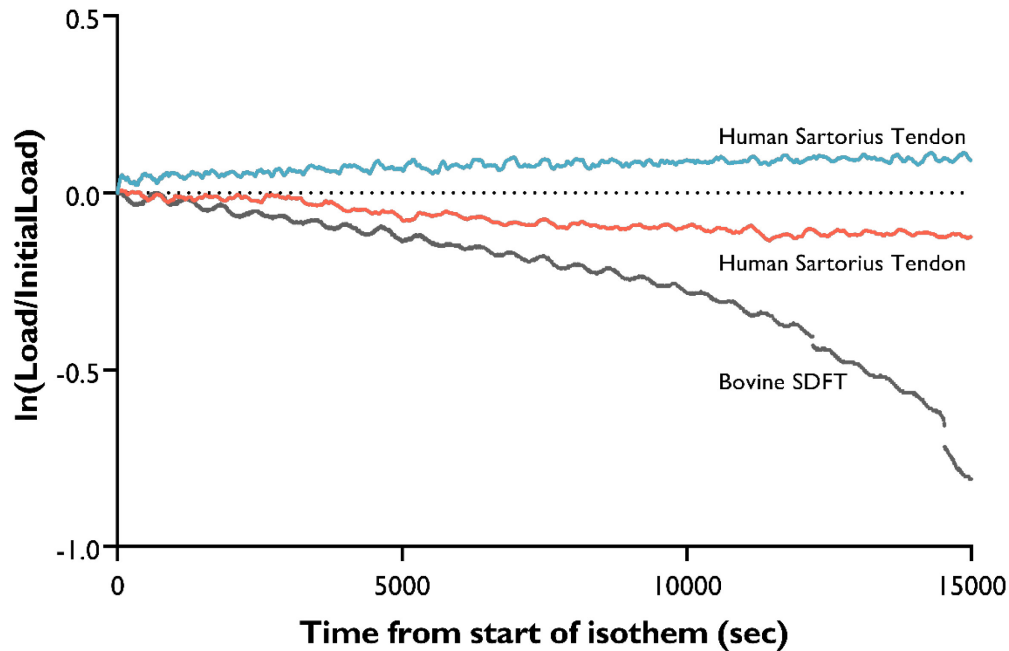


Figure 5.1 Graph of  $\ln\left(\frac{\text{Load}}{\text{Initial Load}}\right)$  on the y-axis and the time from the start of the isotherm on the x-axis in order to illustrate the differences in thermally stable crosslinking and subsequent isothermal behaviour of the human sartorius tendon and the bovine SDFT. In 61% of the human sartorius tendon HIT strip samples, isothermal contraction (blue curve) was observed. However, in the proportion of sartorius tendon samples that displayed load decay (red curve), the difference in the density of thermally stable crosslinking between the human sartorius tendon and bovine SDFT (grey curve) is evident. Bovine SDFT data from Herod *et al.*<sup>109</sup>.

during the isotherm. When load decay did occur, it was on the order of days to weeks rather than hours when compared to previously studied bovine tendons<sup>109</sup> that survived the denaturation segment from room temperature to the 90°C isotherm (Figure 5.1). It may be that the changes in thermal stability are found to be independent of changes in the crosslinking profile of the human sartorius tendon as a result of aging. With maturation, it's been suggested that the conversion of divalent to trivalent crosslinking plateaus, with few new crosslinks being formed<sup>242</sup>, and leading to a reduction in tendon collagen turnover<sup>107</sup> with further aging. This notion is supported by Sparavalo<sup>237</sup> wherein an absence of change to thermally stable crosslinking was observed throughout adulthood (post-maturation) as assessed by HIT ( $t_{1/2}$ ), and the amount of load decay remained unchanged in spite of  $\text{NaBH}_4$ -stabilization treatment. The absence of change in  $t_{1/2}$  with aging is likely the result of early and dense enzymatic crosslinking. Subsequently, non-

enzymatic crosslinking then has little thermal or mechanical effect. The attenuated influence of AGE crosslinking on the sartorius tendon may be supported by evidence in the human patellar tendon, wherein the ratio of the concentration of enzymatic crosslink Hyl-Pyr to the non-enzymatic pentosidine was found in excess of twelve times ( $898 \pm 172$  vs.  $73 \pm 13$  mmol/mol), even into the sixth decade of age, despite the 39% and six fold increase in Hyl-Pyr and pentosidine concentration respectively over four decades of adulthood<sup>56</sup>.

*Sartorius Tendon Collagen Molecular Packing may Increase with Aging, Leading to a Decrease in Thermal Stability*

Similar to Miles *et al.*<sup>168</sup>, age-based changes in thermal stability using distilled water as the DSC sample hydrating solution were performed to strictly examine the effects of physical fiber confinement. In the current study, it was found that  $T_d$  ( $p < 0.0001$ ),  $FWHM$  ( $p = 0.0017$ ), and  $h_{wet\ mass}$  ( $p = 0.0199$ ) were inversely related to the tendon collagen water content – and thus to the size of the box<sup>170</sup> – in a combined female and male non-diabetic donor population. With aging, the polymer-in-a-box model<sup>170</sup> suggests that an increase in the size of the box may be observed. This is suggested by the linear increase in tendon water content found ( $p = 0.0064$ ). However, differences in the measured water content which are due to (i) solvation water bound to the collagen molecules, and (ii) free, interfibrillar water are not able to be distinguished in this study. It is possible that the increase in water content may have subsequently increased the configuration entropy of the thermally labile domains. X-ray diffraction studies of human toe extensor tendons have indicated increases in lateral molecular spacing with the formation of AGEs, yet the mechanism of this change with aging remains unclear<sup>118,182</sup>.

In contrast to the present findings of decreased thermal stability, previous studies in animals (e.g. rabbit Achilles and bovine tail tendon) have found that thermal stability increases<sup>251</sup> or remains unchanged<sup>275</sup> with maturation, accompanied by increases in the degree of thermally stable covalent crosslinking<sup>275</sup>, decreases in  $h_{dry\ mass}$ , and no change in the distribution of thermal stabilities<sup>251</sup>. In humans, DSC investigation of the long head of the biceps collagen (using a scanning rate of 0.3°C/min) revealed significant increases

in the thermal stability of collagen ( $T_{peak}$ ) through maturation to young adult (0-35 years) while remaining unchanged with further aging<sup>35</sup>. In studies of aging, it is possible that varying degrees of microtrauma accumulate in the tendon collagen that may produce confounding results. Injury and/or disease has been shown to decrease the enthalpy of collagen denaturation across varying tendons<sup>54,269,270</sup>. Similarly, injury and/or disease have been shown to produce increases in collagen thermal stability of lower limb tendons (e.g. quadriceps/patellar tendon)<sup>271</sup>, this contrasting with decreases found in rotator cuff tendons<sup>54</sup>.

#### *Effect of Test Solution on Thermal Studies*

In contrast to the present study where distilled water was used as the DSC sample hydrating solution, as commonly in the literature, PBS has been used as the hydrating solution to investigate age-related changes in thermal stability and crosslinking<sup>35,251</sup>. The present study using distilled water contrasts with that of Sparavalo<sup>237</sup> in which sartorius tendon collagen thermal stability, assessed via DSC ( $T_{onset}$ ), increased linearly through adulthood (20-60 years). Introduction of a salt solution (PBS) to the collagen molecule in that study may have disrupted hydrogen bonding interactions<sup>97,168</sup> resulting in altered conformational stability. Consistent with previous studies of molecular destabilization in the presence of salt ions<sup>97,116,136</sup>, values of  $T_{onset}$  found in this study were ~1.6°C higher when comparing values to those obtained by Sparavalo<sup>237</sup> (Table 5.2).

#### *5.1.2. Relationships Between Aging and Tendon Mechanical Properties:*

##### *Sartorius Tendon Mechanical Properties Remain Largely Unchanged with Aging*

In large part, the decreases in thermal stability observed in the male and female non-diabetic donor population with aging were not reflected in the tensile failure mechanics and mechanical properties of the sartorius tendon multi-fascicle subsamples. No significant changes in mechanical properties of the tendon samples were observed with aging in the male donor population. By contrast, in the aging female donor population, only a significant negative linear correlation of strength and age, with a

**Table 5.2 Evidence of the decreases in thermal stability of collagen in the presence of a salt ions evaluated via HIT and DSC. Values expressed as mean  $\pm$  SD.**

Tissue	Solution	$T_{onset}$ (°C)	$T_d$ (°C)	$t_{1/2}$ (hr)
Bovine Marginal Chordae Tendineae <sup>116</sup>	Distilled Water	-	69.0 $\pm$ 1.0	47.0 $\pm$ 10.0
	0.1M NaCl	-	66.0 $\pm$ 0.2**	17.0 $\pm$ 2.5**
<b>Human Sartorius Tendon</b>	0.1M PBS <sup>237</sup>	67.2 $\pm$ 0.8**	-	-
	<i>0.1M PBS*</i>	<i>66.1 <math>\pm</math> 0.5**</i>	-	-
	<i>Distilled Water*</i>	<i>68.8 <math>\pm</math> 0.7</i>	-	-

\*Values calculated for tendon collagen from non-diabetic donors. \*\*Significant difference from distilled water values ( $p < 0.05$ ). Italicized data are from current study.

downward trend for toughness ( $p = 0.0708$ ) were observed. Tensile failure mechanics of the multi-fascicle tendon subsamples (e.g. elastic high energy rupture) supported the thermal evidence of a dense network of thermally stable crosslinking (enzymatic and non-enzymatic) from early adulthood to early geriatric age.

The overall absence of changes of the in vitro mechanical properties of the sartorius tendon with age are in partial agreement of studies of lower limb tendons in vivo wherein the modulus remained unchanged<sup>56,57</sup> throughout adulthood. However, in contrast to the current study, the modulus has also been found to decrease with age<sup>137,189,201,205,240</sup> in lower limb tendons. Discrepancies in results between studies may be due to decreases in lower limb muscle strength (sarcopenia)<sup>201</sup>, rate of torque development and activation capacity<sup>240</sup> that occur with aging, which may allow these studies to describe only the low stress region tendon mechanics in vivo.

Further, the relative absence of changes with in the current study has been largely supported by findings in vitro of human lower limb tendons (Table 5.3). Across four decades of adulthood, Sparavalo<sup>237</sup> found that the measured mechanical properties (modulus, strength, and extensibility) of the distal sartorius tendon from male non-diabetic donors (only) remained unchanged. Moreover, in vitro mechanical testing of patellar tendons support the current findings since mechanical properties (e.g. extensibility, toughness) are largely independent of aging post-maturation<sup>34,76,112,121</sup>,



**Table 5.3 Summary of the effects of aging on in vitro mechanical properties of human lower limb tendons. Values expressed as mean  $\pm$  SD.**

Tissue	Strain Rate	Age (years)	Tissue Modulus (MPa)	UTS (MPa)	Failure Strain	Toughness (MJ/m <sup>3</sup> )
Whole Patellar Tendon <sup>109</sup>	200mm/min	29-50	660 $\pm$ 266	65 $\pm$ 15	0.14 $\pm$ 0.06	4.3 $\pm$ 2.5
		64-93	504 $\pm$ 222	54 $\pm$ 10*	0.15 $\pm$ 0.15	3.7 $\pm$ 1.6
Whole Patellar Tendon <sup>76</sup>	10%/sec	18-55	340 $\pm$ 97	78 $\pm$ 19	0.31 $\pm$ 0.06	-
Whole Patellar Tendon <sup>34</sup>	10%/sec	17-54	302 $\pm$ 83**	36 $\pm$ 11	-	-
Sartorius Tendon Multi-Fascicle Subsamples <sup>237</sup>	0.25%/sec	20-40	168 $\pm$ 86	31 $\pm$ 12	0.29 $\pm$ 0.02	5.0 $\pm$ 1.7
		41-60	206 $\pm$ 49	33 $\pm$ 9	0.27 $\pm$ 0.02	5.3 $\pm$ 1.6
<b>Sartorius Tendon Multi-Fascicle Subsamples<sup>9</sup></b>	0.25%/sec	<i>16-40</i>	<i>208 <math>\pm</math> 47</i>	<i>44 <math>\pm</math> 10</i>	<i>0.29 <math>\pm</math> 0.04</i>	<i>6.9 <math>\pm</math> 1.8</i>
		<i>41-60</i>	<i>195 <math>\pm</math> 35</i>	<i>37 <math>\pm</math> 8</i>	<i>0.26 <math>\pm</math> 0.04</i>	<i>5.3 <math>\pm</math> 1.6</i>

\*Significant difference between young and old ( $p < 0.05$ ); \*\*Significant decrease with aging; <sup>9</sup>Inclusive of male non-diabetic, male diabetic, and female non-diabetic population. Italicized data are from current study.

irrespective of donor sex<sup>105</sup>. Contrasting the present study, though, separate studies of patellar tendons have found decreases in strength<sup>121</sup> or modulus<sup>34</sup> with aging. It is possible that differing strain rates (0.25%/sec vs. 10%/sec<sup>76</sup>), sample selection bias (injury), or gripping across studies may add to the literature variance in tendon mechanics with age<sup>105,112,121</sup>.

#### *BMI May Play a Confounding Role in the Study of Aging and Tendon Mechanics*

With the exception of two class III obese individuals (BMI > 40), it might be suggested that donor BMI in the sample population increased linearly with age ( $p = 0.0583$ ). It is possible that an inverse relationship between BMI and physical activity level may be a confounding effect on assessed tendon mechanics with aging. Despite the reported BMI-related decreases in strength and modulus of the multi-fascicle samples from the female donor population, it is possible that rather than triggering an increase in

material properties (e.g. toughness) due to increasing BMI (with potential associated changes in physical activity) and age, an increase in tendon dimensions (tendon hypertrophy) might occur instead<sup>51,57,242</sup>.

## **5.2. Sex-Related Changes in Sartorius Tendon Collagen Thermal Stability and Mechanics**

### *5.2.1. Thermal Stability and Degree of Thermally Stable Crosslinking of Sartorius Tendon Collagen are Independent of Donor Sex*

To the author's knowledge, this is the first study to investigate the influence of a donor's sex on the thermal stability of tendon collagen. As hypothesized, thermal investigations revealed no differences with sex in the thermal stability ( $T_{onset}$ ,  $T_{peak}$ ,  $T_d$ ), distribution of thermal stability ( $FWHM$ ) and the specific enthalpy of denaturation ( $h_{wet\ mass}$  and  $h_{dry\ mass}$ ). Dense thermally stable crosslinking and molecular packing in both sexes was evidenced by high collagen denaturation temperatures and resistance to load decay (female: 71%, male: 54%) under a 90°C isotherm in HIT. A recent biochemical study of human patellar tendon from young adults (21-30 years of age) failed to show that there are sex-linked difference in the mature enzymatic crosslink Hyl-Pyr<sup>152</sup>, supporting the findings of no significant differences in the thermally stable crosslinking of the sartorius tendon collagen analysed via HIT ( $t_{1/2}$ ).

### *5.2.2. Relationships Between Donor Sex and Tendon Mechanics*

#### *Donor Sex Influences Sartorius Tendon Mechanics*

Despite the absence of identifiable sex-linked changes in molecular thermal stability via HIT and DSC, and in contrast to a hypothesis, sartorius tendon multi-fascicle subsamples from female donors were 25% weaker ( $UTS$ ), 38% less tough, and 16% less extensible ( $Strain\ at\ UTS$ ) than were samples from male donors. Despite these findings suggesting a more mechanically fragile sartorius tendon in females, no changes in failure motifs due to overload were observed under SEM between sexes.

In the current literature, there are limited studies investigating sex-related changes of in vitro human tendon mechanical properties (Table 5.4). Magnusson and coworkers<sup>162</sup> likewise identified in vitro a 50% decrease in strength, while reporting a ~53% lower tendon modulus in isolated Achilles tendon fascicles from female donors compared to male donors. Meanwhile, Hashemi *et al.*<sup>105</sup> found that, in contrast to the current study, human patellar tendons mechanical properties from donors aged 17-50 years were independent of sex; however, linear increases in tendon strength and modulus were attributed to tendon mass density. It may be speculated that inconsistencies in the sex-determined differences in mechanical properties in vitro may be masked by the use of differing strain rates (0.25%/sec vs. 100%/sec<sup>105</sup>) and/or by the determination of the sample CSA.

In vivo, in disagreement with the present findings of unchanged sartorius tendon modulus between sexes throughout adulthood, decreased lower limb tendon modulus (patellar<sup>190</sup> and Achilles<sup>46,110,153,190</sup>) has been reported in females. However, one study found that in post-menopausal age the discrepancy in patellar tendon modulus is absent<sup>227</sup>. It is possible that the differences in tendon mechanical properties in vivo between studies are the result of a difference in the maximum voluntary contraction of the acting muscle, tendon length and moment arm length acting upon the tendon within an individual<sup>177,268</sup>.

*Difference in Sartorius Tendon Mechanical Behaviour Between Donor Sexes may be Related to Collagen Content or Sex Hormone Concentrations*

Alternatively, sex-related differences in tendon mechanical properties may not lie at the molecular level as assessed by DSC and HIT. Evidence in human patellar tendons suggests that changes in collagen content<sup>152</sup> and type<sup>102</sup> – in particular collagen type III – may explain differences in tendon collagen between sexes. Furthermore, sex hormones (e.g. estrogen, testosterone) are influential during development and further aging, and may contribute to determining tendon mechanical properties. Testosterone, present in 7-8 times higher concentration in males has proven to be correlated with increased stiffness and collagen synthesis rates<sup>3,102</sup>. Meanwhile, there have been findings of reduced

**Table 5.4 Summary of in vitro mechanical studies identifying sex-determined differences in human lower limb tendon mechanical properties. Values expressed as mean  $\pm$  SD.**

Tissue	Strain Rate	Sex: Age (years)	Tissue Modulus (MPa)	UTS (MPa)	Failure Strain	Toughness (MJ/m <sup>3</sup> )
Whole Patellar Tendon <sup>105</sup>	100%/s	Female: 17-50	513 $\pm$ 134	60 $\pm$ 17	0.18 $\pm$ 0.03	4.8 $\pm$ 0.8
		Male: 26-50	501 $\pm$ 143	58 $\pm$ 15	0.18 $\pm$ 0.03	4.4 $\pm$ 1.1
Patellar Tendon Fascicle <sup>162</sup>	0.13 mm/s	Female: Young Adult	576 $\pm$ 86	39 $\pm$ 4 <sup>*,<math>\Psi</math></sup>	-	-
		Male: Young Adult	1230 $\pm$ 190 <sup><math>\Phi</math></sup>	76 $\pm$ 16 <sup>*</sup>	-	-
<b>Sartorius Tendon Multi-Fascicle Subsample</b>	0.25%/sec	<i>Female: 16-58</i>	<i>186 <math>\pm</math> 40</i>	<i>34 <math>\pm</math> 7<sup><math>\Psi</math></sup></i>	<i>0.24 <math>\pm</math> 0.04<sup><math>\Psi</math></sup></i>	<i>4.5 <math>\pm</math> 1.1<sup><math>\Psi</math></sup></i>
		<i>Male: 24-59</i>	<i>207 <math>\pm</math> 44</i>	<i>45 <math>\pm</math> 10</i>	<i>0.30 <math>\pm</math> 0.03</i>	<i>7.3 <math>\pm</math> 1.7</i>

\*Measured from printed graph using ImageJ Software.  <sup>$\Psi$</sup> Significant difference from male ( $p < 0.05$ ). Italicized data are from current study.

collagen synthesis rate<sup>152</sup>, decreasing fibrillar diameters and viscoelastic energy dissipation<sup>3,46,102,192</sup> in tendons while in the presence of increased circulating estrogen<sup>85</sup>. Recently, a study by Lee *et al.*<sup>147</sup> showed that in engineered ligaments, inhibition of lysyl oxidase activity (77% after 48 hours) occurred in the presence of high levels of estrogen, possibly reducing the concentration of enzymatic crosslinking – although in the current study, this was not observed via HIT analysis ( $t_{1/2}$ ). In females, despite pregnancy being thought to potentially cause irreversible changes in tendon thermal and mechanical properties due to a combination of cardiovascular changes<sup>132,224</sup> and sex-hormone changes<sup>146</sup>, evidence in the human patellar tendon in vivo shows that mechanical properties remained relatively unchanged<sup>32</sup>.

### 5.3. Diabetes-Related Changes in Sartorius Tendon Collagen Thermal Stability and Mechanics

#### 5.3.1. Relationships Between Diabetes and Tendon Collagen Thermal Stability

##### *Thermal Stability and Thermally Stable Crosslinking Remains Largely Unchanged with Diabetes in Male Donors*

In examining the effects of diabetes on sartorius tendon collagen thermal stability, only an increase in thermal stability in the DSC  $T_{onset}$  – a measure of the onset of the phase transition from helix to near-random coil configuration – was identified using both distilled water and PBS as the hydrating medium, partially confirming the hypothesis of increased thermal stability. Curiously, the absence of significant differences in thermal stability ( $T_d$ ,  $T_{peak}$ ) and tendon water content suggests an overall similarity in molecular packing of the sartorius tendon collagen between non-diabetic and diabetic donors. Similarly, the enthalpy of denaturation ( $h_{wet\ mass}$  and  $h_{dry\ mass}$ ) remained unchanged with diabetic status, despite the suggested narrowing of the distribution of thermal stabilities in tendon collagen from diabetic males ( $p = 0.0944$ ). Independent of diabetic status, consistent findings of isothermal contraction in tendon strip-samples via HIT revealed the continuing presence of dense thermally stable crosslinking with diabetes ( $t_{1/2}$ ).

In support of these findings, Couppé *et al.*<sup>58</sup> provided evidence that the concentrations of the crosslinks pentosidine and Hyl-Pyr in the Achilles tendons of adult humans (45-70 years of age) did not differ significantly between age-matched diabetic and non-diabetic individuals. Furthermore, the mature enzymatic crosslink Hyl-Pyr was found in ~40x the concentration of pentosidine<sup>58</sup>, indicative of the dense thermally stable enzymatic crosslinking present, possibly of comparable crosslinking to that in the human sartorius tendon.

Animal tendon studies have been used to examine the effects of diabetes. Typically, an in vitro glucose or ribose incubation animal model of 14-28 days is used to mimic the enhanced glucose concentration present in an acute hyperglycemic state (Table

5.5) without the other pathophysiological effects of diabetes. For example, a 4-week incubation in a 200mM ribose solution has been suggested to simulate ~20 years of aging and diabetes<sup>150</sup>. In contrast to the observations of a largely insignificant change in thermal stability with diabetic state in the current study, DSC investigations of BTT (28 days, 200mM, ribose)<sup>150</sup> and rabbit Achilles tendon (14 days, 100mg/mL, ribose)<sup>251</sup> have found that, due to the increases in AGE crosslinking, the thermal stability ( $T_{onset}$ ,  $T_{peak}$ ) increases in the presence of a decreased distribution of thermal stabilities ( $FWHM$ ). Similarly, Reihanser and coworkers<sup>206</sup> demonstrated an increase in thermal stability by in vitro glycation of RTT (14 days, 100mmol/L, glucose), with an attenuation of the stabilizing effect of the glycation-induced AGE crosslinks with aging. Compared to the sartorius tendon collagen from the male diabetic donors, the dramatic increases in the thermal stability and decreases in the distribution of thermal stabilities observed in animal models may be indicative of the density of thermally stable crosslinking present, as the proportion of additional AGE crosslinking would be easier to detect.

### 5.3.2. Relationships Between Diabetes and Mechanical Properties in Male Donors

#### *Sartorius Tendons from Male Diabetic Donors Exhibit More Brittle Behaviour*

In the present study, the hypothesis of the sartorius tendon becoming a more brittle and mechanically fragile tissue in the presence of diabetes was confirmed by findings of decreased extensibility (20%) and toughness (38%) when compared to similar aged male donors (Diabetic:  $55.6 \pm 5.3$  years, Non-Diabetic:  $48.1 \pm 7.9$  years). Curiously, the modulus and strength of the sartorius tendon were found to be independent of diabetes in males.

In the literature, studies of diabetes-determined differences in tendon mechanical properties in vitro in animals and humans have provided conflicting results. In support of the current findings, the Achilles tendon modulus in the linear region remained unchanged in dogs with naturally occurring diabetes and who were receiving insulin therapy for 4-9 years<sup>141</sup>. In vitro studies of diabetes-induced rats and mice have shown in contrast to the current work, a decrease in the modulus of lower limb tendons

**Table 5.5 Summary of thermal Studies (HIT/DSC) of tendon collagen subject to in vitro glycation or natural diabetes. Values expressed as mean  $\pm$  SD.**

<b>Tissue</b>	<b>Reducing Sugar (Concentration), Incubation Duration</b>	<b>Heating Rate (°C/min)</b>	$\Delta T_d$ (°C)	$\Delta T_{onset}$ (°C)	$\Delta T_{peak}$ (°C)	$\Delta FWHM$ (°C)	$\Delta h$ (J/g)
Rabbit Achilles Tendon (8-9 M.O.) <sup>251</sup>	Ribose (100 mg/mL), 14 days	5	-	-	+ 4.1*	-1.0*	-7.1*
Rabbit Achilles Tendon (28-34 M.O.) <sup>251</sup>	Ribose (100mg/mL), 14 days	5	-	-	+ 3.4*	-1.1*	-1.8*
Steer Tail Tendon (18-30 M.O.) <sup>150</sup>	Ribose (200 mM), 28 days	10	-	+1.7 $\pm$ 0.5*	+1.6 $\pm$ 0.5*	-	-0.8 $\pm$ 0.5*
<b>Human Sartorius Tendon (38-60 Y.O.)</b>	<i>Diabetes, N/A</i>	5	<i>-0.68</i>	<i>+0.68*</i>	<i>+0.36</i>	<i>-0.15<sup>ϕ</sup></i>	<i>-1.69</i>

\*Significant difference from control or non-diabetic tendon sample ( $p < 0.05$ ). <sup>ϕ</sup>Difference suggests significance ( $p = 0.0998$ ). Italicized data are from current study.

(Achilles<sup>36,81,173</sup>, patellar<sup>55</sup>), with inconsistent decreases in the *UTS*<sup>36,218</sup> and toughness<sup>218</sup> across studies. In humans, there have been few studies investigating diabetes-based changes in the mechanical properties of the Achilles tendon (Table 5.6). Consistent with the sartorius tendon multi-fascicle subsamples, despite the extreme change in strain rate in vitro (0.25%/sec vs. ~100%/sec), extensibility and toughness were decreased in the Achilles tendon samples from the diabetic donors<sup>98</sup>. In disagreement with the current findings, the modulus and/or strength were lowered in the diabetic Achilles tendon samples<sup>94,98</sup>. However, the results obtained in the studies by Grant *et al.*<sup>94</sup> and Guney *et al.*<sup>98</sup> may be confounded by the combined influence of diabetes *and* a specific pathological condition of interest (e.g. diabetic foot ulcers<sup>94</sup> and Charcot's foot<sup>98</sup>). Variability in the harvesting and storage of the Achilles tendon samples from diabetic and non-diabetic donors within the study by Grant *et al.*<sup>94</sup> may further confound mechanical testing results. Unlike in the previously described studies of symptomatic diabetic individuals, the current study investigated only the influence of diabetes on tendon mechanics.

### 5.3.3. Diabetic Tendon Coloration Remains Largely Unchanged

In the current study, there was no consistent evidence of altered tendon coloring in the sartorius tendon samples due to the combined effect of diabetes and aging. In contrast to the findings in this study, in the literature, the typical brilliant pearl white of tendon collagen is consistently replaced by a yellow-golden coloring in diabetic<sup>95,174,236</sup> and in vitro glycated<sup>41,81,135,150,231,260</sup> collagenous tissues. It is possible that the expected change might be the result of an elevated accumulation of the fluorescent AGE crosslinks (e.g. pentosidine)<sup>14</sup>. However it is possible that in the sartorius tendon, similar to evidence in the human Achilles tendons from older individuals (Non-Diabetic:  $59 \pm 7$  years, Diabetic:  $58 \pm 5$  years)<sup>58</sup>, the concentration of the fluorescent pentosidine crosslinks may be independent of diabetic status. Furthermore, evidence in the study of humans patellar tendons suggests that regular physical activity reduces the accumulation of AGE crosslinks<sup>57</sup>. Unfortunately, information regarding potential confounding



**Table 5.6 Summary of the influence of diabetes on the in vitro mechanical properties of human lower limb tendons. Values expressed as mean  $\pm$  SD.**

Tissue	Strain Rate	Diabetic Status: Age (years)	Tissue Modulus (MPa)	UTS (MPa)	Failure Strain	Toughness (J/m <sup>3</sup> )
Whole Achilles Tendon <sup>98</sup>	10%/sec	ND: 48 $\pm$ 21	414 $\pm$ 67	-	0.30 $\pm$ 0.10	1.2 $\pm$ 0.3
		D: 69 $\pm$ 11	347 $\pm$ 68*	-	0.20 $\pm$ 0.03*	1.0 $\pm$ 0.3*
Whole Achilles Tendon <sup>94</sup>	10%/sec	ND: N/A	272 $\pm$ 86	37 $\pm$ 28	-	-
		D: N/A	80 $\pm$ 48*	17 $\pm$ 11*	-	-
<b>Sartorius Tendon Multi-Fascicle Subsample</b>	0.25%/sec	<i>ND: 48 <math>\pm</math> 8</i>	<i>196 <math>\pm</math> 43</i>	<i>44 <math>\pm</math> 11</i>	<i>0.30 <math>\pm</math> 0.03</i>	<i>7.3 <math>\pm</math> 2.0<sup><math>\delta</math></sup></i>
		<i>D: 55 <math>\pm</math> 5</i>	<i>199 <math>\pm</math> 30</i>	<i>36 <math>\pm</math> 6</i>	<i>0.24 <math>\pm</math> 0.02*</i>	<i>4.7 <math>\pm</math> 0.9*<sup><math>\delta</math></sup></i>

\*Significantly different from non-diabetic population ( $p < 0.05$ ).  <sup>$\delta$</sup> MJ/m<sup>3</sup>. Italicized data are from current study.

variables of physical activity level or blood sugar regulation of the diabetic donors for this study was not provided.

#### 5.4. Tensile Failure Mechanics and SEM Structural Studies

##### 5.4.1. Tensile Failure Mechanics of the Sartorius Tendon Reflects Dense Crosslinking

Tensile failure mechanics of the sartorius tendon multi-fascicle samples consisted of a high-energy, elastic, piecewise brittle snapping as observed in other mechanical studies of tendons in vitro performed by Bennett *et al.*<sup>30</sup> and Sparavalo<sup>237</sup>, with the snapping clearly audible over the sounds of the hydraulic system. This brittle behaviour was found to be independent of donor age, sex and diabetic status, contrasting with a previous study by Guney *et al.*<sup>98</sup> wherein Achilles tendons from diabetic donors underwent a more gradual failure. As shown in Figure 5.2, the brittle piecewise failure of the densely crosslinked sartorius tendon contrasted with the tensile failure mechanics of the weakly crosslinked bovine CDET, that failed as a single component in a gradual manner (a parabolic shaped plastic region)<sup>109</sup>. Perhaps indicative of the increase in brittle

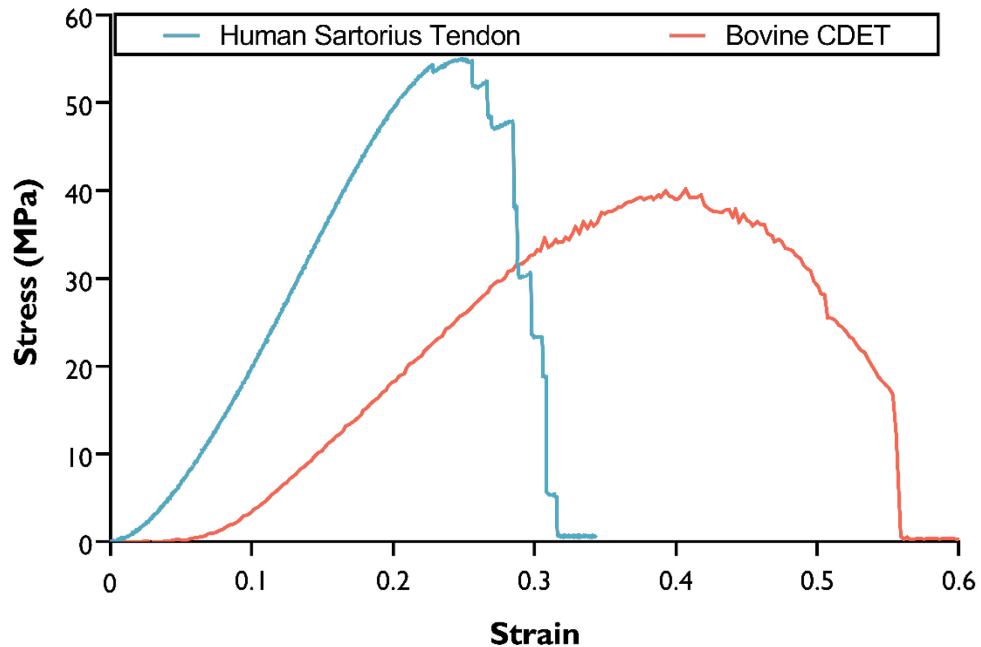


**Figure 5.2** Representative normalized stress-strain curves of the human sartorius tendon (blue) and the bovine CDET (red). A marked difference in the failure mechanics are observed. The densely crosslinked sartorius tendon multi-fascicle subsample fails in a brittle piecewise manner in contrast to the single component gradual failure of the weakly crosslinked bovine CDET. Bovine CDET data from Herod *et al.*<sup>109</sup>.

behaviour of the tensile failure mechanics, the sartorius tendon multi-fascicle subsamples demonstrated a similar range of modulus and strength, yet were less extensible and tough when compared to previously studied bovine tendons<sup>109,276</sup> (Table 5.7).

#### 5.4.2. Discrete Plasticity is Absent in Overloaded Sartorius Tendon

Overall, consistent with prior SEM investigations in the densely crosslinked sartorius tendon<sup>237</sup>, an *absence* of discrete plasticity and consistent failure motifs at the nanoscale independent of age, sex, and diabetes were observed. Across all donor tendons, evidence of elastic recoil, hairpin turns, local fibril damage and complete fibril breakage of collagen fibrils. In the few (3/19 donors) tendon samples exhibiting apparent plasticity damage – that lacked the primary motifs of discrete plasticity<sup>257</sup> – interkink D-banding was preserved and kinking along often isolated fibrils occurred for at maximum ~200 microns. The tendons from these particular donors (24, 25, and 39 years of age) displayed

**Table 5.7 Summary of in vitro mechanical properties of tendons tested in the Tissue Mechanics Lab demonstrating varying degrees of discrete plasticity damage. Values expressed as mean  $\pm$  SD.**

<b>Tissue</b>	<b>Strain Rate</b>	<b>Tissue Modulus (MPa)</b>	<b>UTS (MPa)</b>	<b>Failure Strain</b>	<b>Toughness (MJ/m<sup>3</sup>)</b>	<b>Degree of Discrete Plasticity?</b>
Steer Tail Tendon <sup>276</sup> (24-30 M.O.)	0.01%/sec	421 $\pm$ 80	60 $\pm$ 10	-	9.1 $\pm$ 3.0	Extensive
Bovine CDET <sup>109</sup> (24-36 M.O.)	10%/sec	151 $\pm$ 46	38 $\pm$ 8	38 $\pm$ 18	14.3 $\pm$ 3.6	Extensive
Bovine SDFT <sup>109</sup> (24-36 M.O.)	10%/sec	102 $\pm$ 34	23 $\pm$ 8	33 $\pm$ 12	6.8 $\pm$ 3.4	Sparse
Human Sartorius Tendon Multi-Fascicle Subsample <sup>237</sup> (Male ND, 20-60 Y.O.)	0.25%/sec	189 $\pm$ 66	32 $\pm$ 10	28 $\pm$ 4	5.2 $\pm$ 1.9	Absent
<b>Human Sartorius Tendon Multi-Fascicle Subsample (16-60 Y.O.)*</b>	<i>0.25%/sec</i>	<i>199 <math>\pm</math> 38</i>	<i>39 <math>\pm</math> 9</i>	<i>27 <math>\pm</math> 4</i>	<i>5.7 <math>\pm</math> 1.8</i>	<i>Absent</i>

\*Inclusive of male non-diabetic, male diabetic and female non-diabetic donor populations. Italicized data are from current study.

greater toughness ( $> 6 \text{ MJ/m}^3$ ) and distribution of thermal stabilities ( $FWHM > 2^\circ\text{C}$ ) while being amongst the donors with the highest proportion of load decay observed via HIT.

From the Tissue Mechanics Lab<sup>109,150,237,257,276</sup> (Table 5.1, Table 5.7), it could be suggested that the formation of discrete plasticity in collagen fibrils occurs within tendons exhibiting a higher average toughness, sparse thermally-stable crosslinking (failure to reach  $90^\circ\text{C}$  isotherm), and a broader average distribution of thermal stabilities. In the sartorius tendon, likely of a similar profile to the patellar tendon<sup>56</sup>, the elevated density of mature enzymatic (Hyl-Pyr) and non-enzymatic (pentosidine) intermolecular crosslinking restricts molecular sliding, thought to be necessary for the formation of discrete plasticity<sup>150</sup>.

Consistent with Sparavalo<sup>237</sup> (Figure 5.3), the high-energy, snapping, piecewise failure of the sartorius tendon multi-fascicle subsample was accompanied by elastic recoil damage at the nanoscale in SEM: balling, twisting and tangling of ruptured fibrils. The formation of hairpin turns in isolated fibrils occurred, at times serially along the length of the fibril. Appearances of hairpin turns occurred in both control and overloaded tendons, possibly in part due to sample preparation, however, with a significantly higher frequency and density in the overloaded specimens. Local fibril damage and complete fibril breakage was observed in isolated or neighboring fibrils, consistent with evidence of local fibril failure discovered via TEM by Meinel and coworkers<sup>164</sup> in a ruptured Achilles tendon of a 29-year old female ballet dancer (Figure 5.4). A feature of importance to note in both the sartorius and Achilles tendon is that disruption of the substructure was present only at the damage sites. Local failure of the collagen fibrils may be indicative of inhomogeneities in collagen stability as displayed in BTT fibril modulus via AFM<sup>24</sup>.

In the present study, qualitative differences in ultrastructure organization were not found to be determined by diabetic state. In contrast, Grant *et al.*<sup>95</sup> described SEM investigations in regions of “twisted”, “curved” and otherwise disorganized Achilles tendon fibrils in 11 of 12 diabetic individuals in comparison to non-diabetic individuals. Comparable contrasting structural changes have been discussed in review papers of

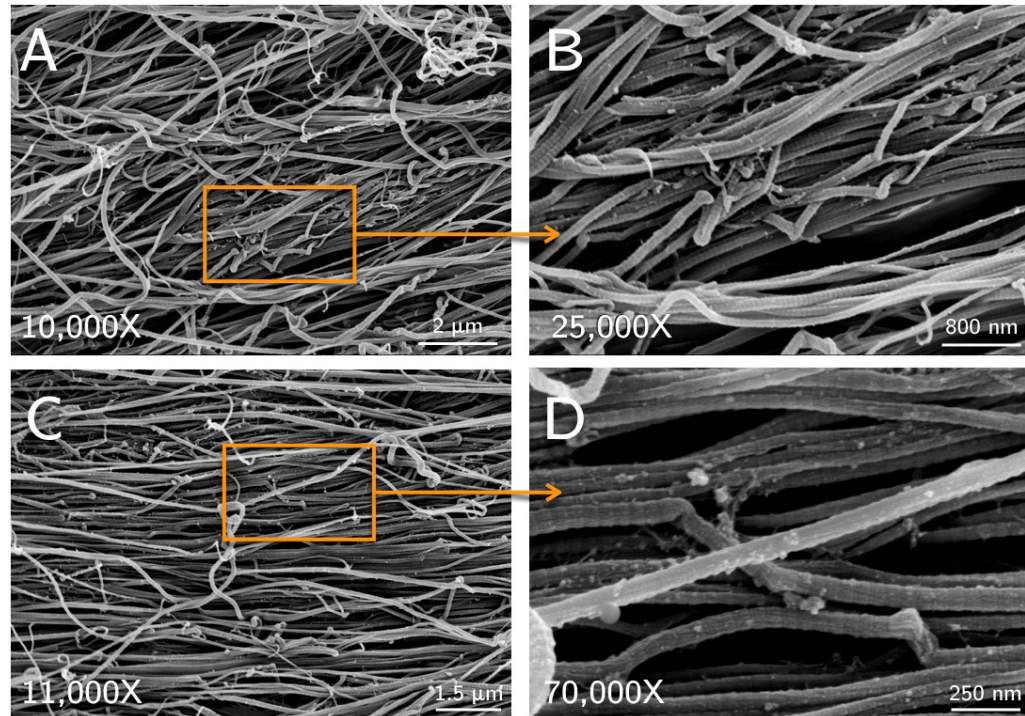


**Figure 5.3 SEM micrographs of overloaded human sartorius tendons revealing hairpin turns, recoiled fibrils and overall disorganization. Reprinted with permission<sup>237</sup>.**

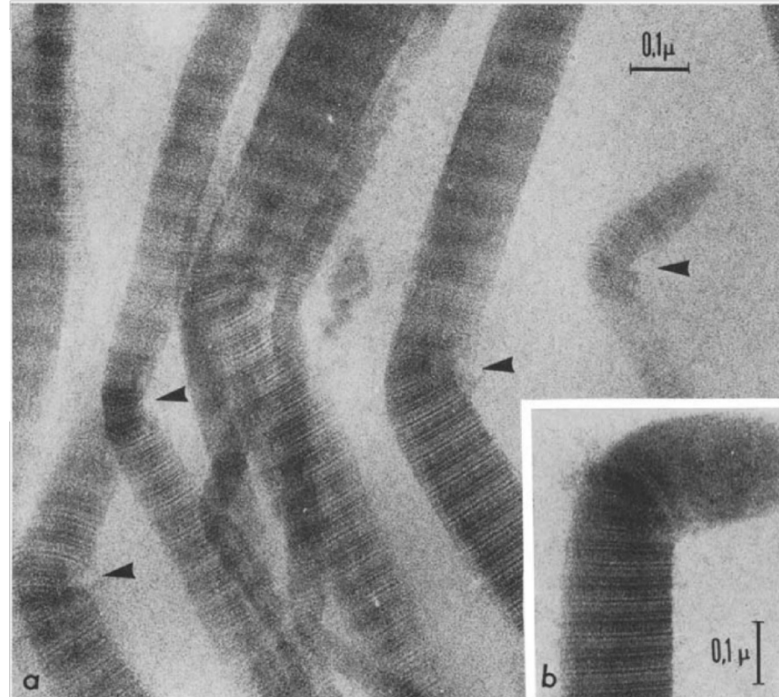


**Figure 5.4 TEM micrograph of local fibril failure (indicated by the black arrow heads) in a ruptured Achilles tendon from a 29-year old female ballet dancer at 38,000x. Reprinted with permission<sup>164</sup>.**

induced diabetic rat model studies, predominantly examining models of the Achilles tendon<sup>188,231</sup>.

## **5.5. Light Microscopy Studies of Structure and Composition**

### *5.5.1. Birefringence: Collagen Crimp Flattening and Period Increases with Aging and Diabetes*

From the preliminary light microscopy studies, few noticeable changes in structure and composition of the sartorius tendon were observed with age. Qualitatively, collagen fiber flattening and crimp length were increased with age under polarized light microscopy. Changes in the collagen crimp were similar between tendons from older non-diabetic and diabetic male donors. Studies of human Achilles tendon<sup>241</sup> and RTT<sup>68</sup> have found a similar loss of crimp amplitude and increase in crimp wavelength of collagen fiber with aging. In light of the observed qualitative flattening of the collagen crimp and increase in crimp wavelength with aging, one would expect a decrease in extensibility, however, this does not agree with the mechanical findings of age-independent extensibility in the current study.

### *5.5.2. H & E Staining: The Human Sartorius Tendon is Highly Cellular, Decreasing with Aging and Diabetes*

H & E staining of nuclei provided evidence of changes in cellular content with aging. Examination of a young female and male non-diabetic donor demonstrated dense nuclei content with no obvious differences between sexes. In the male donors, the density of nuclei appeared to be lower with the combined influence of aging and diabetes, likely indicative of lowered cellular activity and lowered tendon collagen turnover. The result of a qualitative decrease in nuclei content was similarly observed when investigating the sole influence of aging. In support of the current findings, in the human Achilles tendon, a qualitative decrease in nuclei content was observed throughout 4 decades of adulthood (30-66 years of age), and this process appeared to be accelerated in the presence of diabetes<sup>241</sup>. Elsewhere, a study of Achilles tendons provided no comment on the changes

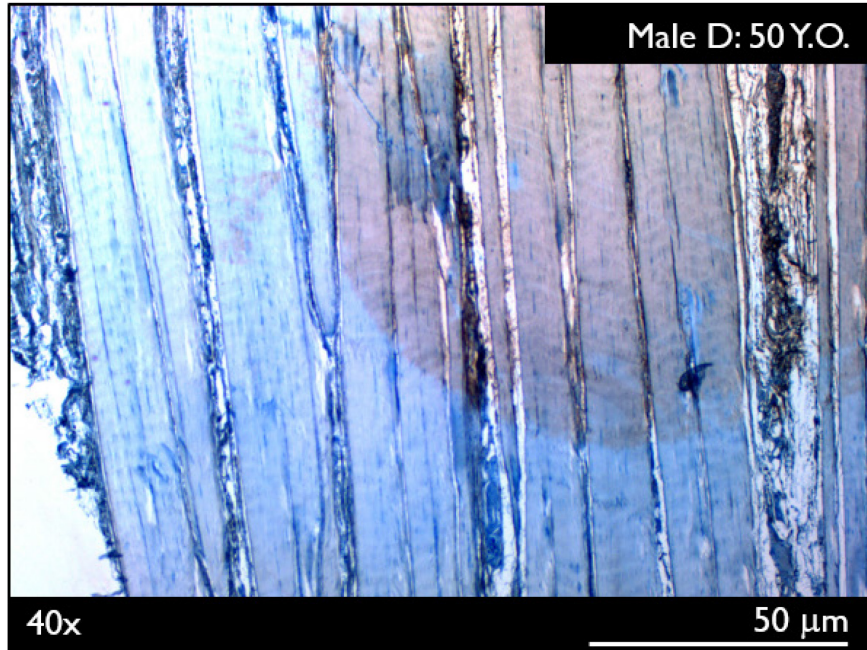
in the content of nuclei between old diabetic and non-diabetic donors<sup>98</sup>; rather, tendon samples from diabetic donors displayed focal regions of collagen fiber disorganization and degeneration that were not observed in the current study. Taken together, the potential effects of a reduced cellular quantity and fiber disorganization support the notion of a reduced healing capacity in tendons from diabetic individuals<sup>236</sup>.

### *5.5.3. $\alpha$ -PEN12: Qualitative Increases in $\alpha$ -PEN12 Epitope Concentration with the Combined Influence of Aging and Diabetes*

In comparing the combined effects of aging and diabetes on pentosidine concentration (the biomarker for AGE accumulation), immunohistochemistry was performed using an antibody for the pentosidine epitope ( $\alpha$ -PEN12). A qualitative increase was identified in the degree of positive (DAB) staining for  $\alpha$ -PEN12 when comparing tendon collagen from an old diabetic and a young non-diabetic donor. While the present study did not differentiate between aging and diabetic state on the concentration of  $\alpha$ -PEN12, previous studies have examined these separately<sup>56,58</sup>. In support of this result, in the human patellar tendon, HPLC analysis has shown a significant six-fold increase in pentosidine accumulation when comparing a young ( $27 \pm 2$ ) and older ( $67 \pm 3$ ) group of male donors<sup>56</sup>. Pentosidine concentration has not been found to be significant between non-diabetic and diabetic donors with similar physical activity levels and age<sup>58</sup>, suggesting that the increase in  $\alpha$ -PEN12 epitope concentration in the sartorius tendon occurring due to the combination of aging and diabetes would be comparable to solely studying the effect of aging.

In preliminary experiments, the use of a heat-induced epitope retrieval method (HIER) denatured much of the collagen on the slides, and it was found that the technique was much more informative without HIER. Positive staining occurred uniformly across collagen fibers. This is confirmed in Figure 5.5, where a drop of the primary was placed on the sample for a short duration ( $< 2$  minutes) and the experiment proceeded according to protocol. Clearly defined edges are displayed where the primary had been placed, suggesting that binding to non-specific endogenous receptors did not occur (which would have resulted in misleading background staining). Further studies are necessary to

**A**



**B**

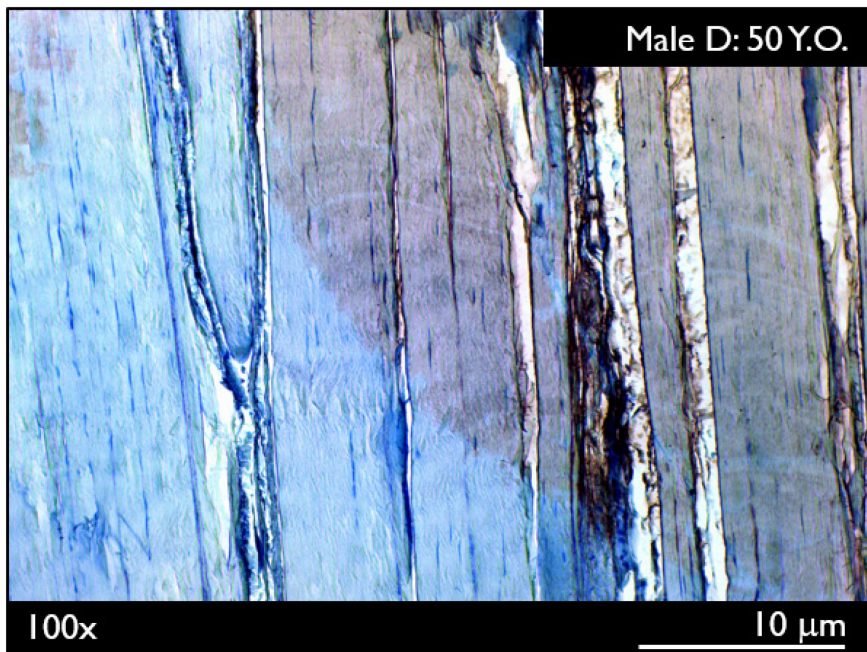


**Figure 5.5** Light microscopy images at 40x and 100x magnification identifying the differences in positive and negative staining of the primary antibody with a clear border where the drop of  $\alpha$ -PEN12 antibody was placed.



independently evaluate the age-related changes in  $\alpha$ -PEN12 concentration and to determine if HIER at various temperatures might be useful to access potential epitopes masked by the 10% formalin fixation.

## 5.6. Summary of Objectives and Hypotheses

### 5.6.1. Study #1 Assessing Collagen Structure and Thermal Stability

**Hypothesis #1:** Thermomechanical behaviour will depend significantly on donor age. With aging, increases in thermally stable crosslinks will further confine the fiber lattice and increase molecular packing resulting in increased overall thermal stability. Aging will result in a decreased distribution of thermal stabilities and an increase in thermally stable crosslinks.

**Conclusion:** With increasing age, it was shown that sartorius tendon collagen thermal stability evaluated by HIT and DSC showed significant decreases in some parameters within the female and male non-diabetic donor populations. Similarly, the distribution of thermal stabilities (*FWMH*) and wet mass enthalpy significantly decreased with age. As sartorius tendon collagen ages, no changes in the concentration of thermally stable crosslinking were observed ( $t_{1/2}$ ) in either sex.

**Hypotheses #2:** Thermomechanical behaviour of tendon collagen over all age ranges will be independent of donor sex. Given the high load-bearing nature of the sartorius tendon and similar tendon compositions between sexes, it is expected that the overall collagen thermal stability, distribution of thermal stabilities (*FWHM*) and thermally stable crosslinking will be independent of sex over all age ranges.

**Conclusion:** No significant changes in thermal stability in tendon collagen were found between female and male non-diabetic donors. Moreover, the distribution of thermal stabilities (*FWHM*), enthalpy of denaturation, and density of thermally stable crosslinking ( $t_{1/2}$ ) did not differ between sexes.

**Hypothesis #3:** Within each sex, diabetic status will significantly determine thermomechanical behaviour of tendon collagen over all age ranges. Accelerated

accumulation of intermolecular glycation crosslinks in tissues from diabetic donors, with regards to the polymer-in-a-box theory<sup>170</sup>, will further increase molecular packing and restrict conformational freedom. Overall collagen thermal stability and total thermally stable crosslinking will be increased, accompanied by a decreased distribution of thermal stabilities in sartorius tendon collagen from the diabetic donors.

**Conclusion:** Thermal stability assessed via DSC revealed an increase in  $T_{onset}$  in tendon collagen from the male diabetic donors when evaluated using both distilled water and PBS as the hydrating solution. However, the distribution of thermal stabilities (*FWHM*), enthalpy of denaturation, HIT  $T_d$ , and isotherm behaviour the thermal stability remained independent of diabetic status in male donors.

#### 5.6.2. Study #2: Assessing Mechanical Behaviour of Sartorius Tendon Collagen

***Hypothesis #1:*** Mechanical behaviour of tendon multi-fascicle subsamples will depend significantly on donor age. With anticipated changes in collagen content and crosslinking profile of aging tendons<sup>66,242</sup>, aging is expected to result in a stiffer, more brittle tissue within each donor population.

**Conclusion:** With aging, no significant changes in tendon multi-fascicle subsample mechanics and tensile properties with age were observed in the male non-diabetic and male diabetic population. Samples from female donors exhibited both a significant decrease in strength and a trend toward decreasing toughness ( $p = 0.0859$ ) with aging.

***Hypotheses #2:*** Mechanical behaviour of tendon multi-fascicle subsamples over all age ranges will be independent of the donor sex. Although minor changes in composition have been observed in human Achilles and patellar tendon studies between sexes<sup>152</sup>, bulk mechanical properties will be independent of sex.

**Conclusion:** Despite an absence of sex-determined difference in the tensile failure mechanics of the sartorius tendon multi-fascicle subsample (e.g. brittle piecewise failure), some mechanical properties were determined by the donor sex. In the female donors, tendon multi-fascicle subsample strength, toughness and extensibility were significantly

lower when compared to the male donor population, while curiously, the modulus remained independent of the donor sex.

***Hypothesis #3:*** Within each sex, diabetic status will significantly determine the mechanical behaviour of the sartorius tendon multi-fascicle subsamples over all age ranges. Further increases in AGE intermolecular crosslink formation will negatively impact tendon multi-fascicle subsample mechanical behaviour, resulting in a stiffer and more brittle tissue.

**Conclusion:** Despite an absence of diabetes-determined differences in the multi-fascicle subsample tensile failure mechanics (e.g. brittle piecewise failure) from male donors, the mechanical properties of toughness and extensibility were reduced in samples from the diabetic males. Unexpectedly, strength and modulus remained unchanged in the similarly aged population: 38-60 years old.

#### *5.6.3. Study #3: Assessing Overload Damage to Tendon Collagen*

***Hypothesis #1:*** Failure mechanisms, as described by an absence of discrete plasticity in a previous study<sup>237</sup>, of tendon collagen will not depend significantly on donor age.

***Hypothesis #2:*** Failure mechanisms of tendon collagen over all age ranges will be independent of the donor sex.

***Hypothesis #3:*** Within each sex, diabetic status will significantly determine the failure mechanisms of tendon collagen over all age ranges. Evidence of more brittle fractures of tendon collagen fibrils from diabetic donors is anticipated.

**Conclusions:** Nanoscale failure mechanics of tendon collagen identified by SEM were independent of donor age, sex and diabetic status. Evidence of an increase in brittle fractures of collagen fibrils from male diabetic donors was not found, and may require further studies. Damage motifs of elastic recoil, hairpin turns, and local fibril failure were observed in all samples. Plasticity damage was rarely observed in younger (24, 25 and 39 Y.O.) and tougher donor tendon multi-fascicle subsamples; nevertheless, the extent of the influence of aging on its formation remains unclear.

#### 5.6.4. Study #4: Histology & Immunohistochemistry

***Hypothesis #1*** In tendon collagen from (i) the older male diabetic donor, expectations are that an increase in collagen crimp wavelength will occur when compared to the tendon from (ii) the young male non-diabetic donor. With the suggested lowered turnover of tendon collagen in the old donor, the increased physical age of the fiber will result in a qualitative increase in the crimp wavelength.

**Conclusion:** In tendon collagen samples from both non-diabetic and diabetic donors in their sixth decade of life, collagen crimp flattening and increase in the crimp wavelength was evident in comparison to a young (24 Y.O.) non-diabetic donor.

***Hypothesis #2*** In tendons from (i) the old diabetic donor, expectations are that a decreased nuclei content via H & E staining will occur when compared to the tendon from (ii) the young non-diabetic donor. With aging and diabetes, marked qualitative decreases in cellular content is anticipated.

**Conclusion:** Although a surprisingly high level of nuclei was present overall in the densely crosslinked sartorius tendon irrespective of age, a qualitative decrease in nuclei content occurred in the older versus younger donor. This decrease in nuclei content with aging appears to be independent of diabetic status.

***Hypothesis #3:*** In the tendon from (i) the older diabetic donor, expectations are that an increased presence of the pentosidine epitope ( $\alpha$ -PEN12) will occur when compared to the tendon from the (ii) young non-diabetic donor.

**Conclusion:** Qualitative increases in the positive staining of the primary antibody for pentosidine ( $\alpha$ -PEN12) were observed in the older male diabetic donor when compared to the younger non-diabetic donor. As this preliminary study has determined changes in pentosidine epitope concentration based on the combined variable of aging and diabetes, future studies are required to differentiate the influence of aging and diabetes.

## Chapter 6: Conclusion

### 6.1. Limitations

The primary constraint on this study occurred in the limited donor supply and information available to us about individual tissue donors. The tissue bank provided us only with age, sex, diabetic status, weight, and height of the donor. Unknown factors influencing tendon health not accounted for in this study include both intrinsic (e.g. genetics) and extrinsic (physical active living) factors. In the diabetic donors, the duration of diabetes and the extent of regulation of blood glucose levels, impacting tendon health and formation of AGEs, remain unknown. The statistical power of the analysis in the sex- and diabetes-related comparative studies examining tendon structure and mechanics were also limited by the sample sizes. In the younger cohorts, only a maximum of two sets of paired tendons under 30 years of age were available in each donor population ( $n_{F,ND} = 2$ ,  $n_{M,ND} = 2$ ,  $n_{M,D} = 0$ ), with the youngest in the male diabetic donor population being 46 years of age. Thus, age-related comparisons within the diabetic population (46-60 years) were insignificant. Moreover, the influence of diabetes could only be inferred from the male data in the absence of sartorius tendons from female diabetic donors. This is especially of importance given results from a previous study that found evidence of Achilles tendon thickening occurred only in females with diabetes<sup>6</sup>.

Histological and immunohistochemical studies were a late addition to the thesis, intended as a preliminary work to qualitatively compare collagen crimp, cellularity and pentosidine epitope content between a younger non-diabetic male donor and an older diabetic donor. Thus, implementation of the light microscopy segment was agreed upon when 4/6 female donor tendons had been used, limiting the diversity of the tendon samples. Compared to animal studies where fixation of tendon specimens is able to occur shortly after the animal is euthanized, the human sartorius tendons were collected and frozen from the NSHA Regional Tissue Bank within 24 hours of tissue harvest prior to dissection and subsequent fixation. Thus, the overall duration of time between harvest to

fixation – during which cellular autolysis and degeneration may occur – of the sartorius tendon would be a limitation.

During mechanical testing preparation, the cross-sectional area of the multi-fascicle subsample was calculated using a line of sight and calculation of an assumed elliptical cross-section. It is possible that inaccurate estimates of the UTS and modulus were obtained due to sample shape. As a tradeoff in facilitating tendon multi-fascicle subsample gripping in tensile overload testing, and replicating the strain rate from the first study of discrete plasticity<sup>257</sup>, the quasistatic strain rate (0.25%/sec) utilized here limits the physiological relevance of the testing, as loading in vivo may reach up to 200%/sec. Although tensile testing of the multi-fascicle bundles provides near-ideal geometry for gripping and allows for multiple tests to be performed, mechanics of whole tendon or fibril level mechanics are predominantly found elsewhere in the literature.

In the thermal studies performed using DSC and HIT, the denaturation temperature evaluated by HIT ( $T_d$ ) was found to consistently precede that evaluated by DSC ( $T_{onset}$ ). This is contrast to what would be thermodynamically expected and may be attributed to the differences in heating rates (~1.5 vs. 5°C/min). Furthermore, comparing the results obtained here and with other thermal studies of human tendon collagen is difficult due in part to the variety of tendons (e.g. patellar/Achilles/rotator cuff tendon) and heating rate – with superheating effects<sup>122</sup> – available for comparison (0.3 vs. 5°C/min)<sup>54,271</sup>.

## **6.2. Future Research Suggestions**

### *6.2.1. In-Depth Light and Scanning Electron Microscopy*

To further improve upon the light microscopy findings, a comparison of serial sections of the tendon tissues at pre-determined locations along the tendon depth is required, in addition to with testing with HIER techniques to potentially uncover masked epitopes not identified in IHC experiments. To add depth, the usage of the Movat Pentachrome kit would uncover the location and concentrations of other ECM components (e.g. proteoglycans, muscle, and elastin). Further, determination of the

nuclear aspect ratio and nuclei counting of H & E stained tendon sections may be used to evaluate changes related to age, sex, and diabetes. In terms of immunohistochemistry, determination on the type of collagens present and cellular activity (e.g. metabolism,  $\alpha$ -SMA) may be performed. In general, a more complete quantitative study with increased number of tendon samples from varying donors and tendon anatomical locations (e.g. Midsubstance, OTJ, MTJ) would improve upon the current findings. Lastly, a study of the changes in fiber structure after multiple overload cycles without rupture could be carried out.

With SEM, determination of changes in fibril diameters and density with donor age, sex, and diabetic status may provide insight into changes in structure and mechanics observed via HIT, DSC, and tensile testing. Moreover, a study of the changes in fibril diameter of damaged versus undamaged fibrils may provide insight on strain energy absorption and dissipation in specific fibrils. In addition to SEM, AFM could be used (similar to the BTT<sup>24</sup> and bovine forelimb tendon<sup>200</sup> studies) to determine overload damage to the internal fibril structure.

### 6.2.2. *In Vitro Diabetes Model*

Determining the alterations in tendon structure and mechanics of a weight-bearing human tendon solely due to accumulation of AGEs has not been performed previously to the author's knowledge. The current study of the effects of diabetes was limited by the lack of knowledge of the diabetic donor's ability to regulate their blood glucose levels (and other factors including activity level) and this may have masked the effects of AGE accumulation occurring in poorly maintained diabetes. Application of in vitro ribose solutions to these (human sartorius) tendons similar to Lee and Veres might be revealing<sup>150</sup>.

### 6.2.3. *Crosslink Analysis and Identification*

HIT and DSC techniques provided valuable (proxy) insight into the changes in density of and types of the crosslinking present (thermally stable vs. thermally labile). Usage of a technique similar to High Performance Liquid Chromatography (HPLC) as

per studies of patellar tendon<sup>56</sup> and BTT<sup>275</sup> may provide important insight in the quantity and concentration of the specific crosslinks present.

#### 6.2.4. *In-Depth Analysis of the Tendon Mechanics*

In-depth evaluation of the stress-strain curves of the tendon fascicles could be performed on three phases. Firstly, determining the extensibility of the tendon based on the beginning of the linear region of the stress-strain curve might reduce manual bias from the variability of the applied preload ( $0.5 \pm 0.25$  N). Secondly, evaluating changes in the post-yield strain energy absorbed may indicate changes with age, sex, and diabetes. Thirdly, determining the differences in failure mechanics after the point of UTS similar to the methods of Guney and coworkers<sup>98</sup> in the Achilles tendons from non-diabetic and diabetic donors could be applied. Lastly, implementation of dynamic mechanical testing to assess viscoelastic properties of the sartorius tendon investigating age-, sex- and diabetes-determined changes.

#### 6.2.5. *Fatigue Subrupture Overload Testing and Usage of a Complementary Set of Human Tendons*

Implementation of a study using *repeated* subrupture overload may provide valuable information on the formation of discrete plasticity in human sartorius tendon collagen fibrils. A previous study of BTT have shown that repeated subrupture overload progressively leads to the increased formation of discrete plasticity damage in tendon collagen fibrils with the number of overload cycles<sup>255</sup>.

In addition to the implementation of a repeated subrupture overload protocol, and similar to the works performed by Herod *et al.*<sup>109</sup>, an experiment in which the differences in structurally proximate, yet functionally distinct human tendons would provide useful information on the differences in positional and energy-storing tendons throughout adulthood. The digital flexor-extensor pair are the likely best candidates.



### 6.3. Concluding Remarks

As an extension of previous work performed by Sparavalo et al<sup>237</sup>, the purpose of this thesis was to determine the differences in sartorius tendon collagen structure and mechanics based on age (16-60 years), sex and diabetes. HIT and DSC revealed some changes in donor tendon structure with aging and diabetes, yet no changes occurred with sex. Compared to male non-diabetic donors, female non-diabetic and male diabetic tissues were found to be less tough and less extensible. In addition, tendons from female donors were weaker than those from the male donors. SEM microscopy revealed no changes in nanoscale failure mechanisms with age, sex and diabetic status. Light microscopy studies revealed a loss of collagen crimp, reduced density of nuclei, and increases in pentosidine epitope accumulation with aging and diabetes. Further, this study was to the author's knowledge, the first to investigate structural changes in tendon collagen based on sex via thermal methods DSC and HIT. In light of these findings, it appears the sartorius tendon is a highly crosslinked structure that remains relatively unchanged with age, sex and diabetes, sacrificing the toughness mechanism of discrete plasticity for molecular stability and strength. This stability of structure with age is belied by the surprisingly high cellular density which is partially retained into early geriatric life. In summary, this novel study has contributed to advancing knowledge in multiple fronts of modern tendon research with potential future applications in healing and treatment of soft tissue injuries, and which could provide insight for tendon and ligament replacements.

## Reference List

1. Abate, M., Schiavone, C., & Salini, V. (2010). Sonographic evaluation of the shoulder in asymptomatic elderly subjects with diabetes. *BMC Musculoskeletal Disorders*, *11*, 278.
2. Abrahams, M. (1967). Mechanical Behaviour of Tendon in Vitro. *Medical & Biological Engineering & Computing*, *5*(5), 433–443.
3. Ackermann, P. W., & Hart, D. A. (Eds.). (2016). *Metabolic Influences on Risk for Tendon Disorders. Advances in Experimental Medicine and Biology*. Switzerland: Springer International Publishing.
4. Ackermann, P. W., & Renström, P. (2012). Tendinopathy in Sport. *Sports Health: A Multidisciplinary Approach*, *4*(3), 193–201.
5. Adams, C. W. M., & Bayliss, O. B. (1973). Acid mucosubstances underlying lipid deposits in ageing tendons and athlerosclerotic arteries. *Athlerosclerosis*, *18*(2), 191–195.
6. Akturk, M., Ozdemir, A., Maral, I., Yetkin, I., & Arslan, M. (2007). Evaluation of Achilles Tendon Thickening in Type 2 Diabetes Mellitus. *Experimental and Clinical Endocrinology & Diabetes : Official Journal, German Society of Endocrinology [and] German Diabetes Association*, *115*(2), 92–96.
7. Aldous, I. G. (2008). *Thermomechanical Stability of Heart Valve Collagen: Differences with Valve Type and Age, and Implications for Remodelling*. Dalhousie University.
8. Alexander, R. M. (1982). The role of tendon elasticity in the locomotion of the camel (Camelus dromedarius). *Journal of Zoology*, *198*(3), 293–313.
9. Alexander, R. M. (1984). Elastic Energy Stores in Running Vertebrates. *Integrative and Comparative Biology*, *24*(1), 85–94.
10. Alexander, R. M. (1991). Energy-saving Mechanisms in Walking and Running. *The Journal of Experimental Biology*, *160*, 55–69.
11. Allain, J. C., Le Lous, M., Bazin, S., Bailey, A. J., Delaunay, A., Lous, M. L. E., & Bazin, S. (1978). Isometric tension developed during heating of collagenous tissues. Relationships with collagen cross-linking. *BBA - Protein Structure*, *533*(1), 147–155.

12. Allain, J. C., Le Lous, M., Cohen-Solal, L., Bazin, S., & Maroteaux, P. (1980). Isometric tensions developed during the hydrothermal swelling of rat skin. *Connective Tissue Research*, 7(3), 127–133.
13. Andreassen, T. T., Seyer-Hansen, K., & Bailey, A. J. (1981). Thermal stability, mechanical properties and reducible cross-links of rat tail tendon in experimental diabetes. *BBA - General Subjects*, 677(2), 313–317.
14. Andreassen, Troels T., Oxlund, H., & Danielsen, C. C. (1988). The influence of non-enzymatic glycosylation and formation of fluorescent reaction products on the mechanical properties of rat tail tendons. *Connective Tissue Research*, 17(1), 1–9.
15. Avery, N. C., & Bailey, A. J. (2005). Enzymic and non-enzymic cross-linking mechanisms in relation to turnover of collagen: Relevance to aging and exercise. *Scandinavian Journal of Medicine and Science in Sports*, 15(4), 231–240.
16. Avery, N. C., & Bailey, A. J. (2006). The effects of the Maillard reaction on the physical properties and cell interactions of collagen. *Pathologie Biologie*, 54(7), 387–395.
17. Badekas, T., Papadakis, S. A., Vergados, N., Galanacos, S. P., Siapkara, A., Forgrave, M., Romansky, N., Mirones, S., Trnka, H. J., & Delmi, M. (2009). Foot and ankle injuries during the Athens 2004 Olympic Games. *Journal of Foot and Ankle Research*, 2, 9.
18. Baer, E., Hiltner, A., & Friedman, B. (1976). Structural hierarchies and interactions in the tendon composite. *Polymer Mechanics*, 12(4), 619–629.
19. Bai, P., Phua, K., Hardt, T., Cernadas, M., & Brodsky, B. (1992). Glycation alters collagen fibril organization. *Connective Tissue Research*, 28(1–2), 1–12.
20. Bailey, A. J. (1968). Intermediate labile intermolecular crosslinks in collagen fibres. *BBA - Protein Structure*, 160(3), 447–453.
21. Bailey, A. J. (2001). Molecular mechanisms of ageing in connective tissues. *Mechanisms of Ageing and Development*, 122(7), 735–755.
22. Bailey, A J, Sims, T. J., Avery, N. C., & Miles, C. A. (1993). Chemistry of collagen cross-links: glucose-mediated covalent cross-linking of type-IV collagen in lens capsules. *Biochemical Journal*, 296(2), 489–496.
23. Bailey, Allen J., Paul, R. G., & Knott, L. (1998). Mechanisms of maturation and ageing of collagen. *Mechanisms of Ageing and Development*, 106(1–2), 1–56.

24. Baldwin, S. J., Kreplak, L., & Lee, J. M. (2016). Characterization via atomic force microscopy of discrete plasticity in collagen fibrils from mechanically overloaded tendons: Nano-scale structural changes mimic rope failure. *Journal of the Mechanical Behavior of Biomedical Materials*, *60*, 356–366.
25. Baldwin, S. J., Kreplak, L., & Lee, J. M. (2019). MMP-9 selectively cleaves non-D-banded material on collagen fibrils with discrete plasticity damage in mechanically-overloaded tendon. *Journal of the Mechanical Behavior of Biomedical Materials*, *95*, 67–75.
26. Baldwin, S. J., Quigley, A. S., Clegg, C., & Kreplak, L. (2014). Nanomechanical mapping of hydrated rat tail tendon collagen I fibrils. *Biophysical Journal*, *107*(8), 1794–1801.
27. Bank, R. A., TeKoppele, J. M., Oostingh, G., Hazleman, B. L., & Riley, G. P. (1999). Lysylhydroxylation and non-reducible crosslinking of human supraspinatus tendon collagen: changes with age and in chronic rotator cuff tendinitis. *Annals of the Rheumatic Diseases*, *58*(1), 35–41.
28. Bear, R. S. (1944). X-Ray Diffraction Studies on Protein Fibers. I. The Large Fiber-Axis Period of Collagen. *Journal of the American Chemical Society*, *66*(8), 1297–1305.
29. Bear, R. S. (1952). The structure of collagen fibrils. *Advances in Protein Chemistry*, *7*, 69–160.
30. Bennett, M. B., Ker, R. F., Dimery, N. J., & Alexander, R. M. (1986). Mechanical properties of various mammalian tendons. *Journal of Zoology*, *209*(4), 537–548.
31. Bentley, J. P. (1979). Aging of collagen. *The Journal of Investigative Dermatology*, *73*(1), 80–83.
32. Bey, M. E., Marzilger, R., Hinkson, L., Arampatzis, A., & Legerlotz, K. (2019). Patellar Tendon Stiffness Is Not Reduced During Pregnancy. *Frontiers in Physiology*, *10*, 334.
33. Bischof, J. C., & He, X. (2005). Thermal stability of proteins. *Annals of the New York Academy of Sciences*, *1066*, 12–33.
34. Blevins, F. T., Hecker, A. T., Bigler, G. T., Boland, A. L., & Hayes, W. C. (1994). The Effects of Donor Age and Strain Rate on the Biomechanical Properties of Bone-Patellar Tendon-Bone Allografts. *The American Journal of Sports Medicine*, *22*(3), 328–333.

35. Bognár, G., Szabó, I., Pintér, C., Ligeti, E., & Lörinczy, D. (2010). Changes in thermal denaturation properties of the long head of the biceps during lifetime. *Journal of Thermal Analysis and Calorimetry*, *102*(1), 65–68.
36. Boivin, G. P., Elenes, E. Y., Schultze, A. K., Chodavarapu, H., Hunter, S. A., & Elased, K. M. (2014). Biomechanical properties and histology of db/db diabetic mouse Achilles tendon. *Muscles, Ligaments and Tendons Journal*, *4*(3), 280–284.
37. Bollen, S. R., & Arvinte, D. (2008). Snapping pes syndrome. *The Journal of Bone and Joint Surgery. British Volume*, *90-B*(3), 334–335.
38. Bolton, N. R. M., Smith, K. E., Pilgram, T. K., Mueller, M. J., & Bae, K. T. (2005). Computed tomography to visualize and quantify the plantar aponeurosis and flexor hallucis longus tendon in the diabetic foot. *Clinical Biomechanics*, *20*, 540–546.
39. Bornstein, P., & Sage, H. (1980). Structurally Distinct Collagen Types. *Annual Review of Biochemistry*, *49*(1), 957–1003.
40. Broom, N. D. (1978). Simultaneous morphological and stress-strain studies of the fibrous components in wet heart valve leaflet tissue. *Connective Tissue Research*, *6*(1), 37–50.
41. Brownlee, M., Vlassara, H., & Cerami, A. (1984). Nonenzymatic glycosylation and the pathogenesis of diabetic complications. *Annals of Internal Medicine*, *101*(4), 527–537.
42. Bruylants, G., Wouters, J., & Michaux, C. (2005). Differential Scanning Calorimetry in Life Science: Thermodynamics, Stability, Molecular Recognition and Application in Drug Design. *Current Medicinal Chemistry*, *12*(17), 2011–2020.
43. Buehler, M. J. (2008). Nanomechanics of collagen fibrils under varying cross-link densities: Atomistic and continuum studies. *Journal of the Mechanical Behavior of Biomedical Materials*, *1*(1), 59–67.
44. Bunn, H. F., & Higgins, P. J. (1981). Reaction of Monosaccharides with Proteins : Possible Evolutionary Significance. *Science*, *213*(4504), 222–224.
45. Bureau of Labour Statistics. (2010). Nonfatal occupational injuries and illnesses requiring days away from work. U.S. Department of Labour.
46. Burgess, K. E., Graham-Smith, P., & Pearson, S. J. (2009). Effect of acute tensile loading on gender-specific tendon structural and mechanical properties. *Journal of Orthopaedic Research*, *27*(4), 510–515.

47. Burner, T., Gohr, C., Mitton-Fitzgerald, E., & Rosenthal, A. K. (2012). Hyperglycemia reduces proteoglycan levels in tendons. *Connective Tissue Research*, 53(6), 535–541.
48. Butler, D. L., Grood, E. S., Noyes, F. R., & Zernicke, R. F. (1978). Biomechanics of Ligaments and Tendons. *Exercise and Sport Sciences Reviews*, 6(1), 125–182.
49. Cagliero, E., Apruzzese, W., Perlmutter, G. S., & Nathan, D. M. (n.d.-aw). Musculoskeletal Disorders of the Hand and Shoulder in Patients with Diabetes Mellitus, 9343(02), 8–11.
50. Cannon, D. J., & Davison, P. F. (1977). Aging, and crosslinking in mammalian collagen. *Experimental Aging Research*, 3(2), 87–105.
51. Carroll, C. C., Dickinson, J. M., Haus, J. M., Lee, G. A., Hollon, C. J., Aagaard, P., Magnusson, S. P., & Trappe, T. A. (2008). Influence of aging on the in vivo properties of human patellar tendon. *Journal of Applied Physiology*, 105(6), 1907–1915.
52. Cavagna, G. A., Heglund, N. C., & Taylor, C. R. (1977). Mechanical work basic mechanisms in terrestrial locomotion : two for minimizing energy expenditure. *American Journal of Physiology*, 235(5), R243-61.
53. Cavan, D., Fernandes, J. da R., Makaroff, L., & Webber, S. (Eds.). (2015). *IDF Diabetes Atlas. International Diabetes Federation (7th ed.)*. Brussels, Belgium: International Diabetes Federation.
54. Chaudhury, S., Holland, C., Porter, D., Tirlapur, U. K., Vollrath, F., & Carr, A. J. (2011). Torn human rotator cuff tendons have reduced collagen thermal properties on differential scanning calorimetry. *Journal of Orthopaedic Research*, 29(12), 1938–1943.
55. Connizzo, B. K., Bhatt, P. R., Liechty, K. W., & Soslowsky, L. J. (2014). Diabetes alters mechanical properties and collagen fiber re-alignment in multiple mouse tendons. *Annals of Biomedical Engineering*, 42(9), 1880–1888.
56. Couppé, C., Hansen, P., Kongsgaard, M., Kovanen, V., Suetta, C., Aagaard, P., Kjaer, M., & Magnusson, S. P. (2009). Mechanical properties and collagen cross-linking of the patellar tendon in old and young men. *Journal of Applied Physiology*, 107(3), 880–886.
57. Couppé, Christian, Svensson, R. B., Grosset, J., Kovanen, V., Nielsen, R. H., Olsen, M. R., Larsen, J. O., Praet, S. F. E., Skovgaard, D., Hansen, M., Aagaard, P., Kjaer,

- M., & Magnusson, S. P. (2014). Life-long endurance running is associated with reduced glycation and mechanical stress in connective tissue. *AGE*, 36(4), 1–20.
58. Couppé, Christian, Svensson, R. B., Kongsgaard, M., Kovanen, V., Grosset, J.-F., Snorgaard, O., Bencke, J., Larsen, J. O., Bandholm, T., Christensen, T. M., Boesen, A., Helmark, I. C., Aagaard, P., Kjaer, M., & Magnusson, S. P. (2016). Human Achilles tendon glycation and function in diabetes. *Journal of Applied Physiology*, 120(2), 130–137.
  59. Cowan, P. M., McGavin, S., & North, A. C. T. (1955). The polypeptide chain configuration of collagen. *Nature*, 176(4492), 1062–1064.
  60. Cronin, N. J., Peltonen, J., Ishikawa, M., Komi, P. V., Avela, J., Sinkjaer, T., & Voigt, M. (2010). Achilles tendon length changes during walking in long-term diabetes patients. *Clinical Biomechanics*, 25(5), 476–482.
  61. Cronkite, A. E. (1936). The tensile strength of human tendons. *The Anatomical Record*, 4(2), 173–186.
  62. D’Ambrogio, E., Giacomozzi, C., Macellari, V., & Uccioli, L. (2005). Abnormal foot function in diabetic patients: the altered onset of Windlass mechanism. *Diabetic Medicine: A Journal of the British Diabetic Association*, 22(12), 1713–1719.
  63. Davison, P. F. (1992). The organization of collagen in growing tensile tissues. *Connective Tissue Research*, 28(3), 171–179.
  64. de Jonge, S., Rozenberg, R., Vieyra, B., Stam, H. J., Aanstoot, H. J., Weinans, H., van Schie, H. T. M., & Praet, S. F. E. (2015). Achilles tendons in people with type 2 diabetes show mildly compromised structure: an ultrasound tissue characterisation study. *British Journal of Sports Medicine*, 49(15), 995–999.
  65. Dean, B. J. F., Dakin, S. G., Millar, N. L., & Carr, A. J. (2017). Review: Emerging concepts in the pathogenesis of tendinopathy. *Surgeon*, 15(6), 349–354.
  66. Derby, B., & Akhtar, R. (Eds.). (2015). *Mechanical Properties of Aging Soft Tissues* (1st ed.). Springer International Publishing.
  67. Devkota, A. C., & Weinhold, P. S. (2003). Mechanical response of tendon subsequent to ramp loading to varying strain limits. *Clinical Biomechanics*, 18(10), 969–974.
  68. Diamant, J., Keller, A., Baer, E., Litt, M., & Arridge, R. G. C. (1972). Collagen; Ultrastructure and Its Relation to Mechanical Properties as a Function of Ageing. *Proceedings of the Royal Society B: Biological Sciences*, 180(1060), 293–315.

69. Dzedzic, D., Bogacka, U., & Ciszek, B. (2014). Anatomy of sartorius muscle. *Folia Morphologica*, 73(3), 359–362.
70. Edouard, P., Feddermann-Demont, N., Alonso, J. M., Branco, P., & Junge, A. (2015). Sex differences in injury during top-level international athletics championships: surveillance data from 14 championships between 2007 and 2014. *British Journal of Sports Medicine*, 49(7), 472–477.
71. Eekhoff, J. D., Fang, F., & Lake, S. P. (2018). Multiscale mechanical effects of native collagen cross-linking in tendon. *Connective Tissue Research*, 59(5), 410–422.
72. Egemen, O., Ozkaya, O., Ozturk, M., Sen, E., Akan, M., Sakiz, D., & Aygit, C. (2012). The Biomechanical and Histological Effects of Diabetes on Tendon Healing: Experimental Study in Rats. *Journal of Hand and Microsurgery*, 4(2), 60–64.
73. Elliott, D. (1965). Structure and function of mammalian tendon. *Biological Reviews*, 40(3), 392–421.
74. Eyre, D. R., Paz, M. A., Gallop, P. M., Sandberg, L. B., Soskel, N. T., & Leslie, J. G. (1984). Cross-Linking in Collagen and Elastin. *Annual Review of Biochemistry*, 53(1), 717–748.
75. Feddermann-Demont, N., Junge, A., Edouard, P., Branco, P., & Alonso, J.-M. (2014). Injuries in 13 international Athletics championships between 2007-2012. *British Journal of Sports Medicine*, 48(7), 513–522.
76. Flahiff, C. M., Brooks, A. T., Hollis, J. M., Vander Schilden, J. L., & Nicholas, R. W. (1995). Biomechanical Analysis of Patellar Tendon Allografts as a Function of Donor Age. *The American Journal of Sports Medicine*, 23(3), 354–358.
77. Flandin, F., Buffevant, C., & Herbage, D. (1984). A differential scanning calorimetry analysis of the age-related changes in the thermal stability of rat skin collagen. *Biochimica et Biophysica Acta (BBA) - Protein Structure and Molecular Enzymology*, 791(2), 205–211.
78. Flory, P. J., & Spurr Jr., O. K. (1961). Melting Equilibrium for Collagen Fibers under Stress. Elasticity in the Amorphous State. *Journal of the American Chemical Society*, 83(6), 1308–1316.
79. Folkhard, W., Mosler, E., Geercken, W., Knörzer, E., Nemetschek-Gansler, H., & Nemetschek, T. (1987). Quantitative analysis of the molecular sliding mechanism in native tendon collagen time-resolved dynamic studies using synchrotron radiation. *International Journal of Biological Macromolecules*, 9(3), 169–175.



80. Fouré, A., Cornu, C., McNair, P. J., & Nordez, A. (2012). Gender differences in both active and passive parts of the plantar flexors series elastic component stiffness and geometrical parameters of the muscle-tendon complex. *Journal of Orthopaedic Research*, 30(5), 707–712.
81. Fox, A. J. S., Bedi, A., Deng, X., Ying, L., Harris, P. E., Warren, R. F., & Rodeo, S. A. (2011). Diabetes mellitus alters the mechanical properties of the native tendon in an experimental rat model. *Journal of Orthopaedic Research*, 29(6), 880–885.
82. Franchi, M., Trirè, A., Quaranta, M., Orsini, E., & Ottani, V. V. V. (2007). Collagen Structure of Tendon Relates to Function. *The Scientific World JOURNAL*, 7, 404–420.
83. Fratzl, P. (2008). *Collagen: Structure and Mechanics*. (P. Fratzl, Ed.). Boston, MA: Springer US.
84. Freedman, K. B., D’Amato, M. J., Nedeff, D. D., Kaz, A., & Bach, B. R. (2003). Arthroscopic Anterior Cruciate Ligament Reconstruction : A Metaanalysis Comparing Patellar Tendon and Hamstring Tendon Autografts. *The American Journal of Sports Medicine*, 31(1), 2–11.
85. Fryhofer, G. W., Freedman, B. R., Hillin, C. D., Salka, N. S., Pardes, A. M., Weiss, S. N., Farber, D. C., & Soslowsky, L. J. (2016). Postinjury biomechanics of Achilles tendon vary by sex and hormone status. *Journal of Applied Physiology*, 121(5), 1106–1114.
86. Gaida, J. E., Ashe, M. C., Bass, S. L., & Cook, J. L. (2009). Is adiposity an under-recognized risk factor for tendinopathy? A systematic review. *Arthritis Care & Research*, 61(6), 840–849.
87. Galeski, A., Kastelic, J., Baer, E., & Kohn, R. R. (1977). Mechanical and structural changes in rat tail tendon induced by alloxan diabetes and aging. *Journal of Biomechanics*, 10(11–12), 775–782.
88. Gautieri, A., Passini, F. S., Silván, U., Guizar-Sicairos, M., Carimati, G., Volpi, P., Moretti, M., Schoenhuber, H., Redaelli, A., Berli, M., & Snedeker, J. G. (2017). Advanced glycation end-products: Mechanics of aged collagen from molecule to tissue. *Matrix Biology*, 59, 95–108.
89. Geeslin, A. G., & Laprade, R. F. (2010). Surgical treatment of snapping medial hamstring tendons. *Knee Surgery Sports Traumatology Arthroscopy*, 18(9), 1294–1296.

90. Gersh, I., & Catchpole, H. R. (1960). The Nature of Ground Substance of Connective Tissue. *Perspectives in Biology and Medicine*, 3(2), 282–319.
91. Giacomozzi, C., D'Ambrogio, E., Uccioli, L., & Macellari, V. (2005). Does the thickening of Achilles tendon and plantar fascia contribute to the alteration of diabetic foot loading? *Clinical Biomechanics*, 20, 532–539.
92. Gai Via, A., Papa, G., Oliva, F., & Maffulli, N. (2016). Tendinopathy. *Current Physical Medicine and Rehabilitation Reports*, 4(1), 50–55.
93. Glazebrook, M. A., Wright Jr., J. R., Langman, M., Stanish, W. D., & Lee, J. M. (2008). Histological analysis of Achilles tendons in an overuse rat model. *Journal of Orthopaedic Research*, 26(6), 840–846.
94. Grant, W. P., Foreman, E. J., Wilson, A. S., Jacobus, D. A., & Kukla, R. M. (2005). Evaluation of Young's modulus in Achilles tendons with diabetic neuroarthropathy. *Journal of the American Podiatric Medical Association*, 95(3), 242–246.
95. Grant, W. P., Sullivan, R., Sonenshine, D. E., Adam, M., Slusser, J. H., Carson, K. A., & Vinik, A. I. (1997). Electron Microscopic Investigation of the Effects of Diabetes Mellitus on the Achilles Tendon. *Journal of Foot and Ankle Surgery*, 36(4), 272–278.
96. Gregg, E. W., Sattar, N., & Ali, M. K. (2016). The changing face of diabetes complications. *The Lancet Diabetes and Endocrinology*, 4(6), 537–547.
97. Grimmer, M., Freudenberg, U., Behrens, S. H., Welzel, P. B., Mu, M., Salchert, K., Taeger, T., Schmidt, K., Pompe, W., & Werner, C. (2007). Electrostatic Interactions Modulate the Conformation of Collagen I, 92(March), 2108–2119.
98. Guney, A., Vatansever, F., Karaman, I., Kafadar, I. H., Oner, M., & Turk, C. Y. (2015). Biomechanical properties of Achilles tendon in diabetic vs. non-diabetic patients. *Experimental and Clinical Endocrinology & Diabetes*, 123(7), 428–432.
99. Gupta, H. S., Seto, J., Krauss, S., Boesecke, P., & Screen, H. R. C. (2010). In situ multi-level analysis of viscoelastic deformation mechanisms in tendon collagen. *Journal of Structural Biology*, 169(2), 183–191.
100. Hall, D. M. B., & Cole, T. J. (2006). What use is the BMI? *Archives of Disease in Childhood*, 91(4), 283–286.
101. Hamlin, C. R., Kohn, R. R., & Luschin, J. H. (1974). Apparent Accelerated Aging of Human Collagen in Diabetes Mellitus. *Diabetes*, 24(10), 902–904.

102. Hansen, M., & Kjaer, M. (2014). Influence of sex and estrogen on musculo-tendinous protein turnover at rest and after exercise. *Exercise and Sport Sciences Reviews*, 183–192.
103. Harkness, R. D. (1961). Biological Functions of Collagen. *Biological Reviews*, 36(4), 399–455.
104. Harkness, R. D. (1970). Crosslinks in collagen and mechanical properties of connective tissues. *Apex*, 4(3), 24–29.
105. Hashemi, J., Chandrashekar, N., & Slauterbeck, J. (2005). The mechanical properties of the human patellar tendon are correlated to its mass density and are independent of sex. *Clinical Biomechanics*, 20(6), 645–652.
106. Haut, R. C. (1985). The Effect of a Lathyrus Diet on the Sensitivity of Tendon to Strain Rate. *Journal of Biomechanical Engineering*, 107(2), 166–174.
107. Heinemeier, K. M., Schjerling, P., Heinemeier, J., Magnusson, S. P., & Kjaer, M. (2013). Lack of tissue renewal in human adult Achilles tendon is revealed by nuclear bomb 14C. *The FASEB Journal*, 27(5), 2074–2079.
108. Henle, T. (2005). Protein-bound advanced glycation endproducts (AGEs) as bioactive amino acid derivatives in foods. *Amino Acids*, 29(4), 313–322.
109. Herod, T. W., Chambers, N. C., & Veres, S. P. (2016). Collagen fibrils in functionally distinct tendons have differing structural responses to tendon rupture and fatigue loading. *Acta Biomaterialia*, 42, 296–307.
110. Hicks, K. M., Onambele-Pearson, G. L., Winwood, K., & Morse, C. I. (2013). Gender differences in fascicular lengthening during eccentric contractions: The role of the patella tendon stiffness. *Acta Physiologica*, 209(3), 235–244.
111. Hodge, A. J., & Petruska, J. A. (1963). Recent Studies with the Electron Microscope on Ordered Aggregates of the Tropocollagen Macromolecule. In G. N. Ramachandran (Ed.), *Aspects of Protein Structure* (pp. 289–300). New York: Academic Press.
112. Hubbard, R. P., & Soutas-Little, R. W. (1984). Mechanical properties of human tendon and their age dependence. *J Biomech Eng*, 106(2), 144–150.
113. Huebschmann, A. G., Regensteiner, J. G., Vlassara, H., & Reusch, J. E. B. (2006). Diabetes and advanced glycoxidation end products. *Diabetes Care*, 29(6), 1420–1432.

114. Ippolito, E., Natali, P. G., Postacchini, F., Accinni, L., & De Martino, C. (1980). Morphological, Immunochemical, and Biochemical Study of Achilles Tendon at Various Ages. *The Journal of Bone and Joint Surgery*, 62-A(4), 583–598.
115. Iwamoto, J., Takeda, T., Sato, Y., & Matsumoto, H. (2008). Retrospective case evaluation of gender differences in sports injuries in a Japanese sports medicine clinic. *Gender Medicine*, 5(4), 405–414.
116. Jahangir, A. (2004). *Thermomechanical Characterization of Rapid Thermal Denaturation in Load-Bearing Collagenous Cardiac Tissues Under Isometric Constraints* (Doctoral dissertation). Dalhousie University.
117. Jain, S. A., Mehr, A., & Pimpalnerkar, A. L. (2010). Snapping sartorius syndrome: A case report. *European Orthopaedics and Traumatology*, 1(6), 237–239.
118. James, V. J., Delbridge, L., McLennan, S. V., & Yue, D. K. (1991). Use of X-ray diffraction in study of human diabetic and aging collagen. *Diabetes*, 40(3), 391–394.
119. Janssen, I., Brown, N. A. T., Munro, B. J., & Steele, J. R. (2015). Variations in jump height explain the between-sex difference in patellar tendon loading during landing. *Scandinavian Journal of Medicine and Science in Sports*, 25(2), 265–272.
120. Järvinen, T. A. H., Järvinen, T. L. N., Kannus, P., Józsa, L., & Järvinen, M. (2004). Collagen fibres of the spontaneously ruptured human tendons display decreased thickness and crimp angle. *Journal of Orthopaedic Research*, 22(6), 1303–1309.
121. Johnson, G. A., Tramaglino, D. M., Levine, R. E., Ohno, K., Choi, N. Y., & Woo, S. L. Y. (1994). Tensile and viscoelastic properties of human patellar tendon. *Journal of Orthopaedic Research*, 12(6), 796–803.
122. Johnson, M., & White, M. A. (2014). Thermal Methods. In D. W. Bruce, D. O'Hare, & R. I. Walton (Eds.), *Multi Length-Scale Characterisation* (Vol. 1, pp. 60–116). United Kingdom: John Wiley & Sons, Ltd.
123. Józsa, L., Réffy, A., Kannus, P., Demel, S., & Elek, E. (1990). Pathological alterations in human tendons. *Archives of Orthopaedic and Trauma Surgery*, 110(1), 15–21.
124. Kannus, P., & Kannus, P. (2000). Structure of the tendon connective tissue. *Scand J Med Sci Sports*, 10(6), 312–320.
125. Kastelic, J, Galeski, A., & Baer, E. (1978). The Multicomposite Structure of Tendon. *Connective Tissue Research*, 6(1), 11–23.

126. Kastelic, John, & Baer, E. (1980). Deformation in Tendon Collagen. *Symposium of the Society for Experimental Biology*, (34), 397–435.
127. Kenedi, R. M., Gibson, T., Evans, J. H., & Barbenel, J. C. (1975). Tissue Mechanics. *Physics in Medicine and Biology*, 20(5), 699–717.
128. Kent, M. J. C., Light, N. D., & Bailey, A. J. (1985). Evidence for glucose-mediated covalent cross-linking of collagen after glycosylation in vitro. *The Biochemical Journal*, 225(3), 745–752.
129. Kiapour, A. M., & Murray, M. M. (2014). Basic science of anterior cruciate ligament injury and repair. *Bone & Joint Research*, 3(2), 20–31.
130. Kjaer, M. (2004). Role of Extracellular Matrix in Adaptation of Tendon and Skeletal Muscle to Mechanical Loading. *Physiological Reviews*, 84(2), 649–698.
131. Klatte-Schulz, F., Minkwitz, S., Schmock, A., Bormann, N., Kurtoglu, A., Tsitsilonis, S., Manegold, S., & Wildemann, B. (2018). Different Achilles Tendon Pathologies Show Distinct Histological and Molecular Characteristics. *International Journal of Molecular Sciences*, 19(2), 404.
132. Knobloch, K., Schreibmueller, L., Meller, R., Busch, K. H., Spies, M., & Vogt, P. M. (2008). Superior Achilles tendon microcirculation in tendinopathy among symptomatic female versus male patients. *The American Journal of Sports Medicine*, 36, 509–514.
133. Knörzer, E., Folkhard, W., Geercken, W., Boschert, C., Koch, M. H. J., Hilbert, B., Krah, H., Mosler, E., Nemetschek-Gansler, H., & Nemetschek, T. (1986). New Aspects of the Etiology of Tendon Rupture. *Archives of Orthopaedic and Traumatic Surgery*, 105, 113–120.
134. Knott, L., & Bailey, A. J. (1998). Collagen cross-links in mineralizing tissues: A review of their chemistry, function, and clinical relevance. *Bone*, 22(3), 181–187.
135. Kohn, R. R., Cerami, A., & Monnier, V. M. (1984). Collagen Aging In Vitro by Nonenzymatic Glycosylation and Browning. *Diabetes*, 33(1), 57–59.
136. Komsa-Penkova, R., Koynova, R., Kostov, G., & Tenchov, B. G. (1996). Thermal stability of calf skin collagen type I in salt solutions. *Biochimica et Biophysica Acta*, 1297(2), 171–181.
137. Kubo, K., Kanehisa, H., Miyatani, M., Tachi, M., & Fukunaga, T. (2003). Effect of low-load resistance training on the tendon properties in middle-aged and elderly women. *Acta Physiologica Scandinavica*, 178(1), 25–32.

138. Kubo, Keitaro, Kanehisa, H., & Fukunaga, T. (2003). Gender differences in the viscoelastic properties of tendon structures. *European Journal of Applied Physiology*, 88(6), 520–526.
139. Kumar, B., Sirisena, D., & Rayner, M. (2013). Proximal sartorius tendon rupture as a cause of traumatic anterior hip pain-a case report of a professional footballer. *Br.J.Sports Med.*, 47(10), 36.
140. Laban, M. M. (1962). Collagen tissue: Implication of its response to stress in vitro. *Archives of Physical Medicine and Rehabilitation*, 43, 461–466.
141. Lancaster, R. L., Haut, R. C., & DeCamp, C. E. (1994). Changes in the mechanical properties of patellar tendon preparations of spontaneously diabetic dogs under long-term insulin therapy. *Journal of Biomechanics*, 27(8), 1105–1108.
142. Laprade, M. D., Kennedy, M. I., Wijdicks, C. A., & Laprade, R. F. (2015). Anatomy and biomechanics of the medial side of the knee and their surgical implications. *Sports Medicine and Arthroscopy Review*, 23(2), 63–70.
143. Le Lous, M., Allain, J. C., Cohen-Solal, L., & Maroteaux, P. (1982). The rate of collagen maturation in rat and human skin. *Connective Tissue Research*, 9(4), 253–262.
144. Le Lous, M., Allain, J. C., Cohen-Solal, L., & Maroteaux, P. (1983). Hydrothermal isometric tension curves from different connective tissues. Role of collagen genetic types and noncollagenous components. *Connective Tissue Research*, 11(2–3), 199–206.
145. Le Lous, M., Cohen-Solal, L., Allain, J. C., Bonaventure, J., & Maroteaux, P. (1985). Age related evolution of stable collagen reticulation in human skin. *Connective Tissue Research*, 13(2), 145–155.
146. Leblanc, D. R., Schneider, M., Angele, P., Vollmer, G., & Docheva, D. (2017). The effect of estrogen on tendon and ligament metabolism and function. *Journal of Steroid Biochemistry and Molecular Biology*, 172, 106–116.
147. Lee, C. A., Lee-Barthel, A., Marquino, L., Sandoval, N., Marcotte, G. R., & Baar, K. (2015). Estrogen inhibits lysyl oxidase and decreases mechanical function in engineered ligaments. *Journal of Applied Physiology*, 118(10), 1250–1257.
148. Lee, J., Kim, K., Jeong, Y., Lee, N. S., Han, S. Y., Lee, C. G., Kim, K., & Han, S. (2014). Pes anserinus and anserine bursa : anatomical study. *Anatomy and Cell Biology*, 47(2), 127–131.

149. Lee, J. M., Pereira, C. A., Abdulla, D., Naimark, W. A., & Crawford, I. (1995). A multi-sample for collagenous denaturation biomaterials temperature tester. *Medical Engineering Physics*, *17*(2), 115–121.
150. Lee, J. M., & Veres, S. P. (2019). Advanced glycation end-product cross-linking inhibits biomechanical plasticity and characteristic failure morphology of native tendon. *Journal of Applied Physiology*, *126*, 832–841.
151. Leff, H. S. (1996). Thermodynamic entropy: The spreading and sharing of energy. *American Journal of Physics*, *64*(10), 1261–1271.
152. LeMoine, J. K., Lee, J. D., & Trappe, T. A. (2008). Impact of sex and chronic resistance training on human patellar tendon dry mass, collagen content, and collagen cross-linking. *AJP: Regulatory, Integrative and Comparative Physiology*, *296*(1), R119–R124.
153. Lepley, A. S., Joseph, M. F., Daigle, N. R., Digiacomio, J. E., Galer, J., Rock, E., Rosier, S. B., & Sureja, P. B. (2018). Gender differences in mechanical properties of the Achilles tendon. *Journal of Strength and Conditioning Research*, *1*.
154. Li, Y., Fessel, G., Georgiadis, M., & Snedeker, J. G. (2013). Advanced glycation end-products diminish tendon collagen fiber sliding. *Matrix Biology*, *32*(3–4), 169–177.
155. Lui, P. P. Y. (2017). Tendinopathy in diabetes mellitus patients—Epidemiology, pathogenesis, and management. *Scandinavian Journal of Medicine and Science in Sports*, *27*(8), 776–787.
156. Maffulli, N, Waterston, S. W., Squair, J., Reaper, J., & Douglas, A. S. (1999). Changing incidence of Achilles tendon rupture in Scotland: a 15-year study. *Clinical Journal of Sport Medicine : Official Journal of the Canadian Academy of Sport Medicine*, *9*(3), 157–160.
157. Maffulli, Nicola, Buono, A. Del, Spiezia, F., Longo, U. G., & Denaro, V. (2012). Light microscopic histology of quadriceps tendon ruptures, 2367–2371.
158. Maffulli, Nicola, Longo, U. G., Maffulli, G. D., Khanna, A., & Denaro, V. (2011). Achilles tendon ruptures in diabetic patients. *Archives of Orthopaedic and Trauma Surgery*, *131*(1), 33–38.
159. Maffulli, Nicola, Orth, F., Barrass, V., Hons, M. S., & Ewen, S. W. B. (2014). Light Microscopic Histology of Achilles Tendon Ruptures A Comparison With Unruptured Tendons, (May).

160. Maganaris, C. N., Narici, M. V., Almekinders, L. C., & Maffulli, N. (2004). Biomechanics and pathophysiology of overuse tendon injuries: Ideas on insertional tendinopathy. *Sports Medicine*, 34(14), 1005–1017.
161. Magnusson, S. P., Beyer, N., Abrahamsen, H., Aagaard, P., Neergaard, K., & Kjaer, M. (2003). Increased Cross-sectional Area and Reduced Tensile Stress of the Achilles Tendon in Elderly Compared With Young Women. *Journal of Gerontology: Biological Sciences*, 58A(2), 123–127.
162. Magnusson, S. P., Hansen, M., Langberg, H., Miller, B., Haraldsson, B., Westh, E. K., Koskinen, S., Aagaard, P., & Kjær, M. (2007). The adaptability of tendon to loading differs in men and women. *International Journal of Experimental Pathology*, 88(4), 237–240.
163. Marieb, E. N., & Hoehn, K. (2013). *Human Anatomy & Physiology*. (S. Beauparlant, Ed.) (9th ed.). Glenview, IL: Pearson Education Inc.
164. Meinel, A., Nemetschek-Gansler, H., Holz, U., Jonak, R., Krahl, H., Nemetschek, T., & Riedl, H. (1977). Fibrilläre Gefügestörung bei Sehnenruptur. *Archiv Für Orthopädische Und Unfall-Chirurgie*, 90(1), 89–94.
165. Menard, D., & Stanish, W. D. (1989). The aging athlete. *The American Journal of Sports Medicine*, 17(2), 187–196.
166. Miles, C. A., & Bailey, A. J. (2001). Thermally labile domains in the collagen molecule. *Micron*, 32(3), 325–332.
167. Miles, C. A., & Burjanadze, T. V. (2001). Thermal stability of collagen fibers in ethylene glycol. *Biophysical Journal*, 80(3), 1480–1486.
168. Miles, Christopher A., Avery, N. C., Rodin, V. V., & Bailey, A. J. (2005). The increase in denaturation temperature following cross-linking of collagen is caused by dehydration of the fibres. *Journal of Molecular Biology*, 346(2), 551–556.
169. Miles, Christopher A., Burjanadze, T. V., & Bailey, A. J. (1995). The Kinetics of the Thermal Denaturation of Collagen in Unrestrained Rat Tail Tendon Determined by Differential Scanning Calorimetry. *Journal of Molecular Biology*, 245(4), 437–446.
170. Miles, Christopher A., & Ghelashvili, M. (1999). Polymer-in-a-box mechanism for the thermal stabilization of collagen molecules in fibers. *Biophysical Journal*, 76(6), 3243–3252.



171. Misof, K., Rapp, G., & Fratzl, P. (1997). A new molecular model for collagen elasticity based on synchrotron x- ray scattering evidence. *Biophysical Journal*, 72(3), 1376–1381.
172. Mochizuki, T., Akita, K., Muneta, T., & Sato, T. (2004). Pes Anserinus: Layered Supportive Structure on the Medial Side of the Knee. *Clinical Anatomy*, 17(1), 50–54.
173. Mohsenifar, Z., Javad Feridoni, M., Bayat, M., Farahani, R., Bayat, S., & Khoshvaghti, A. (2014). Histological and Biomechanical Analysis of the Effects of Streptozotocin- induced Type One Diabetes Mellitus on Healing of Tentomized Achilles Tendons in Rats. *Foot and Ankle Surgery*, 20(3), 186–191.
174. Monnier, V., Kohn, R., & Cerami, A. (1984). Accelerated age-related browning of human collagen in diabetes mellitus. *Proceedings of the National Academy of Sciences*, 81(1), 583–587.
175. Monnier, V. M., & Sell, D. R. (2006). Prevention and Repair of Protein Damage by the Maillard Reaction In Vivo. *Rejuvenation Research*, 9(2), 264–273.
176. Morgan, F. R. (1960). The mechanical properties of collagen fibres: stress-strain curves. *Journal of the Society of Leather Trades Chemists*, 44, 170–182.
177. Morrison, S. M., Dick, T. J. M., & Wakeling, J. M. (2015). Structural and mechanical properties of the human Achilles tendon: Sex and strength effects. *Journal of Biomechanics*, 48(12), 3530–3533.
178. Mosler, E., Folkhard, W., Knörzer, E., & Nemetschek, T. (1985). Stress-induced Molecular Rearrangement in Tendon Collagen. *Journal of Molecular Biology*, 182(4), 589–596.
179. Mott, J. D., Khalifah, R. G., Nagase, H., Shield, C. F. 3rd, Hudson, J. K., & Hudson, B. G. (1997). Nonenzymatic glycation of type IV collagen and matrix metalloproteinase susceptibility. *Kidney International*, 52(5), 1302–1312.
180. Muraoka, T., Muramatsu, T., Fukunaga, T., & Kanehisa, H. (2005). Elastic properties of human Achilles tendon are correlated to muscle strength. *J Appl Physiol*, 99(2), 665–669.
181. Naimark, W. A., Waldman, S. D., Anderson, R. J., Suzuki, B., Pereira, C. A., & Lee, J. M. (1998). Thermomechanical analysis of collagen crosslinking in the developing lamb pericardium. *Biorheology*, 35(1), 1–16.

182. Naresh, M. D., & Brodsky, B. (1992). X-ray diffraction studies on human tendon show age-related changes in collagen packing. *Biochimica et Biophysica Acta*, 1122(2), 161–166.
183. Nemetschek, T., Jonak, R., Nemetschek-Gansler, H., & Riedi, H. (1977). Knickdeformation an Kollagen. *Archiv for Orthop Dische Und Unfall-Chirurgie*, 89, 249–257.
184. Nicholl, I. D., Stitt, A. W., Moore, J. E., Ritchie, A. J., Archer, D. B., & Bucala, R. (1998). Increased levels of advanced glycation endproducts in the lenses and blood vessels of cigarette smokers. *Molecular Medicine*, 4(9), 594–601.
185. Nimni, M. E. (1988). Biochemistry of Normal Tendon and Ligament. In *Collagen: Volume III Biotechnology* (pp. 226–234). Boca Raton, Florida: CRC Press Inc.
186. Nimni, M. E. (Ed.). (1988). *Collagen: Biochemistry* (Vol. I). Boca Raton, Florida: CRC Press Inc.
187. O'Brien, T. D., Reeves, N. D., Baltzopoulos, V., Jones, D. A., & Maganaris, C. N. (2010). Mechanical properties of the patellar tendon in adults and children. *Journal of Biomechanics*, 43(6), 1190–1195.
188. Oliva, F., Piccirilli, E., Berardi, A. C., Frizziero, A., Tarantino, U., & Maffulli, N. (2016). Hormones and tendinopathies: The current evidence. *British Medical Bulletin*, 117(1), 39–58.
189. Onambele, G. L., Narici, M. V, Maganaris, C. N., Gladys, L., Narici, M. V, & Constantinos, N. (2019). Calf muscle-tendon properties and postural balance in old age. *Journal of Applied Physiology*, 100(6), 2048–2056.
190. Onambélé, G. N. L., Burgess, K., & Pearson, S. J. (2007). Gender-specific in vivo measurement of the structural and mechanical properties of the human patellar tendon. *Journal of Orthopaedic Research*, 25(12), 1635–1642.
191. Owen Jr., W. F., Hou, F., Stuart, R. O., Kay, J., Boyce, J., Chertow, G. M., & Schmidt, A. M. (1998).  $\beta$ 2-microglobulin modified with advanced glycation end products modulates collagen synthesis by human fibroblasts. *Kidney International*, 53(5), 1365–1373.
192. Pardes, A. M., Freedman, B. R., Fryhofer, G. W., Salka, N. S., Bhatt, P. R., & Soslowsky, L. J. (2016). Males have Inferior Achilles Tendon Material Properties Compared to Females in a Rodent Model. *Annals of Biomedical Engineering*, 44(10), 2911–2912.

193. Parry, D. A. D., Barnes, G. R. G., & Craig, A. S. (1978). A comparison of the size distribution of collagen fibrils in connective tissues as a function of age and a possible relation between fibril size distribution and mechanical properties. *Proceedings of the Royal Society of London: Biological Sciences*, 203(1152), 305–321.
194. Parry, D. A. D., & Craig, A. S. (1978). Collagen fibrils and elastic fibers in rat-tail tendon: An electron microscopic investigation. *Biopolymers*, 17(4), 843–855.
195. Patterson-Kane, J. C., Wilson, A. M., Firth, E. C., Parry, D. A. D., & Goodshlp, A. E. (1998). Exercise-related alterations in crimp morphology in the central regions of superficial digital flexor tendons from young Thoroughbreds: A controlled study. *Equine Veterinary Journal*, 30(1), 61–64.
196. Petrovic, M., Maganaris, C. N., Deschamps, K., Verschueren, S. M., Bowling, F. L., Boulton, A. J. M., & Reeves, N. D. (2018). Altered Achilles tendon function during walking in people with diabetic neuropathy: implications for metabolic energy saving. *Journal of Applied Biomechanics*, 124(5), 1333–1340.
197. Pluim, B. M., Staal, J. B., Windler, G. E., & Jayanthi, N. (2006). Tennis injuries: occurrence, aetiology, and prevention. *British Journal of Sports Medicine*, 40, 415–424.
198. Prodromos, C. C., Han, Y., Rogowski, J., Joyce, B., & Shi, K. (2007). A meta-analysis of the incidence of anterior cruciate ligament tears as a function of gender, sport, and a knee injury-reduction regimen. *Arthroscopy*, 23(12), 1320–1325.
199. Purslow, P. P., Wess, T. J., & Hukins, D. W. (1998). Collagen orientation and molecular spacing during creep and stress-relaxation in soft connective tissues. *The Journal of Experimental Biology*, 201, 135–142.
200. Quigley, A. S., Bancelin, S., Deska-Gauthier, D., Légaré, F., Kreplak, L., & Veres, S. P. (2018). In tendons, differing physiological requirements lead to functionally distinct nanostructures. *Scientific Reports*, 8(1), 1–14.
201. Quinlan, J., Franchi, M. V, Smith, K., & Szewczyk, N. J. (2017). Muscle and Tendon Contributions to Reduced Rate of Torque Development in Healthy Older Males. *J Gerontol A Bio Sci Med Sci*, 73(4), 539–545.
202. Ramachandran, G. N. (1976). *Biochemistry of Collagen*. (G. N. Ramachandran & A. H. Reddi, Eds.) (1st ed.). New York: Plenum Press.

203. Ramasamy, R., Vannucci, S. J., Shi, S., Yan, D., Herold, K., Yan, S. F., & Schmidt, A. M. (2005). Advanced glycation end products and RAGE : a common thread in aging , diabetes , neurodegeneration , and inflammation. *Glycobiology*, *15*(7), 16R-28R.
204. Ranger, T. A., Wong, A. M. Y., Cook, J. L., & Gaida, J. E. (2016). Is there an association between tendinopathy and diabetes mellitus ? A systematic review with meta-analysis. *British Journal of Sports Medicine*, *50*, 982–989.
205. Reeves, N. D. (2006). Adaptation of the tendon to mechanical usage, *6*(December 2005), 174–180.
206. Reihnsner, R., Pfeiler, W., & Menzel, E. J. (1998). Comparison of normal and in vitro aging by non-enzymatic glycation as verified by differential scanning calorimetry. *Gerontology*, *44*(2), 85–90.
207. Rennie, W. J., & Saifuddin, A. (2005). Pes anserine bursitis : incidence in symptomatic knees and clinical presentation. *Skeletal Radiology*, *34*(7), 395–398.
208. Riemersma, D. J., & Schamhardt, H. C. (1985). In vitro mechanical properties of equine tendons in relation to cross-sectional area and collagen content. *Research in Veterinary Science*, *39*(3), 263–270.
209. Rigby, B. J., Hirai, N., & Spikes, J. D. (1959). The mechanical properties of rat tail tendon. *The Journal of General Physiology*, *43*(2), 265–283.
210. Rigby, B. J., & Mitchell, T. W. (1977). Oxygen Participation in the In Vivo and In Vitro Aging of Collagen Fibres. *Biochemical and Biophysical Research Communications*, *79*(2), 400–405.
211. Rigozzi, S., Müller, R., Stemmer, A., & Snedeker, J. G. (2013). Tendon glycosaminoglycan proteoglycan sidechains promote collagen fibril sliding-AFM observations at the nanoscale. *Journal of Biomechanics*, *46*(4), 813–818.
212. Riley, G. (2004). The pathogenesis of tendinopathy. A molecular perspective. *Rheumatology*, *43*(2), 131–142.
213. Ristolainen, L., Heinonen, A., Waller, B., Kujala, U. M., & Kettunen, J. A. (2009). Gender differences in sport injury risk and types of injuries: a retrospective twelve-month study on cross-country skiers, swimmers, long-distance runners and soccer players. *Journal of Sports Science and Medicine*, *8*(3), 443–451.
214. Robins, S. P., & Bailey, A. J. (1973). Relative Stabilities of the Intermediate Reducible Crosslinks Present in Collagen Fibres. *FEBS Letters*, *33*(2), 167–171.

215. Robins, S. P., Shimokomakit, M., & Bailey, A. J. (1973). The Chemistry of the Collagen Cross-Links : Age-related changes in the reducible components of intact bovine collagen fibres. *Biochem. J*, 131, 771–780.
216. Rosenbloom, A. L., & Silverstein, J. H. (1996). Connective Tissue and Joint Disease in Diabetes Mellitus. *Endocrinology and Metabolism Clinics of North America*, 25(2), 473–483.
217. Ruggeri, A., & Motta, P. M. (Eds.). (1984). *Ultrastructure of the Connective Tissue Matrix* (1st ed.). Boston, MA: Springer US.
218. Sakoma, Y., Furumatsu, T., & Ozaki, T. (2014). Pentosidine Deposition Affects Biomechanical Properties of Achilles Tendon in Diabetic Rats. *Orthop Muscul Syst*, 3(1), 150.
219. Sallis, R. E., Jones, K., Sunshine, S., Smith, G., & Simon, L. (2001). Comparing sports injuries in men and women. *International Journal of Sports Medicine*, 22(6), 420–423.
220. Sandberg, L. B., Soskel, N. T., & Leslie, J. G. (1979). Elastin structure, biosynthesis, and relation to disease states. *The New England Journal of Medicine*, 300(10), 530–534.
221. Sarver, D. C., Kharaz, Y. A., Sugg, K. B., Gumucio, J. P., Comerford, E., & Mendias, C. L. (2017). Sex differences in tendon structure and function. *Journal of Orthopaedic Research*, 35(10), 2117–2126.
222. Sasaki, N., & Odajima, S. (1996). Elongation mechanisms of collagen fibrils and force-strain relations of tendons at each level of structural hierarchy. *Journal of Biomechanics*, 29, 1131–1136.
223. Schnider, S. L., & Kohn, R. R. (1981). Effects of age and diabetes mellitus on the solubility and nonenzymatic glycosylation of human skin collagen. *Journal of Clinical Investigation*, 67(6), 1630–1635.
224. Scott, B. P. (2016). *Physiological Remodelling of Mitral Valve Chordae Tendineae In The Maternal Bovine Heart* (Master's Thesis). Dalhousie University.
225. Screen, H. R. C., Toorani, S., & Shelton, J. C. (2013). Microstructural stress relaxation mechanics in functionally different tendons. *Medical Engineering and Physics*, 35(1), 96–102.

226. Sell, D. R., Nagaraj, R. H., Grandhee, S. K., Odetti, P., Lapolla, A., Fogarty, J., & Monnier, V. M. (1991). Pentosidine: a Molecular Marker for the Cumulative Damage to Proteins in Diabetes, Aging, and Uremia. *Diabetes Metabolism Research and Reviews*, 7(4), 239–251.
227. Seynnes, O. R., Koesters, A., Gimpl, M., Reifberger, A., Niederseer, D., Niebauer, J., Pirich, C., Müller, E., & Narici, M. V. (2011). Effect of alpine skiing training on tendon mechanical properties in older men and women. *Scandinavian Journal of Medicine & Science in Sports*, 21(s1), 39–46.
228. Shadwick, R. E. (1990). Elastic energy storage in tendons: mechanical differences related to function and age. *Journal of Applied Physiology*, 68(3), 1033–1040.
229. Sharma, P., & Maffulli, N. (2005). Tendon Injury and Tendinopathy: Healing and Repair. *The Journal of Bone and Joint Surgery*, 87(1), 187.
230. Shi, D. F., Wang, D. M., Wang, C. T., & Liu, A. (2012). A novel, inexpensive and easy to use tendon clamp for in vitro biomechanical testing. *Medical Engineering and Physics*, 34(4), 516–520.
231. Shi, L., Rui, Y. F., Li, G., & Wang, C. (2015). Alterations of tendons in diabetes mellitus: what are the current findings? *International Orthopaedics*, 39(8), 1465–1473.
232. Simm, A., Müller, B., Nass, N., Hofmann, B., Bushnaq, H., Silber, R., & Bartling, B. (2015). Protein glycation — Between tissue aging and protection. *Experimental Gerontology*, 68, 71–75.
233. Singh, R., Barden, A., Mori, T., & Beilin, L. (2001). Advanced glycation end-products: A review. *Diabetologia*, 44(2), 129–146.
234. Smith, G. I., Atherton, P., Villareal, D. T., Frimel, T. N., Rankin, D., Rennie, M. J., & Mittendorfer, B. (2008). Differences in muscle protein synthesis and anabolic signaling in the postabsorptive state and in response to food in 65-80 year old men and women. *PloS One*, 3(3), e1875.
235. Smith, L. L., Burnet, S. P., & McNeil, J. D. (2003). Musculoskeletal manifestations of diabetes mellitus. *British Journal of Sports Medicine*, 37(1), 30 LP – 35.
236. Snedeker, J. G., & Gautieri, A. (2014). The role of collagen crosslinks in ageing and diabetes - the good, the bad, and the ugly. *Muscles, Ligaments and Tendons Journal*, 4(3), 303–308.

237. Sparavalo, S. (2017). *Age-Related Changes in Structure and Biomechanics of Human Sartorius Tendon Collagen* (Master's Thesis). Dalhousie University.
238. Statistics Canada. (2015). Canadian Community Health Survey: Combined data, 2013/2014. Retrieved September 28, 2017, from <http://www.statcan.gc.ca/daily-quotidien/150624/dq150624b-eng.htm>.
239. Statistics Canada. (2019). Life Expectancy. Retrieved January 20, 2019, from <https://www150.statcan.gc.ca/n1/pub/89-645-x/2010001/life-expectancy-esperance-vie-eng.htm>.
240. Stenroth, L., Peltonen, J., Cronin, N. J., Sipilä, S., & Finni, T. (2012). Age-related differences in Achilles tendon properties and triceps surae muscle architecture in vivo. *Journal of Applied Physiology*, *113*(10), 1537–1544.
241. Strocchi, R., Raspanti, M., Girolami, M., & Giannini, S. (1991). Human Achilles Tendon: Morphological and Morphometric Variations as a Function of Age. *Foot and Ankle*, *12*(2), 100–104.
242. Svensson, R. B., Heinemeier, K. M., Couppé, C., Kjaer, M., & Magnusson, S. P. (2016). Effect of aging and exercise on the tendon. *Journal of Applied Physiology*, *121*(6), 1237–1246.
243. Svensson, R. B., Smith, S. T., Moyer, P. J., & Magnusson, S. P. (2018). Effects of maturation and advanced glycation on tensile mechanics of collagen fibrils from rat tail and Achilles tendons. *Acta Biomaterialia*, *70*, 270–280.
244. Tanaka, S., Avigad, G., Brodsky, B., & Eikenberry, E. F. (1988). Glycation Induces Expansion of the Molecular Packing of Collagen. *Journal of Molecular Biology*, *203*(2), 495–505.
245. Tanaka, S., Avigad, G., Eikenberry, E. F., & Brodsky, B. (1988). Isolation and partial characterization of collagen chains dimerized by sugar-derived cross-links. *Journal of Biological Chemistry*, *263*(33), 17650–17657.
246. Thorpe, C. T., Godinho, M. S. C., Riley, G. P., Birch, H. L., Clegg, P. D., & Screen, H. R. C. (2015). The interfascicular matrix enables fascicle sliding and recovery in tendon, and behaves more elastically in energy storing tendons. *Journal of the Mechanical Behavior of Biomedical Materials*, *52*, 85–94.
247. Thorpe, C. T., Klemm, C., Riley, G. P., Birch, H. L., Clegg, P. D., & Screen, H. R. C. (2013). Helical sub-structures in energy-storing tendons provide a possible mechanism for efficient energy storage and return. *Acta Biomaterialia*, *9*(8), 7948–7956.

248. Thorpe, C. T., Streeter, I., Pinchbeck, G. L., Goodship, A. E., Clegg, P. D., & Birch, H. L. (2010). Aspartic acid racemization and collagen degradation markers reveal an accumulation of damage in tendon collagen that is enhanced with aging. *Journal of Biological Chemistry*, 285(21), 15674–15681.
249. Torp, S., Arridge, R. G. C., Armeniades, C. D., & Baer, E. (1975). Structure-property relationships in tendon as a function of age. *Colston Papers*, 26, 197–221.
250. Torp, S., Baer, E., & Friedman, B. (1975). Effects of age and of mechanical deformation on the ultrastructure of tendon. *Colston Papers*, 26, 223–250.
251. Trębacz, H., Szczęsna, A., & Arczewska, M. (2018). Thermal stability of collagen in naturally ageing and in vitro glycated rabbit tissues. *Journal of Thermal Analysis and Calorimetry*, 134(3), 1903–1911.
252. Tuite, D. J., Renström, P., & O'Brien, M. (1997). The aging tendon. *Scandinavian Journal of Medicine & Science in Sports*, 7(2), 72–77.
253. Veres, S. P., Brennan-pierce, E. P., & Lee, J. M. (2014). Macrophage-like U937 cells recognize collagen fibrils with strain-induced discrete plasticity damage. *Journal of Biomaterial Research*, 103A(1), 397–408.
254. Veres, S. P., Harrison, J. M., & Lee, J. M. (2013). Cross-link stabilization does not affect the response of collagen molecules, fibrils, or tendons to tensile overload. *Journal of Orthopaedic Research*, 31(12), 1907–1913.
255. Veres, S. P., Harrison, J. M., & Lee, J. M. (2013). Repeated subrupture overload causes progression of nanoscaled discrete plasticity damage in tendon collagen fibrils. *Journal of Orthopaedic Research*, 31(5), 731–737.
256. Veres, S. P., Harrison, J. M., & Lee, J. M. (2014). Mechanically overloading collagen fibrils uncoils collagen molecules, placing them in a stable, denatured state. *Matrix Biology*, 33, 54–59.
257. Veres, S. P., & Lee, J. M. (2012). Designed to fail: A novel mode of collagen fibril disruption and its relevance to tissue toughness. *Biophysical Journal*, 102(12), 2876–2884.
258. Viidik, A. (1979). Connective Tissues - Possible Implications of the Temporal Changes for the Aging Process. *Mechanisms of Ageing and Development*, 9(3–4), 267–285.
259. Viidik, A., & Ekholm, R. (1968). Light and electron microscopic studies of collagen fibers under strain. *Anatomy and Embryology*, 127(2), 154–164.



260. Vlassara, H., & Palace, M. R. (2002). Diabetes and advanced glycation endproducts. *Journal of International Meidicine*, 251(2), 87–101.
261. Vogt, B. W., Schleicher, E. D., & Wieland, O. H. (1982).  $\epsilon$ -Amino-Lysine-Bound Glucose in Human Tissues Obtained at Autopsy: Increase in Diabetes Mellitus. *Diabetes*, 31(12), 1123 LP – 1127.
262. Vosseller, J. T., Ellis, S. J., Levine, D. S., Kennedy, J. G., Elliott, A. J., Deland, J. T., Roberts, M. M., & Malley, M. J. O. (2013). Achilles Tendon Rupture in Women.
263. Wang, J. H. C. (2006). Mechanobiology of tendon. *Journal of Biomechanics*, 39(9), 1563–1582.
264. Wasserman. (1956). Intercellular components of connective tissue - origin structure and interrelationship of fibers and ground substance. *Ergebnisse Der Anatomie Und Entwicklungsgeschichte*, 240–333.
265. Weber, J. F., Agur, A. M. R., Fattah, A. Y., Gordon, K. D., & Oliver, M. L. (2015). Tensile mechanical properties of human forearm tendons. *Journal of Hand Surgery (European Volume)*, 40(7), 711–719.
266. Wells, S. M., Adamson, S. L., Langille, B. L., & Lee, J. M. (1998). Thermomechanical Analysis of Collagen Crosslinking in the Developing Ovine Thoracic Aorta. *Biorheology*, 35(6), 399–414.
267. Wess, T. J., Hammersley, A. P., Wess, L., & Miller, A. (1998). Molecular Packing of Type I Collagen in Tendon. *Journal of Structural Biology*, 122, 92–100.
268. Westh, E., Kongsgaard, M., Bojsen-Moller, J., Aagaard, P., Hansen, M., Kjaer, M., & Magnusson, S. P. (2008). Effect of habitual exercise on the structural and mechanical properties of human tendon, in vivo, in men and women. *Scandinavian Journal of Medicine & Science in Sports*, 18(1), 23–30.
269. Wiegand, N., Vámhidy, L., Kereskai, L., & Lorinczy, D. (2010). Differential scanning calorimetric examination of the ruptured Achilles tendon in human. *Thermochimica Acta*, 498(1), 7–10.
270. Wiegand, N., Vámhidy, L., & Lorinczy, D. (2010). Differential scanning calorimetric examination of ruptured Achilles tendons in human. *Journal of Thermal Analysis and Calorimetry*, 498(1), 7–10.
271. Wiegand, N., Vámhidy, L., & Lorinczy, D. (2010). Differential scanning calorimetric examination of ruptured lower limb tendons in human. *Journal of Thermal Analysis and Calorimetry*, 101(2), 487–492.

272. Wiesinger, H. P., Kösters, A., Müller, E., & Seynnes, O. R. (2015). Effects of Increased Loading on in Vivo Tendon Properties: A Systematic Review. *Medicine and Science in Sports and Exercise*, 47(9), 1885–1895.
273. Wilder, R. P., & Sethi, S. (2004). Overuse injuries: tendinopathies, stress fractures, compartment syndrome, and shin splints. *Clinics in Sports Medicine*, 23(1), 55–81.
274. Willett, T. L. (2007). *Molecular-Level Changes in Collagen Due to In vitro Tensile Overload in a Tendon Model* (Doctoral dissertation). Dalhousie University.
275. Willett, T. L., Labow, R. S., Aldous, I. G., Avery, N. C., & Lee, J. M. (2010). Changes in Collagen With Aging Maintain Molecular Stability After Overload: Evidence From an In Vitro Tendon Model. *Journal of Biomechanical Engineering*, 132(3), 031002-1-031002–031008.
276. Willett, T. L., Labow, R. S., Avery, N. C., & Lee, J. M. (2007). Increased Proteolysis of Collagen in an In Vitro Tensile Overload Tendon Model. *Annals of Biomedical Engineering*, 35(11), 1961–1972.
277. Willett, T. L., Labow, R. S., & Lee, J. M. (2008). Mechanical overload decreases the thermal stability of collagen in an in vitro tensile overload tendon model. *Journal of Orthopaedic Research*, 26(12), 1605–1610.
278. Wilson, J. J., & Best, T. M. (2005). Common overuse tendon problems: A review and recommendations for treatment. *American Family Physician*, 72(5), 811–818.
279. Wittstein, J. R., Wilson, J. B., & Moorman, C. T. (2006). Complications Related to Hamstring Tendon Harvest. *Operative Techniques in Sports Medicine*, 14(1), 15–19.
280. Woo, S. L. Y., Gomez, M. A., Woo, Y. K., & Akeson, W. H. (1982). Mechanical Properties of Tendons and Ligaments: II. The relationships of immobilization and exercise on tissue remodeling. *Biorheology*, 19(3), 397–408.
281. Wood, L. K., Arruda, E. M., & Brooks, S. V. (2011). Regional stiffening with aging in tibialis anterior tendons of mice occurs independent of changes in collagen fibril morphology. *Journal of Applied Physiology*, 111(4), 999–1006.
282. Wren, T. A. L., Yerby, S. A., Beaupré, G. S., & Carter, D. R. (2001). Mechanical Properties of the Human Achilles Tendon. *Clinical Biomechanics*, 16(3), 245–251.
283. Yannas, I. V., & Huang, C. (1972). Fracture of tendon collagen. *Journal of Polymer Science*, 10(4), 577–584.

284. Zakaria, M. H. B., Davis, W. A., & Davis, T. M. E. (2014). Incidence and predictors of hospitalization for tendon rupture in Type 2 diabetes: The Fremantle Diabetes Study. *Diabetic Medicine*, 31(4), 425–430.
285. Zhong, S., Wu, B., Wang, M., Wang, X., Yan, Q., Fan, X., Hu, Y., Han, Y., & Li, Y. (2018). The anatomical and imaging study of pes anserinus and its clinical application. *Medicine*, 97(15), 1–9.
286. Zitnay, J. L., & Weiss, J. A. (2018). Load transfer, damage, and failure in ligaments and tendons. *Journal of Orthopaedic Research*, 36(12), 3093–3104.

## **Appendix A: Phosphate Buffer Saline DSC Study, Half-Time of Load Decay and Height-Related Data**

### *DSC Protocol for Usage of PBS as the Hydrating Solution*

For DSC testing, tendon pieces were taken from two ~10 x 10 mm square sections near the middle of tendons (Figure 3.6) from male diabetic and non-diabetic donors due to experimental progression. This resulted in multiple ~2.5 x 2.5 mm samples each weighing  $15 \pm 5$  mg. Samples were placed in 40 mL of freshly prepared phosphate buffer saline. Samples were double rinsed with PBS and stored at 4°C overnight. DSC samples were blotted dry to remove excess water from the surface and weighed before being individually placed and hermetically sealed in 20 $\mu$ L aluminum pans. DSC was performed using a Q200 differential scanning calorimeter (TA Instruments, New Castle, DE) that was calibrated prior to testing with an Indium standard. Samples were run against an empty hermetically sealed reference pan. Pan temperatures were equilibrated at 30°C and the temperature was increased at a linear rate of 5°C per minute to 90°C. During testing, data was recorded at 10 Hz with the resultant endotherm analyzed using Universal Analysis 2000 software (Version 4.5A, TA Instruments). After testing, sealed pans were pierced using a hypodermic needle and stored in a vacuum desiccator with the sample dry mass being weighed once every 24 hours until the mass stabilized.

### *Thermal Stability Remains Largely Unchanged with Age in the Male Diabetic and Non-Diabetic Donor Populations with Changes Related to Solution Type and Diabetic Status*

The preliminary study, performed in an effort to reinforce previous findings in sartorius tendon collagen by Sparavalo et al<sup>237</sup>, revealed only an increase in  $T_{peak}$  ( $p = 0.0196$ ) of the sartorius tendon collagen with age (Figure A.1). Moreover, both of the average values of  $T_{onset}$  ( $p = 0.0033$ ) and  $T_{peak}$  ( $p = 0.0079$ ) were found to be significantly higher in the older male donors (38-60 years of age) with diabetes (Figure A.2). Lastly, the use of phosphate buffer saline produced molecular destabilization exhibited by the significant decreases in  $T_{onset}$  and  $T_{peak}$  when compared to values obtained using distilled water (Figure A.3), however, the difference remained unchanged by age group.

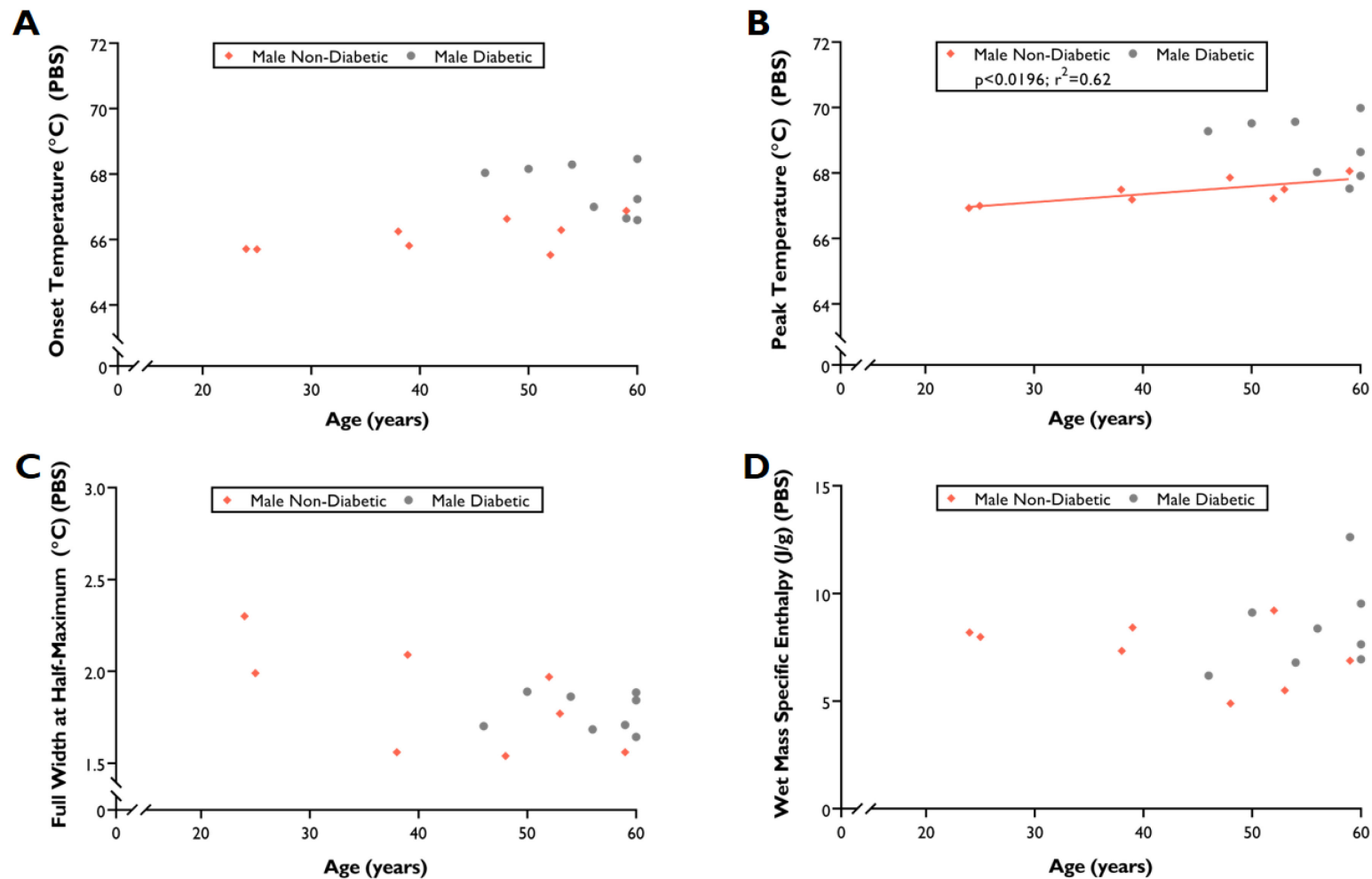


Figure A.1 DSC Properties vs. Age when using PBS as the hydrating solution. Only (A)  $T_{peak}$  was found to have an increasing significant relationship with increasing age in male non-diabetic individuals. Male diabetic and non-diabetic individuals were included in this segment of the study.

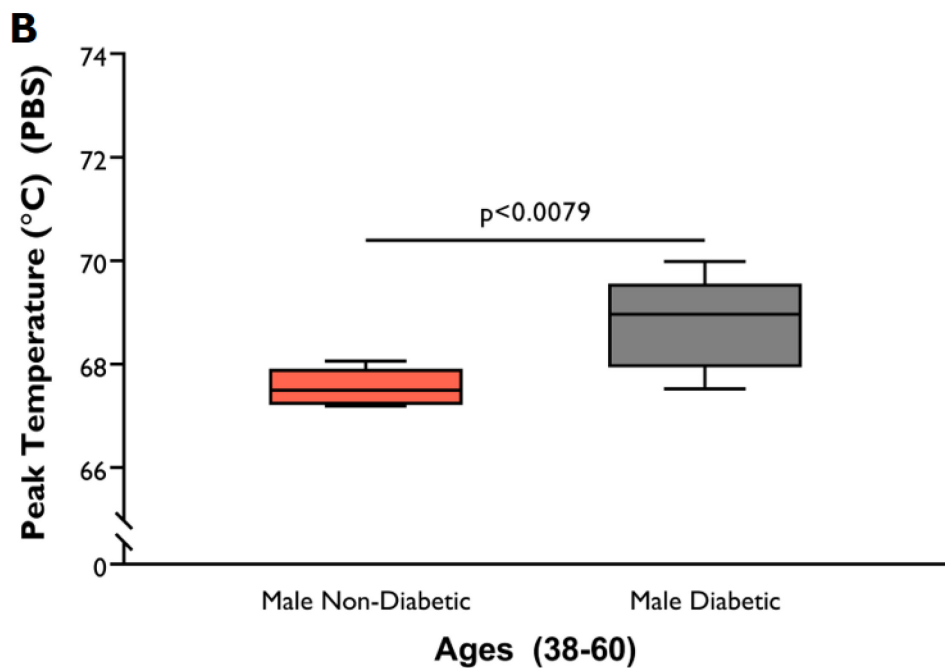
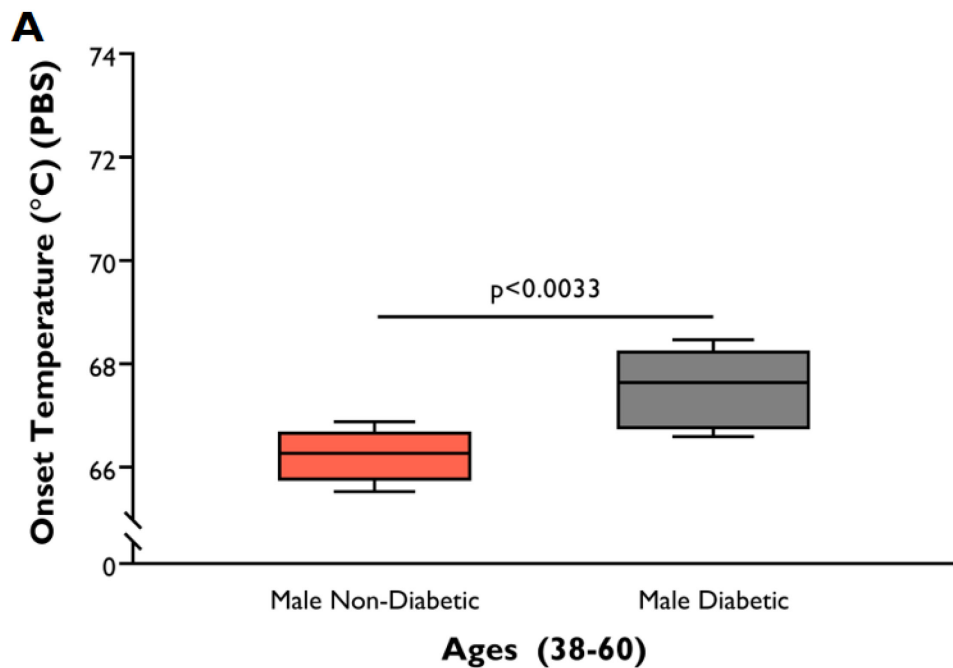


Figure A.2 Evaluating the effect of diabetes in the older male population (38-60) on DSC parameters: (A)  $T_{onset}$  and (B)  $T_{peak}$  using PBS as the hydrating solution.

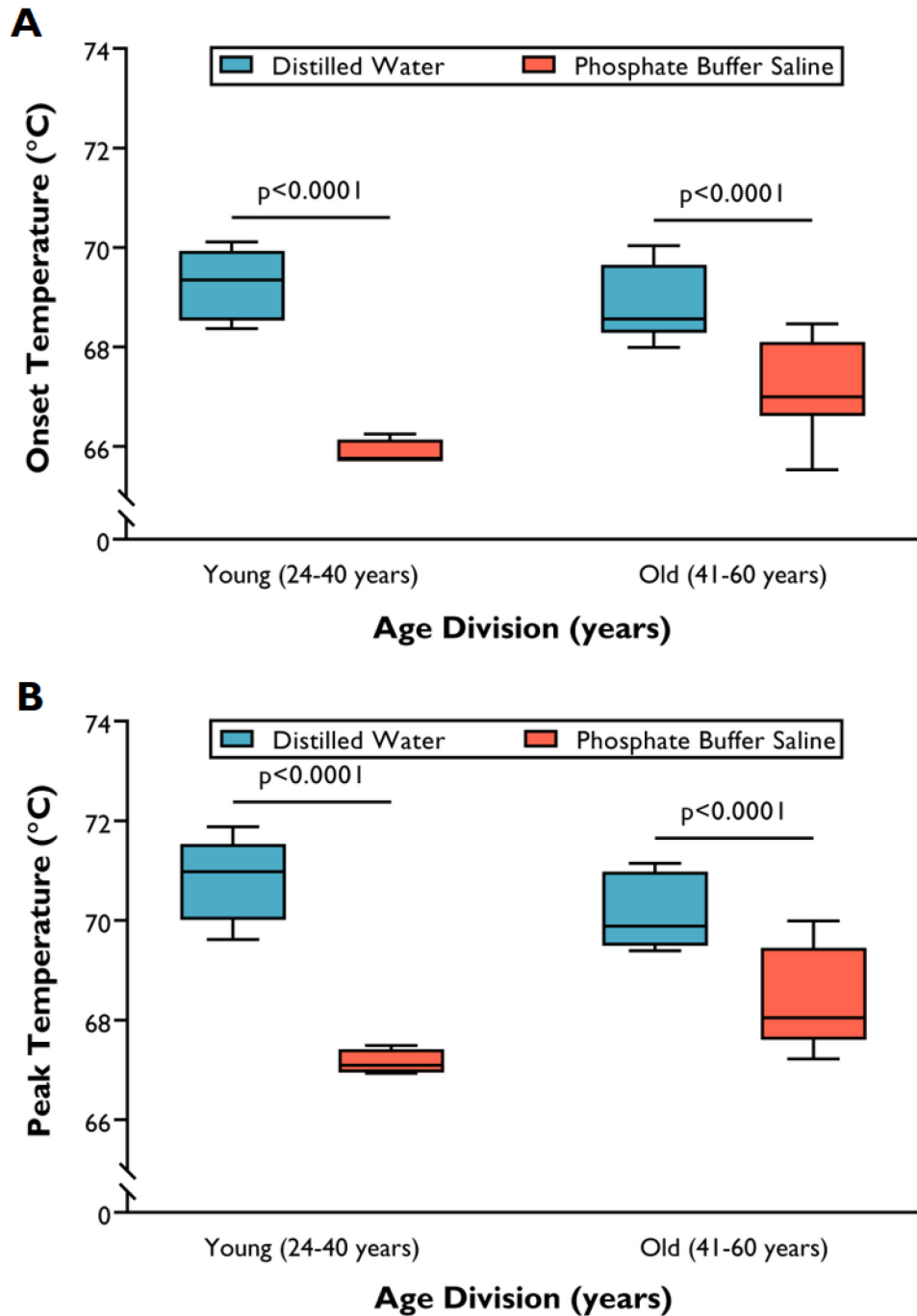


Figure A.3 Combining the Male ND and Male Diabetic data to improve sample sizes, an evaluation of the effects of salt solutions on (A)  $T_{onset}$  and (B)  $T_{peak}$  of tendon collagen in the younger and older populations was performed. Significant molecular destabilization occurs within the younger and older donor population; however, the disparity does not significantly decrease with aging when evaluated using a Two-Way Ordinary ANOVA ( $p > 0.05$ ).

**Table A.1 Half-Time of Load Decay values of samples from female non-diabetic donors. Mean  $\pm$  SD values of  $t_{1/2}$  for each donor population are found in parentheses below their respective names. Values are expressed as mean  $\pm$  SD.**

<b>Donor Population (Average <math>t_{1/2}</math> (hr))</b>	<b>Age (years)</b>	<b>N</b>	<b><math>t_{1/2}</math> (hrs)</b>
<b>Female Non-Diabetic (482 <math>\pm</math> 568)</b>	16	1	302 $\pm$ N/A
	17	1	100 $\pm$ N/A
	44	2	127 $\pm$ 73
	48	0	N/A
	49	2	1,473 $\pm$ 1,147
	58	4	409 $\pm$ 381
	<b>Age</b>	<b>N</b>	<b><math>t_{1/2}</math></b>
<b>Male Non-Diabetic (1,490 <math>\pm</math> 2,370)</b>	24	2	36 $\pm$ 36
	25	3	508 $\pm$ 583
	31	2	6,260 $\pm$ 7,940
	38	5	212 $\pm$ 190
	39	3	440 $\pm$ 309
	48	1	123 $\pm$ N/A
	52	3	508 $\pm$ 539
	53	3	344 $\pm$ 335
	59	3	5,000 $\pm$ 7,710
	<b>Age</b>	<b>N</b>	<b><math>t_{1/2}</math> (hr)</b>
<b>Male Diabetic (757 <math>\pm</math> 677)</b>	46	3	506 $\pm$ 189
	50	0	N/A
	54	3	1,310 $\pm$ 1,980
	56	1	1,625 $\pm$ N/A
	59	0	N/A
	60	1	53 $\pm$ N/A
	60	4	291 $\pm$ 329
	60	0	N/A



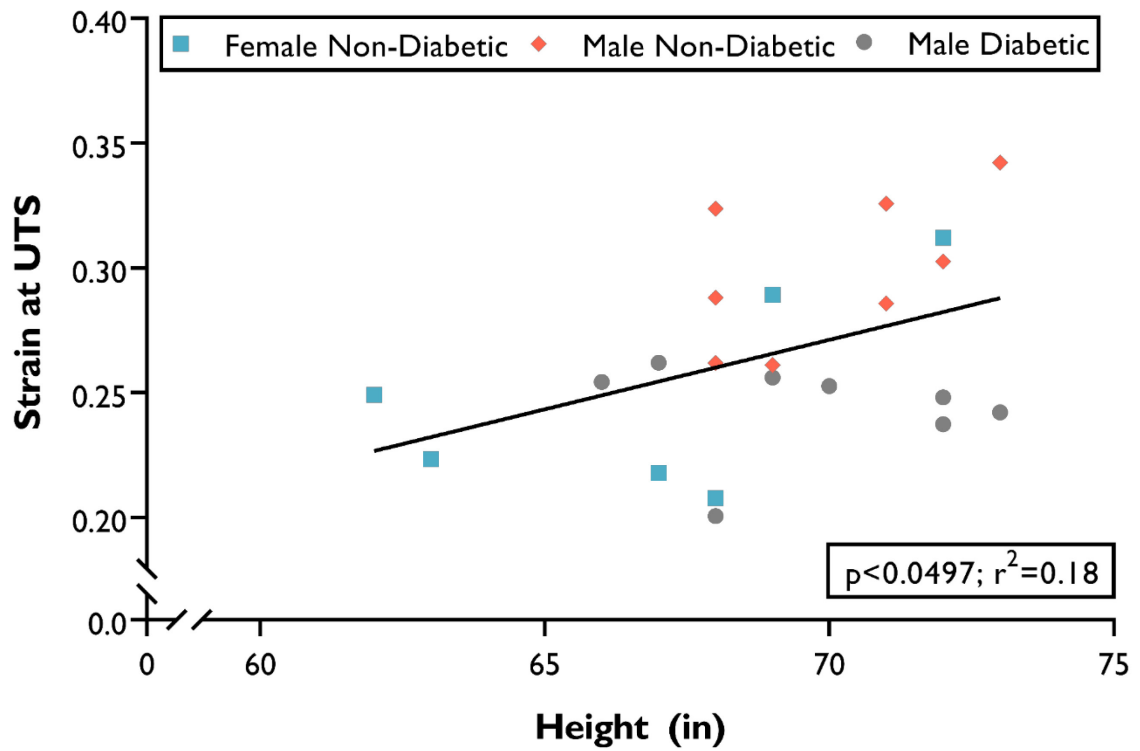


Figure A.4 Strain at UTS increased significantly with increasing height when pooling the entire sample population. Significant relationships were not found for any of the individual donor populations.

## Appendix B: Licenses for Copyrighted Material

---

**From:** Academic UK Non Rightslink  
**Sent:** July 23, 2019 8:17 AM  
**To:** Emile Feniyanos  
**Subject:** FW: Permission Request - Modifying Figure for Thesis

23 July 2019

Dear Emile Feniyanos ,

**Figure 27 from J. Kastelic, A. Galeski & E. Baer (1978) The Multicomposite Structure of Tendon, Connective Tissue Research, 6:1, 11-23, DOI: 10.3109/03008207809152283**

Thank you for your correspondence requesting permission to reproduce the above material from our Journal in your **printed thesis** "Age-, Sex-, and Diabetes-Determined Changes in the Structure and Mechanics of Human Sartorius Tendon Collagen" and to be posted in your university's repository - **Dalhousie University**.

We will be pleased to grant entirely free permission on the condition that you acknowledge the original source of publication and insert a reference to the Journal's web site: [www.tandfonline.com](http://www.tandfonline.com)

Please note that this licence **does not allow you to post our content on any third party websites or repositories**.

Thank you for your interest in our Journal.

With best wishes

Lee-Ann

**Lee-Ann Anderson** – Senior Permissions & Licensing Executive, Journals  
Routledge, Taylor & Francis Group  
3 Park Square, Milton Park, Abingdon, Oxon, OX14 4RN, UK.  
**Permissions Tel: +44 (0)20 7017 7617**  
**Permissions e-mail:** [permissionrequest@tandf.co.uk](mailto:permissionrequest@tandf.co.uk)  
Direct Tel: +44 (0)20 7017 7932  
Web: [www.tandfonline.com](http://www.tandfonline.com)  
e-mail: [lee-ann.anderson@tandf.co.uk](mailto:lee-ann.anderson@tandf.co.uk)



Taylor & Francis is a trading name of Informa UK Limited, registered in England under no. 1072954

[Information Classification: General](#)

---

**From:** Emile Feniyanos <[em903640@dal.ca](mailto:em903640@dal.ca)>  
**Sent:** 28 May 2019 21:14  
**To:** Academic UK Non Rightslink <[permissionrequest@tandf.co.uk](mailto:permissionrequest@tandf.co.uk)>  
**Subject:** Permission Request - Modifying Figure for Thesis

Hello,

[REDACTED]

The journal article of concern:

Title: The Multicomposite Structure of Tendon

Authors: J. Kastelic, A. Galeski & E. Baer

Journal: Connective Tissue Research

Year: 1978

Volume: 6

Issue: 1

DOI: <https://doi.org/10.3109/03008207809152283>

I was looking to modify Figure 27 on page 21. I've attached the modified image to this email.

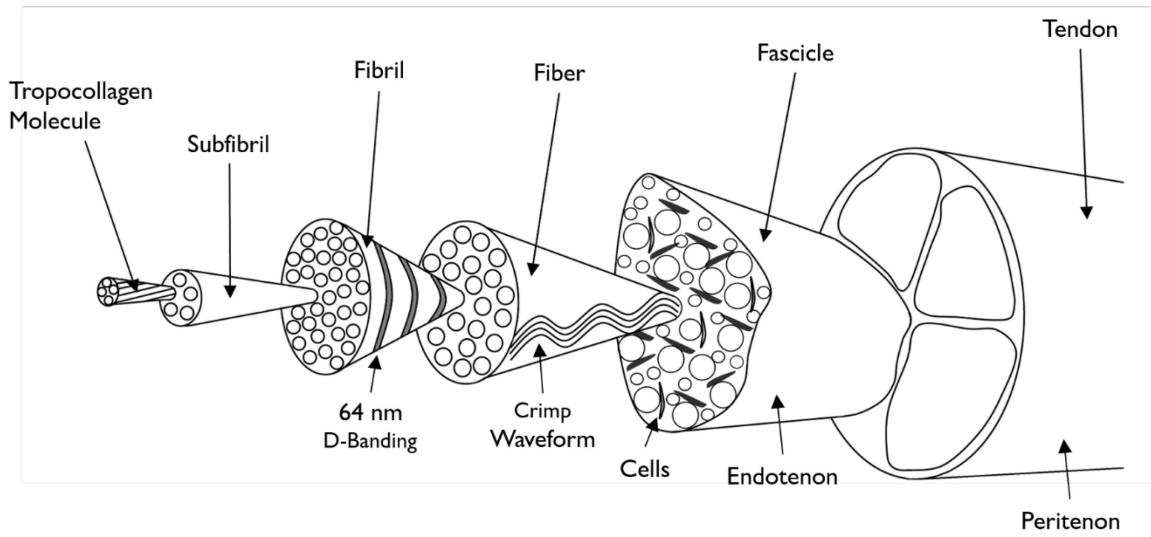
My thesis title: Age-, Sex-, and Diabetes-Determined Changes in the Structure and Mechanics of Human Sartorius Tendon Collagen.

Academic Institute: Dalhousie University



Thanks very much for any assistance,  
Emile

<Modified\_Figure\_27.tiff>



---

**From:** US Journal Permissions  
**Sent:** August 2, 2019 4:38 PM  
**To:** Emile Feniyanos  
**Subject:** RE: Request: Permission Inquiry

August 2, 2019

Dear Ms. Feniyanos,

**Material requested: Figure 1 in  
Jeremy D. Eekhoff, Fei Fang & Spencer P. Lake (2018)  
Multiscale mechanical effects of native collagen cross-linking in tendon,  
Connective Tissue Research, 59:5, 410-422, DOI: [10.1080/03008207.2018.1449837](https://doi.org/10.1080/03008207.2018.1449837)**

Thank you for your correspondence requesting permission to reproduce the above material from our Journal in your **printed thesis** and to be posted in your university's repository – **Dalhousie University**.

We will be pleased to grant entirely free permission on the condition that you acknowledge the original source of publication and insert a reference to the Journal's web site: [www.tandfonline.com](http://www.tandfonline.com)

Please note that this license **does not allow you to post our content on any third party websites or repositories**.

Thank you for your interest in our Journal.

Sincerely,

**Mary Ann Muller** – Permissions Coordinator, US Journals Division



Find digital versions of our articles on: [www.tandfonline.com](http://www.tandfonline.com) to use RightsLink, our online permissions web page, for immediate processing of your permission request.

**Please Note:** Permissions requests for US journals may take up to four weeks for processing due to demand.



**Taylor & Francis Group**  
an informa business

530 Walnut Street – 8<sup>th</sup> floor  
Philadelphia | PA | 19106 | United States of America  
**Direct line:** 215-606-4334



## SPRINGER NATURE LICENSE TERMS AND CONDITIONS

Jun 11, 2019

This Agreement between Dalhousie University -- Emile Feniyanos ("You") and Springer Nature ("Springer Nature") consists of your license details and the terms and conditions provided by Springer Nature and Copyright Clearance Center.

License Number	4606050527289
License date	Jun 11, 2019
Licensed Content Publisher	Springer Nature
Licensed Content Publication	Archiv für orthopädische und Unfall-Chirurgie, mit besonderer Berücksichtigung der Frakturenlehre und der orthopädisch-chirurgischen Technik
Licensed Content Title	Knickdeformationen an Kollagen
Licensed Content Author	Th. Nemetschek, R. Jonak, A. Meinel et al
Licensed Content Date	Jan 1, 1977
Licensed Content Volume	89
Licensed Content Issue	3
Type of Use	Thesis/Dissertation
Requestor type	academic/university or research institute
Format	print and electronic
Portion	figures/tables/illustrations
Number of figures/tables/illustrations	2
Will you be translating?	yes, without original language
Number of languages	1
Circulation/distribution	<501
Author of this Springer Nature content	no
Title	Age-, Sex-, and Diabetes-Determined Changes in the Structure and Mechanics of Human Sartorius Tendon Collagen.
Institution name	Dalhousie University
Expected presentation date	Jul 2019
Portions	Figure 1 on page 251. Figure 3 on page 253
Specific Languages	English
Requestor Location	Dalhousie University 5981 University Avenue  Halifax, NS B3H4R2 Canada Attn: Emile Feniyanos
Total	<b>0.00 CAD</b>
Terms and Conditions	

Springer Nature Terms and Conditions for RightsLink Permissions

**Springer Nature Customer Service Centre GmbH (the Licensor)** hereby grants you a non-exclusive, world-wide licence to reproduce the material and for the purpose and requirements specified in the attached copy of your order form, and for no other use, subject to the conditions below.

1. The Licensor warrants that it has, to the best of its knowledge, the rights to license reuse of this material. However, you should ensure that the material you are requesting is original to the Licensor and does not carry the copyright of another entity (as credited in the published version).

If the credit line on any part of the material you have requested indicates that it was reprinted or adapted with permission from another source, then you should also seek permission from that source to reuse the material.

2. Where **print only** permission has been granted for a fee, separate permission must be obtained for any additional electronic re-use.
3. Permission granted **free of charge** for material in print is also usually granted for any electronic version of that work, provided that the material is incidental to your work as a whole and that the electronic version is essentially equivalent to, or substitutes for, the print version.
4. A licence for 'post on a website' is valid for 12 months from the licence date. This licence does not cover use of full text articles on websites.
5. Where '**reuse in a dissertation/thesis**' has been selected the following terms apply: Print rights of the final author's accepted manuscript (for clarity, NOT the published version) for up to 100 copies, electronic rights for use only on a personal website or institutional repository as defined by the Sherpa guideline ([www.sherpa.ac.uk/romeo/](http://www.sherpa.ac.uk/romeo/)).
6. Permission granted for books and journals is granted for the lifetime of the first edition and does not apply to second and subsequent editions (except where the first edition permission was granted free of charge or for signatories to the STM Permissions Guidelines <http://www.stm-assoc.org/copyright-legal-affairs/permissions/permissions-guidelines/>), and does not apply for editions in other languages unless additional translation rights have been granted separately in the licence.
7. Rights for additional components such as custom editions and derivatives require additional permission and may be subject to an additional fee. Please apply to [Journalpermissions@springernature.com](mailto:Journalpermissions@springernature.com)/[bookpermissions@springernature.com](mailto:bookpermissions@springernature.com) for these rights.
8. The Licensor's permission must be acknowledged next to the licensed material in print. In electronic form, this acknowledgement must be visible at the same time as the figures/tables/illustrations or abstract, and must be hyperlinked to the journal/book's homepage. Our required acknowledgement format is in the Appendix below.
9. Use of the material for incidental promotional use, minor editing privileges (this does not include cropping, adapting, omitting material or any other changes that affect the meaning, intention or moral rights of the author) and copies for the disabled are permitted under this licence.
10. Minor adaptations of single figures (changes of format, colour and style) do not require the Licensor's approval. However, the adaptation should be credited as shown in Appendix below.

#### Appendix — Acknowledgements:

##### **For Journal Content:**

Reprinted by permission from [the Licensor]: [Journal Publisher (e.g. Nature/Springer/Palgrave)] [JOURNAL NAME] [REFERENCE CITATION (Article name, Author(s) Name), [COPYRIGHT] (year of publication)]

##### **For Advance Online Publication papers:**

Reprinted by permission from [the Licensor]: [Journal Publisher (e.g. Nature/Springer/Palgrave)] [JOURNAL

**NAME** [REFERENCE CITATION (Article name, Author(s) Name), [COPYRIGHT] (year of publication), advance online publication, day month year (doi: 10.1038/sj.[JOURNAL ACRONYM].)]

**For Adaptations/Translations:**

Adapted/Translated by permission from [the Licensor]: [Journal Publisher (e.g. Nature/Springer/Palgrave)] [JOURNAL NAME] [REFERENCE CITATION (Article name, Author(s) Name), [COPYRIGHT] (year of publication)]

**Note: For any republication from the British Journal of Cancer, the following credit line style applies:**

Reprinted/adapted/translated by permission from [the Licensor]: on behalf of Cancer Research UK: : [Journal Publisher (e.g. Nature/Springer/Palgrave)] [JOURNAL NAME] [REFERENCE CITATION (Article name, Author(s) Name), [COPYRIGHT] (year of publication)]

**For Advance Online Publication papers:**

Reprinted by permission from The [the Licensor]: on behalf of Cancer Research UK: [Journal Publisher (e.g. Nature/Springer/Palgrave)] [JOURNAL NAME] [REFERENCE CITATION (Article name, Author(s) Name), [COPYRIGHT] (year of publication), advance online publication, day month year (doi: 10.1038/sj.[JOURNAL ACRONYM])]

**For Book content:**

Reprinted/adapted by permission from [the Licensor]: [Book Publisher (e.g. Palgrave Macmillan, Springer etc)] [Book Title] by [Book author(s)] [COPYRIGHT] (year of publication)

**Other Conditions:**

Version 1.1

Questions? [customercare@copyright.com](mailto:customercare@copyright.com) or +1-855-239-3415 (toll free in the US) or +1-978-646-2777.

---

---



## ELSEVIER LICENSE TERMS AND CONDITIONS

Jul 24, 2019

This Agreement between Dalhousie University -- Emile Feniyanos ("You") and Elsevier ("Elsevier") consists of your license details and the terms and conditions provided by Elsevier and Copyright Clearance Center.

License Number	4616010497894
License date	Jun 25, 2019
Licensed Content Publisher	Elsevier
Licensed Content Publication	Biophysical Journal
Licensed Content Title	Designed to Fail: A Novel Mode of Collagen Fibril Disruption and Its Relevance to Tissue Toughness
Licensed Content Author	Samuel P. Veres, J. Michael Lee
Licensed Content Date	Jun 20, 2012
Licensed Content Volume	102
Licensed Content Issue	12
Licensed Content Pages	9
Start Page	2876
End Page	2884
Type of Use	reuse in a thesis/dissertation
Intended publisher of new work	other
Portion	figures/tables/illustrations
Number of figures/tables/illustrations	1
Format	both print and electronic
Are you the author of this Elsevier article?	No
Will you be translating?	No
Original figure numbers	Figure 3
Title of your thesis/dissertation	Age-, Sex-, and Diabetes-Determined Changes in the Structure and Mechanics of Human Sartorius Tendon Collagen.
Publisher of new work	Dalhousie University
Expected completion date	Jul 2019
Estimated size (number of pages)	1
Requestor Location	Dalhousie University 5981 University Avenue

Halifax, NS B3H4R2

Canada  
Attn: Emile Feniyanos  
GB 494 6272 12  
Publisher Tax ID  
Total **0.00 CAD**  
Terms and Conditions

#### INTRODUCTION

1. The publisher for this copyrighted material is Elsevier. By clicking "accept" in connection with completing this licensing transaction, you agree that the following terms and conditions apply to this transaction (along with the Billing and Payment terms and conditions established by Copyright Clearance Center, Inc. ("CCC"), at the time that you opened your Rightslink account and that are available at any time at <http://myaccount.copyright.com>).

#### GENERAL TERMS

2. Elsevier hereby grants you permission to reproduce the aforementioned material subject to the terms and conditions indicated.
3. Acknowledgement: If any part of the material to be used (for example, figures) has appeared in our publication with credit or acknowledgement to another source, permission must also be sought from that source. If such permission is not obtained then that material may not be included in your publication/copies. Suitable acknowledgement to the source must be made, either as a footnote or in a reference list at the end of your publication, as follows:  
"Reprinted from Publication title, Vol /edition number, Author(s), Title of article / title of chapter, Pages No., Copyright (Year), with permission from Elsevier [OR APPLICABLE SOCIETY COPYRIGHT OWNER]." Also Lancet special credit - "Reprinted from The Lancet, Vol. number, Author(s), Title of article, Pages No., Copyright (Year), with permission from Elsevier."
4. Reproduction of this material is confined to the purpose and/or media for which permission is hereby given.
5. Altering/Modifying Material: Not Permitted. However figures and illustrations may be altered/adapted minimally to serve your work. Any other abbreviations, additions, deletions and/or any other alterations shall be made only with prior written authorization of Elsevier Ltd. (Please contact Elsevier at [permissions@elsevier.com](mailto:permissions@elsevier.com)). No modifications can be made to any Lancet figures/tables and they must be reproduced in full.
6. If the permission fee for the requested use of our material is waived in this instance, please be advised that your future requests for Elsevier materials may attract a fee.
7. Reservation of Rights: Publisher reserves all rights not specifically granted in the combination of (i) the license details provided by you and accepted in the course of this licensing transaction, (ii) these terms and conditions and (iii) CCC's Billing and Payment terms and conditions.
8. License Contingent Upon Payment: While you may exercise the rights licensed immediately upon issuance of the license at the end of the licensing process for the transaction, provided that you have disclosed complete and accurate details of your proposed use, no license is finally effective unless and until full payment is received from you (either by publisher or by CCC) as provided in CCC's Billing and Payment terms and conditions. If full payment is not received on a timely basis, then any license preliminarily granted shall be deemed automatically revoked and shall be void as if never granted. Further, in the event that you breach any of these terms and conditions or any of CCC's Billing and Payment terms and conditions, the license is automatically revoked and shall be void as if never granted. Use of materials as described in a revoked license, as well as any use of the materials beyond the scope of an unrevoked license, may constitute copyright infringement and publisher reserves the right to take any and all action to protect its copyright in the materials.
9. Warranties: Publisher makes no representations or warranties with respect to the licensed material.
10. Indemnity: You hereby indemnify and agree to hold harmless publisher and CCC, and their respective officers, directors, employees and agents, from and against any and all claims arising out of your use of the licensed material other than as specifically authorized pursuant to this license.
11. No Transfer of License: This license is personal to you and may not be sublicensed, assigned, or transferred by you to any other person without publisher's written permission.
12. No Amendment Except in Writing: This license may not be amended except in a writing signed by both parties (or, in the case of publisher, by CCC on publisher's behalf).
13. Objection to Contrary Terms: Publisher hereby objects to any terms contained in any purchase order, acknowledgment, check endorsement or other writing prepared by you, which terms are inconsistent with these terms and conditions or CCC's Billing and Payment terms and conditions. These terms and conditions, together with CCC's Billing and Payment terms and conditions (which are incorporated herein), comprise the entire agreement between you and publisher (and CCC) concerning this licensing transaction. In the event of any conflict between your obligations established by these terms and conditions and those established by CCC's Billing and Payment terms and conditions, these terms and conditions shall control.

14. Revocation: Elsevier or Copyright Clearance Center may deny the permissions described in this License at their sole discretion, for any reason or no reason, with a full refund payable to you. Notice of such denial will be made using the contact information provided by you. Failure to receive such notice will not alter or invalidate the denial. In no event will Elsevier or Copyright Clearance Center be responsible or liable for any costs, expenses or damage incurred by you as a result of a denial of your permission request, other than a refund of the amount(s) paid by you to Elsevier and/or Copyright Clearance Center for denied permissions.

#### LIMITED LICENSE

The following terms and conditions apply only to specific license types:

15. **Translation:** This permission is granted for non-exclusive world **English** rights only unless your license was granted for translation rights. If you licensed translation rights you may only translate this content into the languages you requested. A professional translator must perform all translations and reproduce the content word for word preserving the integrity of the article.

16. **Posting licensed content on any Website:** The following terms and conditions apply as follows: Licensing material from an Elsevier journal: All content posted to the web site must maintain the copyright information line on the bottom of each image; A hyper-text must be included to the Homepage of the journal from which you are licensing at <http://www.sciencedirect.com/science/journal/xxxxx> or the Elsevier homepage for books at <http://www.elsevier.com>;

Central Storage: This license does not include permission for a scanned version of the material to be stored in a central repository such as that provided by Heron/XanEdu.

Licensing material from an Elsevier book: A hyper-text link must be included to the Elsevier homepage at <http://www.elsevier.com>. All content posted to the web site must maintain the copyright information line on the bottom of each image.

**Posting licensed content on Electronic reserve:** In addition to the above the following clauses are applicable: The web site must be password-protected and made available only to bona fide students registered on a relevant course. This permission is granted for 1 year only. You may obtain a new license for future website posting.

17. **For journal authors:** the following clauses are applicable in addition to the above:

#### Preprints:

A preprint is an author's own write-up of research results and analysis, it has not been peer-reviewed, nor has it had any other value added to it by a publisher (such as formatting, copyright, technical enhancement etc.).

Authors can share their preprints anywhere at any time. Preprints should not be added to or enhanced in any way in order to appear more like, or to substitute for, the final versions of articles however authors can update their preprints on arXiv or RePEc with their Accepted Author Manuscript (see below).

If accepted for publication, we encourage authors to link from the preprint to their formal publication via its DOI. Millions of researchers have access to the formal publications on ScienceDirect, and so links will help users to find, access, cite and use the best available version. Please note that Cell Press, The Lancet and some society-owned have different preprint policies. Information on these policies is available on the journal homepage.

**Accepted Author Manuscripts:** An accepted author manuscript is the manuscript of an article that has been accepted for publication and which typically includes author-incorporated changes suggested during submission, peer review and editor-author communications.

Authors can share their accepted author manuscript:

- immediately
  - via their non-commercial person homepage or blog
  - by updating a preprint in arXiv or RePEc with the accepted manuscript
  - via their research institute or institutional repository for internal institutional uses or as part of an invitation-only research collaboration work-group
  - directly by providing copies to their students or to research collaborators for their personal use
  - for private scholarly sharing as part of an invitation-only work group on commercial sites with which Elsevier has an agreement
- After the embargo period
  - via non-commercial hosting platforms such as their institutional repository
  - via commercial sites with which Elsevier has an agreement

In all cases accepted manuscripts should:

- link to the formal publication via its DOI
- bear a CC-BY-NC-ND license - this is easy to do

- if aggregated with other manuscripts, for example in a repository or other site, be shared in alignment with our hosting policy not be added to or enhanced in any way to appear more like, or to substitute for, the published journal article.

**Published journal article (JPA):** A published journal article (PJA) is the definitive final record of published research that appears or will appear in the journal and embodies all value-adding publishing activities including peer review coordination, copy-editing, formatting, (if relevant) pagination and online enrichment.

Policies for sharing publishing journal articles differ for subscription and gold open access articles:

**Subscription Articles:** If you are an author, please share a link to your article rather than the full-text. Millions of researchers have access to the formal publications on ScienceDirect, and so links will help your users to find, access, cite, and use the best available version.

Theses and dissertations which contain embedded PJAs as part of the formal submission can be posted publicly by the awarding institution with DOI links back to the formal publications on ScienceDirect.

If you are affiliated with a library that subscribes to ScienceDirect you have additional private sharing rights for others' research accessed under that agreement. This includes use for classroom teaching and internal training at the institution (including use in course packs and courseware programs), and inclusion of the article for grant funding purposes.

**Gold Open Access Articles:** May be shared according to the author-selected end-user license and should contain a [CrossMark logo](#), the end user license, and a DOI link to the formal publication on ScienceDirect.

Please refer to Elsevier's [posting policy](#) for further information.

18. **For book authors** the following clauses are applicable in addition to the above: Authors are permitted to place a brief summary of their work online only. You are not allowed to download and post the published electronic version of your chapter, nor may you scan the printed edition to create an electronic version. **Posting to a repository:** Authors are permitted to post a summary of their chapter only in their institution's repository.

19. **Thesis/Dissertation:** If your license is for use in a thesis/dissertation your thesis may be submitted to your institution in either print or electronic form. Should your thesis be published commercially, please reapply for permission. These requirements include permission for the Library and Archives of Canada to supply single copies, on demand, of the complete thesis and include permission for Proquest/UMI to supply single copies, on demand, of the complete thesis. Should your thesis be published commercially, please reapply for permission. Theses and dissertations which contain embedded PJAs as part of the formal submission can be posted publicly by the awarding institution with DOI links back to the formal publications on ScienceDirect.

#### **Elsevier Open Access Terms and Conditions**

You can publish open access with Elsevier in hundreds of open access journals or in nearly 2000 established subscription journals that support open access publishing. Permitted third party re-use of these open access articles is defined by the author's choice of Creative Commons user license. See our [open access license policy](#) for more information.

#### **Terms & Conditions applicable to all Open Access articles published with Elsevier:**

Any reuse of the article must not represent the author as endorsing the adaptation of the article nor should the article be modified in such a way as to damage the author's honour or reputation. If any changes have been made, such changes must be clearly indicated.

The author(s) must be appropriately credited and we ask that you include the end user license and a DOI link to the formal publication on ScienceDirect.

If any part of the material to be used (for example, figures) has appeared in our publication with credit or acknowledgement to another source it is the responsibility of the user to ensure their reuse complies with the terms and conditions determined by the rights holder.

#### **Additional Terms & Conditions applicable to each Creative Commons user license:**

**CC BY:** The CC-BY license allows users to copy, to create extracts, abstracts and new works from the Article, to alter and revise the Article and to make commercial use of the Article (including reuse and/or resale of the Article by commercial entities), provided the user gives appropriate credit (with a link to the formal publication through the relevant DOI), provides a link to the license, indicates if changes were made and the licensor is not represented as endorsing the use made of the work. The full details of the license are available at <http://creativecommons.org/licenses/by/4.0>.

**CC BY NC SA:** The CC BY-NC-SA license allows users to copy, to create extracts, abstracts and new works from the Article, to alter and revise the Article, provided this is not done for commercial purposes, and that the user gives appropriate credit (with a link to the formal publication through the relevant DOI), provides a link to the license, indicates if changes were made and the licensor is not represented as endorsing the use made of the work. Further, any new works must be made available on the same conditions. The full details of the license are available at <http://creativecommons.org/licenses/by-nc-sa/4.0>.

**CC BY NC ND:** The CC BY-NC-ND license allows users to copy and distribute the Article, provided this is not done for commercial purposes and further does not permit distribution of the Article if it is changed or edited in any way, and provided the user gives appropriate credit (with a link to the formal publication through the relevant DOI), provides a link to the license, and that the licensor is not represented as endorsing the use made of the work. The full details of the license are available at <http://creativecommons.org/licenses/by-nc-nd/4.0>. Any commercial reuse of Open Access articles published with a CC BY NC SA or CC BY NC ND license requires permission from Elsevier and will be subject to a fee.

Commercial reuse includes:

- Associating advertising with the full text of the Article
- Charging fees for document delivery or access
- Article aggregation
- Systematic distribution via e-mail lists or share buttons

Posting or linking by commercial companies for use by customers of those companies.

20. **Other Conditions:**

v1.9

Questions? [customercare@copyright.com](mailto:customercare@copyright.com) or +1-855-239-3415 (toll free in the US) or +1-978-646-2777.



## THE AMERICAN PHYSIOLOGICAL SOCIETY LICENSE TERMS AND CONDITIONS

Jun 11, 2019

This Agreement between Dalhousie University -- Emile Feniyanos ("You") and The American Physiological Society ("The American Physiological Society") consists of your license details and the terms and conditions provided by The American Physiological Society and Copyright Clearance Center.

License Number	4605991196829
License date	Jun 11, 2019
Licensed Content Publisher	The American Physiological Society
Licensed Content Publication	Journal of Applied Physiology
Licensed Content Title	Advanced glycation end-product cross-linking inhibits biomechanical plasticity and characteristic failure morphology of native tendon
Licensed Content Author	J. Michael Lee, Samuel P. Veres
Licensed Content Date	Apr 1, 2019
Licensed Content Volume	126
Licensed Content Issue	4
Type of Use	Thesis/Dissertation
Requestor type	non-profit academic/educational
Readers being charged a fee for this work	No
Format	print and electronic
Portion	figures/tables/images
Number of figures/tables/images	2
Will you be translating?	no
World Rights	no
Order reference number	
Title	Age-, Sex-, and Diabetes-Determined Changes in the Structure and Mechanics of Human Sartorius Tendon Collagen.
Institution name	Dalhousie University
Expected presentation date	Jul 2019
Portions	Figure 4 on page 835 Figure 7 on page 838
Requestor Location	Dalhousie University 5981 University Avenue  Halifax, NS B3H4R2 Canada Attn: Emile Feniyanos
Billing Type	Invoice

**Billing Address**

Dalhousie University  
5981 University Avenue

Halifax, NS B3H4R2  
Canada  
Attn: Emile Feniyanos

**Total****0.00 CAD****Terms and Conditions**

## Terms and Conditions:

©The American Physiological Society (APS). All rights reserved. The publisher for this requested copyrighted material is APS. By clicking "accept" in connection with completing this license transaction, you agree to the following terms and conditions that apply to this transaction. At the time you opened your Rightslink account you had agreed to the billing and payment terms and conditions established by Copyright Clearance Center (CCC) available at <http://myaccount.copyright.com>

The APS hereby grants to you a nonexclusive limited license to reuse published material as requested by you, provided you have disclosed complete and accurate details of your proposed reuse of articles, figures, tables, images, and /or data in new or derivative works. Licenses are for a one-time English language use with a maximum distribution equal to the number of copies identified by you in the licensing process, unless additional options for translations or World Rights were included in your request. Any form of print or electronic republication must be completed within three years from the date hereof. Copies prepared before then may be distributed thereafter

The following conditions are required for a License of Reuse:

**Attribution:** You must publish in your new or derivative work a citation to the original source of the material(s) being licensed herein, including publication name, author(s), volume, year, and page number prominently displayed in the article or within the figure/image legend.

**Abstracts:** APS Journal article abstracts may be reproduced or translated for noncommercial purposes without requesting permission, provided the citation to the original source of the materials is included as noted above ("Attribution"). Abstracts or portions of abstracts may not be used in advertisements or commercial promotions.

**Non-profit/noncommercial reuse:** APS grants permission for the free reuse of APS published material in new works published for educational purposes, provided there is no charge or fee for the new work and/or the work is not directly or indirectly commercially supported or sponsored. Neither original authors nor non-authors may reuse published material in new works that are commercially supported or sponsored including reuse in a work produced by a commercial publisher without seeking permission.

**Video and photographs:** Some material published in APS publications may belong to other copyright holders and cannot be republished without their permission. The copyright holder of photographs must be ascertained from the original source by the permission requestor. Videos and podcasts may not be rebroadcast without proper attribution and permission as requested here. For further inquiries on reuse of these types of materials, please contact [cvillemez@the-aps.org](mailto:cvillemez@the-aps.org)

**Figures/Tables/Images** are available to the requestor from the APS journals website at <http://www.the-aps.org/publications/journals/>. The obtaining of content is a separate transaction and does not involve Rightslink or CCC, and is the responsibility of the permission seeker. Higher resolution images are available at additional charge from APS; please contact [cvillemez@the-aps.org](mailto:cvillemez@the-aps.org)

**Original Authors of Published Works:** To see a full list of original authors rights concerning their own published work <http://www.the-aps.org/publications/authorinfo/copyright.htm>

Content reuse rights awarded by the APS may be exercised immediately upon issuance of this license, provided full disclosure and complete and accurate details of the proposed reuse have been made; no license is finally granted unless and until full payment is received either by the publisher or by CCC as provided in CCC's Billing and Payment Terms and Conditions. If full payment is not received on a timely basis, then any license preliminarily granted shall be deemed automatically revoked and shall be void as if never granted. Further, in the event that you breach any of these Terms and Conditions or any of CCC's Billing and Payment Terms and Conditions, the license is automatically revoked and shall be void as if never granted. Use of materials as described in a revoked license, as well as any use of the materials beyond the scope of the license, may constitute copyright infringement and the Publisher reserves the right to take action to protect its copyright of its materials.

The APS makes no representations or warranties with respect to the licensed material. You hereby indemnify and agree to hold harmless the publisher and CCC, and their respective officers, directors, employees and agents, from and

against any and all claims arising out of your use of the licensed material other than as specifically authorized pursuant to this license.

This license is personal to you /your organization and may not be sublicensed, assigned, or transferred by you /your organization to another person /organization without the publisher's permission. This license may not be amended except in writing signed by both parties, or in the case of the publisher, by CCC on the publisher's behalf.

The APS reserves all rights not specifically granted in the combination of (i) the license details provided by you and accepted in the course of this licensing transaction, (ii) these Terms and Conditions and (iii) CCC's Billing and Payment Terms and Conditions.

v1.0

Questions? [customercare@copyright.com](mailto:customercare@copyright.com) or +1-855-239-3415 (toll free in the US) or +1-978-646-2777.

---

---



## ELSEVIER LICENSE TERMS AND CONDITIONS

Jun 11, 2019

This Agreement between Dalhousie University -- Emile Feniyanos ("You") and Elsevier ("Elsevier") consists of your license details and the terms and conditions provided by Elsevier and Copyright Clearance Center.

License Number	4597841133089
License date	May 28, 2019
Licensed Content Publisher	Elsevier
Licensed Content Publication	Journal of the Mechanical Behavior of Biomedical Materials
Licensed Content Title	Characterization via atomic force microscopy of discrete plasticity in collagen fibrils from mechanically overloaded tendons: Nano-scale structural changes mimic rope failure
Licensed Content Author	Samuel J. Baldwin, Laurent Kreplak, J. Michael Lee
Licensed Content Date	Jul 1, 2016
Licensed Content Volume	60
Licensed Content Issue	n/a
Licensed Content Pages	11
Start Page	356
End Page	366
Type of Use	reuse in a thesis/dissertation
Portion	figures/tables/illustrations
Number of figures/tables/illustrations	1
Format	both print and electronic
Are you the author of this Elsevier article?	No
Will you be translating?	No
Original figure numbers	Figure 9 on page 363
Title of your thesis/dissertation	Age-, Sex-, and Diabetes-Determined Changes in the Structure and Mechanics of Human Sartorius Tendon Collagen.
Publisher of new work	Dalhousie University
Expected completion date	Jul 2019
Estimated size (number of pages)	1
Requestor Location	Dalhousie University 5981 University Avenue  Halifax, NS B3H4R2 Canada Attn: Emile Feniyanos

Publisher Tax ID GB 494 6272 12  
Total **0.00 CAD**  
Terms and Conditions

#### INTRODUCTION

1. The publisher for this copyrighted material is Elsevier. By clicking "accept" in connection with completing this licensing transaction, you agree that the following terms and conditions apply to this transaction (along with the Billing and Payment terms and conditions established by Copyright Clearance Center, Inc. ("CCC"), at the time that you opened your Rightslink account and that are available at any time at <http://myaccount.copyright.com>).

#### GENERAL TERMS

2. Elsevier hereby grants you permission to reproduce the aforementioned material subject to the terms and conditions indicated.
3. Acknowledgement: If any part of the material to be used (for example, figures) has appeared in our publication with credit or acknowledgement to another source, permission must also be sought from that source. If such permission is not obtained then that material may not be included in your publication/copies. Suitable acknowledgement to the source must be made, either as a footnote or in a reference list at the end of your publication, as follows:  
"Reprinted from Publication title, Vol /edition number, Author(s), Title of article / title of chapter, Pages No., Copyright (Year), with permission from Elsevier [OR APPLICABLE SOCIETY COPYRIGHT OWNER]." Also Lancet special credit - "Reprinted from The Lancet, Vol. number, Author(s), Title of article, Pages No., Copyright (Year), with permission from Elsevier."
4. Reproduction of this material is confined to the purpose and/or media for which permission is hereby given.
5. Altering/Modifying Material: Not Permitted. However figures and illustrations may be altered/adapted minimally to serve your work. Any other abbreviations, additions, deletions and/or any other alterations shall be made only with prior written authorization of Elsevier Ltd. (Please contact Elsevier at [permissions@elsevier.com](mailto:permissions@elsevier.com)). No modifications can be made to any Lancet figures/tables and they must be reproduced in full.
6. If the permission fee for the requested use of our material is waived in this instance, please be advised that your future requests for Elsevier materials may attract a fee.
7. Reservation of Rights: Publisher reserves all rights not specifically granted in the combination of (i) the license details provided by you and accepted in the course of this licensing transaction, (ii) these terms and conditions and (iii) CCC's Billing and Payment terms and conditions.
8. License Contingent Upon Payment: While you may exercise the rights licensed immediately upon issuance of the license at the end of the licensing process for the transaction, provided that you have disclosed complete and accurate details of your proposed use, no license is finally effective unless and until full payment is received from you (either by publisher or by CCC) as provided in CCC's Billing and Payment terms and conditions. If full payment is not received on a timely basis, then any license preliminarily granted shall be deemed automatically revoked and shall be void as if never granted. Further, in the event that you breach any of these terms and conditions or any of CCC's Billing and Payment terms and conditions, the license is automatically revoked and shall be void as if never granted. Use of materials as described in a revoked license, as well as any use of the materials beyond the scope of an unrevoked license, may constitute copyright infringement and publisher reserves the right to take any and all action to protect its copyright in the materials.
9. Warranties: Publisher makes no representations or warranties with respect to the licensed material.
10. Indemnity: You hereby indemnify and agree to hold harmless publisher and CCC, and their respective officers, directors, employees and agents, from and against any and all claims arising out of your use of the licensed material other than as specifically authorized pursuant to this license.
11. No Transfer of License: This license is personal to you and may not be sublicensed, assigned, or transferred by you to any other person without publisher's written permission.
12. No Amendment Except in Writing: This license may not be amended except in a writing signed by both parties (or, in the case of publisher, by CCC on publisher's behalf).
13. Objection to Contrary Terms: Publisher hereby objects to any terms contained in any purchase order, acknowledgment, check endorsement or other writing prepared by you, which terms are inconsistent with these terms and conditions or CCC's Billing and Payment terms and conditions. These terms and conditions, together with CCC's Billing and Payment terms and conditions (which are incorporated herein), comprise the entire agreement between you and publisher (and CCC) concerning this licensing transaction. In the event of any conflict between your obligations established by these terms and conditions and those established by CCC's Billing and Payment terms and conditions, these terms and conditions shall control.
14. Revocation: Elsevier or Copyright Clearance Center may deny the permissions described in this License at their sole discretion, for any reason or no reason, with a full refund payable to you. Notice of such denial will be made using the

contact information provided by you. Failure to receive such notice will not alter or invalidate the denial. In no event will Elsevier or Copyright Clearance Center be responsible or liable for any costs, expenses or damage incurred by you as a result of a denial of your permission request, other than a refund of the amount(s) paid by you to Elsevier and/or Copyright Clearance Center for denied permissions.

#### LIMITED LICENSE

The following terms and conditions apply only to specific license types:

15. **Translation:** This permission is granted for non-exclusive world **English** rights only unless your license was granted for translation rights. If you licensed translation rights you may only translate this content into the languages you requested. A professional translator must perform all translations and reproduce the content word for word preserving the integrity of the article.

16. **Posting licensed content on any Website:** The following terms and conditions apply as follows: Licensing material from an Elsevier journal: All content posted to the web site must maintain the copyright information line on the bottom of each image; A hyper-text must be included to the Homepage of the journal from which you are licensing at <http://www.sciencedirect.com/science/journal/xxxx> or the Elsevier homepage for books at <http://www.elsevier.com>;

Central Storage: This license does not include permission for a scanned version of the material to be stored in a central repository such as that provided by Heron/XanEdu.

Licensing material from an Elsevier book: A hyper-text link must be included to the Elsevier homepage at <http://www.elsevier.com>. All content posted to the web site must maintain the copyright information line on the bottom of each image.

**Posting licensed content on Electronic reserve:** In addition to the above the following clauses are applicable: The web site must be password-protected and made available only to bona fide students registered on a relevant course. This permission is granted for 1 year only. You may obtain a new license for future website posting.

17. **For journal authors:** the following clauses are applicable in addition to the above:

#### Preprints:

A preprint is an author's own write-up of research results and analysis, it has not been peer-reviewed, nor has it had any other value added to it by a publisher (such as formatting, copyright, technical enhancement etc.).

Authors can share their preprints anywhere at any time. Preprints should not be added to or enhanced in any way in order to appear more like, or to substitute for, the final versions of articles however authors can update their preprints on arXiv or RePEc with their Accepted Author Manuscript (see below).

If accepted for publication, we encourage authors to link from the preprint to their formal publication via its DOI. Millions of researchers have access to the formal publications on ScienceDirect, and so links will help users to find, access, cite and use the best available version. Please note that Cell Press, The Lancet and some society-owned have different preprint policies. Information on these policies is available on the journal homepage.

**Accepted Author Manuscripts:** An accepted author manuscript is the manuscript of an article that has been accepted for publication and which typically includes author-incorporated changes suggested during submission, peer review and editor-author communications.

Authors can share their accepted author manuscript:

- immediately
  - via their non-commercial person homepage or blog
  - by updating a preprint in arXiv or RePEc with the accepted manuscript
  - via their research institute or institutional repository for internal institutional uses or as part of an invitation-only research collaboration work-group
  - directly by providing copies to their students or to research collaborators for their personal use
  - for private scholarly sharing as part of an invitation-only work group on commercial sites with which Elsevier has an agreement
- After the embargo period
  - via non-commercial hosting platforms such as their institutional repository
  - via commercial sites with which Elsevier has an agreement

In all cases accepted manuscripts should:

- link to the formal publication via its DOI
- bear a CC-BY-NC-ND license - this is easy to do

- if aggregated with other manuscripts, for example in a repository or other site, be shared in alignment with our hosting policy not be added to or enhanced in any way to appear more like, or to substitute for, the published journal article.

**Published journal article (JPA):** A published journal article (PJA) is the definitive final record of published research that appears or will appear in the journal and embodies all value-adding publishing activities including peer review coordination, copy-editing, formatting, (if relevant) pagination and online enrichment.

Policies for sharing publishing journal articles differ for subscription and gold open access articles:

**Subscription Articles:** If you are an author, please share a link to your article rather than the full-text. Millions of researchers have access to the formal publications on ScienceDirect, and so links will help your users to find, access, cite, and use the best available version.

Theses and dissertations which contain embedded PJAs as part of the formal submission can be posted publicly by the awarding institution with DOI links back to the formal publications on ScienceDirect.

If you are affiliated with a library that subscribes to ScienceDirect you have additional private sharing rights for others' research accessed under that agreement. This includes use for classroom teaching and internal training at the institution (including use in course packs and courseware programs), and inclusion of the article for grant funding purposes.

**Gold Open Access Articles:** May be shared according to the author-selected end-user license and should contain a [CrossMark logo](#), the end user license, and a DOI link to the formal publication on ScienceDirect.

Please refer to Elsevier's [posting policy](#) for further information.

18. **For book authors** the following clauses are applicable in addition to the above: Authors are permitted to place a brief summary of their work online only. You are not allowed to download and post the published electronic version of your chapter, nor may you scan the printed edition to create an electronic version. **Posting to a repository:** Authors are permitted to post a summary of their chapter only in their institution's repository.

19. **Thesis/Dissertation:** If your license is for use in a thesis/dissertation your thesis may be submitted to your institution in either print or electronic form. Should your thesis be published commercially, please reapply for permission. These requirements include permission for the Library and Archives of Canada to supply single copies, on demand, of the complete thesis and include permission for Proquest/UML to supply single copies, on demand, of the complete thesis. Should your thesis be published commercially, please reapply for permission. Theses and dissertations which contain embedded PJAs as part of the formal submission can be posted publicly by the awarding institution with DOI links back to the formal publications on ScienceDirect.

#### **Elsevier Open Access Terms and Conditions**

You can publish open access with Elsevier in hundreds of open access journals or in nearly 2000 established subscription journals that support open access publishing. Permitted third party re-use of these open access articles is defined by the author's choice of Creative Commons user license. See our [open access license policy](#) for more information.

#### **Terms & Conditions applicable to all Open Access articles published with Elsevier:**

Any reuse of the article must not represent the author as endorsing the adaptation of the article nor should the article be modified in such a way as to damage the author's honour or reputation. If any changes have been made, such changes must be clearly indicated.

The author(s) must be appropriately credited and we ask that you include the end user license and a DOI link to the formal publication on ScienceDirect.

If any part of the material to be used (for example, figures) has appeared in our publication with credit or acknowledgement to another source it is the responsibility of the user to ensure their reuse complies with the terms and conditions determined by the rights holder.

#### **Additional Terms & Conditions applicable to each Creative Commons user license:**

**CC BY:** The CC-BY license allows users to copy, to create extracts, abstracts and new works from the Article, to alter and revise the Article and to make commercial use of the Article (including reuse and/or resale of the Article by commercial entities), provided the user gives appropriate credit (with a link to the formal publication through the relevant DOI), provides a link to the license, indicates if changes were made and the licensor is not represented as endorsing the use made of the work. The full details of the license are available at <http://creativecommons.org/licenses/by/4.0>.

**CC BY NC SA:** The CC BY-NC-SA license allows users to copy, to create extracts, abstracts and new works from the Article, to alter and revise the Article, provided this is not done for commercial purposes, and that the user gives appropriate credit (with a link to the formal publication through the relevant DOI), provides a link to the license, indicates if changes were made and the licensor is not represented as endorsing the use made of the work. Further, any new works must be made available on the same conditions. The full details of the license are available at <http://creativecommons.org/licenses/by-nc-sa/4.0>.

**CC BY NC ND:** The CC BY-NC-ND license allows users to copy and distribute the Article, provided this is not done for commercial purposes and further does not permit distribution of the Article if it is changed or edited in any way, and provided the user gives appropriate credit (with a link to the formal publication through the relevant DOI), provides a link to the license, and that the licensor is not represented as endorsing the use made of the work. The full details of the license are available at <http://creativecommons.org/licenses/by-nc-nd/4.0>. Any commercial reuse of Open Access articles published with a CC BY NC SA or CC BY NC ND license requires permission from Elsevier and will be subject to a fee.

Commercial reuse includes:

- Associating advertising with the full text of the Article
- Charging fees for document delivery or access
- Article aggregation
- Systematic distribution via e-mail lists or share buttons

Posting or linking by commercial companies for use by customers of those companies.

20. **Other Conditions:**

v1.9

Questions? [customercare@copyright.com](mailto:customercare@copyright.com) or +1-855-239-3415 (toll free in the US) or +1-978-646-2777.

---

---

## ELSEVIER LICENSE TERMS AND CONDITIONS

Jul 24, 2019

This Agreement between Dalhousie University -- Emile Feniyanos ("You") and Elsevier ("Elsevier") consists of your license details and the terms and conditions provided by Elsevier and Copyright Clearance Center.

License Number	4616090840193
License date	Jun 25, 2019
Licensed Content Publisher	Elsevier
Licensed Content Publication	Journal of the Mechanical Behavior of Biomedical Materials
Licensed Content Title	MMP-9 selectively cleaves non-D-banded material on collagen fibrils with discrete plasticity damage in mechanically-overloaded tendon
Licensed Content Author	Samuel.J. Baldwin, Laurent Kreplak, J. Michael. Lee
Licensed Content Date	Jul 1, 2019
Licensed Content Volume	95
Licensed Content Issue	n/a
Licensed Content Pages	9
Start Page	67
End Page	75
Type of Use	reuse in a thesis/dissertation
Portion	figures/tables/illustrations
Number of figures/tables/illustrations	1
Format	both print and electronic
Are you the author of this Elsevier article?	No
Will you be translating?	No
Original figure numbers	Figure 7
Title of your thesis/dissertation	Age-, Sex-, and Diabetes-Determined Changes in the Structure and Mechanics of Human Sartorius Tendon Collagen.
Publisher of new work	Dalhousie University
Expected completion date	Jul 2019
Estimated size (number of pages)	1
Requestor Location	Dalhousie University 5981 University Avenue  Halifax, NS B3H4R2 Canada Attn: Emile Feniyanos

Publisher Tax ID GB 494 6272 12  
Total **0.00 CAD**  
Terms and Conditions

#### INTRODUCTION

1. The publisher for this copyrighted material is Elsevier. By clicking "accept" in connection with completing this licensing transaction, you agree that the following terms and conditions apply to this transaction (along with the Billing and Payment terms and conditions established by Copyright Clearance Center, Inc. ("CCC"), at the time that you opened your Rightslink account and that are available at any time at <http://myaccount.copyright.com>).

#### GENERAL TERMS

2. Elsevier hereby grants you permission to reproduce the aforementioned material subject to the terms and conditions indicated.
3. Acknowledgement: If any part of the material to be used (for example, figures) has appeared in our publication with credit or acknowledgement to another source, permission must also be sought from that source. If such permission is not obtained then that material may not be included in your publication/copies. Suitable acknowledgement to the source must be made, either as a footnote or in a reference list at the end of your publication, as follows:  
"Reprinted from Publication title, Vol /edition number, Author(s), Title of article / title of chapter, Pages No., Copyright (Year), with permission from Elsevier [OR APPLICABLE SOCIETY COPYRIGHT OWNER]." Also Lancet special credit - "Reprinted from The Lancet, Vol. number, Author(s), Title of article, Pages No., Copyright (Year), with permission from Elsevier."
4. Reproduction of this material is confined to the purpose and/or media for which permission is hereby given.
5. Altering/Modifying Material: Not Permitted. However figures and illustrations may be altered/adapted minimally to serve your work. Any other abbreviations, additions, deletions and/or any other alterations shall be made only with prior written authorization of Elsevier Ltd. (Please contact Elsevier at [permissions@elsevier.com](mailto:permissions@elsevier.com)). No modifications can be made to any Lancet figures/tables and they must be reproduced in full.
6. If the permission fee for the requested use of our material is waived in this instance, please be advised that your future requests for Elsevier materials may attract a fee.
7. Reservation of Rights: Publisher reserves all rights not specifically granted in the combination of (i) the license details provided by you and accepted in the course of this licensing transaction, (ii) these terms and conditions and (iii) CCC's Billing and Payment terms and conditions.
8. License Contingent Upon Payment: While you may exercise the rights licensed immediately upon issuance of the license at the end of the licensing process for the transaction, provided that you have disclosed complete and accurate details of your proposed use, no license is finally effective unless and until full payment is received from you (either by publisher or by CCC) as provided in CCC's Billing and Payment terms and conditions. If full payment is not received on a timely basis, then any license preliminarily granted shall be deemed automatically revoked and shall be void as if never granted. Further, in the event that you breach any of these terms and conditions or any of CCC's Billing and Payment terms and conditions, the license is automatically revoked and shall be void as if never granted. Use of materials as described in a revoked license, as well as any use of the materials beyond the scope of an unrevoked license, may constitute copyright infringement and publisher reserves the right to take any and all action to protect its copyright in the materials.
9. Warranties: Publisher makes no representations or warranties with respect to the licensed material.
10. Indemnity: You hereby indemnify and agree to hold harmless publisher and CCC, and their respective officers, directors, employees and agents, from and against any and all claims arising out of your use of the licensed material other than as specifically authorized pursuant to this license.
11. No Transfer of License: This license is personal to you and may not be sublicensed, assigned, or transferred by you to any other person without publisher's written permission.
12. No Amendment Except in Writing: This license may not be amended except in a writing signed by both parties (or, in the case of publisher, by CCC on publisher's behalf).
13. Objection to Contrary Terms: Publisher hereby objects to any terms contained in any purchase order, acknowledgment, check endorsement or other writing prepared by you, which terms are inconsistent with these terms and conditions or CCC's Billing and Payment terms and conditions. These terms and conditions, together with CCC's Billing and Payment terms and conditions (which are incorporated herein), comprise the entire agreement between you and publisher (and CCC) concerning this licensing transaction. In the event of any conflict between your obligations established by these terms and conditions and those established by CCC's Billing and Payment terms and conditions, these terms and conditions shall control.
14. Revocation: Elsevier or Copyright Clearance Center may deny the permissions described in this License at their sole discretion, for any reason or no reason, with a full refund payable to you. Notice of such denial will be made using the

contact information provided by you. Failure to receive such notice will not alter or invalidate the denial. In no event will Elsevier or Copyright Clearance Center be responsible or liable for any costs, expenses or damage incurred by you as a result of a denial of your permission request, other than a refund of the amount(s) paid by you to Elsevier and/or Copyright Clearance Center for denied permissions.

#### LIMITED LICENSE

The following terms and conditions apply only to specific license types:

15. **Translation:** This permission is granted for non-exclusive world **English** rights only unless your license was granted for translation rights. If you licensed translation rights you may only translate this content into the languages you requested. A professional translator must perform all translations and reproduce the content word for word preserving the integrity of the article.

16. **Posting licensed content on any Website:** The following terms and conditions apply as follows: Licensing material from an Elsevier journal: All content posted to the web site must maintain the copyright information line on the bottom of each image; A hyper-text must be included to the Homepage of the journal from which you are licensing at <http://www.sciencedirect.com/science/journal/xxxx> or the Elsevier homepage for books at <http://www.elsevier.com>;

Central Storage: This license does not include permission for a scanned version of the material to be stored in a central repository such as that provided by Heron/XanEdu.

Licensing material from an Elsevier book: A hyper-text link must be included to the Elsevier homepage at <http://www.elsevier.com>. All content posted to the web site must maintain the copyright information line on the bottom of each image.

**Posting licensed content on Electronic reserve:** In addition to the above the following clauses are applicable: The web site must be password-protected and made available only to bona fide students registered on a relevant course. This permission is granted for 1 year only. You may obtain a new license for future website posting.

17. **For journal authors:** the following clauses are applicable in addition to the above:

#### Preprints:

A preprint is an author's own write-up of research results and analysis, it has not been peer-reviewed, nor has it had any other value added to it by a publisher (such as formatting, copyright, technical enhancement etc.).

Authors can share their preprints anywhere at any time. Preprints should not be added to or enhanced in any way in order to appear more like, or to substitute for, the final versions of articles however authors can update their preprints on arXiv or RePEc with their Accepted Author Manuscript (see below).

If accepted for publication, we encourage authors to link from the preprint to their formal publication via its DOI. Millions of researchers have access to the formal publications on ScienceDirect, and so links will help users to find, access, cite and use the best available version. Please note that Cell Press, The Lancet and some society-owned have different preprint policies. Information on these policies is available on the journal homepage.

**Accepted Author Manuscripts:** An accepted author manuscript is the manuscript of an article that has been accepted for publication and which typically includes author-incorporated changes suggested during submission, peer review and editor-author communications.

Authors can share their accepted author manuscript:

- immediately
  - via their non-commercial person homepage or blog
  - by updating a preprint in arXiv or RePEc with the accepted manuscript
  - via their research institute or institutional repository for internal institutional uses or as part of an invitation-only research collaboration work-group
  - directly by providing copies to their students or to research collaborators for their personal use
  - for private scholarly sharing as part of an invitation-only work group on commercial sites with which Elsevier has an agreement
- After the embargo period
  - via non-commercial hosting platforms such as their institutional repository
  - via commercial sites with which Elsevier has an agreement

In all cases accepted manuscripts should:

- link to the formal publication via its DOI
- bear a CC-BY-NC-ND license - this is easy to do



- if aggregated with other manuscripts, for example in a repository or other site, be shared in alignment with our hosting policy not be added to or enhanced in any way to appear more like, or to substitute for, the published journal article.

**Published journal article (JPA):** A published journal article (PJA) is the definitive final record of published research that appears or will appear in the journal and embodies all value-adding publishing activities including peer review co-ordination, copy-editing, formatting, (if relevant) pagination and online enrichment.

Policies for sharing publishing journal articles differ for subscription and gold open access articles:

**Subscription Articles:** If you are an author, please share a link to your article rather than the full-text. Millions of researchers have access to the formal publications on ScienceDirect, and so links will help your users to find, access, cite, and use the best available version.

Theses and dissertations which contain embedded PJAs as part of the formal submission can be posted publicly by the awarding institution with DOI links back to the formal publications on ScienceDirect.

If you are affiliated with a library that subscribes to ScienceDirect you have additional private sharing rights for others' research accessed under that agreement. This includes use for classroom teaching and internal training at the institution (including use in course packs and courseware programs), and inclusion of the article for grant funding purposes.

**Gold Open Access Articles:** May be shared according to the author-selected end-user license and should contain a [CrossMark logo](#), the end user license, and a DOI link to the formal publication on ScienceDirect.

Please refer to Elsevier's [posting policy](#) for further information.

18. **For book authors** the following clauses are applicable in addition to the above: Authors are permitted to place a brief summary of their work online only. You are not allowed to download and post the published electronic version of your chapter, nor may you scan the printed edition to create an electronic version. **Posting to a repository:** Authors are permitted to post a summary of their chapter only in their institution's repository.

19. **Thesis/Dissertation:** If your license is for use in a thesis/dissertation your thesis may be submitted to your institution in either print or electronic form. Should your thesis be published commercially, please reapply for permission. These requirements include permission for the Library and Archives of Canada to supply single copies, on demand, of the complete thesis and include permission for Proquest/UML to supply single copies, on demand, of the complete thesis. Should your thesis be published commercially, please reapply for permission. Theses and dissertations which contain embedded PJAs as part of the formal submission can be posted publicly by the awarding institution with DOI links back to the formal publications on ScienceDirect.

#### **Elsevier Open Access Terms and Conditions**

You can publish open access with Elsevier in hundreds of open access journals or in nearly 2000 established subscription journals that support open access publishing. Permitted third party re-use of these open access articles is defined by the author's choice of Creative Commons user license. See our [open access license policy](#) for more information.

#### **Terms & Conditions applicable to all Open Access articles published with Elsevier:**

Any reuse of the article must not represent the author as endorsing the adaptation of the article nor should the article be modified in such a way as to damage the author's honour or reputation. If any changes have been made, such changes must be clearly indicated.

The author(s) must be appropriately credited and we ask that you include the end user license and a DOI link to the formal publication on ScienceDirect.

If any part of the material to be used (for example, figures) has appeared in our publication with credit or acknowledgement to another source it is the responsibility of the user to ensure their reuse complies with the terms and conditions determined by the rights holder.

#### **Additional Terms & Conditions applicable to each Creative Commons user license:**

**CC BY:** The CC-BY license allows users to copy, to create extracts, abstracts and new works from the Article, to alter and revise the Article and to make commercial use of the Article (including reuse and/or resale of the Article by commercial entities), provided the user gives appropriate credit (with a link to the formal publication through the relevant DOI), provides a link to the license, indicates if changes were made and the licensor is not represented as endorsing the use made of the work. The full details of the license are available at <http://creativecommons.org/licenses/by/4.0>.

**CC BY NC SA:** The CC BY-NC-SA license allows users to copy, to create extracts, abstracts and new works from the Article, to alter and revise the Article, provided this is not done for commercial purposes, and that the user gives appropriate credit (with a link to the formal publication through the relevant DOI), provides a link to the license, indicates if changes were made and the licensor is not represented as endorsing the use made of the work. Further, any new works must be made available on the same conditions. The full details of the license are available at <http://creativecommons.org/licenses/by-nc-sa/4.0>.

**CC BY NC ND:** The CC BY-NC-ND license allows users to copy and distribute the Article, provided this is not done for commercial purposes and further does not permit distribution of the Article if it is changed or edited in any way, and provided the user gives appropriate credit (with a link to the formal publication through the relevant DOI), provides a link to the license, and that the licensor is not represented as endorsing the use made of the work. The full details of the license are available at <http://creativecommons.org/licenses/by-nc-nd/4.0>. Any commercial reuse of Open Access articles published with a CC BY NC SA or CC BY NC ND license requires permission from Elsevier and will be subject to a fee.

Commercial reuse includes:

- Associating advertising with the full text of the Article
- Charging fees for document delivery or access
- Article aggregation
- Systematic distribution via e-mail lists or share buttons

Posting or linking by commercial companies for use by customers of those companies.

20. **Other Conditions:**

v1.9

Questions? [customercare@copyright.com](mailto:customercare@copyright.com) or +1-855-239-3415 (toll free in the US) or +1-978-646-2777.

---

---

**ELSEVIER LICENSE  
TERMS AND CONDITIONS**

Jul 24, 2019

---

This Agreement between Dalhousie University -- Emile Feniyanos ("You") and Elsevier ("Elsevier") consists of your license details and the terms and conditions provided by Elsevier and Copyright Clearance Center.

License Number	4635460121359
License date	Jul 24, 2019
Licensed Content Publisher	Elsevier
Licensed Content Publication	Acta Biomaterialia
Licensed Content Title	Collagen fibrils in functionally distinct tendons have differing structural responses to tendon rupture and fatigue loading
Licensed Content Author	Tyler W. Herod,Neil C. Chambers,Samuel P. Veres
Licensed Content Date	Sep 15, 2016
Licensed Content Volume	42
Licensed Content Issue	n/a
Licensed Content Pages	12
Start Page	296
End Page	307
Type of Use	reuse in a thesis/dissertation
Intended publisher of new work	other
Portion	figures/tables/illustrations
Number of figures/tables/illustrations	1
Format	both print and electronic
Are you the author of this Elsevier article?	No
Will you be translating?	No
Original figure numbers	Figure 6 on page 302
Title of your thesis/dissertation	Age-, Sex-, and Diabetes-Determined Changes in the Structure and Mechanics of Human Sartorius Tendon Collagen.
Publisher of new work	Dalhousie University
Expected completion date	Jul 2019
Estimated size (number of pages)	1
Requestor Location	Dalhousie University 5981 University Avenue

Halifax, NS B3H4R2

	Canada
	Attn: Emile Feniyanos
Publisher Tax ID	GB 494 6272 12
Total	0.00 CAD
Terms and Conditions	

#### INTRODUCTION

1. The publisher for this copyrighted material is Elsevier. By clicking "accept" in connection with completing this licensing transaction, you agree that the following terms and conditions apply to this transaction (along with the Billing and Payment terms and conditions established by Copyright Clearance Center, Inc. ("CCC"), at the time that you opened your Rightslink account and that are available at any time at <http://myaccount.copyright.com>).

#### GENERAL TERMS

2. Elsevier hereby grants you permission to reproduce the aforementioned material subject to the terms and conditions indicated.

3. Acknowledgement: If any part of the material to be used (for example, figures) has appeared in our publication with credit or acknowledgement to another source, permission must also be sought from that source. If such permission is not obtained then that material may not be included in your publication/copies. Suitable acknowledgement to the source must be made, either as a footnote or in a reference list at the end of your publication, as follows:

"Reprinted from Publication title, Vol /edition number, Author(s), Title of article / title of chapter, Pages No., Copyright (Year), with permission from Elsevier [OR APPLICABLE SOCIETY COPYRIGHT OWNER]." Also Lancet special credit - "Reprinted from The Lancet, Vol. number, Author(s), Title of article, Pages No., Copyright (Year), with permission from Elsevier."

4. Reproduction of this material is confined to the purpose and/or media for which permission is hereby given.

5. Altering/Modifying Material: Not Permitted. However figures and illustrations may be altered/adapted minimally to serve your work. Any other abbreviations, additions, deletions and/or any other alterations shall be made only with prior written authorization of Elsevier Ltd. (Please contact Elsevier at [permissions@elsevier.com](mailto:permissions@elsevier.com)). No modifications can be made to any Lancet figures/tables and they must be reproduced in full.

6. If the permission fee for the requested use of our material is waived in this instance, please be advised that your future requests for Elsevier materials may attract a fee.

7. Reservation of Rights: Publisher reserves all rights not specifically granted in the combination of (i) the license details provided by you and accepted in the course of this licensing transaction, (ii) these terms and conditions and (iii) CCC's Billing and Payment terms and conditions.

8. License Contingent Upon Payment: While you may exercise the rights licensed immediately upon issuance of the license at the end of the licensing process for the transaction, provided that you have disclosed complete and accurate details of your proposed use, no license is finally effective unless and until full payment is received from you (either by publisher or by CCC) as provided in CCC's Billing and Payment terms and conditions. If full payment is not received on a timely basis, then any license preliminarily granted shall be deemed automatically revoked and shall be void as if never granted. Further, in the event that you breach any of these terms and conditions or any of CCC's Billing and Payment terms and conditions, the license is automatically revoked and shall be void as if never

granted. Use of materials as described in a revoked license, as well as any use of the materials beyond the scope of an unrevoked license, may constitute copyright infringement and publisher reserves the right to take any and all action to protect its copyright in the materials.

9. Warranties: Publisher makes no representations or warranties with respect to the licensed material.

10. Indemnity: You hereby indemnify and agree to hold harmless publisher and CCC, and their respective officers, directors, employees and agents, from and against any and all claims arising out of your use of the licensed material other than as specifically authorized pursuant to this license.

11. No Transfer of License: This license is personal to you and may not be sublicensed, assigned, or transferred by you to any other person without publisher's written permission.

12. No Amendment Except in Writing: This license may not be amended except in a writing signed by both parties (or, in the case of publisher, by CCC on publisher's behalf).

13. Objection to Contrary Terms: Publisher hereby objects to any terms contained in any purchase order, acknowledgment, check endorsement or other writing prepared by you, which terms are inconsistent with these terms and conditions or CCC's Billing and Payment terms and conditions. These terms and conditions, together with CCC's Billing and Payment terms and conditions (which are incorporated herein), comprise the entire agreement between you and publisher (and CCC) concerning this licensing transaction. In the event of any conflict between your obligations established by these terms and conditions and those established by CCC's Billing and Payment terms and conditions, these terms and conditions shall control.

14. Revocation: Elsevier or Copyright Clearance Center may deny the permissions described in this License at their sole discretion, for any reason or no reason, with a full refund payable to you. Notice of such denial will be made using the contact information provided by you. Failure to receive such notice will not alter or invalidate the denial. In no event will Elsevier or Copyright Clearance Center be responsible or liable for any costs, expenses or damage incurred by you as a result of a denial of your permission request, other than a refund of the amount(s) paid by you to Elsevier and/or Copyright Clearance Center for denied permissions.

#### LIMITED LICENSE

The following terms and conditions apply only to specific license types:

15. **Translation:** This permission is granted for non-exclusive world **English** rights only unless your license was granted for translation rights. If you licensed translation rights you may only translate this content into the languages you requested. A professional translator must perform all translations and reproduce the content word for word preserving the integrity of the article.

16. **Posting licensed content on any Website:** The following terms and conditions apply as follows: Licensing material from an Elsevier journal: All content posted to the web site must maintain the copyright information line on the bottom of each image; A hyper-text must be included to the Homepage of the journal from which you are licensing at <http://www.sciencedirect.com/science/journal/xxxxx> or the Elsevier homepage for books at <http://www.elsevier.com>; Central Storage: This license does not include permission for a scanned version of the material to be stored in a central repository such as that provided by Heron/XanEdu.

Licensing material from an Elsevier book: A hyper-text link must be included to the Elsevier homepage at <http://www.elsevier.com>. All content posted to the web site must maintain the copyright information line on the bottom of each image.

**Posting licensed content on Electronic reserve:** In addition to the above the following clauses are applicable: The web site must be password-protected and made available only to bona fide students registered on a relevant course. This permission is granted for 1 year only. You may obtain a new license for future website posting.

**17. For journal authors:** the following clauses are applicable in addition to the above:

**Preprints:**

A preprint is an author's own write-up of research results and analysis, it has not been peer-reviewed, nor has it had any other value added to it by a publisher (such as formatting, copyright, technical enhancement etc.).

Authors can share their preprints anywhere at any time. Preprints should not be added to or enhanced in any way in order to appear more like, or to substitute for, the final versions of articles however authors can update their preprints on arXiv or RePEc with their Accepted Author Manuscript (see below).

If accepted for publication, we encourage authors to link from the preprint to their formal publication via its DOI. Millions of researchers have access to the formal publications on ScienceDirect, and so links will help users to find, access, cite and use the best available version. Please note that Cell Press, The Lancet and some society-owned have different preprint policies. Information on these policies is available on the journal homepage.

**Accepted Author Manuscripts:** An accepted author manuscript is the manuscript of an article that has been accepted for publication and which typically includes author-incorporated changes suggested during submission, peer review and editor-author communications.

Authors can share their accepted author manuscript:

- immediately
  - via their non-commercial person homepage or blog
  - by updating a preprint in arXiv or RePEc with the accepted manuscript
  - via their research institute or institutional repository for internal institutional uses or as part of an invitation-only research collaboration work-group
  - directly by providing copies to their students or to research collaborators for their personal use
  - for private scholarly sharing as part of an invitation-only work group on commercial sites with which Elsevier has an agreement
- After the embargo period
  - via non-commercial hosting platforms such as their institutional repository
  - via commercial sites with which Elsevier has an agreement

In all cases accepted manuscripts should:

- link to the formal publication via its DOI
- bear a CC-BY-NC-ND license - this is easy to do
- if aggregated with other manuscripts, for example in a repository or other site, be shared in alignment with our hosting policy not be added to or enhanced in any way to appear more like, or to substitute for, the published journal article.

**Published journal article (JPA):** A published journal article (PJA) is the definitive final record of published research that appears or will appear in the journal and embodies all value-adding publishing activities including peer review co-ordination, copy-editing, formatting, (if relevant) pagination and online enrichment.

Policies for sharing publishing journal articles differ for subscription and gold open access articles:

**Subscription Articles:** If you are an author, please share a link to your article rather than the full-text. Millions of researchers have access to the formal publications on ScienceDirect, and so links will help your users to find, access, cite, and use the best available version. Theses and dissertations which contain embedded PJAs as part of the formal submission can be posted publicly by the awarding institution with DOI links back to the formal publications on ScienceDirect.

If you are affiliated with a library that subscribes to ScienceDirect you have additional private sharing rights for others' research accessed under that agreement. This includes use for classroom teaching and internal training at the institution (including use in course packs and courseware programs), and inclusion of the article for grant funding purposes.

**Gold Open Access Articles:** May be shared according to the author-selected end-user license and should contain a [CrossMark logo](#), the end user license, and a DOI link to the formal publication on ScienceDirect.

Please refer to Elsevier's [posting policy](#) for further information.

18. **For book authors** the following clauses are applicable in addition to the above:

Authors are permitted to place a brief summary of their work online only. You are not allowed to download and post the published electronic version of your chapter, nor may you scan the printed edition to create an electronic version. **Posting to a repository:** Authors are permitted to post a summary of their chapter only in their institution's repository.

19. **Thesis/Dissertation:** If your license is for use in a thesis/dissertation your thesis may be submitted to your institution in either print or electronic form. Should your thesis be published commercially, please reapply for permission. These requirements include permission for the Library and Archives of Canada to supply single copies, on demand, of the complete thesis and include permission for Proquest/UMI to supply single copies, on demand, of the complete thesis. Should your thesis be published commercially, please reapply for permission. Theses and dissertations which contain embedded PJAs as part of the formal submission can be posted publicly by the awarding institution with DOI links back to the formal publications on ScienceDirect.

#### **Elsevier Open Access Terms and Conditions**

You can publish open access with Elsevier in hundreds of open access journals or in nearly 2000 established subscription journals that support open access publishing. Permitted third party re-use of these open access articles is defined by the author's choice of Creative Commons user license. See our [open access license policy](#) for more information.

#### **Terms & Conditions applicable to all Open Access articles published with Elsevier:**

Any reuse of the article must not represent the author as endorsing the adaptation of the article nor should the article be modified in such a way as to damage the author's honour or reputation. If any changes have been made, such changes must be clearly indicated.

The author(s) must be appropriately credited and we ask that you include the end user license and a DOI link to the formal publication on ScienceDirect.

If any part of the material to be used (for example, figures) has appeared in our publication with credit or acknowledgement to another source it is the responsibility of the user to ensure their reuse complies with the terms and conditions determined by the rights holder.

#### **Additional Terms & Conditions applicable to each Creative Commons user license:**

**CC BY:** The CC-BY license allows users to copy, to create extracts, abstracts and new works from the Article, to alter and revise the Article and to make commercial use of the Article (including reuse and/or resale of the Article by commercial entities), provided the

user gives appropriate credit (with a link to the formal publication through the relevant DOI), provides a link to the license, indicates if changes were made and the licensor is not represented as endorsing the use made of the work. The full details of the license are available at <http://creativecommons.org/licenses/by/4.0>.

**CC BY NC SA:** The CC BY-NC-SA license allows users to copy, to create extracts, abstracts and new works from the Article, to alter and revise the Article, provided this is not done for commercial purposes, and that the user gives appropriate credit (with a link to the formal publication through the relevant DOI), provides a link to the license, indicates if changes were made and the licensor is not represented as endorsing the use made of the work. Further, any new works must be made available on the same conditions. The full details of the license are available at <http://creativecommons.org/licenses/by-nc-sa/4.0>.

**CC BY NC ND:** The CC BY-NC-ND license allows users to copy and distribute the Article, provided this is not done for commercial purposes and further does not permit distribution of the Article if it is changed or edited in any way, and provided the user gives appropriate credit (with a link to the formal publication through the relevant DOI), provides a link to the license, and that the licensor is not represented as endorsing the use made of the work. The full details of the license are available at <http://creativecommons.org/licenses/by-nc-nd/4.0>. Any commercial reuse of Open Access articles published with a CC BY NC SA or CC BY NC ND license requires permission from Elsevier and will be subject to a fee.

Commercial reuse includes:

- Associating advertising with the full text of the Article
- Charging fees for document delivery or access
- Article aggregation
- Systematic distribution via e-mail lists or share buttons

Posting or linking by commercial companies for use by customers of those companies.

#### 20. Other Conditions:

v1.9

Questions? [customercare@copyright.com](mailto:customercare@copyright.com) or +1-855-239-3415 (toll free in the US) or +1-978-646-2777.

---

---





**Permissions**

4th Floor, Auto Atlantic  
Corner, Hertzog Boulevard &  
Heerengracht  
Cape town, 8001  
South Africa  
USAPermissions@pearson.com

Jun 12, 2019

PE Ref # 209088

Emile Feniyanos  
DALHOUSIE UNIVERSITY  
5981 University Avenue  
Halifax, NS  
CANADA

Dear Emile Feniyanos,

You have our permission to include content from our text, *HUMAN ANATOMY & PHYSIOLOGY, 9th Ed.* by *MARIEB, ELAINE N.; HOEHN, KATJA*, in your dissertation or masters thesis at Dalhousie University.

Content to be included is:

- Page 364 Figure 10.20 (a)

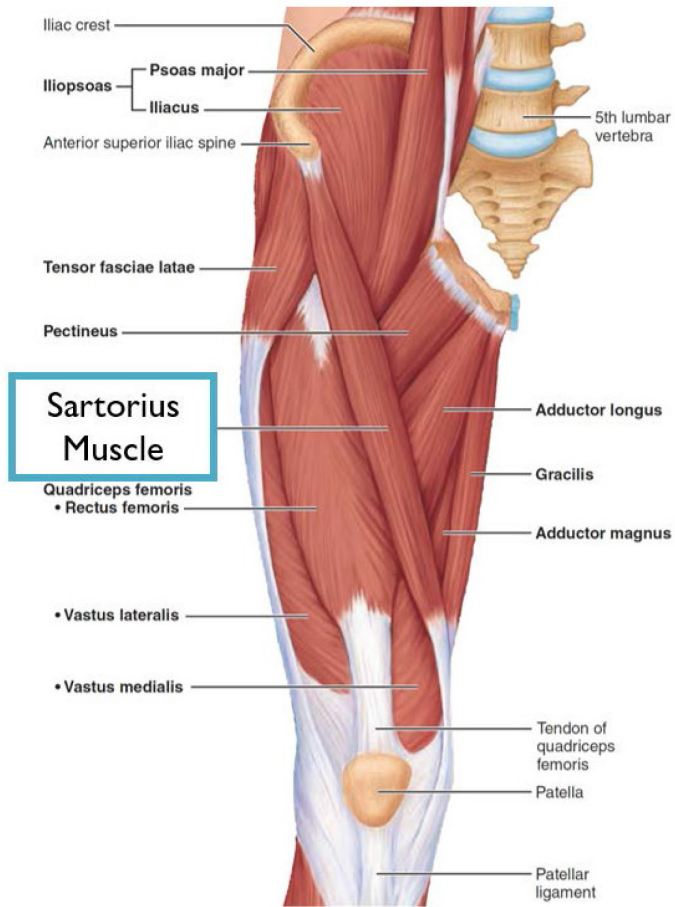
Please credit our material as follows:

*MARIEB, ELAINE N.; HOEHN, KATJA, HUMAN ANATOMY & PHYSIOLOGY, 9th, ©2013. Reprinted by permission of Pearson Education, Inc., New York.*

Sincerely,

Gaynor Thomas, Global Permissions Granting Analyst

A



---

**From:** Wiley Global Permissions  
**Sent:** July 23, 2019 4:53 AM  
**To:** Emile Feniyanos  
**Subject:** RE: NON RIGHTSLINK : Permission request to reuse only a portion of a figure

Dear Emile,

Thank you for your email.

Permission is granted for you to use the material requested for your thesis/dissertation subject to the usual acknowledgements (author, title of material, title of book/journal, ourselves as publisher) and on the understanding that you will reapply for permission if you wish to distribute or publish your thesis/dissertation commercially.

You should also duplicate the copyright notice that appears in the Wiley publication in your use of the Material. Permission is granted solely for use in conjunction with the thesis, and the material may not be posted online separately.

Any third-party material is expressly excluded from this permission. If any material appears within the article with credit to another source, authorisation from that source must be obtained.

*Please note in your publication that the figure has been adapted and to reference the original.*

Should you require any further information, please do not hesitate to contact me.

Kind regards,

**Paisley Chesters**  
**Permissions Co-Ordinator**

Wiley  
The Atrium  
Southern Gate  
Chichester  
West Sussex  
PO19 8SQ  
[www.wiley.com](http://www.wiley.com)

**WILEY**

John Wiley & Sons Limited is a private limited company registered in England with registered number 641132.  
Registered office address: The Atrium, Southern Gate, Chichester, West Sussex, United Kingdom. PO19 8SQ

---

**From:** Emile Feniyanos <em903640@dal.ca>  
**Sent:** 22 July 2019 17:14  
**To:** Wiley Global Permissions <permissions@wiley.com>  
**Subject:** NON RIGHTSLINK : Permission request to reuse only a portion of a figure

Hello,

My name is Emile Feniyanos and I was inquiring about reusing a figure in my thesis at Dalhousie University and planned to only include a portion of the figure (see original and cropped image attached)

My thesis title : Age-, Sex-, and Diabetes-Determined Changes in the Structure and Mechanics of Human Sartorius Tendon Collagen.

University: Dalhousie University, Halifax, Nova Scotia, Canada

Information about the journal article where the figure derives from:

Licensed Content Publisher John Wiley and Sons  
Licensed Content Publication Journal of Orthopaedic Research  
Licensed Content Title Cross-link stabilization does not affect the response of collagen molecules, fibrils, or tendons to tensile overload  
Licensed Content Author Samuel P. Veres, Julia M. Harrison, J. Michael Lee

DOI: <https://doi.org/10.1002/jor.22460>

Figure to be reused: Figure # 1 on page 1908 (or the third page) of the journal article – upon confirmation of my supervisor, the only further change would be to add an arrow and label “Sample” pointing to the sample held between the grips.

Thanks,  
Emile Feniyanos

## SPRINGER NATURE LICENSE TERMS AND CONDITIONS

Jun 11, 2019

This Agreement between Dalhousie University -- Emile Feniyanos ("You") and Springer Nature ("Springer Nature") consists of your license details and the terms and conditions provided by Springer Nature and Copyright Clearance Center.

License Number	4606050819468
License date	Jun 11, 2019
Licensed Content Publisher	Springer Nature
Licensed Content Publication	Archiv für orthopädische und Unfall-Chirurgie, mit besonderer Berücksichtigung der Frakturenlehre und der orthopädisch-chirurgischen Technik
Licensed Content Title	Fibrilläre Gefügestörung bei Sehnenruptur
Licensed Content Author	A. Meinel, H. Nemetschek-Gansler, U. Holz et al
Licensed Content Date	Jan 1, 1977
Licensed Content Volume	90
Licensed Content Issue	1
Type of Use	Thesis/Dissertation
Requestor type	academic/university or research institute
Format	print and electronic
Portion	figures/tables/illustrations
Number of figures/tables/illustrations	1
Will you be translating?	yes, without original language
Number of languages	1
Circulation/distribution	<501
Author of this Springer Nature content	no
Title	Age-, Sex-, and Diabetes-Determined Changes in the Structure and Mechanics of Human Sartorius Tendon Collagen.
Institution name	Dalhousie University
Expected presentation date	Jul 2019
Portions	Figure 1 on page 91.
Specific Languages	English
Requestor Location	Dalhousie University 5981 University Avenue  Halifax, NS B3H4R2 Canada Attn: Emile Feniyanos
Total	<b>0.00 CAD</b>
Terms and Conditions	

Springer Nature Terms and Conditions for RightsLink Permissions

**Springer Nature Customer Service Centre GmbH (the Licensor)** hereby grants you a non-exclusive, world-wide licence to reproduce the material and for the purpose and requirements specified in the attached copy of your order form, and for no other use, subject to the conditions below.

1. The Licensor warrants that it has, to the best of its knowledge, the rights to license reuse of this material. However, you should ensure that the material you are requesting is original to the Licensor and does not carry the copyright of another entity (as credited in the published version).  
  
If the credit line on any part of the material you have requested indicates that it was reprinted or adapted with permission from another source, then you should also seek permission from that source to reuse the material.
2. Where **print only** permission has been granted for a fee, separate permission must be obtained for any additional electronic re-use.
3. Permission granted **free of charge** for material in print is also usually granted for any electronic version of that work, provided that the material is incidental to your work as a whole and that the electronic version is essentially equivalent to, or substitutes for, the print version.
4. A licence for 'post on a website' is valid for 12 months from the licence date. This licence does not cover use of full text articles on websites.
5. Where '**reuse in a dissertation/thesis**' has been selected the following terms apply: Print rights of the final author's accepted manuscript (for clarity, NOT the published version) for up to 100 copies, electronic rights for use only on a personal website or institutional repository as defined by the Sherpa guideline ([www.sherpa.ac.uk/romeo/](http://www.sherpa.ac.uk/romeo/)).
6. Permission granted for books and journals is granted for the lifetime of the first edition and does not apply to second and subsequent editions (except where the first edition permission was granted free of charge or for signatories to the STM Permissions Guidelines <http://www.stm-assoc.org/copyright-legal-affairs/permissions/permissions-guidelines/>), and does not apply for editions in other languages unless additional translation rights have been granted separately in the licence.
7. Rights for additional components such as custom editions and derivatives require additional permission and may be subject to an additional fee. Please apply to [Journalpermissions@springernature.com](mailto:Journalpermissions@springernature.com)/[bookpermissions@springernature.com](mailto:bookpermissions@springernature.com) for these rights.
8. The Licensor's permission must be acknowledged next to the licensed material in print. In electronic form, this acknowledgement must be visible at the same time as the figures/tables/illustrations or abstract, and must be hyperlinked to the journal/book's homepage. Our required acknowledgement format is in the Appendix below.
9. Use of the material for incidental promotional use, minor editing privileges (this does not include cropping, adapting, omitting material or any other changes that affect the meaning, intention or moral rights of the author) and copies for the disabled are permitted under this licence.
10. Minor adaptations of single figures (changes of format, colour and style) do not require the Licensor's approval. However, the adaptation should be credited as shown in Appendix below.

#### Appendix — Acknowledgements:

**For Journal Content:**

Reprinted by permission from [the Licensor]: [Journal Publisher (e.g. Nature/Springer/Palgrave)] [JOURNAL NAME] [REFERENCE CITATION (Article name, Author(s) Name), [COPYRIGHT] (year of publication)]

**For Advance Online Publication papers:**

Reprinted by permission from [the Licensor]: [Journal Publisher (e.g. Nature/Springer/Palgrave)] [JOURNAL

NAME] [REFERENCE CITATION (Article name, Author(s) Name), [COPYRIGHT] (year of publication), advance online publication, day month year (doi: 10.1038/sj.[JOURNAL ACRONYM].)

**For Adaptations/Translations:**

Adapted/Translated by permission from [the Licensor]: [Journal Publisher (e.g. Nature/Springer/Palgrave)] [JOURNAL NAME] [REFERENCE CITATION (Article name, Author(s) Name), [COPYRIGHT] (year of publication)]

**Note: For any republication from the British Journal of Cancer, the following credit line style applies:**

Reprinted/adapted/translated by permission from [the Licensor]: on behalf of Cancer Research UK: : [Journal Publisher (e.g. Nature/Springer/Palgrave)] [JOURNAL NAME] [REFERENCE CITATION (Article name, Author(s) Name), [COPYRIGHT] (year of publication)]

**For Advance Online Publication papers:**

Reprinted by permission from The [the Licensor]: on behalf of Cancer Research UK: [Journal Publisher (e.g. Nature/Springer/Palgrave)] [JOURNAL NAME] [REFERENCE CITATION (Article name, Author(s) Name), [COPYRIGHT] (year of publication), advance online publication, day month year (doi: 10.1038/sj.[JOURNAL ACRONYM])]

**For Book content:**

Reprinted/adapted by permission from [the Licensor]: [Book Publisher (e.g. Palgrave Macmillan, Springer etc)] [Book Title] by [Book author(s)] [COPYRIGHT] (year of publication)

**Other Conditions:**

Version 1.1

Questions? [customer-care@copyright.com](mailto:customer-care@copyright.com) or +1-855-239-3415 (toll free in the US) or +1-978-646-2777.



## Re: Permission to use a Figure in Thesis

Sara Sparavalo [REDACTED]

Tue 5/28/2019 4:29 PM

To: Emile Fenianos [REDACTED]

[REDACTED]  
Absolutely, please do :).

[REDACTED]  
Sara

On May 28, 2019, at 16:10, Emile Fenianos [REDACTED] wrote:

Hi Sara,

[REDACTED]  
In terms of reprinted materials, I would like to include the following figure from your thesis.

Figure 4.17.

I've also attached the figure to the email that I would like to use in my thesis.

Thanks,  
Emile

<Figure 4.17.jpg>



<Figure 4.17.tif>

